GEOTECHNICAL INVESTIGATION ON THE BEHAVIOUR OF FIBRE-MIXED BLACK COTTON SOIL UNDER THE INFLUENCE OF VARIOUS PERMEANTS FOR BARRIER APPLICATION

Thesis

submitted in partial fulfillment of the requirements

for the degree of

DOCTOR OF PHILOSOPHY

by

NUTHALAPATI MAHESH BABU

(Roll No. 186104109)

Department of Civil Engineering

Indian Institute of Technology, Guwahati

Guwahati – 781039, India

January 2025

TH-3665_186104109

TH-3665_186104109

CERTIFICATE

This is to certify that the thesis entitled **"Geotechnical Investigation on The Behaviour of Fibre-Mixed Black Cotton Soil Under The Influence of Various Permeants for Barrier Application"** submitted by **Nuthalapati Mahesh Babu,** Roll No. 186104109, to the Indian Institute of Technology, Guwahati, for the award of the degree of Doctor of Philosophy in Civil Engineering is a record of bonafide research work carried out by him under my supervision and guidance. The thesis work, in my opinion, has reached the requisite standard fulfilling the requirement for the degree of Doctor of Philosophy.

The results contained in this thesis have not been submitted in part or full to any other University or Institute for award of any degree or diploma.

(Dr Anil Kumar Mishra)

Professor

Department of Civil Engineering

Indian Institute of Technology Guwahati

Date:

IIT Guwahati

STATEMENT

I do hereby declare that the matter embodied in this thesis is the result of investigations carried out by me in the Department of Civil Engineering, Indian Institute of Technology Guwahati, Assam, India.

In keeping with the general practice of reporting scientific observations, due acknowledgements have been made wherever the work described is based on the findings of other investigators.

(Nuthalapati Mahesh Babu)

Date:

IIT-Guwahati

TH-3665_186104109

ACKNOWLEDGEMENTS

I thank **God** for **His** grace, guidance, protection, and support throughout this journey, working through the kindness and assistance of many people along the way.

I sincerely express my profound gratitude to all those whose unwavering support and encouragement have enabled me to pursue my research and successfully submit this PhD thesis. First and foremost, I extend my heartfelt appreciation and deep gratitude to my thesis supervisor and research guide, **Prof. Anil Kumar Mishra**, for his meticulous guidance, unwavering encouragement, patience, and invaluable support throughout my PhD journey. Once again, I extend my deepest thanks to him from the bottom of my heart.

After that, I would like to express my sincere gratitude to the chairman of my Doctoral Committee, Prof. S. Sreedeep, and committee members Dr. K. Ravi and Prof. S. K. Majumder for their valuable insights, constructive feedback, and encouragement. I would also like to express my gratitude to the other faculty members of the Geotechnical Engineering Division, Civil Engineering Department, for their valuable suggestions and support throughout my PhD journey. I am also deeply thankful to the Ministry of Human Resource Development, India, for its essential financial support, which enabled me to pursue my studies.

I am also deeply grateful to **Mr. Hari Ram Upadhyaya** and Mr. Ashim for their unwavering assistance during various phases of my research work. Their help has been invaluable in ensuring the smooth progress of my study. Furthermore, I would like to express my appreciation to the office staff of the Civil Engineering Department for their support in administrative matters, which greatly facilitated my research process.

I would like to express my heartfelt appreciation to all my Assembly elders and members for their continuous support and encouragement, which have played a crucial role in my growth. I am thankful to my closest friend and mentor Dr. Anil Kumar (EEE), for standing with me through both challenging and joyful moments. My special thanks to Dr. Jaswant Gangolu (Structures) for his encouragement and support during my PhD journey. I am grateful to Venkat Anna and Pabllbi Akka for the wonderful moments and opportunities we shared. Their presence has been truly special in my journey. I am truly thankful to Dr. Saswat Ray, my senior, for her constant support and motivation during the initial stages of my journey.

TH-3665_186104109

My special thanks to my friends Jogi (helpful man) and Ganesh from the physics lab, who patiently helped me and with me during my PhD. Also, I am grateful to my friends Sam, Patanjali, Prasanna (B. Tech friend), Jerison Anna (Structural engineer), Feba Akka, Tharun Anna, Rajashekar Anna (Chemical) and family, Sunil Anna, Joel, Vivek, Sakesh, Anil (Mechanical), Joel (IITM M. Tech), Joshua, Praneet, Kireeti, Silvanus, Suresh Anna, and many others. Their support, kindness, and the valuable lessons I have learned from them have truly enriched my journey. I am thankful to my favourite B. Tech lecturer, Ummi Salma, who taught Geotechnical engineering subject.

Also, I am thankful to my seniors Dr. Chandra Gupt Bhanu and Dr. Krishanu Mukhrejee, for their support in my research. I am thankful to my colleagues and friends Chandra, Sreekant, Subhash (M. Tech), Abhishek (M. Tech), Asish (M. Tech), Alok, Riya, Maruti, Sai (M. Tech), Abhishek Anna, Sai (Ph.D) for their support in my work.

Finally, but most importantly, I would like to thank my Parents (**Srinivasa Rao and Koteswaramma**), who taught me the value of hard work and moral values. Without them, I am nothing. I am grateful for their unconditional love, support, and guidance. I would like to express my joy to my younger brother N. Venkatesh (who looks older than me), friendly and supportive.

NUTHALAPATI MAHESH BABU

TH-3665_186104109

ABSTRACT

The rapid growth in population, urbanization, and industrial expansion lead to the significant accumulation of solid waste highlighting the critical need for safe and engineered disposal systems rather than traditional open dumping practices. Engineered disposal systems are designed to isolate both domestic and industrial wastes from the natural environment by placing geotechnical barrier systems. These clay barriers are designed to act as impermeable layers, ensuring effective containment and minimizing or avoiding the potential for groundwater contamination. The distinctive characteristics like high swelling ability, high adsorption capacity, and very low hydraulic conductivity of clay make it preferable as a barrier material for effective waste containment systems. Usually, bentonites are extensively used as engineered barrier materials because of its high ability to meet the requirements for effective barrier performance. The use of bentonites is associated with two significant challenges. Firstly, their availability in India is geographically restricted, mainly limited to the state of Rajasthan. Secondly, bentonites exhibit high shrinkage and compressibility tendencies due to the presence of the predominant clay mineral montmorillonite, which can lead to significant desiccation cracks, compromising the purpose of hydraulic barrier application. Hence, it becomes imperative to explore alternative naturally available clayey soils that can serve as effective barrier materials without compromising the essential performance criteria for barrier applications.

In this study, naturally available black cotton (BC) soil is employed as a barrier material based on its widespread availability and mineralogical composition, with montmorillonite being the predominant mineral. However, BC soil is also susceptible to significant shrinkage phenomenon. Extensive research focused on over the past few decades has demonstrated that clays have reduced susceptibility to shrinkage when added with fibres. Therefore, considering the engineering, economic, and environmental benefits a composite of waste tire fibre and BC soil is utilized as a hydraulic barrier. Here, the suitability of waste tire content for use with BC soil was evaluated by incorporating waste tire fibres at the concentration levels of 5, 10, and 15% by dry weight of BC soil.

The long-term effectiveness of fibre-mixed BC soil liner as a hydraulic barrier can be adversely affected by the permeation of various hazardous chemicals present in landfill leachate, leading to groundwater contamination if the engineering behaviour of barrier material is not thoroughly examined. Therefore, it is very crucial to test barrier material under

the permeation of various salts and heavy metals, which are predominant in landfill leachate. For this reason, fibre-mixed BC soil was tested under two inorganic salts (NaCl and $CaCl_2$) at two concentrations of 0.1 and 1.0N, three heavy metals (two cationic: Pb(II) and Cd(II), one anionic: Cr(VI)) at three concentrations of 100, 500, and 1000 ppm, and two synthetic leachates (MSW leachate and fly ash leachate) to assess its suitability as a hydraulic barrier.

The test results indicated a substantial decrease in the swelling potentials, swelling pressures, and time for 90% consolidation of BC soil as a consequence of the significant increase in tire fibre content by up to 15%. However, the compression index of BC soil decreased up to 10% of fibre inclusions but showed a slight increase when the fibre content was raised from 10 to 15%. The hydraulic conductivity of BC soil increased by multiple folds with the rise in fibre content. However, all hydraulic conductivity values of fibre-mixed soil remained within the acceptable limit ($<10^{-7}$ cm/s); meanwhile, the UCS value of BC soil exceeded the required threshold (>200 kPa) with the incorporation of 15% tire-fibre content. The experimental results showed a significant reduction in Atterberg limits and free swell indices with all chemical solutions. Also, engineering properties such as oedometer swelling heights, swelling pressures, and time for 90% consolidation of all fibre-mixed BC soil samples under the permeation of inorganic salts, heavy metals, and synthetic leachates were reduced considerably at high concentrations, irrespective of fibre content. All measured swelling values of fibre-mixed BC soil samples were predicted using the rectangular hyperbola model under various permeants and found a good correlation between measured and predicted swelling potentials, irrespective of permeant type. The time and swelling observed in the primary swelling stages of all samples varied depending on the type and concentration of permeant. However, the coefficient of consolidation and hydraulic conductivity values of all samples rose to multiple folds because of these chemical permeants, irrespective of fibre content. On the other hand, compression indices of all fibre-mixed BC soil samples were reduced marginally with the rise in the concentration of inorganic salts and heavy metals including synthetic leachates. Concentration and cation valency play vital roles in altering these engineering properties of fibre-mixed BC soil. Test results revealed that the hydromechanical characteristics of all fibre-mixed BC soil samples were influenced more significantly by divalent cations from $CaCl_2$ concentrations than with monovalent cations from NaCl at the same concentration levels. Cr(VI) permeants exhibited a more pronounced impact on the swelling, consolidation, and hydraulic properties of all fibre-mixed soils than with divalent heavy metal permeants due to valency and concentrations of K^+ ions from

TH-3665_186104109

$K_2Cr_2O_7$ solution. The The UCS values of all fibre-mixed soil samples were slightly reduced with Cr(VI) permeants, whereas marginally increased with Cd(II) and Pb(II), irrespective of fibre content. Synthetic fly ash leachate had shown a more significant impact on geotechnical properties of barrier material than synthetic MSW leachate due to elevated concentration of heavy metals present in fly ash leachate. However, the UCS values of all fibre-mixed soil samples exhibited a declining trend with both leachates. The hydraulic conductivity of 15% fibre-mixed soil exhibited a surpassing value at any given consolidation pressure under permeation of synthetic leachates and inorganic salt permeations at 1.0N concentration. Laboratory results clearly highlighted the importance of evaluating the influence of various permeants on the geotechnical properties of fibre-mixed soils.

KEYWORDS: Black cotton soil; landfill liner, waste tire fibres, inorganic salts; heavy metals; synthetic leachates; liquid limit; swelling pressure; coefficient of consolidation; hydraulic conductivity; compressibility

TH-3665_186104109

TABLE OF CONTENTS

		Page No.
	ACKNOWLEDGEMENT	iii-iv
	ABSTRACT	v-vii
	LIST OF FIGURES	xi-xvi
	LIST OF TABLES	xvii-xviii
	ABBREVIATIONS	xix
	SYMBOLS USED	xx
CHAPTER 1	**INTRODUCTION**	**1-5**
1.1.	General	1
1.2.	Outline of the thesis	4
CHAPTER 2	**BACKGROUND AND LITERATURE SURVEY**	**6-61**
2.1.	General	6
2.2.	Waste management and disposal	6
2.3.	Landfill liner	7
2.4.	Landfill design approaches in various countries	9
2.5.	Key design parameters for landfill liners	10
2.5.1.	Hydraulic conductivity	10
2.5.2.	Settlement	10
2.5.3.	Shear strength	11
2.5.4.	Volumetric shrinkage	11
2.6.	Black cotton (BC) soil	11
2.6.1.	General	11
2.6.2.	Problems associated with black cotton soil	12
2.6.3.	Identification of expansiveness of black cotton soil	14
2.6.4.	Structure of montmorillonite	16
2.6.5.	Swelling mechanism of expansive black cotton soils	18
	2.6.5.1. Inner-crystalline swelling	18
	2.6.5.2. Osmotic swelling	19
2.6.6.	Diffuse Double Layer	21
	2.6.6.1. Factors influencing diffuse double layer thickness	22
2.6.7.	Black cotton soil treatment techniques	23
2.6.8.	Use of black cotton soil as landfill liner	24
2.7.	Review of literature on clay-waste tire mix	25
2.8.	Formation of leachate from MSW	42
2.8.1.	Leachate composition	42
2.8.2.	Influence of leachates on barrier material	43
2.9.	Review of literature on salt solutions' interaction with clay	44
2.10.	Sources and consequences of heavy metals in leachate	51
2.11.	Review of literature on heavy metals' interaction with clay	53
2.12.	Review of literature on leachates' interaction with clay	56
2.13.	Critical analysis of the reviewed literature	59
2.14.	Research gap and objectives of the study	60

CHAPTER 3 MATERIALS AND METHODOLOGY 62-80

3.1. General 62
3.2. Plan of research work 62
3.3. Collection of BC soil and its characterization 64
3.4. Tire fibre and its characterization 68
3.5. Permeant solutions 70
3.5.1. Inorganic salt solutions 70
3.5.2. Heavy metal solutions 70
3.5.3. Synthetic leachates 71
3.6. Preparation of BC soil-tire fibre mix 72
3.7. Testing Methodology 74
3.7.1. Free swell index determination 74
3.7.2. Atterberg limits determination 74
3.7.3. Compaction properties determination 75
3.7.4. Swelling potentials and swelling pressures determination 75
3.7.5. Hydraulic conductivity (k) determination 77
3.7.6. Unconfined compression strength (UCS) estimation 79

CHAPTER 4 INFLUENCE OF TIRE FIBRE ON THE BEHAVIOUR OF BC SOIL 81-101

4.1. Introduction 81
4.2. Test Result and Discussion 83
4.2.1. Compaction characteristics 83
4.2.2. Time-swelling relationship 84
4.2.3. Swelling pressures and Swelling potentials 86
4.2.4. Swelling prediction using RH model 87
4.2.5. Coefficient of consolidation (c_v) 90
4.2.6. Time for 90% consolidation (t_{90}) 92
4.2.7. Void ratio vs pressure (e-log P) relationship 94
4.2.8. Compression index (C_c) 95
4.2.9. Hydraulic conductivity (k) 95
4.2.10. Unconfined compressive strength (UCS) 97
4.3. Summary 100

CHAPTER 5 INFLUENCE OF SALT PERMEANTS ON THE BEHAVIOUR OF FIBRE-MIXED BC SOIL 102-145

5.1. Introduction 102
5.2. Test Result and Discussion 103
5.2.1. Atterberg limits 103
5.2.2. Free swell index (FSI) 105
5.2.3. Time-swelling relationship 107
5.2.4. Swelling pressures and swelling potentials 115
5.2.4. Coefficient of consolidation (c_v) 120
5.2.5. Time for 90% consolidation (t_{90}) 124
5.2.6. Void ratio vs pressure (e-log P) relationship 128
5.2.7. Compression index (C_c) 129
5.2.8. Hydraulic conductivity (k) 132

TH-3665_186104109

5.2.9.	Unconfined compressive strength (UCS)	140
5.3.	Summary	143
CHAPTER 6	**INFLUENCE OF HEAVY METAL CONCENTRATIONS ON THE BEHAVIOUR OF FIBRE-MIXED BC SOIL**	**146-212**
6.1.	Introduction	146
6.2.	Test Result and Discussion	148
6.2.1.	Atterberg limits	148
6.2.2.	Free swell index (FSI)	150
6.2.3.	Time vs swelling behaviour	152
6.2.4.	Swelling pressures and swelling potentials	162
6.2.5.	Coefficient of consolidation (c_v)	170
6.2.6.	Time for 90% consolidation (t_{90})	176
6.2.7.	Void ratio vs pressure (e-log P) relationship	188
6.2.8.	Hydraulic conductivity (k)	189
6.2.9.	Compression index (C_c)	188
6.2.10.	FESEM behaviour	199
6.2.11.	Unconfined compressive strength (UCS)	202
6.3.	Summary	210
CHAPTER 7	**INFLUENCE OF SYNTHETIC LEACHATES ON THE BEHAVIOUR OF FIBRE-MIXED BC SOIL**	**213-249**
7.1.	Introduction	213
7.2.	Test Result and Discussion	214
7.2.1.	Leachates' influence on Atterberg limits	214
7.2.2.	Influence of leachates on free swell index	215
7.2.3.	Influence of leachates on time-swelling relationship	216
7.2.4.	Influence of leachates on Swelling pressures and swelling potentials	225
7.2.5.	Influence of leachates on coefficient of consolidation (c_v)	227
7.2.6.	Influence of leachates on time for 90% consolidation (t_{90})	231
7.2.7.	Influence of leachates on void ratio – pressure (e-log$P$) relationship	235
7.2.8.	Influence of leachates on compression index (C_c)	238
7.2.9.	Influence of leachates on hydraulic conductivity (k)	239
7.2.9.	Influence of leachates on UCS behaviour	245
7.3.	Summary	248
CHAPTER 8	**CONCLUSION AND SCOPE FOR FUTURE WORK**	**249-252**
8.1.	Conclusion	249
8.2.	Scientific contributions and practical significance	251
8.3.	Future scope of the study	251
	REFERENCES	**253-270**
	LIST OF PUBLICATIONS	**271-272**

TH-3665_186104109

LIST OF FIGURES

Figure No.	Caption	Page No.
2.1	Typical liner systems	8
2.2	Liner systems specified in Europe and America	9
2.3	Japanese liner systems	10
2.4	Black cotton soil (before and after pulverization)	12
2.5	Typical cracks in black soils during the dry season	14
2.6	Structure of montmorillonite	17
2.7.a	Inner-crystalline swelling of sodium montmorillonite.	19
2.7.b	The structure of water molecule	19
2.8.a	Two negatively charged clay layers with ion cloud.	21
2.8.b	Negatively charged clay surface, ions in the diffuse double layer and ions in the pore water.	21
2.9	Gouy-Chapman diffuse double layer theory	22
2.10	Stacking and burning of waste tires	25
2.11	Waste tire applications in the civil engineering field	26
2.12	Waste tire classifications	27
3.1	Research design	63
3.2.a	BC soil used in this study	64
3.2.b	Particle size distribution curve of BC soil	64
3.3.a	XRD analysis of BC soil	65
3.3.b	EDX analysis of BC soil	65
3.4	FTIR analysis of BC soil	66
3.5.a	FESEM image of BCS at 20000 x magnification	67
3.5.b	TG curve of BC soil	67
3.6	Tire fibres used in this research	68
3.7.a	EDX analysis of tire fibre	69
3.7.b	FESEM analysis of tire fibre	69
3.8.a	FTIR analysis of tire fibre	70
3.8.b	TGA analysis of tire fibre.	70
3.9	BC soil-tire fibre mix	73
3.10	Determination of swelling pressure and swelling potential	76
3.11	Consolidation testing setup	78
3.12	Taylor square root-of time fitting method	79
3.13	UCS testing setup	80
4.1	Compaction curves for BC soil-tire fibre mixes	83
4.2	Representation of swelling stages from swelling curve (S-curve)	85
4.3	Time-swell plot of fibre-mixed BC soil with DI water	85
4.4	Linearized representation of swelling potential data for BC soil-tire fibre mixes	88
4.5	Correlation between measured swell vs observed swell	89
4.6	Consolidation pressure vs coefficient of consolidation (c_v) plot for various fibre-mixed BC soil with DI water	90

TH-3665_186104109

4.7	Fibre content vs coefficient of consolidation plots with DI water at different consolidation pressures	91
4.8	Consolidation pressure vs time for 90% consolidation (t_{90}) plot for various fibre-mixed BC soil with DI water	92
4.9	Fibre content vs t_{90} plots with DI water at different consolidation pressures	93
4.10	Void ratio-pressure plots for various fibre-mixed BC soil with DI water	94
4.11	Compression index of fibre-mixed BC soil with DI water	95
4.12	Hydraulic conductivity vs void ratio plots for various fibre-mixed BC soil with DI water	96
4.13	Hydraulic conductivity vs consolidation pressure plots for various fibre-mixed BC soil with DI water	96
4.14	UCS of fibre-mixed BC soil with DI water	98
4.15	Typical failure pattern of fibre-mixed samples (0, 5, 10, and 15%) after UCS testing	99
5.1	Atterberg limits of BC soil with NaCl and $CaCl_2$ salt solutions	104
5.2	Free swelling index (FSI) of BC soil with NaCl and $CaCl_2$ salt solutions	106
5.3	Liquid limit versus FSI of BC soil with salts of various concentrations solutions	106
5.4	Time-swelling plot of BC soil with NaCl and $CaCl_2$ salt permeants	109
5.5	Time-swelling plot of 5% fibre-mixed BC soil with NaCl and $CaCl_2$ salt permeants	109
5.6	Time-swelling plot of 10% fibre-mixed BC soil with NaCl and $CaCl_2$ salt permeants	110
5.7	Time-swelling plot of 15% fibre-mixed BC soil with NaCl and $CaCl_2$ salt permeants	110
5.8	Linearized representation of swelling potential data for BC soil under different salt permeants	111
5.9	Linearized representation of swelling potential data for 5% fibre-mixed BC soil under different salt permeants	111
5.10	Linearized representation of swelling potential data for 10% fibre-mixed BC soil under different salt permeants	112
5.11	Linearized representation of swelling potential data for 15% fibre-mixed BC soil under different salt permeants	112
5.12	Correlation between measured swell vs predicted swell of all fibre-mixed samples under various salt permeant concentrations	119
5.13	Consolidation pressure vs coefficient of consolidation (c_v) plots for pure BC soil with various concentrations of salt permeants	121
5.14	Consolidation pressure vs coefficient of consolidation (c_v) plots for 5% fibre-mixed BC soil with various concentrations of salt permeants	122
5.15	Consolidation pressure vs coefficient of consolidation (c_v) plots for 10% fibre-mixed BC soil with various concentrations of salt permeants	122
5.16	Consolidation pressure vs coefficient of consolidation (c_v) plots for 15% fibre-mixed BC soil with various concentrations of salt permeants	123
5.17	Fibre content vs coefficient of consolidation plot with various salt permeant concentrations at a consolidation pressure of 784.5 kPa	123
5.18	Consolidation pressure vs time for 90% consolidation (t_{90}) plots for pure BC soil with various salt permeant concentrations	125

TH-3665_186104109

5.19	Consolidation pressure vs time for 90% consolidation (t_{90}) plots for 5% fibre-mixed BC soil with various salt permeant concentrations	126
5.20	Consolidation pressure vs time for 90% consolidation (t_{90}) plots for 10% fibre-mixed BC soil with various salt permeant concentrations	126
5.21	Consolidation pressure vs time for 90% consolidation (t_{90}) plots for 15% fibre-mixed BC soil with various salt permeant concentrations	127
5.22	Fibre content vs time for 90% consolidation (t_{90}) plot with various salt permeant concentrations at the consolidation pressure of 784.5 kPa	127
5.23	Void ratio (e) vs consolidation pressure (P) plots for pure BC soil with various salt permeant concentrations	130
5.24	Void ratio (e) vs consolidation pressure (P) plots for 5% fibre-mixed BC soil with various salt permeant concentrations	130
5.25	Void ratio (e) vs consolidation pressure (P) plots for 10% fibre-mixed BC soil with various salt permeant concentrations	131
5.26	Void ratio (e) vs consolidation pressure (P) plots for 15% fibre-mixed BC soil with various salt permeant concentrations	131
5.27	Compression index (C_c) of fibre-mixed BC soil with various salt permeant concentrations	132
5.28	Hydraulic conductivity vs void ratio plots for pure BC soil with various salt permeant concentrations	136
5.29	Hydraulic conductivity vs void ratio plots for 5% fibre-mixed BC soil with various salt permeant concentrations	137
5.30	Hydraulic conductivity vs void ratio plots for 10% fibre-mixed BC soil with various salt permeant concentrations	137
5.31	Hydraulic conductivity vs void ratio plots for 15% fibre-mixed BC soil with various salt permeant concentrations	138
5.32	Fibre content vs Hydraulic conductivity plots for fibre-mixed BC soil with various salt permeant concentrations at the void ratio of 0.75	138
5.33	FESEM images of BC soil with various salt permeant concentrations after completion of consolidation tests	139
5.34	Axial stress vs axial strain curves for pure BC soil with various salt permeant concentrations	141
5.35	Axial stress vs axial strain curves for 5% fibre-mixed BC soil with various salt permeant concentrations	141
5.36	Axial stress vs axial strain curves for 10% fibre-mixed BC soil with various salt permeant concentrations	142
5.37	Axial stress vs axial strain curves for 15% fibre-mixed BC soil with various salt permeant concentrations	142
6.1	Atterberg limits of BC soil with heavy metal solutions	149
6.2	Free swelling index of BC soil with heavy metal solutions	151
6.3	Relationship between liquid limit versus FSI of BC soil	151
6.4a, b,&c	Time vs swelling relationship of pure BC soil with heavy metal permeants	153
6.4d, e,&f	Linear representation of swelling behavior of pure BC soil with RH model permeated with heavy metals	153
6.5a, b,&c	Time vs swelling relationship of 5 % fibre-mixed BC soil with heavy metal permeants	154
6.5d, e,&f	Linear representation of swelling behaviour of 5% fibre-mixed BC soil with RH model permeated with heavy metals	154

TH-3665_186104109

6.6a, b,&c	Time vs swelling relationship of 10 % fibre-mixed BC soil with heavy metal permeantscondition	155
6.6d, e,&f	Linear representation of swelling behaviour of 10% fibre-mixed BC soil with RH model permeated with heavy metals	155
6.7a, b,&c	Time vs swelling relationship of 15 % fibre-mixed BC soil with heavy metal permeantscondition	156
6.7d, e,&f	Linear representation of swelling behaviour of 15% fibre-mixed BC soil with RH model permeated with heavy metals	156
6.8	Correlation between measured swell vs predicted swell of all fibre-mixed samples under various heavy metal permeant concentrations	170
6.9	Coefficient of consolidation vs consolidation pressure plots of BC soil with heavy metal permeants	172
6.10	Coefficient of consolidation vs consolidation pressure plots of 5% fibre-mixed BC soil with heavy metal permeants	173
6.11	Coefficient of consolidation vs consolidation pressure plots of 15% fibre-mixed BC soil with heavy metal permeants	174
6.12	Coefficient of consolidation vs consolidation pressure plots of 15% fibre-mixed BC soil with heavy metal permeants	175
6.13	Fibre content vs coefficient of consolidation (c_v) plot with various heavy metal permeant concentrations at the consolidation pressure of 784.5 kPa	176
6.14	Time taken for 90% consolidation vs consolidation pressure plots of BC soil with heavy metal permeants	178
6.15	Time taken for 90% consolidation vs consolidation pressure plots of 5% fibre-mixed BC soil with heavy metal permeants	179
6.16	Time taken for 90% consolidation vs consolidation pressure plots of 10% fibre-mixed BC soil with heavy metal permeants	180
6.17	Time taken for 90% consolidation vs consolidation pressure plots of 15% fibre-mixed BC soil with heavy metal permeants	181
6.18	Fibre content vs time for 90% consolidation (t_{90}) plot with various heavy metal permeant concentrations at the consolidation pressure of 784.5 kPa.	182
6.19	Void ratio (e) vs consolidation pressure plots for pure BC soil with various heavy metal permeant concentrations	184
6.20	Void ratio (e) vs consolidation pressure plots for 5% fibre-mixed BC soil with various heavy metal permeant concentrations	185
6.21	Void ratio (e) vs consolidation pressure plots for 10% fibre-mixed BC soil with various heavy metal permeant concentrations	186
6.22	Void ratio (e) vs consolidation pressure plots for 15% fibre-mixed BC soil with various heavy metal permeant concentrations	187
6.23	Compression index (C_c) of fibre-mixed BC soil with various salt permeant concentrations	188
6.24	Hydraulic conductivity (k) vs void ratio plots for pure BC soil with various heavy metal permeant concentrations	194
6.25	Hydraulic conductivity (k) vs void ratio plots for 5% fibre-mixed BC soil with various heavy metal permeant concentrations	195
6.26	Hydraulic conductivity (k) vs void ratio plots for 10% fibre-mixed BC soil with various heavy metal permeant concentrations	196
6.27	Hydraulic conductivity (k) vs void ratio plots for 15% fibre-mixed BC soil with various heavy metal permeant concentrations	197

TH-3665_186104109

6.28	FESEM images of BC soil with lead permeant concentrations	199
6.29	FESEM images of BC soil with cadmium permeant concentrations	200
6.30	FESEM images of BC soil with hexavalent chromium permeant concentrations	201
6.31	Axial stress vs axial strain curves for pure BC soil with various heavy metal permeant concentrations	204
6.32	Axial stress vs axial strain curves for 5% fibre-mixed BC soil with various heavy metal permeant concentrations	205
6.33	Axial stress vs axial strain curves for 10% fibre-mixed BC soil with various heavy metal permeant concentrations	206
6.34	Axial stress vs axial strain curves for 15% fibre-mixed BC soil with various heavy metal permeant concentrations	207
7.1	Atterberg limits of BC soil with synthetic leachates	214
7.2	Free swell index of BC soil with synthetic leachates	215
7.3	Time-swell plot of pure BC soil under synthetic leachates' permeations	217
7.4	Time-swell plot of 5% fibre-mixed BC soil under synthetic leachates' permeations	218
7.5	Time-swell plot of 10% fibre-mixed BC soil under synthetic leachates' permeations	218
7.6	Time-swell plot of 15% fibre-mixed BC soil under synthetic leachates' permeations	219
7.7	Linearized representation of swelling data for BC soil with RH model permeated with leachates	219
7.8	Linearized representation of swelling data for 5% fibre-mixed BC soil with RH model permeated with leachates	220
7.9	Linearized representation of swelling data for 10% fibre-mixed BC soil with RH model permeated with leachates	220
7.10	Linearized representation of swelling data for 15% fibre-mixed BC soil with RH model permeated with leachates	221
7.11	Correlation between measured swell vs observed swell of all fibre-mixed BC soils under permeation of leachates	221
7.12	Consolidation pressure vs coefficient of consolidation (c_v) plots for pure BC soil under permeation of synthetic leachates	228
7.13	Consolidation pressure vs coefficient of consolidation (c_v) plots for 5% fibre-mixed BC soil under permeation of synthetic leachates	228
7.14	Consolidation pressure vs coefficient of consolidation (c_v) plots for 10% fibre-mixed BC soil under permeation of synthetic leachates	229
7.15	Consolidation pressure vs coefficient of consolidation (c_v) plots for 15% fibre-mixed BC soil under permeation of synthetic leachates	229
7.16	Fibre content vs coefficient of consolidation plot with synthetic leachate permeants at the consolidation pressure of 784.5 kPa	230
7.17	Consolidation pressure vs time for 90% consolidation (t_{90}) plots for pure BC soil under permeation of synthetic leachates	231
7.18	Consolidation pressure vs time for 90% consolidation (t_{90}) plots for 5% fibre-mixed BC soil under permeation of synthetic leachates	231
7.19	Consolidation pressure vs time for 90% consolidation (t_{90}) plots for 10% fibre-mixed BC soil under permeation of synthetic leachates	232
7.20	Consolidation pressure vs time for 90% consolidation (t_{90}) plots for 15% fibre-mixed BC soil under permeation of synthetic leachates	232

TH-3665_186104109

7.21	Fibre content vs time for 90% consolidation plot with synthetic leachate permeants at the consolidation pressure of 784.5 kPa	233
7.22	Void ratio (*e*) vs consolidation pressure plots for pure BC soil under permeation of synthetic leachates	235
7.23	Void ratio (*e*) vs consolidation pressure plots for 5% fibre-mixed BC soil under permeation of synthetic leachates	235
7.24	Void ratio (*e*) vs consolidation pressure plots for 10% fibre-mixed BC soil under permeation of synthetic leachates	236
7.25	Void ratio (*e*) vs consolidation pressure plots for 15% fibre-mixed BC soil under permeation of synthetic leachates	236
7.26	Compression index (C_c) of fibre-mixed BC soil under permeation of synthetic leachates	237
7.27	Hydraulic conductivity (*k*) vs void ratio plots for pure BC soil under permeation of synthetic leachates	241
7.28	Hydraulic conductivity (*k*) vs void ratio plots for 5% fibre-mixed BC soil under permeation of synthetic leachates	241
7.29	Hydraulic conductivity (*k*) vs void ratio plots for 10% fibre-mixed BC soil under permeation of synthetic leachates	242
7.30	Hydraulic conductivity (*k*) vs void ratio plots for 15% fibre-mixed BC soil under permeation of synthetic leachates	242
7.31	Fibre content vs hydraulic conductivity plots for fibre-mixed BC soil with synthetic leachate permeants cat the void ratio of 0.75	243
7.32	FESEM image of BC soil after permeation of synthetic MSW leachate	243
7.33	FESEM image of BC soil after permeation of synthetic fly ash leachate	244
7.34	Axial stress vs axial strain behaviour of BC soil with synthetic leachates	245
7.35	Axial stress vs axial strain behaviour of 5% fibre-mixed BC soil with synthetic leachates	245
7.36	Axial stress vs axial strain behaviour of 10% fibre-mixed BC soil with synthetic leachates	246
7.37	Axial stress vs axial strain behaviour of 10% fibre-mixed BC soil with synthetic leachates	246
7.38	Peak strength values of fibre-mixed BC soil with synthetic leachates	247

TH-3665_186104109

LIST OF TABLES

Table No.	Caption	Page No.
2.1	Classification of expansive soil based on the liquid limit	15
2.2	Differential free swell IS: 2720 (Part 40) 1977	15
2.3	Expansive soil classification based on the free swell ratio	16
2.4	Summary of clay -tire fibre mix literature	35
2.5	Summary of literature on salt solutions' interaction with clay	48
2.6	Summary of literature on heavy metals' interaction with clay	55
2.7	Summary of literature on leachates' interaction with clay	58
3.1	Properties of BC soil used in this study	66
3.2	XRF result of BC soil	67
3.3	Elemental analysis of single tire fibre	69
3.4	Composition of synthetic MSW leachate	72
3.5	Composition of synthetic fly ash leachate	72
4.1	Time and percent swells of fibre-mixed BC soil with DI water	86
4.2	Swelling pressures and swelling potentials fibre-mixed BC soil with DI water	87
4.3	Predicted swelling potentials (RH model) vs measured swelling potential values	89
4.4	Peak strength and peak strain values of fibre-mixed BC soil with DI water	98
5.1	Time and percent swells of pure BC soil with various salt permeant concentrations	113
5.2	Time and percent swell of 5% fibre-mixed BC soil with various salt permeant concentrations	113
5.3	Time and percent swells of 10% fibre-mixed BC soil with various salt permeant concentrations	114
5.4	Time and percent swells of 15% fibre-mixed BC soil with various salt permeant concentrations	114
5.5	Swelling pressures of fibre-mixed BC soil with various salt permeant concentrations	117
5.6	Swelling potentials of fibre-mixed BC soil with various salt permeant concentrations	117
5.7	Predicted swelling potentials (RH model) vs measured swelling potential values of fibre-mixed samples under various salt permeant concentrations	118
5.8	Hydraulic conductivity vs consolidation pressure values for pure BC soil with various salt permeant concentrations	134
5.9	Hydraulic conductivity vs consolidation pressure values for 5% fibre-mixed BC soil with various salt permeant concentrations	135
5.10	Hydraulic conductivity vs consolidation pressure values for 10% fibre-mixed BC soil with various salt permeant concentrations	135
5.11	Hydraulic conductivity vs consolidation pressure values for 15% fibre-mixed BC soil with various salt permeant concentrations	136

TH-3665_186104109

5.12	Peak strength values of fibre-mixed BC soil with various salt permeant concentrations	143
5.13	Peak strain values of fibre-mixed BC soil with various salt permeant concentrations	143
6.1	Time and percent swells of pure BC soil with various heavy metal permeant concentrations	159
6.2	Time and percent swells of 5% fibre-mixed BC soil with various heavy metal permeant concentrations	160
6.3	Time and percent swells of 10% fibre-mixed BC soil with various heavy metal permeant concentrations	161
6.4	Time and percent swells of 15% fibre-mixed BC soil with various heavy metal permeant concentrations	162
6.5	Swelling pressures of fibre-mixed BC soil with various salt permeant concentrations	164
6.6	Swelling potentials of fibre-mixed BC soil with various heavy metal permeant concentrations	165
6.7	Predicted swelling potentials (RH model) vs measured swelling potential values of BC soil samples under various heavy metal permeant concentrations	166
6.8	Predicted swelling potentials (RH model) vs measured swelling potential values of 5% fibre-mixed BC soil samples under various heavy metal permeant concentrations	167
6.9	Predicted swelling potentials (RH model) vs measured swelling potential values of 10% fibre-mixed BC soil samples under various heavy metal permeant concentrations	168
6.10	Predicted swelling potentials (RH model) vs measured swelling potential values of 15% fibre-mixed BC soil samples under various heavy metal permeant concentrations	169
6.11	Hydraulic conductivity vs consolidation pressure values for fibre-mixed BC soil samples with various heavy metal permeant concentrations	191
6.12	Hydraulic conductivity values of fibre-mixed BC soil (at e = 0.75) under various heavy metal permeants	198
6.13	Peak strength values of fibre-mixed BC soil with various heavy metal concentrations	208
6.14	Peak strain values of fibre-mixed BC soil with various heavy metal concentrations	209
7.1	Time vs swelling percentage relationship of fibre-mixed BC soil with synthetic leachates	222
7.2	Predicted swelling potentials (RH model) vs measured swelling potential values of fibre-mixed BC soil samples under permeation of leachates	225
7.3	Swelling pressures and swelling potentials of fibre-mixed BC soil with synthetic leachates	226
7.4	Hydraulic conductivity vs consolidation pressure values for fibre-mixed BC soil with synthetic leachate permeants	240

TH-3665_186104109

LIST OF ABBREVIATIONS

L	Litre
mL	Millilitre
mg	Milligram
ppm	Parts per million
MSW	Municipal Solid Waste
BC soil	Black Cotton soil
TF	Tire Fibre
MDD	Maximum Dry Density
OMC	Optimum Moisture Content
DDL	Diffuse Double Layer
CEC	Cation Exchange Capacity
IS	Indian Standards
ASTM	American Society for Testing and Materials
GCL	Geosynthetic Clay Liner
UCS	Unconfined Compressive Strength
USEPA	United States Environmental Protection Agency
FESEM	Field emission scanning electron microscopy
XRD	X-ray diffraction
FTIR	Fourier Transform Infrared
TGA	Thermogravimetric Analysis
EDX	Energy Dispersive X-ray
XRF	X-ray Fluorescence
FSI	Free Swell Index
DI water	De-ionized water
USCS	Unified Soil Classification System
SML	Synthetic MSW Leachate
SFL	Synthetic Fly ash Leachate
LL	Liquid Limit
PL	Plastic Limit
PI	Plasticity Index
SPo	Swelling Potential
SPr	Swelling Pressure

TH-3665_186104109

SYMBOLS USED

k	Hydraulic conductivity
γ_d	Dry density
m_v	Coefficient of volume change
c_v	Coefficient of consolidation
t_{90}	Time for 90% of consolidation
C_c	Compression index
e	Void raio
ΔP	Change in pressure
Δe	Change in void ratio
T_v	Time factor
γ_w	Unit weight of the pore fluid
G_s	Specific gravity of soil solid particles
N	Normality
M	Molarity
P	Pressure
σ_1	Major principal stress

TH-3665_186104109

CHAPTER 1

INTRODUCTION

1.1. General

The rapid population growth and fast industrialization has led to generation of a massive amount of municipal solid waste (MSW) across the globe. The generation of MSW was about 2.01 billion tonnes per year in 2016 and is expected to increase by about 3.4 billion tonnes per year in 2050 (Malav et al., 2020). This vast amount of MSW generation causes major environmental problems, especially in developing countries like India. Landfilling is the most reliable technique to dispose of MSW and is followed by many countries, such as the USA, Canada, Japan and many European countries (Qian et al., 2002; Agamuthu, 2013). Clay liners play a vital role in a landfill systems, which are provided to restrict the migration of leachate into the groundwater (Rubinos and Spagnoli, 2018). The high swelling tendency, low hydraulic conductivity ($<10^{-7}$ cm/s), and tolerable shear strength (>200 kPa) are the critical parameters of clay liners to prevent the migration of leachate to the groundwater (USEPA, 1988; Benson et al., 1999). Expansive clays are associated with excessive swelling and low hydraulic conductivity characteristics, rendering them unsuitable for civil engineering applications such as buildings, pavements, and foundations (Mishra et al., 2008). In contrast, these characteristics of expansive clays are more beneficial for geoenvironmental applications such as landfill liners, backfills at nuclear repository sites, cutoff walls, and drilling fluids, which would be effective in preventing the harmful contamination of groundwater due to the migration of leachate (Sharma and Reddy, 2004; Narani et al., 2020).

Usually, bentonite clays (rich in montmorillonite) are typically employed as a liner material because of their high adsorption and swelling capacity, low hydraulic conductivity (k), and adequate shear strength properties (Dutta and Mishra, 2015; Narani et al., 2020; Ray et al., 2021(a)). However, bentonite is not a locally available material, and it needs to be imported from the places where it is produced (Sivapullaiah and Baig, 2011). Bentonite is susceptible to shrinkage when it dries, which leads to an increase in hydraulic conductivity and a reduction in the shear strength. Past studies (Taheri et al., 2018; Nasab and Keykha, 2020; Mukherjee and Mishra, 2021) have shown that the shrinkage behaviour of the bentonite can be reduced by addition of sand to the bentonite. As sands are also scarce and costly in India

TH-3665_186104109

(Gupt et al., 2021); hence, finding an efficient and economical material for clay liners instead of bentonites and sand bentonite mixtures in landfills is necessitous.

Black cotton (BC) soils are expansive clays that are naturally abundant in India and occupy roughly 20×10^4 square miles of land, which is almost 20% of India's entire land mass (Babu et al., 2008). These soils fall into the smectite category and are widely distributed throughout the southern (states of Andhra Pradesh, Karnataka, Telangana, and Tamilnadu), central (states of Madya Pradesh and Maharashtra), western (states of Rajasthan and Gujarat), and northern (states of Uttar Pradesh) regions of India (Kumar et al., 2007; Srivastava et al., 2014). These smectite group soils are rich in montmorillonite mineral, which leads to the formation of the diffuse double layer (DDL) when it comes in contact with water, resulting in swelling and low hydraulic conductivity (k) values (Madsen and Vonmoos, 1989; Dutta and Mishra, 2016(a)). Due to its high swelling and low permeability characterstics, the BC soil can be considered as an alternate material to replace bentonite as a landfill liner material.

Similar to bentonite, the shrinkage behaviour of expansive BC soil leads to desiccation cracking and can weaken its usability as a liner material (Rayhani et al., 2008). Past literature has revealed that fibre reinforcement is a better approach to controlling the cracking potential of expansive soil. Many researchers examined the influence of polypropylene and polyester fibres on the desiccation behaviour of clayey soils for landfill application (Harianto et al., 2008; Tang et al., 2012; Divya et al., 2014; Chaduvula et al., 2017) and observed a significant reduction in crack width, length, and connectivity networks at the optimum percentage of fibre content. However, due to the high cost of conventional fibres, the overall cost of the liner may rise significantly (Mukherjee and Mishra, 2019a) due to the inclusion of fibres. Therefore, it is desirable to research a new reinforcing material which is innovative, cost-effective, and capable of enhancing the engineering behaviour of liners.

A large number of waste tires have been produced worldwide due to the increasing demand for automobiles. It is predicted that 1.2 billion units of waste tires will be generated annually by 2030 (Arulrajah et al., 2019; Narani et al., 2020). These waste tyres pose significant challenges to the environment as illegal burning can release some toxic gases, such as benzene, styrene, butadiene, hydrocarbons, SO_2, CO, NO, etc. (Liu et al., 2020), and particulate matter impacting the air quality. Therefore, the efficient way to deal with the

TH-3665_186104109

generation of waste tire rubber is re-utilization. Many researchers have used these waste tire rubbers in numerous geotechnical and geoenvironmental applications (Cetin et al., 2006; Seda et al., 2007; Trouzine et al., 2012; Srivastava et al., 2014; Yadav and Tiwari, 2017; Chegenizadeh et al., 2018; Soltani et al., 2019; Mistry et al.,2020; Akbarimehr et al., 2021; Haq et al., 2024). Notably, few researchers (Cokca and Yilmaz, 2004; Narani et al., 2020; Mukherjee and Mishra, 2021) in the past have primarily focused on the utilization of these waste tires by incorporating them into bentonite mixtures for landfill liner application and found a significant reduction in shrinkage behaviour of liner material. Although most of the past research has focused much on using bentonite-tire and bentonite-sand-tire mixtures for liner application, no detailed study has been conducted on the use of BC soil-tire fibre composition as landfill liners in barrier applications.

The waste which is disposed of in landfills gets decomposed with time and produces toxic chemicals known as leachates. Leachate generation is a critical environmental issue, particularly in the context of waste management, as it involves the production of liquid that percolates through solid waste in landfills and extracts dissolved or suspended contaminants. These leachates generally consist of inorganic chemicals (such as Na^{+} and Ca^{2+}) (Kjeldsen et al., 2002; Tatsi and Zouboulis, 2002), heavy metals (such as Pb(II), Cd(II), Cr(VI)) and organic chemicals (alcohols and acids) (Mishra et al., 2005; Li and Li, 2001; Li et al., 2007; Chalermyanont et al., 2009; Dutta and Mishra, 2016(b); Ray et al., 2021(b)). When these chemicals come in contact with the liner material, the properties of the liner material, such as swelling and hydraulic conductivity, get affected significantly due to a reduction in the diffuse double layer (DDL) thickness (Shackelford et al., 2000; Shariatmadari et al., 2011; Dutta and Mishra, 2016(a); Jadda and Bag, 2020; He et al., 2021). Hence, it is imperative to investigate the behaviour of barrier material in the presence of various chemicals present in the leachate.

Many studies (Shackelford et al., 2000; Mishra et al., 2009; Shariatmadari et al., 2011; Zhu et al., 2013; Dutta and Mishra, 2015; Dutta and Mishra, 2016(b); Xu et al., 2018; Chai and Fu, 2020; Jadda and Bag, 2020; Gupt et al., 2020; He et al., 2021; Ray et al., 2022(b); Namadi et al., 2023) have been conducted in the past to investigate the effect of inorganic salts, heavy metals, and leachates on the hydraulic, swelling, and adsorption behaviour of bentonites, sand-bentonite composites, and soil-bentonite mixtures. These studies have shown that the

TH-3665_186104109

swelling and hydraulic conductivity of liner material are affected significantly due to the permeation of these chemicals.

Since, the BC soil and tire fibre composite might act as a replacement of bentonite and as a liner material, it is quite essential to investigate the impact of various contaminants present in the leachate on the swelling and hydraulic conductivity behaviour on BC soil and tire fibre composite. However, so far, no study has been carried out to investigate these behaviours in the presence of the contaminants present in the leachate. Therefore, it is essential to determine the impact of various chemicals, such as inorganic salts, heavy metals, and leachates, on the hydromechanical characteristics of fibre-mixed BC soils. The compressibility of the liner material is also a critical property which aids in the assessment of its settlement as a result of the overburdened weight of waste at the waste disposal site (Mishra et al., 2010). Since the consolidation parameters, such as compression index (C_c), coefficient of consolidation (c_v), and duration to complete 90% of the consolidation (t_{90}), give an overview of the compressibility characteristic of soil, studying these parameters has garnered significant attention among researchers due to their significance in the compressibility behaviour. Therefore, it is essential to study the consolidation behaviour of BC soil under the impact of waste tire fibre in detail. Also, it is crucial to study the influence of various chemicals on the consolidation behaviour of tire fibre-mixed BC soil.

1.2. Outline of the thesis

The thesis is divided into eight chapters, with brief summaries of each chapter provided below:

Chapter 1 provides an explanation of the issue statement's introduction as well as the importance of its resolution. It also gives a chapter plan that covers the complete thesis organization.

Chapter 2 describes the research background and thoroughly analyses the literature on the suitability of expansive soils for geoenvironmental applications, fibre-clay interaction, and clay-leachate interaction. In this chapter, the study's objectives and importance are also discussed.

TH-3665_186104109

Chapter 3 provides the materials used and methodologies followed to meet the specific research objectives. The basic properties of different materials are also included in this chapter.

Chapter 4 examines the influence of tire fibres on the engineering properties such as compaction, swelling, consolidation, compressibility, hydraulic conductivity and shear strength of black cotton soil.

Chapter 5 investigates the effect of inorganic salt permeants on index properties such as the free swell index and Atterberg limits of BC soil and engineering properties such as swelling, consolidation, hydraulic conductivity, compressibility, and shear strength of fibre-mixed black cotton soil.

Chapter 6 presents the influence of heavy metal permeants (Pb(II), Cd(II), Cr(VI)) ranging from 100 to 1000 ppm on index properties of BC soil and engineering properties like swelling (swell pressures and swell potentials), consolidation parameters (time for 90% consolidation and coefficient of consolidation) void ratio-pressure relationships, and shear strength of fibre-mixed black cotton soil.

Chapter 7 provides information on the impact of synthetic municipal solid waste and fly ash leachates on free swelling, Atterberg limits of BC soil, and the engineering behaviour of fibre-mixed black cotton soil.

Chapter 8 summarises the concluding remarks and limitations of the present study. Also, the future scope of this present work has been reported in this chapter.

TH-3665_186104109

CHAPTER 2

BACKGROUND AND LITERATURE SURVEY

2.1. General

Clay liner functions as an impermeable barrier between leachate and groundwater in landfills. Expansive soils are commonly used as barrier materials due to their high swelling capacity and low hydraulic conductivity, which effectively mitigate the risk of groundwater contamination by restricting pollutant migration. Expansive soils have the ability to form a diffuse double layer (DDL) with water, resulting in high swelling capacities and low hydraulic conductivities (Olson and Mesri, 1970). The liner's potential is threatened by two issues: shrinkage cracks and chemical attacks. It is crucial to take these issues into account when evaluating the potential liner material. Therefore, this chapter presents a detailed analysis of the research application background and relevant published literature, identifying gaps in the existing research knowledge and shaping the framework for the study's design.

2.2. Waste management and disposal

In today's world, urbanization and industrialization have led to the generation of vast amounts of waste, which significantly pollutes the geo-environment and groundwater. The volume of waste produced by both developed and developing countries continues to rise due to increasing resource consumption and higher living standards. In recent years, the rapid growth in urban waste production has become a pressing global issue. It is estimated that approximately 4 billion tonnes of waste are generated worldwide each year, with this figure steadily increasing. Global municipal solid waste (MSW) is expected to grow from 1.3 billion tonnes in 2010 to 2.2 billion tonnes in 2025, according to Hoornweg and Bhada (2012). Landfilling is an acceptable and recommended approach for MSW dumping in many countries around the world (Rowe et al., 1997). While incineration, recycling, and composting have contributed more and more to the management of solid waste in Western communities over the last few decades, waste disposal in landfills (or landfilling) continues to be a common form of managing waste worldwide (Rubinos and Spagnoli 2018). Most developed nations also depend on landfilling as a vital part of solid waste management infrastructure, including many EU countries and the USA (Agamuthu 2013).

TH-3665_186104109

Waste materials are primarily classified into municipal solid waste (MSW) and industrial waste. Industrial waste comprises a variety of products, including incinerated wastes, sewage, waste oils, acids, alkalis, plastics, textiles, paper, organic residues, solid animal remains, metal scraps, concrete, ceramics, slag, refuse, animal excreta, ash, and carcasses. Conversely, MSW denotes non-industrial garbage, predominantly generated by households and encompassing waste from commercial enterprises such as offices and restaurants. Specific categories of garbage, including explosive, toxic, or infectious materials, are designated as "specially controlled municipal solid waste" or "specially controlled industrial waste." These are governed by rigorous restrictions during the processing and disposal stages to reduce dangers to human health and the environment.

In affluent nations, the per capita trash generation ranges from 0.4 to 1.1 kg daily, with certain urban areas surpassing 2.4 kg per day and even greater amounts in tourist destinations. These statistics underscore the urgent necessity for efficient waste management techniques to tackle the escalating difficulties of trash generation and disposal. Globally, the production of municipal solid waste (MSW) is estimated to range between 1.7 and 1.9 billion metric tonnes (UNEP, 2010). In the United States alone, approximately 258 million tonnes of MSW were generated in 2014. Out of this, over 89 million tonnes were recycled or composted, about 33 million tonnes underwent energy recovery through combustion, and more than 136 million tonnes, exceeding 50%, were disposed of in landfills (UNEP, 2010; Rubinos and Spagnoli, 2018). India, as reported by the Central Pollution Control Board in 2016, produces around 52 million tonnes of waste annually, equating to roughly 0.144 million tonnes daily. Research consistently indicates that using landfill liners is an effective approach for the safe disposal of municipal solid waste.

2.3. Landfill liner

The design of waste disposal facilities typically includes a barrier to separate the waste from groundwater, aiming to minimize pollutant migration and reduce environmental impacts. The effectiveness of such facilities is directly tied to their design and long-term performance. Commonly, compacted clay liners and composite liner systems incorporating geomembranes are employed for this purpose (Fig. 2.1. b & c). Landfilling, as an engineered method for municipal solid waste (MSW) disposal, ensures minimal environmental hazards by safely confining waste.

TH-3665_186104109

A landfill liner is a substantial barrier made from compacted natural clay or synthetic materials such as geomembranes or geosynthetic clay liners. Its primary function is to prevent leachate from contaminating groundwater by controlling its movement. The cross-section of a typical waste disposal site is shown in Fig. 2.1(a). Clay liners are frequently used due to their low hydraulic conductivity and strong adsorption capacity, which effectively limit the transportation of contaminants and reduce the risk of groundwater pollution.

Liners are essential for two primary reasons. First, if the natural soil consists of fractured clay, a liner is necessary to prevent contaminants from travelling through these fractures. Second, when the surrounding natural soil lacks sufficiently low hydraulic conductivity to serve as an effective barrier, a liner must be installed. In cases where the initial design does not provide adequate assurance of minimal groundwater contamination, additional engineering measures, such as a secondary leachate collection system or a hydraulic control layer, may be implemented to enhance protection.

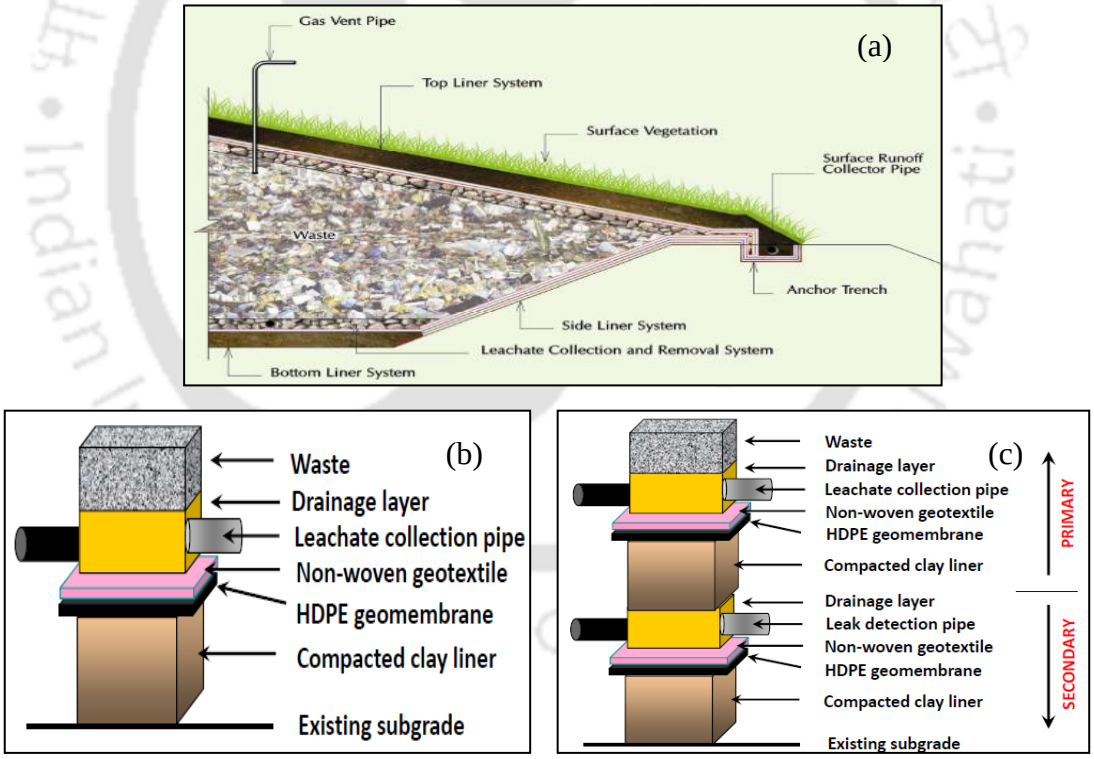

Fig. 2.1 Typical liner systems: (a) Typical cross-section of the landfill; (b) Single composite liner system; (c) Double composite liner system (Hughes et al. 2007).

2.4. Landfill design approaches in various countries

The writing of the Council Directive on the landfill of waste was initiated by the European Commission in the late 1980s. In 1999, the directive was ultimately agreed upon, proposing

TH-3665_186104109

that landfill liners should meet at least one of the hydraulic conductivity and thickness requirements to safeguard soil, groundwater, and surface water.

Landfill for inert waste:

Hydraulic conductivity (k) < $1x10^{-7}$ m/sec; thickness > 1m

Landfill for non-hazardous waste:

Hydraulic conductivity (k) < $1x10^{-9}$ m/sec; thickness > 1m

Landfill for hazardous waste:

Hydraulic conductivity (k) < $1x10^{-9}$ m/sec; thickness > 5m

In Fig. 2.2 and 2.3, the mineral barrier thickness and hydraulic conductivity parameters utilized in liners are observed to vary across countries. For the United States and the United Kingdom, the barrier's thickness should be less than 0.6 m and 1 m, respectively, and the hydraulic conductivity (k) should be less than 10^{-9} m/sec. k should be less than 10^{-9} m/sec, and the barrier thickness should be less than 5 m for Japan.

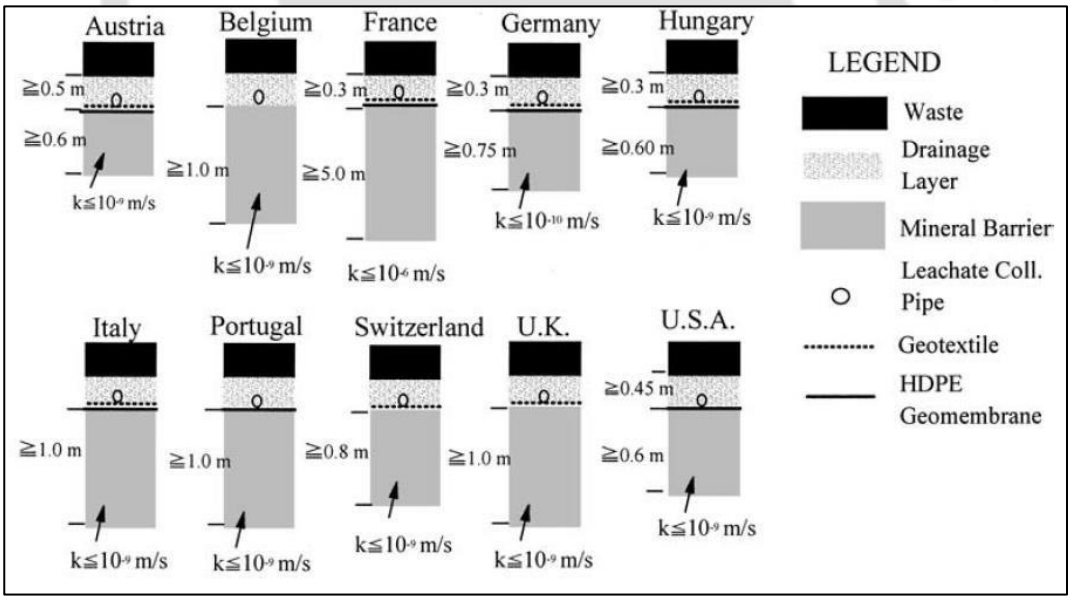

Fig. 2.2. Liner systems specified in Europe and America (Chai and Miura 2002).

TH-3665_186104109

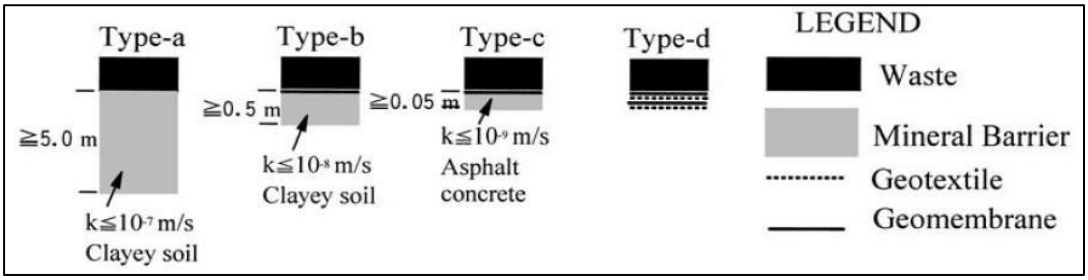

Fig. 2.3. Japanese liner systems (Chai and Miura 2002).

2.5. Key design parameters for landfill liners

2.5.1. Hydraulic conductivity

The hydraulic conductivity of the soil is a critical requirement that must be met for it to be used as a liner or cover material in a landfill. Many environmental agencies and researchers (USEPA 1988; Koerner and Daniel 1997; Hauser et al. 2001) have suggested that the landfill liner and cover material should have at least a hydraulic conductivity value of 10^{-9} m/sec and 10^{-7} m/sec or less, respectively. Mitchell and Jaber (1990) reported that the amount of moisture and dry density impacts the ability of soil to limit flow transmission. The soil particles are distributed in a scattered pattern, resulting in the lowest hydraulic conductivity values (k) when the placement conditions have a high dry density and a damp of optimum moisture content. In contrast, a dry compaction side develops a flocculated pattern, which results in enhanced water flow paths and a higher k. Clods and macropores are broken up, and the clay can be rapidly remoulded on the wet optimum side. The total hydraulic conductivity is also limited due to the minimal hydraulic conductivity of clay micropores.

2.5.2. Settlement

Settlement is a critical factor, which influences the performance of final covers. As per, Koerner and Daniel (1997), all solid waste settles over time, resulting in the subsidence of the upper surface and the engineered cover. In order to guarantee the final cover's long-term stability and efficacy, it is imperative to obtain precise design estimates of differential and total settlement. The cover material is typically supported by a soil foundation layer that is laid over the solid waste mass. The final grade of the soil foundation layer is adjusted to account for the anticipated settlement after placement. Typically, landfill liners and covers are constructed using synthetic materials (geomembranes, geonets, geotextiles, etc.) in conjunction with clayey soils. The long-term performance of the landfill system may be

TH-3665_186104109

compromised by the excessive deformation and cracking of the cover that may result from the non-uniform deposition of waste materials in landfills. The discharge of leachate into the surrounding soil/groundwater system may be the result of differential settlement of compacted clay liners, which is caused by compaction over weak ground or over soft spots in an underlying drainage layer (Maher and Ho, 1994). In addition, Scalia et al. (2017) conducted an investigation into the differential settlement of the barrier system after 14 years of service and discovered a substantial total differential settlement of barrier soil.

2.5.3. Shear strength

In order to preserve the integrity of landfill liners, compacted clay liners (CCLs) must possess sufficient shear strength. Benson and Othman (1993) suggested that the hydraulic barrier should also be physically stable for it to be used as a landfill material, and it should have enough shear strength to prevent sliding on the slope. A minimum unconfined compressive strength of 200 kPa, which was arbitrarily selected for rigid clay, was proposed by Daniel and Wu (1993).

2.5.4. Volumetric shrinkage

In order to achieve low hydraulic conductivity values of compacted soil, clays that are employed as barrier materials are usually placed and compacted at the wet of optimum water content. Therefore, the shrinkage tendency of compacted clay increases parallelly with the increase in moulding water content. Liner desiccation or shrinkage cracking may manifest when they are exposed to the atmosphere during humid weather, which can lead to a significant increase in hydraulic conductivity. The volumetric shrinkage during drying should not exceed 4%, as established by Daniel and Wu (1993) in their study of clayey soil in West Texas.

2.6. Black cotton (BC) soil

2.6.1. General

Expansive soil deposits are present in the arid and semi-arid regions. Around 0.3 million m^2 of India's soil was covered by the expansive soils. These soils originated from the basaltic traps, the ferruginous gneisses, and the schists of central and south-central India (Chen 2012). Black Cotton Soil, a type of expansive soil, is widely available in India and covers approximately 17% of the country's land area. These tropical black clays vary in color, ranging from light grey to dark grey and black. The name "Black Cotton Soil" originates

TH-3665_186104109

from its dark color (Fig. 2.4) and its exceptional suitability for cultivating cotton The names black tropical clay and black cotton soil may both be used mutually (Osinubi 2015). These soils cover more than one-fifth of the area of India and are present in the states of Maharashtra, Gujarat, Utter Pradesh to the south, Rajasthan to the east, Madhya Pradesh to the south and west, and a few areas of Andhra Pradesh, Karnataka, and Tamil Nadu (Kumar et al. 2007). These soils are not only located in India but also in Africa, Ethiopia, Australia, Israel, Jordan, the U.S.A, China, and so on (Babu et al. 2008 and Gobinath et al. 2016). According to Etim et al. (2017), about three percent of the world's land area is covered by black cotton soils. Atahu et al. (2019) mentioned around 40% of the total area in Ethiopia is covered with black cotton soils. The surveys previously mentioned indicated that there is a significant prevalence of black cotton soils worldwide.

Fig. 2.4. Black cotton soil (before and after pulverization).

2.6.2. Problems associated with black cotton soil

Black cotton soils are categorized under the smectite group soils (rich in montmorillonite minerals) and contain high plastic clays, which are responsible for problems in the construction of civil engineering structures (Etim et al., 2017). Montmorillonite is the predominant mineral found in Black Cotton Soils. Its presence causes significant volume changes when transitioning between dry and wet states. High swell pressures are exhibited in a saturated condition, whereas shrinkage occurs in dry conditions (Osinubi, 2015). Montmorillonite clays have 2:1 layers structurally consisting of two tetrahedral sheets with an octahedral sheet between them and allowing isomorphous replacement in the sheets, thereby demonstrating a high degree of exchange cations, hydration, and swelling (Amadi, 2014).

TH-3665_186104109

The swelling phenomenon occurs in the montmorillonite mineral due to the presence of a weak bond between the elements. The swelling can occur in two stages in montmorillonite; those are inner crystalline swelling and outer crystalline swelling, which leads to double-layer repulsion. The expansion of soil depends on several conditions, such as initial compaction conditions, moisture content, and the type of clay minerals and cations present in the soil (Shukla and Parihar, 2016). In subsequent discussions, the montmorillonite mineral will be explained in detail.Weak strength, weak workability, high volumetric uncertainty, and low durability in response to environmental changes are the critical characteristics of Black cotton soils (Amadi, 2014). Due to their volume change behaviour during wet and dry conditions (Chen 2012), BC soil poses a significant challenge for engineering structures like pavements, buildings, earth structures, etc. The presence of montmorillonite minerals in black cotton soils is the reason for moisture variations and volume change behaviour, which results in damage to structures. In the USA only, the damage to civil engineering structures built on expansive soils is nearly about 10 billion dollars annually, and the annual financial loss by expansive soils is more than the loss due to the combination of earthquakes, floods, hurricanes, and tornadoes (Chen 2012, and Jones and Holtz 1973). Due to its lightweight, pavements located over the expansive soils undergo heaving due to swelling and cracking due to shrinkage. Similarly, in the case of buildings like dwelling houses, which transfer the light load to soils also experienced cracks (Fig. 2.5) due to the presence of expansive soils such as black cotton soil. Earth structures like canals, barriers, etc., experienced slope failures and caused severe damage (Mishra et al. 2008) due to the volume change tendencies of these soils. These soils exhibit more significant variation in shear strength, compressibility, and swelling, which results in low bearing capacity values and differential settlement occurrence in the case of foundations (Babu et al. 2008). Awareness of compressibility and permeability is required in several engineering problems concerning seepage, settlement, and structural stability (Mir and Sridharan 2014). Therefore, based on the available literature it can be concluded that these BC soils possess hazardous consequences on all geotechnical applications. Hence, it is essential to focus on identifying the degree of expansiveness of BC soils, and exploring treatment methods to enable their effective use in field applications.

TH-3665_186104109

Fig.2.5. Typical cracks in black soils during the dry season: (a) field condition; (b) pavements; (c) buildings (Atahu et al. 2019).

2.6.3. Identification of expansiveness of black cotton soil

According to Sridharan et al. (2016), the degree of the expansiveness of soils can be identified by the following two methods.

(a) Inferential testing methods (direct and indirect methods)
(b) Mineralogical identification testing methods

Inferential testing methods establish a correlation between the index properties of fine-grained soils and their clay mineralogical composition to estimate swell potential. These methods are categorized into direct and indirect approaches. Indirect methods assess the degree of soil expansiveness using parameters such as liquid limit, plasticity index, shrinkage limit, shrinkage ratio, and particle size distribution. Table 2.1 illustrates an example of expansive soil classification based on liquid limit values and their associated swell potential.

TH-3665_186104109

Table 2.1. Classification of expansive soil based on the liquid limit (Sridharan et al., 2016)

Swell potential	Liquid limit (%)		
	Chen (1965)	IS: 1498 (1970)	Senthanet et al. (1977)
Low	<30	20-35	<50
Medium	30-40	35-50	50-60
High	40-60	50-70	>60
Very high	>60	70-90	-

Direct methods for measuring swell potential are categorized into two main types: oedometer tests and free swell tests. Free swell tests include variations such as free swell value, differential free swell, and free swell ratio. These tests are commonly employed to assess the swelling characteristics of expansive soils due to their simplicity and cost-effectiveness. Among these, the differential free swell test is a standard procedure. According to IS: 2720 (Part III-1980), the test involves using 10 grams of soil, and the free swell index value is calculated using the following formula.

$$\text{DFS}=\frac{(\text{Settled soil volume in water-Settled soil volume in kerosene})}{\text{Settled soil volume in kerosene}}\times 100$$

Kerosene is employed due to its nature as a non-polar liquid, which prevents soil expansion. As per the IS code, the subsequent Table 2.2 illustrates the degree of swelling of the oedometer.

Table 2.2. Differential free swell IS: 2720 (Part 40) 1977

S.No	DFS	Degree of Expansion
1	< 20%	Low
2	20 - 35%	Moderate
3	35 – 50%	High
4	>50%	Very High

TH-3665_186104109

The free swell ratio is the ratio of the equilibrium sediment volume of 10 grammes of soil (passing through a 425-micron sieve) in a 100 ml container of distilled water to its sediment volume in kerosene. The following table shows the swelling potential of soil based on the free swell ratio and oedometer expansion values according to Sridharan and Prakash (2000).

Table 2.3. Expansive soil classification based on the free swell ratio

Free swell value	Oedometer expansion (%)	Clay type	Soil expansivity
<1	<1	Non-swelling	Negiligible
1-1.5	1-5	Mixture of swelling and Non-swelling	Low
1.5-2	5-15	Swelling	Moderate
2-4	15-25	Swelling	High
>4	<1	Swelling	Very high

However, mineralogical testing involves techniques such as X-ray diffraction analysis, differential thermal analysis, chemical analysis, dye adsorption, and scanning electron microscopy (SEM). These methods effectively and accurately identify clay minerals in expansive soils, but they have limitations in characterizing swelling behaviour. According to Sridharan and Keshavamurthy (2016), these methods are not cost-effective and require a high level of expertise for mineral identification. Reddy et al. (2020) concluded that soils exhibiting a high free swell index and liquid limit, combined with the presence of montmorillonite, are inherently expansive. Therefore, it is important to understand the mechanism of montmorillonite in expansive soils.

2.6.4. Structure of montmorillonite

The primary mineralogical components of clay particles are phyllosilicates, and their effective diameter is less than 2 microns. Phyllosilicates consist of a tetrahedral sheet of silica (SiO_2) and an octahedral sheet of aluminum (Al^{3+}) or magnesium (Mg^{2+}) oxides. Montmorillonite is a 2:1 mineral that consists of an octahedral sheet inserted between two silica sheets, as displayed in Fig. 2.6. The silica and gibbsite sheets are arranged in a manner that the ends of the tetrahedra from each silica sheet and one hydroxyl layer of the octahedral sheet form a shared layer. Successive layers of these sheets are held together by van der Waals forces and cations that balance the charge deficiencies within the structure. However,

TH-3665_186104109

van der Waals bonds are relatively weak, allowing water or other polar liquids to easily penetrate between the layers, leading to significant expansion. The lateral dimensions of the mineral range from 1,000 to 50,000 A^0, with a thickness of 10 to 50 A^0.

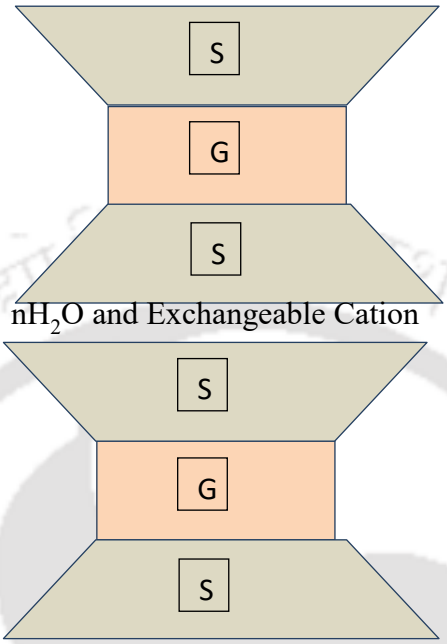

Fig. 2.6. Structure of Montmorillonite.

The layers formed in this structure are continuous along the 'a' and 'b' directions and are stacked vertically along the 'c' direction. Successive layers are held together by weak van der Waals forces and cations that compensate for charge deficiencies within the structure. These weak bonds can be easily disrupted, allowing the layers to separate through the adsorption of water or other polar liquids. The basal spacing in the 'c' direction, denoted as d (001), varies widely, ranging from approximately 0.96 nm (1 nm = 10^{-6} mm) to complete separation.

The principal mineral of BC soil is montmorillonite. A montmorillonite particle in the dry state is reminiscent of a closed book, which is composed of numerous thin crystalline sheets that are bound together by weak van der Waals forces and cations. The crystal structure of each sheet contains charge deficiencies that are neutralised by the presence of cations that are loosely attached to the surface. When the dried montmorillonite clay and water are combined, water is drawn into the montmorillonite particles to hydrate the surface of the elemental sheets and the cations. When sodium montmorillonite and freshwater are combined, the fluid that enters the particles forms dense, viscous diffuse ionic layers around

TH-3665_186104109

the layer, causing the montmorillonite particles to swell, potentially to the point of complete separation of the sheets. However, the salt solutions or high cation concentrations minimize the separation distance between sheets.

2.6.5. Swelling mechanism of expansive black cotton soils

The swelling mechanism of expansive soils which are rich in montmorillonite mineral can take place in two stages which are crystalline swelling and osmotic swelling (Norish and Qurirk, 1954).

2.6.5.1. Inner crystalline swelling

The initial mechanism that occurs when montmorillonite absorbs water is crystalline swelling. This process increases the distance between the unit layers of montmorillonite, leading to an expansion in its volume and the development of swelling pressure. During inner-crystalline swelling, the volume of montmorillonite can double. The polarity of water molecules plays a crucial role in this process. When cations become hydrated, water molecules align their negative dipoles toward the cations, thereby weakening the electrostatic interactions between the negatively charged layers and the interlayer cations. Inner-crystalline swelling, also known as Type I swelling, is a process in which expandable 2:1 phyllosilicates sequentially incorporate one, two, three, or four discrete layers of water molecules (H_2O) into the mineral interlayers (Norrish, 1954). In this process, swelling occurs prior to osmotic swelling (Type II), which is driven by long-range electrical diffuse double-layer interactions. Figures 2.7.a and 2.7.b illustrate the inner-crystalline swelling of sodium montmorillonite. Inner-crystalline swelling involves a balance between the attractive and repulsive forces acting between adjacent interlayer surfaces (Norrish, 1954; Van Olphen, 1965; Kittrick, 1969). The net potential energy of interaction in inner-crystalline swelling is primarily governed by electrostatic attraction between exchangeable cations and the negatively charged basal surfaces of the clay (Laird, 1996, 2006). The positively charged cations act as charge bridges linking adjacent clay layers. Conversely, the hydration energy of the exchangeable cations drives the net repulsive forces. Under unsaturated conditions or saturated conditions with high electrolyte concentrations, net attractive forces dominate. In contrast, under fully saturated conditions with low electrolyte concentrations, net repulsive forces become dominant.

TH-3665_186104109

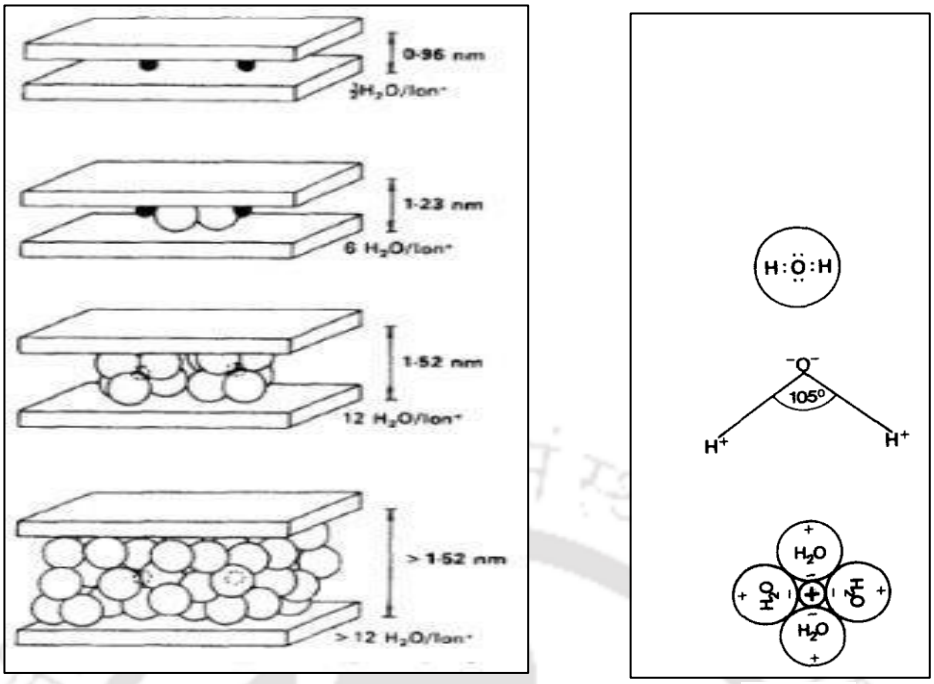

(a) (b)

Fig. 2.7. (a) Inner-crystalline swelling of sodium montmorillonite. Given are the layer distances and the maximum number of water molecules per sodium ion (Kraehenbuehl et al., 1987); **(b)** The structure of water molecule.

2.6.5.2. Osmotic swelling

The osmotic phase of swelling follows the hydration phase but occurs only when the exchange sites contain monovalent cations (Jellander et al., 1988; Mc Bride, 1994; Norrish and Quirk, 1954; Prost et al., 1998). The interlayer region retains numerous layers of water molecules during the osmotic phase. The number of layers of water molecules at equilibrium is proportional to the cation concentration in the bulk water (Norrish, 1954; Onikata et al., 1999; Zhang et al., 1995). Accordingly, when the bulk water contains a low concentration of monovalent cations, and monovalent cations occupy the exchange sites, a larger fraction of the total water is bound, and less mobile water is available for flow resulting in a lower value of hydraulic conductivity. This condition is commonly observed when sodium-montmorillonite are hydrated and/or permeated with DI water (Alther et al., 1985; Gleason et al., 1997; Lutz and Kemper, 1959; Petrov and Rowe, 1997; Ruhl and Daniel, 1997; Shackelford et al., 2000). When polyvalent cations occupy the exchange sites, only the hydration phase occurs. The interlayer expands until it contains four monolayers of water and then expands no further (Jellander et al., 1988; Mc Bride, 1994; Norrish and Quirk, 1954;

TH-3665_186104109

Posner and Quirk, 1964; Prost et al., 1998). There are several explanations for the lack of additional interlayer swelling when polyvalent cations occupy the exchange sites, but consensus does not exist regarding which explanation is correct (Mc Bride, 1994). Nevertheless, the absence of the osmotic phase is well documented experimentally in the literature (Mc Bride, 1994; Norrish and Quirk, 1954; Posner and Quirk, 1964; Prost et al., 1998). Lack of an osmotic phase is evident in the free swelling of calcium-montmorillonite, which typically is about 3 mL/2g even when DI water is the hydrating liquid. In contrast, the free swelling of sodium-montmorillonite typically exceeds 30 mL/2g in dilute monovalent solutions or DI water (Lin and Benson, 2000; Egloffstein, 2020).

In sodium-montmorillonite, the swelling can result in the complete separation of the layers. The driving force for the osmotic swelling is the large difference in concentration between the ions electrostatically held close to the clay surface and the ions in the pore water of the rock (Fig. 2.8.a). Irregularities in the crystal lattice are manifested by an excess negative charge, which must be compensated by positive ions close to the surface of the clay. The concentration of positive ions close to the surface is thus too high, while that of negative ions is very small. The positive ion concentration decreases with increasing distance from the surface, whereas the concentration of negative ions increases. The negatively charged clay surface and the cloud of ions form the diffuse electric double layer (Fig. 2.8.b). A high negative potential exists directly at the surface of the clay layer. The value of this potential is reduced, with increasing distance from the surface and reaches zero in the pore water. When two such negative potential fields overlap, they repel each other and cause the observed swelling in clay. The profile of the potential curves, and therefore the repulsion at a given distance varies with the valence and the radius of the counter-ions in the double layer and with the concentration of electrolytes in the pore water. A transformation of sodium montmorillonite into its calcium form or an increase in the electrolyte concentration in the pore water results in the decrease in the double layer thickness and a reduction in the swelling stress.

TH-3665_186104109

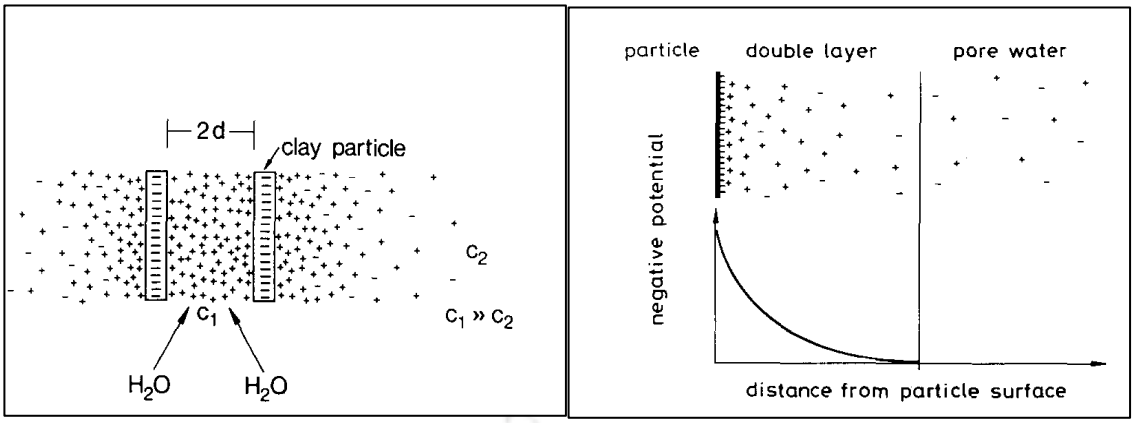

(a) **(b)**

Figure 2.8. (a) Two negatively charged clay layers with ion cloud. The ion concentration C_1 between the layers is much higher than the ion concentration C_2 in the pore water. An equilibration of the concentration can only be reached through the penetration of water into the space between clay layers, since the interlayer cations are fixed electrostatically by the negative charge of the layers (osmotic swelling) (Van Olphen, 1965); **(b)** Negatively charged clay surface, ions in the diffuse double layer and ions in the pore water. The distribution of the negative potential changes with the valence and the radius of the ions in the double layer and with the electrolyte concentration in the pore water.

2.6.6. Diffuse double layer

In dry clay, the negative charge of the particle is balanced by exchangeable cations like Ca+2, Mg+2, Na+, and K+ surrounding the particles being held by electrostatic attraction. Cations in excess of those needed to neutralize the electronegativity of the clay particles and associated anions are present as salt precipitates. When the water is added, the precipitates can go into solution. The interlayer cations within the clay particles, due to the electrostatic attraction of the negatively charged surfaces, pull water molecules because of their hydration energy upon wetting. Highly concentrated cations along the charged surfaces try to diffuse away from the surfaces to equalize concentration throughout the clay water solution. The action of two opposing tendencies leads to specific ion distribution along with the clay particles in the clay water suspension. The concentration of the counterions near the particle surface is high and decreases with an increase in the distance from the surface. The charged surface and the distributed charge in the adjacent phase are together termed as the diffuse

TH-3665_186104109

double layer (DDL). There are various models explaining the phenomenon of diffused double layer, but one of the most widely used was the Gouy-Chapman model.

Gouy (1910)-Chapman (1913) developed a model to explain the variation of potential with respect to distance from the surface of the clay platelet based on certain assumptions, such as the presence of a single exchangeable cation at the clay surface and the particles are assumed to be in the form of parallel plates only. Two studies have been done initially considering only a single clay plate and then by considering the interaction of the clay particles. When only a single clay plate was considered, the potential along the surface was observed to be greater and decreased with an increase in the distance from the surface, which becomes zero when equilibrium, i.e., the bulk solution, is reached. The distance from the surface of the clay plate to the bulk solution is termed as the thickness of the diffuse double layer.

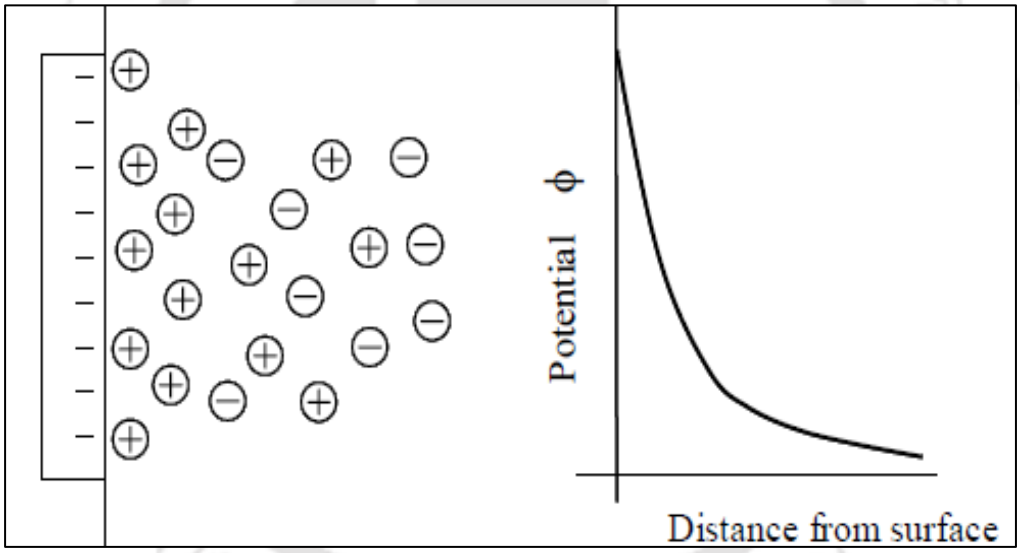

Fig. 2.9. Gouy-Chapman diffuse double layer theory

2.6.6.1. Factors influencing diffuse double layer thickness

The thickness of the diffuse double layer is influenced by factors such as electrolyte concentration, ion valence, dielectric constant, temperature, the size of hydrated ions, pH, and anion adsorption.

- Electrolyte concentration: The thickness of the diffuse double layer varies inversely with the square root of the pore water concentration. An increase in electrolyte concentration lowers the surface potential under constant surface charge conditions,

TH-3665_186104109

causing the potential to decay more rapidly with distance and reducing the thickness of the diffuse layer.

- Cation Valence: The thickness of the diffuse double layer varies inversely with the valence of the cation.
- Effect of Temperature: The thickness of the diffuse double layer is directly proportional to the square root of the temperature.
- Dielectric constant: The thickness of DDL is directly proportional to the square root of the dielectric constant.
- Size of hydrated cation: The thickness of DDL is directly proportional to the size of the hydrated cation.

2.6.7. Black cotton soil treatment techniques

According to Ikeagwuani and Nwonu (2019), expansive soils are stabilized by mechanical techniques such as compaction, prewetting, wetting-drying cycles, reinforcement, and solid wastes, and by chemical processes such as adding traditional and non-traditional agents. Babu et al. (2008) also mentioned the swelling of black cotton soils could be controlled by chemical stabilization, reinforcement, provision of geomembranes, and cohesion non-swelling (CNS) layer techniques. However, these methods are expensive for small-scale projects like constructing small-height bunds. Generally, cementitious additives (lime, cement, etc.), chemicals (NaCl, $MgCl_2$, KCl, etc.), and non-cementitious additives (fly ash, GGBS, stone dust, rice husk ash, etc.) are used for stabilization purposes (Malik and Priyadarshee 2018).

The disadvantage of some mechanical techniques is that they require more physical presence in the field for quality control, which is an important and time-consuming process. In the case of prewetting and wetting-drying cycles, the expected outcome may not come and is unsuitable for too expansive soils.

The disadvantages of chemical techniques are the field condition result may vary with controlled laboratory conditions, especially because some harmful compounds may be released during the reaction process, which leads to ground contamination (Ikeagwuani and Nwonu 2019). Over the past few decades, chemical stabilizations have been performed by using lime, cement, etc. However, in the present scenario, the usage of cement and lime is decreased because they are not economically reasonable and also produce greenhouse gases like carbon dioxide and nitrogen oxide during their production process (Murmu et al. 2020).

TH-3665_186104109

These are some disadvantages of both mechanical and chemical stabilizations. Malik and Priyadarshee (2018) reported the utilization of locally available waste materials as stabilization materials is the best way in both economically and environmentally. From all considerations, the stabilization techniques might have produced good results for moderate to low swell soils. Still, in the case of highly expansive soils, the laboratory results may not simulate field results. As a result, it is imperative to investigate the potential of highly expansive black cotton soils in engineering applications where their distinctive characteristics are well-suited, such as geoenvironmental applications, including landfill barriers.

2.6.8. Use of black cotton soil as landfill liner

Generally, clay-rich soils are preferred in waste containment systems because they have very low hydraulic conductivity values and great adsorption capacity. Black cotton soil is also rich in clay content and can be used as a barrier material in landfill lining systems. Also, Bc soil possesses high swelling pressures-swelling potentials, and low hydraulic conductivities (Nwaiwu et al., 2012; Mir and Sridharan, 2014; Gobinath et al., 2016; Yohanna et al., 2022). The problems associated with the usage of expansive BC soil as landfill liners are the formation of desiccation cracks and leachate interaction. Desiccation cracks occur due to the high swell shrink behaviour of soil, which leads to more significant distress in impervious barriers of landfill systems, which generate leachate and pollute land and groundwater. These desiccation cracks are responsible for increased hydraulic conductivity because the cracks act as drainage paths. Therefore, it is important to arrest this shrinkage phenomenon. In past literature, studies suggested that the incorporation of traditional fibres controlled this shrinkage and cracking tendencies (Miller and Rifai, 2004; Harianto et al., 2008; Tang et al., 2012; Chaduvula et al. 2017). However, the use of these traditional fibres is neither cost-effective nor addresses the pressing environmental challenges. On the other hand, many researchers have been focusing on the use of waste materials in geotechnical and geoenvironmental applications. The utilization of waste tires in civil engineering applications has gained significant attention due to their durability and enhanced engineering properties. Moreover, reusing waste tires helps alleviate the burden on rubber landfills, contributing to sustainable waste management. The detailed literature review on waste tire usage in clays for geotechnical and geoenvironmental fields is discussed below. Thereafter, literature on the influence of leachates on landfill barriers also will be discussed.

TH-3665_186104109

2.7. Review of literature on clay-waste tire mix

The rapid expansion of automobile utilization results in an immense quantity of tire waste being produced annually. According to previous studies, nearly 1.5 billion waste tires are produced every year globally, and around 1000 million tires per year approach the end of their serviceable life (Yadav and Tiwari 2017, Mukherjee and Mishra 2017). The USA only delivers 270 million waste tires per year, as per data obtained from the Rubber Manufacturer Association, 2000. Around 45% of 270 million waste tires are stored in storage yards, landfills (Fig. 2.10), or illegal dumpsites. (Siddique and Naik, 2004). Some countries in Europe and states in the USA have used this tire waste for fuel, on roads, and in similar applications. But in the Asian continent, some developing countries like India and China are still following standard disposal methods into landfills or dumping illegally. (Hoan and Chan, 2010).

Fig. 2.10. Stacking and burning of waste tires (Liu et al., 2018)

A large number of scrap tires are placed in landfills, stockpiles and hence could rise in the occupation of a wide range of land. So, some countries are burnt off the waste tires (Fig. 2.10) without effective recycling (Yoon et al. 2008), which causes the discharge of hazardous fumes comprising several benzene compounds, styrene, butadiene, hydrocarbons, SO_2, CO, and NO, etc. These toxic gases have been shown to have a significantly detrimental impact on both the environment and human health. So, the storing and burning of waste tires cause serious effects not only on the environment but also on the water, soil, and air that finally threaten human life (Liu et al. 2020). Hence the efficient way to deal with the generation of waste tire rubber is re-utilisation. Many researchers have used these waste tire rubbers in numerous civil engineering applications such as soil stabilization, road construction, concrete, and motor works (Fig. 2.11). Geotechnical engineering is the essential branch of civil engineering, which includes the application of soil mechanics and foundations to the study and design of geotechnical systems such as embankments, dams, tunnels, canals, and

TH-3665_186104109

foundations for bridges, roads, buildings, and solid waste disposal systems. Each application of soil mechanics involves difficulty because of the variability of soils and their stratification, composition, and engineering properties. For an effective way to reuse tire waste, many investigations have been carried out to examine the effect of waste tires in numerous geotechnical engineering applications, such as subgrade backfilling, landfill, retaining wall, foundation and slope reinforcement, etc.

Fig. 2.11. Waste tire applications in the civil engineering field.

The recycled tire waste is obtainable in many forms like chips, fibres, powders, crumbs, etc. Various researchers have studied the influence of varied tire content types and their sizes on different soils. According to ASTM D6270-08, tire waste is classified into ground rubber, rough shreds, granulated rubber, tire chips, tire shreds, powdered rubber, etc. Nazim and Hall, 2010 and Busic et al. 2018 mentioned that waste tire rubber classified as shredded rubber aggregate (13 to 76 mm), crumb rubber (0.425 to 4.75 mm), ground rubber (0.425 mm down), and rubber fibre (average size of 12.5 mm length).

Based on the earlier classification of waste tire type and size various investigations are done on sandy, and clayey soils mixed with tire waste and examined the engineering properties of soils including compression and deformation behaviour, dynamic properties, shear properties, etc. (Liu et al., 2020).

TH-3665_186104109

Fig. 2.12. Waste tire classifications.

In this literature, the main focus is on clayey-type soils and their swelling, shrinkage compressibility, consolidation, and strength behavior by the addition of tire content. Potential applications have been identified in accordance with the observed results.

Al-Tabba et al. (1997) Al-Tabba et al. (1997) investigated the impact of rubber tire particles of varying sizes (1-4 mm, 4-8 mm, and 8-12 mm) on three types of soils. The soils used in their study included bentonite, kaolin, and kaolin-lime mixtures. Their findings indicated a reduction in maximum dry density (MDD) with no significant change in the optimum moisture content (OMC). The unconfined compressive strength (UCS) of the soil samples also decreased as tire content increased. Additionally, the hydraulic conductivity was observed to decline with higher tire content, and the resulting values were deemed appropriate for landfill applications.

A. Al-Tabba and T. Aravinthan (1998) conducted tests on natural over-consolidated clay mixed with a shredded tire with a proportion of 6 and 15 % by soil weight. In this study, they conducted tests on paraffin-treated shredded tires incorporated with soil. The study revealed that the maximum dry density decreased due to the low specific gravity of the shredded tire, while the optimum moisture content remained unchanged. It was also observed that the unconfined compressive strength (UCS) of the clay-tire mix reduced to 40% of the strength of untreated clay. The permeability of the clay-tire mixtures increased when distilled water

TH-3665_186104109

was used as the permeant. In contrast, a decrease in permeability was noted when paraffin was used as the permeant. Additionally, the amount of swelling decreased with distilled water as the permeant but increased when paraffin was used. The concentrations of copper and nickel in the waste tire–clay mixtures were measured by performing leaching studies. Leaching results for Cu and Ni, showed that the presence of tire material has an insignificant influence on their leachability.

Cokca and Yilmaz (2004) performed laboratory tests on bentonite-added fly ash treated with rubber. They concluded that hydraulic conductivity and compressibility were increased with increased rubber content. It was also observed that the swell pressure increased as the bentonite content was increased. Finally, they concluded that incorporating 10% rubber content and bentonite added with fly ash would be suitable materials for liner construction after considering the hydraulic conductivity property value. The leachate analysis outcome of fly ash -tire-bentonite mixtures indicated that these materials do not pose any significant environmental risk, as the levels of cadmium, lead, selenium, barium, mercury, arsenic, chromium, and silver were within non-hazardous limits.

Cetin et al. (2006) studied on geotechnical properties of clayey soil treated with fine (passed through 0.425 mm) and coarse-grained (passed through 4.75mm and retained on 2 mm) tire chips. The findings showed that the Atterberg limits of clayey soil decreased as the tire chip content increased, with proportions ranging from 0% to 50% by weight in increments of 10%. The MDD value of clay decreased with an increase in the fine tire chips than the coarse tire chips. They reported that the shear strength was increased from 110 kPa to 140 kPa due to the rise in the fine tire content from 0 to 30%, respectively. The cohesion of clay increased for an increase in the fine and coarse tire content up to 40%, whereas the angle of internal friction decreased. It was found that hydraulic conductivity was lower in coarse-grained tire chips compared to fine-grained chips when subjected to normal pressures ranging from 100 to 350 kPa.

Ozkul and Baykal (2006) examined undrained and drained responses of low plasticity kaolinite clay treated with 10% tire buffings at standard and modified compaction energies. The results indicated that the drained strengths remained consistent under both standard and modified compaction energies. On the other hand, the undrained strength varied under modified compaction energy. They concluded that the findings were favorable for using the material as backfill in earthen dams.

TH-3665_186104109

Akbulut et al. (2007) conducted tests on three different types of clay soils (CH type) treated with tire fibre as 1,2,3,4 and 5% and synthetic fibres (Polyethene and polypropylene fibres) at the level of 0.1,0.2, 0.3, 0.4 and 0.5% by weight. They found that the UCS values of clay samples increased due to the increase in the fire content by up to 2%, and the UCS of clay soils was given the maximum value of 0.2% of synthetic fibres. The cohesive value was also increased due to the inclusion of natural and synthetic fibres for 10mm lengths. They examined dynamic behaviour too, and the results showed an improvement in damping ratio and shear modulus.

Seda et al. (2007) performed laboratory tests on expansive soil treated with 20% tire rubber and concluded that the MDD value of the expansive soil rubber mix was decreased and the OMC value remained the same. They also observed that the swell pressures were controlled by the addition of tire rubber. They suggested that the rubber clayey soil mix would be suitable as backfill material.

Hoan Ho et al. (2010) conducted consolidation tests on cement-stabilized kaolin lay mixed with rubber chips on 0, 5, 10, and 15% by weight. They concluded that the stiffness of the soil improved as the rubber content increased from 0% to 15%, accompanied by the addition of a small amount of cement. The coefficient of compressibility (C_c) and the coefficient of re-compressibility (C_r) were decreased due to the increase in the rubber chips content.

Patil et al. (2011) conducted the one-dimensional swell test on expansive soil consisting of 25% Wyoming sodium bentonite and 75% clean silica sand with poor gradation. They performed various tests on expansive soil mixed with sand and granular tire rubber independently and it was concluded that the swelling was effectively controlled with an increase in both sand and tire content.

Marefat and Soltani-Jigeh (2011) investigated the impact of tire chips on the strength behavior of clayey soil. Their study involved conducting consolidated undrained tests on soil samples mixed with tire chips of three different sizes (1.28 mm, 3.56 mm, and 5.53 mm) at proportions of 10%, 20%, and 30% by weight under effective confining pressures of 100, 200, and 300 kPa. They observed that the friction angle increased with tire chip content up to 10%, but further addition of tire chips resulted in a decrease.

Jafari and Eshnaashari (2012) conducted UCS tests on lime stabilized clayey soil reinforced with waste tire cord at a level of 0.5, 1, and 1.5% by dry weight of soil. The results showed that the UCS of 4% lime stabilized specimens was increased from 0 to 1.5% under 28 days

TH-3665_186104109

caring period, respectively. A similar trend was observed due to the addition of 8% lime and three different percentages (0 to 1.5%) of tire fibres. They also noticed that the durability index was also improved under freeze-thaw conditions due to inclusion of fibres.

Trouzine et al. (2012) examined the effect of tire fibres at the level of 10%,20%,25% and 50% by weight on two clayey soils, namely, low plasticity clay (CL) and high plasticity clay (CH) and found that the swell pressures and swell potentials were decreased due to the addition of tire fibres from 10 to 50%. They noticed that the compression and re-compression indexes were also increased due to the increase in tire content.

Asadzadeh and Ersizad (2013) conducted consolidation tests on low plasticity clayey soil treated with 10, 20, and 30% tire chips of 1.275mm size. They reported that the compression index was reduced, and the swell index was increased due to increased fibre content. They also found that the cohesion value was raised and the angle of internal friction was decreased due to the increase in tire fibre content.

Kim and Kang (2013) conducted laboratory experiments on composite geomaterial (CGM) composed of dredged clay, cement, bottom ash, and rubber particles. They concluded tests on GGM samples treated with three different bottom ash contents and five different tire contents. They reported that MDD, UCS, and CBR values of the soil mix were decreased due to the addition of rubber content.

Kalkan (2013) investigated the consolidation properties of clayey soil blended with silica fume and rubber fibres. They performed tests on clayey soil-silica fume mixture and clayey soil-silica fume-rubber fibre mixture. In this study, the composition of silica fume and rubber fibres were 10 and 20% and 1, 2, 3 and 4%, respectively. They reported that the UCS of clayey soil increased due to the upsurge in the silica fume by up to 20% and fibres at 2%. They observed a reduction in both swelling pressure and hydraulic conductivity with the incorporation of a silica fume-rubber fibre mixture.

Srivastava et al. (2014) examined the geotechnical properties of black cotton soil treated with coarse (passing through 4.75mm and retained on 2.0mm) and fine (passing through 2mm and retained on 0.075mm) waste shredded tire at the level of 5%, 10%, 15% and 20% by dry weight. They reported that the liquid limit and plastic limit of soil were decreased due to the addition of coarse and fine shredded tires. The compaction results showed that the MDD and OMC values were reduced due to the addition of coarse and fine fractions. They concluded that the undrained cohesion values were increased up to 60% due to the increase in the coarse

TH-3665_186104109

size shredded tire up to 5%. The swell pressure was decreased due to the inclusion of tire content, and consolidation parameters (C_c, c_v, k) were increased by the addition of tire content. Finally, they suggested that the soil with coarse tire fractions was suitable for the backfill of embankments.

Dunham-Friel and Carraro (2014) conducted a consolidated undrained triaxial test on expansive soil treated with waste glass and rubber fibre. The results indicated that the MDD was decreased by the addition of rubber fibre, and OMC remained the same. A similar trend was noticed in the case of the waste glass soil mixture. From triaxial tests, they found that the critical friction angle was improved due to the increase in fibre contents and waste glass. However, the peak friction angle was increased due to the addition of waste glass; in contrast, it was found to decrease with the addition of rubber fibres when compared to untreated soil.

Cabalar et. al (2014) evaluated the performance of clay stabilized with lime in the proportion of 0, 2, 4, and 6 and reinforced with tire buffings in the proportion of 0, 5, 10, and 15%. They conducted CBR and UCS tests on three different mixtures of clay-lime, clay-tire buffings and clay-lime-tire buffings. They suggested that the inclusion of fibres in clay treated with a small amount of lime gave satisfactory results economically and environmentally. They noted that incorporating rubber content led to reductions in swelling, MDD, and UCS values.

Razali et al. (2015) examined the effect of tire chips and fly ash on cement-stabilized clayey soil at in the proportion of 5, 10 and 15%. The results showed that the UCS value was increased due to the addition of 15% fly ash and 10% tire chips individually. Similar results were observed in the CBR test also.

Xin et al. (2015) performed consolidated undrained and isotropic compression tests on cement-stabilized clayey soil reinforced with tire chips with an average size of 4.5mm. They reported that the undrained shear strength of cement stabilized clayey soil increases due to an increase in the fibre content. They observed that there was a significant reduction of pore water pressure by the addition of rubber content. The compressibility was increased due to an increase in tire content, whereas decreased due to the addition of cement.

Priyadarshee et al. (2015) conducted a comparative study on kaoline clay treated with tire crumbles (1, 2, 5, 10, and 20% by weight) and fly ash and reported that the MDD was decreased with the addition of tire crumbles and observed an increase in CBR value with the addition of tire crumbles up to 5%, beyond that the values were decreased.

TH-3665_186104109

Tajdini et al. (2016) performed unconsolidated undrained (UU) and consolidated drained (CD) tests on kaolin clay reinforced with crumb rubber at the level of 5, 10, and 15% by weight and reported that the angle of internal fractions and shear strength values of the clay-tire mix was increased under drained condition compared to those mix under undrained condition. The CBR value was also increased due to an increase in rubber content by up to 5% and beyond that, the CBR value was decreased.

Roustaei et al. (2016) performed UU triaxial test on clayey soil treated with tire crumbs as 0, 0.5, 1, 1.5, 2, and 2.5% of the weight of soil under different confining pressures with the soil subjected to different freeze-thaw cycles and observed that the cohesion decreased due to the addition of crumb rubber under freeze-thaw conditions.

Mukherjee and Mishra (2017) carried out a series of consolidation triaxial and unconfined compressive strength tests on sand bentonite mix reinforced with tire fibres in a proportion of 5, 10, and 15% by weight. In this study, they used 10% bentonite and 90% sand, and results showed an increment in cohesion due to the inclusion of tire fibres up to 10%. They reported that the hydraulic conductivity (k) and the coefficient of consolidation (c_v) were increased with an increase in tire chips content. They observed that UCS results in an increment in the failure strain due to the addition of rubber. Finally, they suggested that the sand bentonite mix of 10% tire chips was suggested for landfill applications.

Yadav and Tiwari (2017) studied the effect of rubber fibre on cement-stabilized clayey soil. The test results demonstrated that MDD and OMC values were decreased due to increased fibre content. They also reported that the UCS value of cement-stabilized clayey soil was maximum at 5% of tire content, and the improvement in CBR value was observed at 2.5% fibre content of 6% cement-stabilized soil. They concluded that swelling pressure diminished as tire content increased and cement content decreased.

Chegenizadeh et al. (2018) investigated the influence of coarse tire crumbs and fine tire powder on soil-bentonite mixtures for backfill application in slurry trench walls. They found a significant hike in coefficient of consolidation and compressibility values with the inclusion of both rubber types. Also, a significant hike in hydraulic conductivity values was observed with coarse tire crumbs than with powder.

Soltani et al. (2019) conducted UCS and consolidation tests on expansive soil reinforced with coarse (4.75-1.18mm) and fine (1.18-0.075mm) tire rubber at the level of 5, 10, 20, and 30% by dry weight. They reported that the coarse rubber soil mix was given maximum UCS

TH-3665_186104109

at 10% of inclusion than the fine rubber addition. It was also observed that adding rubber content led to a reduction in both the compression index and swelling behaviour.

Abbaspour et al. (2019) studied the effect of waste textile tire fibres on clayey and sandy soils. In this study, tests were performed by adding 0.5, 1, 3, and 4% tire fibres on both soils. The results showed an increment in both cohesion and angle of internal friction with the addition of 1% tire fibre content of sandy soil whereas in case of clayey soil, cohesion was increased and the angle of internal friction was decreased. CBR values of clayey soil were reduced due to an increase in fibre content, but in the case of sandy soil, they observed an increment in CBR value at an optimum level of 2% fibre content. Failure strains were increased by the addition of fibre content of 1% in both soils.

Bekhiti et al. (2019) investigated the unconfined compressive strength (UCS) and swelling behavior of cement-stabilized clay mixed with waste tire rubber at proportions of 0%, 0.5%, 1%, and 2% by weight. Laboratory tests demonstrated that the addition of both rubber and cement improved the consistency limits of the soil. The study incorporated cement contents of 5%, 7.5%, and 10% by weight of the soil. The results indicated that the UCS of the cement-stabilized soil increased with the inclusion of rubber. Additionally, the swell pressure and swell potential were significantly reduced by adding 2% tire rubber and 10% cement to the soil. However, the compression index and re-compression index were found to increase with higher fibre content.

Irani and Ghasemi (2019) examined the compaction and strength properties of clayey sand treated with lime and reinforced with shredded tire and tire cord scrap as 0, 0.5, 1, 1.5, and 2.5% by weight of soil. In this study, the clayey sand was first stabilized with lime at proportions of 2%, 4%, and 6% by weight, followed by the incorporation of shredded tire and tire cord scrap. It was reported that the inclusion of fibres, such as shredded tire and cord scrap, resulted in a reduction in both MDD and OMC. The UCS value was achieved with the addition of 6% lime and 0.5% tire additives.

Mukherjee and Mishra (2019(b)) investigated consolidation parameters of sand bentonite (80:20) mix reinforced with tire fibres at a level of 5%, 10%, and 15% by dry weight and observed that the decrement in a void ratio by the addition of tire content. They reported the compression index of the SB 20 mix was decreased due to an increase in fibre content from 0 to 5% after it was increased due to the rise in tire content from 10% to 15%.

TH-3665_186104109

Hasan et al. (2020) studied the effect of tire crumb rubber on expansive soil with the proportion of 1, 3, 5 and 10% by weight. They concluded that adding crumb rubber led to a reduction in swell pressure, compression index, and consolidation coefficient values. Also, it was noticed a significant decrement in MDD value by the inclusion of fibres.

Narani et al. (2020) conducted laboratory studies on sodium bentonite mixed with tire fibres of 0, 1, 3, and 4% by weight. They reported that the MDD values were decreased by the addition of fibre content. It was observed that swelling potential decreased with an increase in fibre content up to 3%, while the addition of rubber fibres resulted in higher hydraulic conductivity. They observed that the addition of rubber content decreased the desiccation crack formations compared to untreated specimens. Finally, they suggested that the expansive soil of a 3% tire fibre mix was suitable for liner material.

Akbarimehr et. al (2021) explored the geotechnical properties of Tehran low plasticity clay mixed with rubber granules (0-50%), results showed that increasing the rubber content reduced the MDD and UCS values. The results indicated that the mixtures were suitable for use as lightweight filler materials in geotechnical applications with an optimal fibre content of up to 10%.

Mistry et al. (2021) focused on the three aspect ratios (9, 6.4, 4.5) of waste tire fibre content (0.25 -15) on high plasticity clayey soil. They observed a significant reduction in swelling, time for 90% consolidation, and permeability values of expansive soil with the hike in fibre content. Fibre contents with lower aspect ratios demonstrated a more pronounced reduction in these properties compared to those with higher aspect ratios. Finally, they suggested this waste tire fibre mix for sustainable construction applications.

Erenson (2023) investigated the use of waste tire rubber particles (0, 5, 10, and 15%) on the engineering performance of five types of clayey soils. Test results revealed a significant reduction in liquid limit, linear shrinkage, and dispersion potential of clayey soils with the hike in fibre content.

Haq et al. (2024) explore the potential of weak Indian clayey soil stabilized with lime and waste rubber tire powder (0-15%). Results showed a significant reduction in MDD and plasticity properties of clayey soil. Whereas OMC, cohesion, and CBR values of lime-stabilized clayey soil were increased with the rise in rubber powder content up to 12.5%. The cost-benefit analysis demonstrated cost reductions of up to 19% for foundation applications and 39% for pavement applications.

TH-3665_186104109

Table 2.4. Summary of clay -tire fibre mix literature

Authors	Type of Clay	Type of Tire	Amount of Tire content	Important Results
Al-Tabba et al. (1997)	Bentonite, Kaolin, and Kaoline-lime mix	Shredded tire	2-20% (1-4, 4-8, and 8-12 mm)	▪ MDD declined ▪ OMC increased slightly ▪ UCS decreased
A. Al-Tabba and T. Aravinthan (1998)	Over consolidated fissured clay	Shredded tire	6 to 8% (1-4 and 4-8 mm)	▪ UCS decreased ▪ The swelling reduced when water as permeant and increased when paraffin as permeant ▪ Swell pressures decreased
Cokca and Yilmaz (2004)	Bentonite-fly ash mix	Granular rubber	0-10% by dry weight (0.1 – 1 mm)	▪ MDD decreased ▪ UCS decreased ▪ Secant modulus reduced ▪ *k* value increased ▪ Compressibility increased ▪ Non-hazardous leachate found in tested mixtures by leachate analysis
Cetin et al. (2006)	Cohesive clayey soil	Coarse-grained and fine-grained tire chips	10,20,30,40, and 50% by weight [(2 - 4.75 mm) and (<0.425 mm)]	▪ OMC raised with fine-grained chips ▪ MDD declined with both tire chips ▪ Cohesion value increased up to 40% for fine and coarse-grained chips ▪ The angle of internal friction reduced up to 40% for both tire chips ▪ *k* value increased at lower overburden pressures and higher tire contents

TH-3665_186104109

Authors	Type of Clay	Type of Tire	Amount of Tire content	Important Results
Ozkul and Baykal (2006)	Kaolin clay	Tire buffings	10% by weight (4-15 mm length)	▪ Undrained shear strength increased under modified compaction energy compared to standard compaction energy. ▪ Drained shear strength remained the same for both compaction energies
Akbulut et al. (2007)	Highly compressibility clays	Tire fibres	0, 1, 2, and 3% (2-5, 5-10- and 10-15-mm lengths)	▪ UCS value increased up to 2% tire fibre ▪ Highest cohesion value observed at 10 mm length fibres
Seda et al. (2007)	CH-type clayey soil	Granular tire	20 % by weight (< 6.7 mm)	▪ Swell pressures and swell potentials reduced
Ho et al. (2010)	Cement-stabilized Kaolin clay	Tire chips	5, 10, and 15% (2 to 5 mm)	▪ Coefficient of compressibility (C_c) decreased ▪ Coefficient of re-compressibility (C_r) decreased
Patil et al. (2011)	Sand-bentonite mix	Tire fibre	0, 0.2 and 0.36 fractions by volume of solid	▪ Swelling decreased
Marefat and Soltani-Jigeh (2011)	Clayey soil	Tire chips	10, 20, and 30% by weight (1.28, 3.56, and 5.53mm)	▪ Friction angle increased up to 10% tire chips then decreased. ▪ Cohesion increased

TH-3665_186104109

Authors	Type of Clay	Type of Tire	Amount of Tire content	Important Results
Jafari and Eshnaashari (2012)	Low plasticity clayey soil	Tire fibres	0.5%, 1%, and 1.5% by weight (20 mm length)	▪ UCS value increased ▪ Durability index increased
Trouzine et al. (2012)	Medium and high plasticity clays	Rubber fibres	10, 20, 25, and 50% by weight (7 mm length)	▪ Swell pressures and swell potentials decreased ▪ Compressibility index and re-compression index increased
Asadzadeh and Ersizad (2013)	Low plasticity clay	Tire chips	10, 20, and 30% (1.275 mm)	▪ Swell index increased ▪ Cohesion value increased ▪ Compression Index reduced
Kim and Kang (2013)	Low plasticity clay	Rubber particles	20, 50, 75 and 100% by weight (0.1-2mm)	▪ MDD decreased ▪ UCS value decreased ▪ CBR value decreased
Kalkan (2013)	Expansive clay (LL =72)	Tire fibres	1-4% by weight (5-10 mm length)	▪ OMC and MDD reduced ▪ Swelling pressure reduced ▪ *k* value increased with fibre ▪ Cohesion increased up to 2% fibre
Srivastava et al. (2014)	Black cotton soil	Tire shreds	5-20% by weight (4.75-2mm & 2-0.425mm)	▪ MDD and OMC decreased ▪ Swelling pressures decreased ▪ UCS increased up to 5% ▪ *k* value increased
Dunham-Friel and Carraro (2014)	Expansive soil	Granular rubber	20% by weight (4.8 & 6.7 mm length)	▪ MDD decreased ▪ Friction angles increased

TH-3665_186104109

Authors	Type of Clay	Type of Tire	Amount of Tire content	Important Results
Cabalar et.al (2014)	Clayey soil (L=49.5)	Tire buffings	5, 10, and 15% by weight	▪ Swelling decreased ▪ CBR values decreased ▪ UCS values decreased
Razali et al. (2015)	Low plasticity clayey soil	Tire chips	5, 10, and 15% by weight	▪ CBR value increased up to 10% chips ▪ UCS value increased up to 5% chips
Xin et al. (2015)	Low plasticity clayey soil	Tire chips	0 to 120% by weight (4.5 mm length)	▪ Pore water pressure reduced ▪ Undrained shear strength increased
Priyadarshee et al. (2015)	Kaolin-fly ash mix	Tire crumbles	1, 2, 5, 10, and 20% by weight	▪ MDD value decreased ▪ Strength and stiffness increased ▪ CBR value increased up to 5 % tire crumbles
Tajdini et al. (2016)	Kaolinite	Crumb rubber	5, 10, and 15% by weight	▪ Shear strength increased under the drained condition and decreased under undrained condition ▪ CBR value increased up to 5% rubber
Roustaei et al. (2016)	Low plasticity clayey soil	Tire crumbs	0.5, 1, 1.5, 2 and 2.5% by weight (4.75-0.6 mm length)	▪ Cohesion values decreased under freeze-thaw conditions ▪ Strain softening behaviour increased with tire content

TH-3665_186104109

Authors	Type of Clay	Type of Tire	Amount of Tire content	Important Results
Mukherjee and Mishra (2017)	Sand bentonite mix (90:10)	Tire fibres	5, 10, and 15% by dry weight (4.75 to 2 mm)	▪ MDD decreased ▪ Large failure strains observed in UCS due to fibre increment ▪ *k* value increased ▪ Cohesion increased up to 10% tire fibre ▪ Compression index decreased up to 10% tire fibre
Yadav and Tiwari (2017)	Expansive clay (LL = 34.2)	Tire fibres	2.5, 5, 7.5, and 10% by dry weight (15 mm length)	▪ OMC and MDDdecreased ▪ UCS value increased up to 5% tire content ▪ CBR values increased up to 2.5 % tire content ▪ Swelling reduced
Chegenizadeh et al. (2018)	Soil-bentonite mix	Coarse tire crumbs and fine tire powder	2, 5, and 10% by dry weight	▪ Coefficient of consolidation increased ▪ Compression index increased ▪ Coefficient of permeability increased
Soltani et al. (2019)	Kaolinite-bentonite mixture (85:15)	Tire rubber (coarse and powder)	5, 10, 20, and 30% by dry weight (4.75 – 1.18 mm & 1.18 0.75 mm)	▪ Swell-shrink behaviour reduced ▪ Compression index reduced

TH-3665_186104109

Authors	Type of Clay	Type of Tire	Amount of Tire content	Important Results
Abbaspour et al. (2019)	Low compressibility clay	Tire fibres	0.5, 1, 3, and 4% by weight (20 – 40 mm length)	▪ MDD decreased ▪ CBR and UCS values decreased ▪ Ductility increased ▪ Angle of internal friction increased
Bekhiti et al. (2019)	Cement-stabilized bentonite	Tire fibres	0.5, 1, and 2% by weight (average of 8mm length)	▪ Liquid limit decreased ▪ UCS increased ▪ Swelling pressure and swell potential decreased
Irani and Ghasemi (2019)	Sand with clayey fines (LL = 35)	Tire cord scrap and shredded tire	0.5, 1, 1.5, and 2.5% by dry weight	▪ MDD and OMC decreased ▪ UCS value increased up to 5% tire content ▪ UCS increased up to 0.5% tire content
Mukherjee and Mishra (2019b)	Sand bentonite mix (80:20)	Tire fibres	5, 10, and 15% by weight (4.75 to 2 mm sieved)	▪ *k* value increased ▪ Undrained shear strength increased ▪ Swell pressures diminished ▪ Compression index decreased up to 5% tire content
Narani et al. (2020)	Sodium bentonite	Tire fibres	0, 1, 3, and 4% by weight (20-40mm)	▪ Swelling potential decreased up to 3% tire fibre ▪ Split tensile strength increased ▪ *k* value increased ▪ Volumetric shrinkage decreased ▪ Desiccation crack formations decreased

TH-3665_186104109

Authors	Type of Clay	Type of Tire	Amount of Tire content	Important Results
Akbarimehr et. al (2021)	Low compressibility clay	Tire shreds	10, 20, 30, 40 and 50% by weight	▪ OMC increased and MDD decreased ▪ UCS decreased ▪ Failure strains increased ▪ Angle of internal friction increased up to 10% tire content
Mistry et al. (2021)	High plasticity clay (LL = 65%)	Tire fibres	0.25, 0.5, and 1.0% by weight (three different aspect ratios)	▪ Swelling and compressibility behaviour reduced ▪ Rate of consolidation increased ▪ *k* value values hiked ▪ No significant change in MDD
Erenson (2023)	Clayey soils (Bentonite, Kaolin clays, Ball clay, and solid waste dam clay)	Rubber granules	5, 10, and 15% by weight (passing through 1.6 mm sieve)	▪ Atterberg limits decreased ▪ Linear shrinkage reduced ▪ Dispersion potential reduced for all clayey samples
Haq et al. (2024)	Lime stabilized clayey soil (LL = 38.7%)	Tire powder	2.5-15% (1-0.08 mm sieved)	▪ MDD increased and OMC decreased ▪ CBR and cohesion values increased up to 12.5% tire content

TH-3665_186104109

2.8. Formation of leachate from MSW

Leachate is produced through various chemical and biological processes occurring within solid waste in landfills and can pose significant risks to surrounding soil and groundwater if not effectively managed. Leachates are typically categorized into aqueous solutions containing water-miscible contaminants, non-aqueous liquids composed of organic compounds that are water-immiscible, or combinations of both, leading to the development of two distinct phases. Properly designed and managed modern landfills are equipped to prevent leachate from escaping into the environment. The landfill liner acts as a protective barrier, preventing the potentially hazardous leachate from polluting underlying groundwater resources.

2.8.1. Leachate composition

Pollutants in municipal solid waste (MSW) and industrial landfill leachate can be categorized into four main groups:

Dissolved Organic Matter: This includes compounds quantified as Chemical Oxygen Demand (COD) or Total Organic Carbon (TOC), such as volatile fatty acids (which accumulate during the acid phase of waste stabilization) and more resistant compounds like humic- and fulvic-like substances (Christensen and Kjeldsen, 1989).

Inorganic Macro-Components: These include ions such as calcium (Ca^{2+}), magnesium (Mg^{2+}), sodium (Na^{+}), potassium (K^{+}), ammonium (NH_4^{+}), iron (Fe^{2+}), manganese (Mn^{2+}), chloride (Cl^{-}), sulfate (SO_4^{2-}), and hydrogen carbonate (HCO_3^{-}) (Norouzi et al., 2022).

Heavy Metals: Examples include lead (Pb^{2+}), cadmium (Cd^{2+}), chromium (Cr^{3+}), copper (Cu^{2+}), nickel (Ni^{2+}), and zinc (Zn^{2+}).

Xenobiotic Organic Compounds (XOCs): These originate from industrial or household chemicals and are typically found in low concentrations (generally below 1.0 mg/L per compound). They include aromatic hydrocarbons, phenols, chlorinated aliphatics, and pesticides.

The composition of these pollutants in leachate varies depending on factors such as waste type, landfill age, and site management practices. Landfill leachate often contains elevated levels of BOD, COD, ammonia, chloride, sodium, potassium, hardness, and boron. Additionally, raw leachate frequently exceeds drinking water standards for heavy metal

TH-3665_186104109

concentrations, posing risks to human health. The presence of toxic substances is influenced by the nature of the waste deposited and can vary significantly.

2.8.2. Influence of leachates on barrier material

Chemicals present in landfill leachate with low dielectric constants, high electrolyte concentrations, or elevated cation valence can cause the bentonite's diffuse double layer to contract, increasing hydraulic conductivity (Olson and Mesri, 1970; Dutta and Mishra 2015). High concentrations of cations such as sodium, calcium, potassium, etc. in leachate can trigger ion exchange reactions, which diminish the swelling capacity of clay and lead to an increase in its hydraulic conductivity capacity (Booker et al., 1995). Prolonged exposure to acidic or saline leachate can lead to the dissolution of minerals and weakening of the clay structure/matrix, further increasing hydraulic conductivity (Gleason et al., 1997). Hence, designing an effective clay barrier requires a thorough understanding of the contaminant composition, the extent of contaminant accumulation within the liner material, and its impact on the clay structure, which ultimately influences the barrier's swelling properties and hydraulic conductivity. Therefore, it is very essential to understand the barrier material engineering performance under the influence of leachate conditions. Since leachate is a complex mixture of different chemical constituents, it is very essential to test the barrier material under the impact of individual salts and heavy metals for understanding the unique contributions like cation type, valency, concentration, dielectric constant, etc on hydromechanical beahviour of barrier material. For instance, monovalent cations such as sodium tend to induce dispersion in clay minerals, while divalent cations like calcium encourage flocculation, impacting clay mineral’s engineering properties such as swelling and hydraulic conductivity (Mitchell and Soga, 2005). Heavy metals such as cadmium and lead may form complexes or precipitates, altering the chemical compatibility of the clay matrix. Therefore, the impacts of salts and heavy metals allow researchers and engineers to design more robust and efficient barrier systems. A comprehensive review of the effects of individual inorganic salts and heavy metals on barrier materials is presented below, providing valuable insights into their impact on liner stability.

TH-3665_186104109

2.9. Review of literature on salt solutions' interaction with clay

The availability of land is hard to find for dumping municipal solid waste, so this huge amount of waste is reduced by incineration with the residue of bottom ash and fly ash which is responsible for the presence of cations like Ca and Na in clay liner (Mishra et al. 2005). The hydraulic conductivity is related to the diffuse double-layer thickness, so the presence of these cations in waste suppresses the diffuse double-layer thickness due to high electrolyte concentrations and results in the increment in hydraulic conductivity (Ruhl and Daniel, 1997). The higher hydraulic conductivity values lead to contamination of the ground.

This study investigates the impact of various solutions with differing concentrations on the hydromechanical properties of clay liners, as detailed below.

Petrov and Rowe (1997) studied the effect of NaCl salt solutions (concentration as 0.01, 0.1, 0.6, and 2.0 M) on geosynthetic clay liner (GCL). It was observed that the hydraulic conductivity of the GCL increased when permeated with salt solutions of varying concentrations. Specifically, a rise in NaCl solution concentration resulted in higher hydraulic conductivity values compared to those obtained with distilled water. They also reported that liquid limit values were decreased with an increasing concentration of salt solutions.

Shackelford et al. (2000) studied the effect of non-polar solutions like NaCl, $ZnCl_2$, and $CaCl_2$ as permeants on the hydraulic conductivity of GCLs. The findings indicated that permeant solutions with a high concentration of monovalent cations and a low concentration of divalent cations lead to a substantial increase in hydraulic conductivity.

Jo et al. (2001) investigated the swell and consolidation behaviour of non-prehyadrated GCLs permeated with salt solutions of NaCl, KCl, LiCl, $CaCl_2$, $MgCl_2$, $ZnCl_2$, $CuCl_2$, and $LaCl_3$. They reported that the swelling and hydraulic conductivity values were increased for trivalent cation solutions compared to monovalent cation solutions. In this study, strong acid (HCl) strong base (NaOH) solutions were used to examine the effect of pH on swelling and hydraulic conductivity of GCLs. From the results, they reported that significant swelling had occurred in strong base solutions, whereas the lowest swelling occurred in strong acid solutions.

Lee and Shackelford (2005) studied the effect of hydraulic conductivity on two geosynthetic clay liners (GCLs) containing different qualities of bentonites. This study utilized water and

TH-3665_186104109

$CaCl_2$ solutions with concentrations of 5, 10, 20, 50, 100, and 500 mM as permeants in GCLs. They observed that GCL with higher quality bentonites (GCL-HQB) possessed a lesser value of hydraulic conductivity compared to lower quality bentonites (GCL-LCB) when water was used as permeant. They also observed a higher increase in hydraulic conductivity in GCL-HQB compared to GCL-LQB when permeated with $CaCl_2$ solutions.

Mishra et al. (2005) investigated the effect of salt solutions on basalt soil and bentonite mixture. In this study, NaCl and $CaCl_2$ solutions with varying concentrations of 0, 0.001, 0.01, and 1M were utilized. The results reported that the hydraulic conductivity values were increased due to the increase in salt solution concentrations. In contrast, liquid limit and compression index values were decreased with an increase in the concentration of both $CaCl_2$ and NaCl.

Singh and Prasad (2007) investigated the impact of aluminum hydroxide and acetic acid, which are commonly found in landfill leachate, on bentonite. The study reported a reduction in differential free swelling by 47% with acetic acid and 49% with aluminum hydroxide compared to deionized (DI) water. The findings also revealed that the hydraulic conductivity of bentonite decreased by 12% with aluminum hydroxide and 17% with acetic acid. Additionally, swelling pressure was reduced by 82% and 20% with the addition of aluminum hydroxide and acetic acid, respectively.

Arasan et al. (2010) examined the impact of various inorganic salt solutions of concentrations varying from 0.01 to 1.0M on the swelling pressure of compacted clays. Results showed that for CL clay, swelling pressure increased with higher salt concentrations, whereas for CH clay, swelling pressure decreased as salt concentrations increased. The behavior varied due to differences in clay mineral compositions.

Shirazi et al. (2011) investigated the impact of salinity on the swelling behavior of compacted bentonite. They determined that the swelling rate was more influenced by the concentration of NaCl than by the initial dry density or loading conditions. Their results indicated a significant reduction in the liquid limit, from 497% to 112%, when the permeant was switched from deionized (DI) water to a 0.5 M NaCl solution, while the plastic limit showed an increase.

Shariatmadari et al. (2011) investigated the effect of inorganic salt solutions (NaCl, $CaCl_2$, and $MgCl_2$) on the free swelling, liquid limit, compaction and consolidation properties of two types of clay bentonite mixtures. In this study, bentonite clay in two proportions of 10%

TH-3665_186104109

and 20% by weight were added to low-plasticity clay. The findings revealed a reduction in liquid limit, swelling volume, maximum dry density (MDD), and compressibility, while hydraulic conductivity showed an increase.

Zhu et al. (2013) studied the effect of salt solutions (NaCl and $CaCl_2$) with varying concentrations from 0.1M to 2M on GMZ01 bentonite. GMZ01 represents the place Ga0MiaoZi was located in China. Their results indicated that the swell pressures of bentonite were decreased with the increase in the concentration of salt solutions. This increment was significant in $CaCl_2$ permeant than NaCl. The hydraulic conductivity of GMZ01 bentonite increased more significantly with NaCl than with $CaCl_2$ as permeants at higher concentrations.

Rao et al. (2013) examined black cotton soil's (liquid limit of 82) swelling mechanisms inundated by NaCl solution up to 4.0M concentration and stated that both crystalline swelling and double layer swelling mechanisms were responsible with distilled water and 0.1M NaCl solution. Also, they observed a significant reduction in swelling potentials with the hike in the concentration of pore fluid.

Dutta and Mishra (2015) investigated the effect of NaCl and $CaCl_2$ salt solutions on the consolidation behaviour of two compacted bentonites and reported that the free swelling, liquid limit, swelling pressure, and swelling potential of the bentonites were decreased due to the increase in salt concentration. Bentonite with NaCl solution showed a higher of these values in contrast to the same concentration of $CaCl_2$ solution. They also noted that hydraulic conductivity increased more with $CaCl_2$ solution compared to the same concentration of NaCl solution.

Zhang et al. (2016) examined the effects of salt solution concentration (0.1-1.0M) on the mechanical behaviour (Strength) and microstructure of GMZ07 bentonite-sand (50:50) mixture, considered for high-level radioactive waste isolation in China. Tests reveal that shear strength increases with salt concentration due to a rise in friction angle, while cohesion remains unaffected. Compression tests show similar compressibility across all salt concentration.

Dutta and Mishra (2016a) examined the influence of NaCl and $CaCl_2$ salt solutions of different concentrations, on consolidation behaviour of two compacted bentonites. They

TH-3665_186104109

reported that the C_c, m_v, and t_{90} of the bentonites decreased, whereas, c_v increased with the increase in salt concentration. They also observed that an increment in C_c, m_v and t_{90} values for higher quality bentonite than lower quality bentonite because of the higher quality bentonite exhibited higher cation exchange capacity, exchangeable sodium percentage and swelling capacity.

Ramya et al. (2018) studied the effect of NaCl solution of varying concentrations, on consolidation properties of black cotton soil. They reported that the coefficient of consolidation was increased with increase in salt concentration. Whereas, the coefficient of compression decreased for the same concentration. The liquid limit of the soil was found to decrease progressively with an increase in NaCl concentration.

Xu et al. (2018) tested the influence of deflection and Ca^{2+} (up to 5g/l) concentrations on the permeability behaviour of sand bentonite mixture. Permeability increased with deflection, exceeding 10^{-7} cm/s when the intact layer was less than 50–60 mm thick. Bentonite-sand mixtures pre-soaked in Ca^{2+} solutions leaked under the settlement, while unsoaked mixtures did not, highlighting calcium's impact on swelling. Ion exchange converts Na-bentonite to Ca-bentonite when Ca^{2+} concentration is more than double Na^{+}, reducing swelling and increasing permeability.

Chai and Tao Fu (2020) investigated the influence of three chemical additives (NaCl, $CaCl_2$, and $FeCl_3$) of various concentrations (0.1-1.0 mol/L), on consolidation behaviour of slurry soil. They reported that the compression index (C_c) and hydraulic conductivity values were increased with an increase in concentration and cationic valence of chemical additives because of the diffuse double layer thickness was compressed due to chemical additives.

Ying et al. (2021) focused on the liquid limit and sediment behaviour of two soils; Na-bentonite (630 LL) and silty soil (29 LL) under the influence of NaCl solution at various percentage levels. They found that significant reduction in both sediment volume and liquid limit values at the higher percentage of NaCl solution with Na-bentonite clay, whereas they observed a reverse trend in both properties for silty soil. It is essential to understand the barrier material consolidation, strength, and permeability characteristics for landfill liner purposes.

Jadda and Bag (2020) investigated two distinct bentonites (monovalent and divalent) in the salt environment and discovered that hydraulic conductivity values of monovalent bentonite were increased about 76 times and 41 times for 1N NaCl and $CaCl_2$ electrolyte solutions,

TH-3665_186104109

respectively compared to distilled water. However, this increment was less in the case of divalent bentonite. Swelling pressures exhibited lower values with monovalent bentonites compared to divalent in the presence of salts.

Song et al. (2024) investigated the shear strength and microstructural behaviour of compacted bentonite utilizing two saturation methods: constant-vertical stress (CP) and constant-volume (CV). Findings revealed that shear strength increases with rising vertical stress and salt solution concentration. Samples prepared using CV method pronounced higher strength with distilled water, whereas samples prepared using CP method demonstrated higher strength with saline solutions.

Table 2.5. Summary of literature on salt solutions' interaction with clay.

Authors	Clay type	Salt solution type	Important findings
Petrov and Rowe (1997)	Bentonite	NaCl	▪ Hydraulic conductivity value increased from 10^{-9} to 10^{-6} cm/s for 2N concentration ▪ Liquid limit (LL) reduced from 530 to 96%
Shackelford et al. (2000)	Three different GCL's constituted bentonite as clay	NaCl & $CaCl_2$	▪ Hydraulic conductivity value increased significantly due to a low concentration of $CaCl_2$ and a high concentration of NaCl cations
Jo et al. (2001)	GCL constituted bentonite as clay (67% montmorillonite)	Monovalent, divalent, and trivalent cation solutions	▪ Hydraulic conductivity value increased with an increase in the valency of cations of pore fluid ▪ Stong base solutions pronounced less swelling values
Lee and Shackelford (2005)	Two bentonites	$CaCl_2$	▪ Hydraulic conductivity increased for high-quality bentonite compared to low-quality bentonite

TH-3665_186104109

Authors	Clay type	Salt solution type	Important findings
Mishra et al. (2005)	Basalt soil-bentonite mix	NaCl and $CaCl_2$	▪ Hydraulic conductivity values increased ▪ Liquid limit and compression index value decreased by increasing the concentration of salt solutions
Singh and Prasad (2007)	Bentonite	Aluminium hydroxide and acetic acid	▪ Differential free swelling decreased ▪ Hydraulic conductivity of bentonite decreased by 12% by aluminium hydroxide
Arasan et al. (2010)	Low plasticity and high plasticity clayey soils	KCl, $CaCl_2$, $FeCl_3$, and NH_4Cl	▪ Swelling pressures increased at 1M concentration for low plasticity clayey soil ▪ Swelling pressures decreased for high-plasticity soil
Shirazi et al. (2011)	Bentonite	NaCl	▪ LL decreased and plastic limit increased ▪ Swelling decreased
Shariatmadari et al. (2011)	Clay-bentonite mixture	NaCl, $CaCl_2$, and $MgCl_2$	▪ LL decreased ▪ MDD decreased ▪ Swelling volume decreased ▪ Hydraulic conductivity increased
Zhu et al. (2013)	GMZO1 Bentonite	NaCl and $CaCl_2$	▪ Swell pressures increased more by $CaCl_2$ permeant than NaCl ▪ Hydraulic conductivity increased more by NaCl than $CaCl_2$
Rao et al. (2013)	Black cotton soil	NaCl	▪ Swelling potentials decreased with an upsurge in concentration

TH-3665_186104109

Authors	Clay type	Salt solution type	Important findings
Dutta and Mishra (2015)	Two bentonites	NaCl and $CaCl_2$	▪ Free swelling, liquid limit, swelling pressure and swelling potential of the bentonites decreased ▪ Hydraulic conductivity increased
Zhang et al. (2016)	Bentonite-sand mixture	NaCl	▪ Liquid limit decreased ▪ Shear strength increased at high concentration
Dutta and Mishra (2016a)	Two bentonites	NaCl and $CaCl_2$	▪ Coefficient of compressibility (C_c), the time required for 90% consolidation (t_{90}) decreased with an increase in concentration ▪ Coefficient volume change (m_v) decreased
Xu et al. (2018)	Sand-bentonite mixture	$CaCl_2$	▪ Permeability increased ▪ Deflection increased ▪ Swelling properties reduced
Ramya et al. (2018)	Black cotton soil	NaCl	▪ MDD increased ▪ LL decreased ▪ Coefficient of compressibility decreased ▪ Hydraulic conductivity increased
Chai and Tao Fu (2020)	Marine clay	NaCl, $CaCl_2$, and $FeCl_3$	▪ Compression index (C_c) and hydraulic conductivity values increased with an increase in concentration and cationic valence
Jadda and Bag (2020)	Monovalent and divalent bentonites	NaCl and $CaCl_2$	▪ Free swell decreased ▪ Hydraulic conductivity increased ▪ Swelling pressures decreased ▪ Monovalent bentonite experienced significant variations than divalent bentonite at high concentrations

TH-3665_186104109

Authors	Clay type	Salt solution type	Important findings
Ying et al. (2021)	Two individual soils (Bentonite and silty soil)	NaCl	▪ LL, sediment volume increased with an increase in the percentage of NaCl solution for slity soils. ▪ For bentonite, these properties were reduced significantly
Song et al. (2024)	Bentonite	NaCl	▪ Shear strength raised with the hike in NaCl solution from 0.01 to 1.0M ▪ Aggregation of clay particles observed at high concentration

2.10. Sources and consequences of heavy metals in leachate

Heavy metals are frequently present in various waste streams, landfill leachates, and contribute significantly to contamination at hazardous waste sites. In municipal solid waste and residual agricultural waste, heavy metal concentrations typically range from 0 to 100 ppm, whereas in sewage sludge, mining waste, and industrial waste, concentrations can vary between 100 and 10,000 ppm (Yong and Perno, 1991). Landfill leachate typically contains heavy metals such as lead (Pb), cadmium (Cd), chromium (Cr), copper (Cu), nickel (Ni), iron (Fe), and selenium (Se). While the specific types and concentrations of heavy metals vary between landfills, their levels frequently exceed permissible limits, posing significant environmental and health risks. This underscores the need for stringent monitoring and advanced treatment strategies to mitigate the impact of these contaminants.

The presence of metal species in landfill leachate is a critical environmental concern due to the hazardous effects of heavy metals on the geo-environment. Unlike organic pollutants, heavy metals cannot be degraded or destroyed, and they often enter human and animal systems through food, water, and air. In trace amounts, certain heavy metals like copper, nickel, and zinc are essential for various biological functions, serving as catalysts in specific enzymatic reactions. However, when their concentrations exceed permissible limits, they can disrupt metabolic processes by binding indiscriminately to biomolecules and causing oxidative stress. This can lead to cellular damage, including membrane degradation and

TH-3665_186104109

DNA alterations (mutagenesis). Acute exposure to high levels of heavy metals can result in toxicity, while prolonged low-level exposure may trigger allergies, chronic illnesses, or even cancers. Heavy metals in the environment originate from various sources, including natural geological processes, industrial activities, agricultural practices, pharmaceutical waste, domestic effluents, and atmospheric deposition (He et al., 2005). Human exposure to heavy metals predominantly stems from anthropogenic activities, such as mining and smelting operations, industrial manufacturing and applications, as well as the utilization of metal-based compounds in domestic and agricultural settings (He et al., 2005; Casarett, 2008). Cadmium is widely utilized in various industrial processes, with significant applications in the production of alloys, pigments, and batteries (Wilson, 1988). While the use of cadmium in batteries has seen notable growth in recent years, other sources include emissions from paint pigments, batteries, industrial tools, and Cd-coated household waste, such as certain hand tools and home appliances, are the primary sources of cadmium content in landfills (Gujre et al., 2021). Elevated Cd levels in groundwater cause hazardous consequences on human health. These high quantities of cadmium trigger major health problems, including vomiting, severe stomach discomfort, bone fracture, infertility, and even damage to the central nervous system (which causes psychological disorders), as well as kidney and liver damage (Saha and Sanyal, 2010; Sobti and Singh, 2019). Likewise, lead is a major heavy metal frequently detected in leachates, primarily due to its extensive use in various industrial processes. The most prevalent sources of Pb in solid wastes are batteries, electronic goods, fertilizer and petrochemical wastes, and oil refineries, resulting in dangerous health effects such as diarrhea, anemia, and poisoning that causes brain, liver, and kidney failure (Gupt et al., 2020; Amiri et al., 2022). Excessive zinc exposure poses significant health risks to humans through inhalation, dermal contact, and ingestion, causing respiratory, gastrointestinal, and neurological issues, as well as increasing prostate cancer risk (Plum et al., 2010). Chromium contamination primarily originates from industrial waste sources such as tannery sludge, electroplating processes, and steel production. Hexavalent chromium [Cr(VI)], a particularly toxic form (due to its high water solubility), is frequently identified in landfill leachates (Zayed & Terry, 2003). This hexavalent chromium sources from various industrial activities such as dyes and pigments, wood and leather preservation, electroplating plants, and chromium slags, causing rhinitis, skin diseases, and cancer (Zhu and Liu, 2018; Yang et al., 2021). In landfills, Cr(VI) typically exists as anionic complexes such as Chromate (CrO_4^{2-}), Bichromate (Cr_2O^{7-}), and hydrogen chromate ($HCrO_4^-$) (Banchhor et al.,

TH-3665_186104109

2020; Yang et al., 2021). Considering their prevalence and toxicological significance, three heavy metals were chosen for evaluating leachate under varying concentrations: two cationic species, lead and cadmium, and one anionic species, hexavalent chromium. The following section provides a detailed review of the interactions between clay and heavy metals, highlighting key mechanisms and findings from existing literature.

2.11. Review of literature on heavy metals' interaction with clay

Li and Li (2001) examined the sorption of heavy metals and the hydraulic conductivity characteristics of three different bentonite-based mixtures: sand-bentonite, sand-bentonite-forest soil, and sand-bentonite-spruce bark. Their study, which focused on the presence of cadmium (Cd), lead (Pb), and copper (Cu), found that the forest soil mixture demonstrated the highest capacity for heavy metal retention. Also, they discovered a higher permeability behaviour for cadmium (4.5 times) and copper (2.5 times) compared to lead. Abollino et al. (2003) investigated the adsorption behaviour of heavy metals on Na-montmorillonite and found that the metal retention capacity decreases as pH levels drop. Lo et al. (2004) conducted batch sorption and column experiments to examine the transport of heavy metals in saturated sand and bentonite-soil mixtures. Their study demonstrated that, under an effective stress of 34.5 kPa, the permeability of compacted sand was approximately six orders of magnitude higher than that of the bentonite-soil mixture when permeated with solutions containing Pb, Zn, and Cd. Chalermyanont et al. (2009) examined the sorption capacity of two clayey soils (marine and lateritic) for various heavy metals (Pb, Cr, Cd, Ni, and Zn) at concentrations ranging from 0.0001 to 1M. They discovered that marine soil had a higher adsorption capacity than lateritic soil, with Cr having the highest adsorption capacity, followed by Pb, Cd, Ni, and Zn. Saha and Sanyal (2010) focused on cadmium metal removal from wastewater with the help of Indian expansive soil and observed that the soil was more effective in removing Cd from wastewater (90-95%) at a pH of 5.5. Du et al. (2015) carried out consolidation tests to assess the compressibility and hydraulic conductivity of clayey soil/calcium-bentonite backfills subjected to varying levels of lead (Pb) contamination. Their findings indicated that Pb-contaminated backfills exhibited a hydraulic conductivity increase by a factor of fifty compared to uncontaminated backfills. Additionally, as Pb concentration increased, there was a notable reduction in the liquid limit, compression index, and pH. Li et al. (2015) studied the hydraulic and mechanical performance of Chinese clay under Pb solutions ranging from 0 to 20,000 mg/L and noticed a 15 times higher permeability values and 1.6 times greater cohesion values at the maximum

TH-3665_186104109

lead solution concentration. Mohammed et al. (2016) evaluated the effectiveness of red earth soil (RS) and black cotton soil (BCS) in attenuating Cd(II) and Ni(II) from aqueous solutions using batch equilibrium tests. The Langmuir isotherm provided a better fit than the Freundlich isotherm. Results indicated that Cd had higher sorption than Ni in both soils, with BCS showing greater retention capacity than RS. Dutta and Mishra (2016b) investigated the impact of lead, copper, and zinc metal permeants on the performance of two bentonites. Substantial decline in free swell, liquid limit, and swelling pressure values observed at high concentrations. Experimental outcomes found a reduction in swelling potential values of higher quality bentonite of about 41.5, 38.9, and 36.4% for 1000 ppm lead, copper, and zinc solutions, respectively, compared to Deionized water (DI water). Li et al. (2017) conducted batch studies and permeability tests on shale-clay composite with different heavy metals. They found an increment in permeability (k) for higher shale content, and they found the highest adsorption capacity for shale-clay (10:90) composite was for Cd, followed by Cr, Pb, and Zn. Taheri et al. (2018) discovered a considerable decrement (68%) in cohesion value at the maximum Pb concentration (20 cmol/kg soil) with sand bentonite (80:20) mixture. Moghal et al. (2020) evaluated the effect of various heavy metal solutions at two different concentrations (i.e. 50 and 100 ppm) on the compressibility and strength behaviour of two expansive soils and observed an increase in the UCS values with a rise in all metal concentrations from 0 to 100 ppm. Fan et al. (2020) discovered lower swelling potentials for sodium bentonite with Cr (VI) solution than Pb-Zn solution at the same concentration. Yang et al. (2021) performed hydraulic conductivity tests on the soil-bentonite mix with a 1000 ppm concentration of Cr(VI) permeants and found a significant increment in permeability values. Ray et al. (2022a) studied the consolidation properties of Indian bentonite under the Pb permeants (0-1000 ppm) and observed that the co-efficient of compressibility (m_v) and time for 90% consolidation (t_{90}) values declined due to an increase in the Pb concentration from 0 to 1000 ppm. However, coefficient of consolidation (c_v) values increased at higher concentrations. The summary of this literature is presented in Table 2.6 below.

TH-3665_186104109

Table 2.6. Summary of literature on heavy metals' interaction with clay.

Authors	Clay type	Heavy metal type	Important findings
Li and Li (2001)	Sand-bentonite, sand-soil-bentonite, and sand-bentonite-spruce bark	Pb, Cd, and Cu	▪ Adsorption capacity decreased with a reduction in pH. ▪ Hydraulic conductivity increased with heavy metal concentrations ▪ Cd showed higher *k* than Pb
Abollino et al. (2003)	Bentonite	Cd, Cr, Pb, Mn, Ni, and Cu	▪ Retention capacity decreases with a decrease in pH
Lo et al. (2004)	Bentonite-soil and sand	Pb, Cd, and Zn	▪ Hydraulic conductivity of sand increased significantly than soil-bentonite mix
Chalermyanont et al. (2009)	Marine soil and lateritic soil	Pb, Cr, Cd, Ni, and Zn	▪ High adsorption capacity observed with marine soil than with lateritic soil
Saha and Sanyal (2010)	Indian expansive soil	Cd	▪ Good adsorption capacity of Cd from wastewater was observed at a pH of 5.5
Du et al. (2015)	Clayey soil-calcium-bentonite	Pb	▪ LL, compression index, and hydraulic conductivity decreased with Pb solutions
Li et al. (2015)	Chinese clay	Pb	▪ Permeability decreased with a rise in the concentration of lead ▪ Cohesion value increased
Mohammed et al. (2016)	Red soil and black cotton soil	Cd and Ni	▪ Higher retention capacity observed with black cotton soil than with red soil
Dutta and Mishra (2016b)	Two bentonites	Pb, Cu, and Zn	▪ Free swell and LL decreased ▪ Swelling pressure and swelling potentials reduced at higher concentrations

TH-3665_186104109

Authors	Clay type	Heavy metal type	Important findings
Li et al. (2017)	Shale-clay (10:90) mix	Pb, Cd, Cr, and Zn	▪ Permeability is directly proportional to the addition of shale content ▪ Highest adsorption capacity observed with Cd followed by Cr, Pb, and Zn
Taheri et al. (2018)	Sand-bentonite (80:10) mix	Pb	▪ Cohesion and permeability increased at maximum concentration
Moghal et al. (2020)	Two expansive soils	Pb, As, Cr, Cu, Hg, and Zn	▪ Low liquid limit soil showed higher compression index at higher concentrations ▪ UCS increased at higher concentrations for two soils
Fan et al. (2020)	Polymer-treated sodium-activated calcium bentonite	Pb-Zn mix and Cr(VI)	▪ Swell index decreased at higher concentrations of Cr(VI) than Pb-Zn ▪ Hydraulic conductivity values increased
Yang et al. (2021)	Polymerized calcium bentonite	Cr(VI)	▪ Hydraulic conductivity raised ▪ Compression index reduced marginally
Ray et al. (2022c)	Bentonite	Pb	▪ Co-efficient of compressibility and time for 90% consolidation values declined ▪ Coefficient of consolidation values raised

2.12. Review of literature on leachates' interaction with clay

In the past, few studies on both real and synthetic leachates have investigated their impact on barrier materials, focusing on the influence of various constituents on hydromechanical behavior and sorption characteristics. Ruhl and Daniel (1997) carried out experiments to assess the effects of both simulated and real MSW leachate on geosynthetic clay liners (GCLs). Their findings indicated that hydraulic conductivity was greater when exposed to simulated MSW leachate compared to real MSW leachate. Shan et al. (2002) examined the

TH-3665_186104109

influence of real MSW along with other individual pore fluids on the hydraulic conductivity of geosynthetic clay liners (GCLs). Results showed that both the hydrating and permeating liquids significantly affect GCL performance. They reported a significant reduction in the free swell and hydraulic conductivity values of bentonite with MSW leachate. Pivato and Raga (2006) examined the attenuation of ammonium from MSW landfill leachate and its impact on the sorption capacity of bentonite. Their study revealed that bentonite exhibits a high capacity for ammonium sorption. Bouazza et al. (2013) examined the effects of highly acidic leachates on needle-punched geosynthetic clay liners (GCLs) and observed that hydraulic conductivity increased as leachate concentration intensified. Xue and Zhang (2014) assessed the impact of landfill leachate concentration on the degradation of solidified clay liners. Results showed that higher leachate concentrations led to a significant reduction in unconfined compressive strength and an increase in hydraulic conductivity. The leachate altered the clay's compact structure, increasing large pore proportions while reducing medium and micropores, making the material more prone to deformation. Chen et al. (2018) investigated the impact of synthetic coal combustion product leachate on the hydraulic conductivity of geosynthetic clay liners (GCLs). Their findings indicated that pre-permeating GCLs with deionized (DI) water before introducing leachate resulted in hydraulic conductivity increasing by as much as threefold. Shariatmadari et al. (2018) investigated the impact of landfill leachate on the geotechnical properties of contaminated soils near dump sites in Iran. Results showed that higher leachate concentrations led to a reduction in uniaxial shear strength and corresponding strains. Also, it was noticed a decline in cohesion and permeability coefficient. Demdoum et al. (2020) examined the compressibility, hydraulic conductivity, shear strength, and chemical properties of compacted bentonite-geomaterial mixtures for landfill bottom liners in the presence of MSW landfill leachate. Findings indicated that leachate lowered compressibility and hydraulic conductivity while enhancing compressive and tensile strength. Shear strength increased with higher calcareous sand content, with contaminated mixtures exhibiting greater cohesion and a reduced friction angle. The $B_{10}CS_{20}T_{70}$ mixture (10% bentonite, 20% calcareous sand, 70% tuff) was identified as the most effective option for landfill liner applications. Ray et al. (2022) evaluated the impact of fly ash, sewage sludge, and paper mill leachates on two Indian bentonites with different mineralogical compositions. Results showed that liquid limit, free swell, swelling potential, swelling pressure, shear strength, and consolidation parameters decreased, while hydraulic conductivity and the coefficient of consolidation increased.

TH-3665_186104109

Bentonite with higher cation exchange capacity (CEC) and swelling ability experienced greater variations in these properties. Among the leachates, fly ash leachate caused the most significant changes in bentonite behavior.

Table 2. Summary of literature on leachates' interaction with clay.

Authors	Clay type	Leachate type	Important findings
Ruhl and Daniel (1997)	Geosynthetic clay liner	Simulated and real MSW	▪ Real MSW leachate exhibited lower aggressiveness in the rise of *k* values compared to simulated MSW leachate
Shan et al. (2002)	Geosynthetic clay liner	Real MSW, acidic water, saline water, and Gasoline	▪ Free swell index reduced up to 50% with MSW ▪ Hydraulic conductivity increased
Pivato and Raga (2006)	Bentonite	Real MSW	▪ Bentonite exhibits a high capacity for ammonium sorption.
Bouazza et al. (2013)	Geosynthetic clay liner	Strong acidic synthetic leachate	▪ Hydraulic conductivity increased
Xue and Zhang (2014)	Medium compressibility clay	Real MSW	▪ UCS decreased ▪ Hydraulic conductivity increased
Chen et al. (2018)	Geosynthetic clay liner	Synthetic leachate of coal combustion	▪ Hydraulic conductivity increased up to 3 times than DI water
Shariatmadari et al. (2018)	Low-plasticity clayey soil	Real MSW leachate	▪ Permeability reduced ▪ UCS reduced ▪ Volumetric strains increased
Demdoum et al. (2020)	Benoite-geomaterials mix	Real MSW leachate	▪ Shear strength increased ▪ Compressibility and angle of internal friction lowered ▪ Permeability decreased

TH-3665_186104109

Authors	Clay type	Leachate type	Important findings
Ray et al. (2022b)	Two bentonites	Synthetic leachates (Fly ash, Papermill, and sewage sludge)	▪ Permeability and coefficient of consolidation increased ▪ Swelling potential and LL decreased ▪ Fly ash leachate is more influential compared to others

2.13. Critical analysis of the reviewed literature

The integration of compacted clay barriers within landfill containment systems is essential to mitigate the environmental and geotechnical challenges posed by uncontrolled solid waste disposal. The stability of engineered barriers is governed by key geotechnical and physicochemical properties, including exceptional swelling capacity, extremely low hydraulic conductivity, optimal shear strength, superior adsorption potential, and minimal volumetric shrinkage, ensuring long-term integrity and performance in waste containment systems. The literature indicates that bentonite is widely preferred as a landfill liner due to its high absorption capacity and low hydraulic conductivity. However, its availability in India is primarily restricted to Rajasthan, making frequent imports costly, necessitating the exploration of more cost-effective alternatives for landfill applications. The BC soil, naturally abundant in montmorillonite, exhibits high swelling potential and low hydraulic conductivity, making it a promising alternative for landfill liners and it spans over one-fifth of India's total land area soil. The BC soil is highly susceptible to shrinkage due to its expansive nature. The literature review provides substantial evidence that waste tire fibr

es effectively mitigate shrinkage potential and enhance the cracking resistance of barrier materials (Narani et al., 2020; Mukherjee & Mishra, 2021). However, extensive literature analysis reveals that waste tire fibres significantly influence the hydromechanical properties of barrier materials, leading to notable variations in their performance. Therefore, a comprehensive understanding of the geotechnical properties of BC soil mixed with tire fibres is essential for optimizing its performance as a hydraulic barrier.

The reviewed literature indicates that the presence of various chemicals in leachate significantly impacts geotechnical properties, including swelling, consolidation, hydraulic conductivity, and shear strength. These alterations are primarily attributed to the shrinkage

TH-3665_186104109

of the diffuse double layer, influenced by the cationic composition of the leachate, which affects soil structure and behaviour. The variations in the geotechnical properties of barrier materials are influenced by soil type, mineralogical composition, and cation exchange capacity. The literature review highlights that inorganic salts and heavy metals in landfill leachate are key contributors to the deterioration and compromised effectiveness of liner materials. Therefore, a comprehensive evaluation of barrier materials is necessary under varying concentrations, cationic compositions, and valence states of salts and heavy metals to ensure their long-term stability and functional integrity.

2.14. Research gap and objectives of the study

In this study, BC soil incorporated with waste tire fibres was chosen as a barrier material for landfill barrer application. The literature survey emphasizes that, despite effective shrinkage control, the incorporation of waste tire fibres induces notable changes in the engineering properties of landfill liners. Numerous studies have examined the impact of tire content on bentonite and sand-bentonite mixtures for geoenvironmental applications. However, limited knowledge is available on the impact of waste tire content on the engineering behaviour of BC soil. Also, extensive literature is available on the influence of inorganic salts on various bentonite types and sand-bentonite mixtures. However, research on their effects on Black Cotton (BC) soils remains limited. Therefore, a comprehensive investigation into the effects of inorganic salt concentrations, cationic composition, and valence states on the engineering behavior of BC soil is crucial for ensuring its suitability in geoenvironmental applications.

Given the significant concern of heavy metal accumulation in landfills, it is imperative to investigate the effects of individual metal species at elevated concentrations on barrier material properties. A thorough understanding of the influence of metal type, concentration, and valency is essential for assessing their impact on the geotechnical performance and long-term stability of landfill barriers. However, most of the researchers focused on divalent and trivalent heavy metal concentrations on the adsorption and hydraulic behaviour of bentonites and sand bentonite mixtures. However, understanding the impact of hexavalent heavy metals, such as Cr(VI), on the engineering behavior of barrier materials is crucial, as its accumulation in landfills is both highly toxic and significant. Also, no detailed literature is available on the influence of heavy metal concentrations on the geotechnical properties like swelling, compressibility, and hydraulic conductivity of BC soil.

TH-3665_186104109

Although several studies have investigated fibre-mixed soil composites and recommended them for use as barrier materials, there remains a research gap regarding the impact of leachate interaction on these fibre-mixed soils. Due to the high surface roughness of tire fibres, a detailed analysis of the influence of inorganic salts and heavy metals on the fluid transport mechanisms in fibre-mixed soils is critical for understanding their hydromechanical behavior. However, no study has been done on the influence of various chemical permeants on the hydromechanical behaviour of fibre-mixed BC soil for barrier application in landfills.

The reviewed of the literature suggested that it is important to understand the barrier material behaviour under the influence of real and synthetic leachates to simulate the field condition and understand the overall chemical compatibility of the barrier material. However, comprehensive studies on the influence of leachates on the hydraulic, consolidation, and compressibility characteristics of Black Cotton (BC) soil and fibre-mixed soils remain unexplored.

Therefore, the main objective of the present study is to examine the influence of various inorganic salts, heavy metals, and leachates on the engineering behaviour of fibre-mixed black cotton soil. To achieve this objective, the detailed scopes of the present study are:

I. To study the influence of waste tire fibres (0, 5, 10, and 15% by weight) on the engineering behaviour of black cotton soil. (Compaction, swelling, consolidation, hydraulic, and unconfined compressive strength (UCS)).
II. To study the effect of various concentrations of inorganic salt solutions (NaCl and $CaCl_2$) on the swelling, consolidation, hydraulic conductivity, and UCS of fibre-mixed black cotton soil samples.
III. To study the effect of various concentrations of heavy metals (Pb(II), Cd(II), Cr(VI)) on the engineering behaviour of fibre-mixed black cotton soil samples.
IV. To study the hydro-mechanical behaviour of fibre-mixed black cotton soil samples under the influence of both synthetic municipal solid waste and fly ash leachates.

TH-3665_186104109

CHAPTER 3

MATERIALS AND METHODOLOGY

3.1. General

This chapter provides a comprehensive explanation of the materials utilized and experimental methodologies employed to conduct the research. The methods for determining the swelling pressure, swelling potential and hydraulic conductivity from one-dimensional consolidation experiments have also been described.

3.2. Plan of research work

To accomplish the objectives of the current investigation, the complete research was conducted in four phases, as shown below. Figure 3.1 illustrates the overarching objective and its division into constituent phases.

Phase I deals with gathering the materials and analyzing their basic characteristics. In addition, this phase investigated the influence of tire content on the engineering properties of BC soil in the presence of DI water, including compaction, swelling, consolidation, compressibility, hydraulic conductivity, and unconfined compressive strength (UCS).

In **Phase II**, index properties like Atterberg limits and free swell index of BC soil were determined in the presence of monovalent (NaCl) and divalent ($CaCl_2$) inorganic salt solutions at two different concentrations (0.1 and 1N), including DI water. Then, a series of consolidation experiments were conducted on all fibre-mixed soil samples (0, 5, 10, and 15%) inundated with salt permeants to evaluate the change in their swelling, consolidation, hydraulic, and compressibility properties. The UCS behaviour of all fibre-mixed soil samples was also examined in the presence of inorganic salt permeants by performing laboratory experiments.

Phase III deals with the influence of heavy metals [Pb(II), Cd(II), and Cr(VI)] on index properties of BC soil at three different concentrations (100, 500 and 1000 ppm). In this phase, laboratory studies also assessed and compared the engineering properties of all fibre-mixed soil samples (consolidation, hydraulic conductivity, compressibility, and shear strength).

TH-3665_186104109

Fig. 3.1. Research design.

TH-3665_186104109

The investigation and comparison of **Phase IV** focused on the impact of two synthetic leachates (MSW and fly ash) on the Atterberg limits, the free swelling behaviour of BC soil, and their impact on the engineering behaviour of fibre-mixed soil samples.

3.3. Collection of BC soil and its characterization

For this research work the BC soil was collected from the East Godavari district in Andhra Pradesh state, India. To prevent the presence of organic matter and roots, the soil was excavated 1.5 meters below ground level. The collected soil sample was pulverized, and a 425µ passing sample [Fig. 3.1(a)] was employed throughout this work. Table 3.1 lists the physical properties of BC soil and the proportion of clay content [Fig. 3.1(b)] in the soil was assessed using hydrometer analysis in accordance with ASTM D422 (2007). As per ASTM D854 (2014) and ASTM D4318 (2010), the specific gravity and Atterberg limits of BC soil were determined. The organic content of BC soil was determined as per ASTM D2974 (2020), Method A.

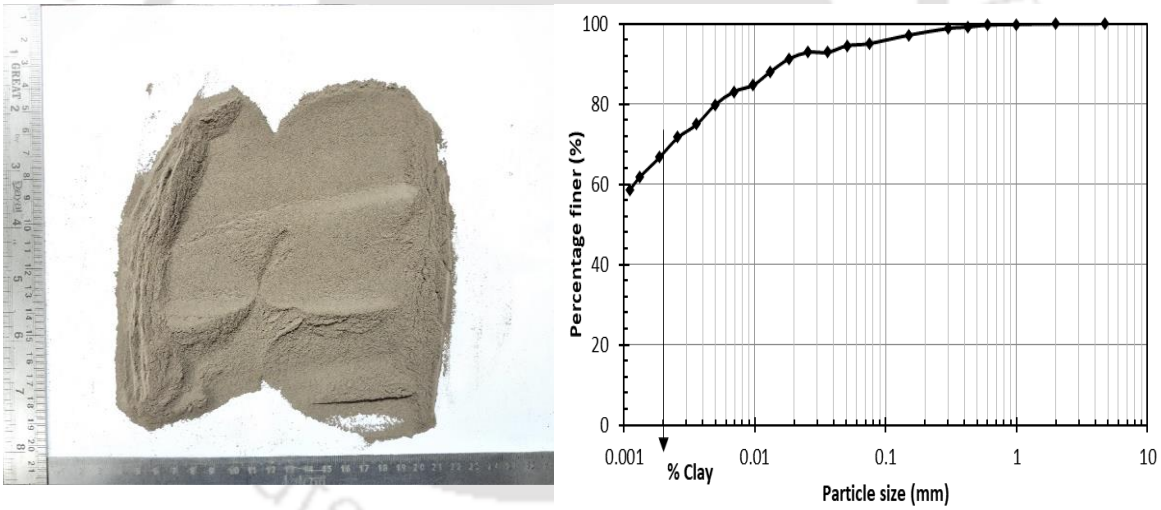

(a) (b)

Fig. 3.2. (a) BC soil used in this study; (b) Particle size distribution curve of BC soil.

Microstructural analyses were conducted on BC soil to identify important properties like mineralogy, primary elements, morphology, functional groups, elemental composition, and change in mass over temperature changes. X-ray diffraction (XRD) technique was used to identify the basic minerals present in the BC soil with a step size of 0.02° from 3° to 70°. The XRD image of BC soil was represented in Fig. 3.2(a), and Montmorillonite $[Na, Ca)_{0.3}$ $(Al, Mg)_2$ Si_4O_{10} $(OH)_2.xH_2O)]$, Quartz $[SiO_2]$, and Calcite $[CaCO_3]$ are the prevalent

TH-3665_186104109

minerals observed in BC soil. The montmorillonite content in BC soil was found to be 42.6%. The Energy dispersive X-ray (EDX) technique was carried out to determine the major elements present in BC soil. The plot in Fig. 1 indicates the presence of Oxygen, Silicon, and Iron in significant amounts, followed by traces of Aluminium, Magnesium, Potassium, etc., as displayed in Fig. 3.2(b).

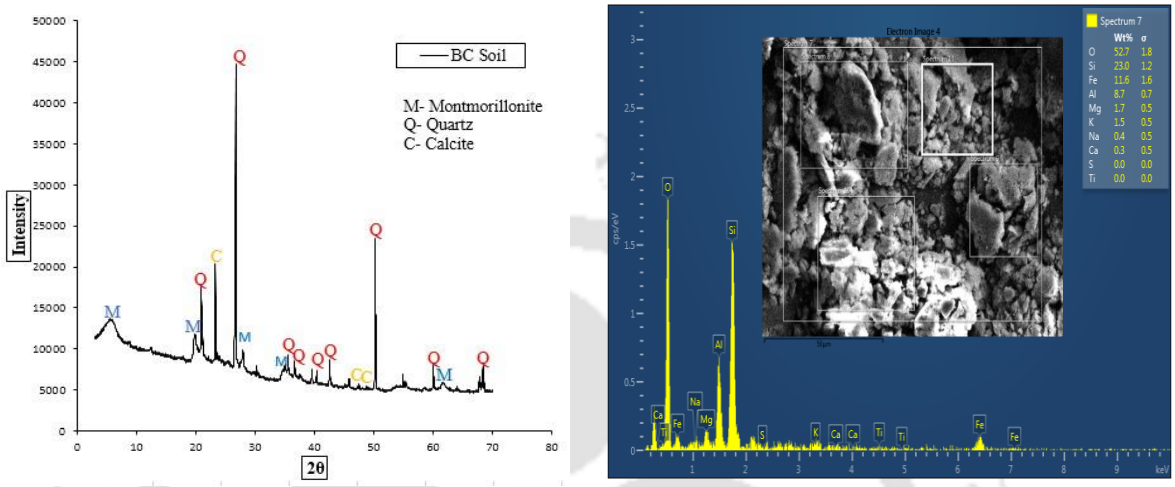

(a) (b)

Fig. 3.3. (a) XRD analysis of BC soil; (b) EDX analysis of BC soil.

Table 3.2 represents the elemental composition of BC soil determined by performing the X-ray fluorescence (XRF) analysis. Fourier transform infrared spectroscopy (FTIR) analysis was conducted on BC soil at ambient temperature by keeping the spectral range 4000-400 cm^{-1} to determine the important functional groups of soil. The broad patterns of Si-O observed in the infra ray spectroscopy investigations of BC soil suggested the presence of quartz, as depicted in Fig. 3.4. The presence of stretching vibration bands at 3400-3800 cm^{-1} indicates the potential for O–H stretching vibration of the silanol (Si-OH) groups in BC soil. The surface morphology of BC soil was observed by conducting Field emission scanning electron microscopy (FESEM) (Sigma, Germany) on soil. Before performing the test, the dry BC soil sample was kept in an oven at 60°C for one day to avoid charge since it was moisture-sensitive. Then, the sample was placed on aluminium stubs with the help of carbon tabe. Finally, the gold coating was applied to the sample using a sputter coater prior to analysis. The plot in Fig. 3.5(a) illustrates the FESEM of BC soil, which exhibited a flaky-shaped structure as a result of the presence of montmorillonite mineral (Mitche and Soga, 2005). Thermogravimetric analysis (TGA) was done on BC soil, which would show the

TH-3665_186104109

thermal resistance of soil by measuring the variation in mass due to changes in temperature levels.

Table 3.1. Properties of BC soil used in this study

Property	Black cotton soil
Liquid limit	85%
Plastic limit	38%
Plasticity index	47%
Shrinkage limit	10%
Specific gravity	2.59
Free swell index	196%
Clay content	68%
Silt content	22.7%
Sand content	9.3%
USCS classification	High plasticity clay (CH)
Organic content	2.63%
Montmorillonite content	42.6%
pH	8.5

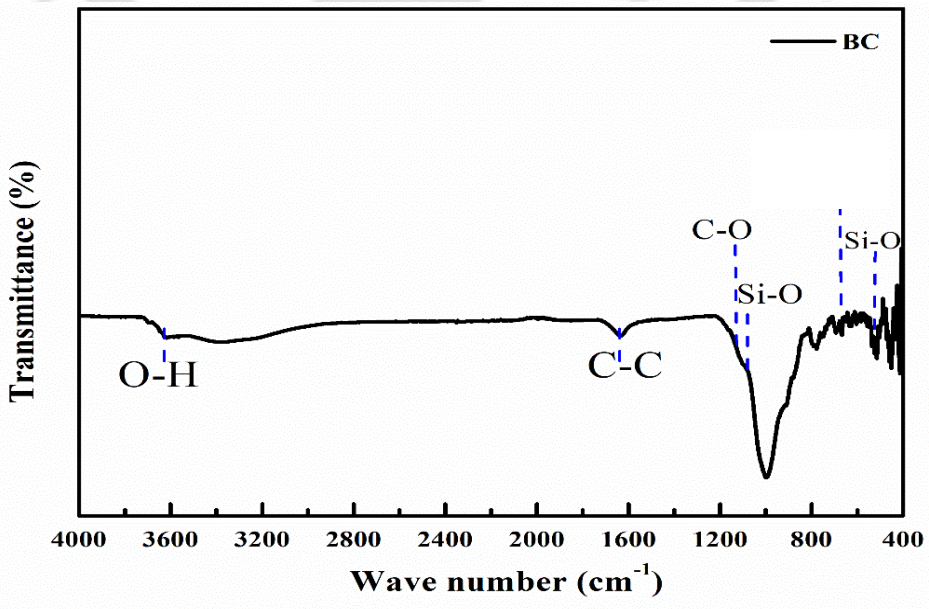

Fig. 3.4. FTIR analysis of BC soil.

TH-3665_186104109

Table 3.2. XRF result of BC soil

Element oxides	BC soil
SiO_2	51.69%
Al_2O_3	13.29%
Fe_2O_3	16.12%
MnO	0.14%
MgO	2.50%
CaO	1.16%
Na_2O	1.04%
K_2O	1.66%
TiO_2	1.42%
P_2O_5	0.18%

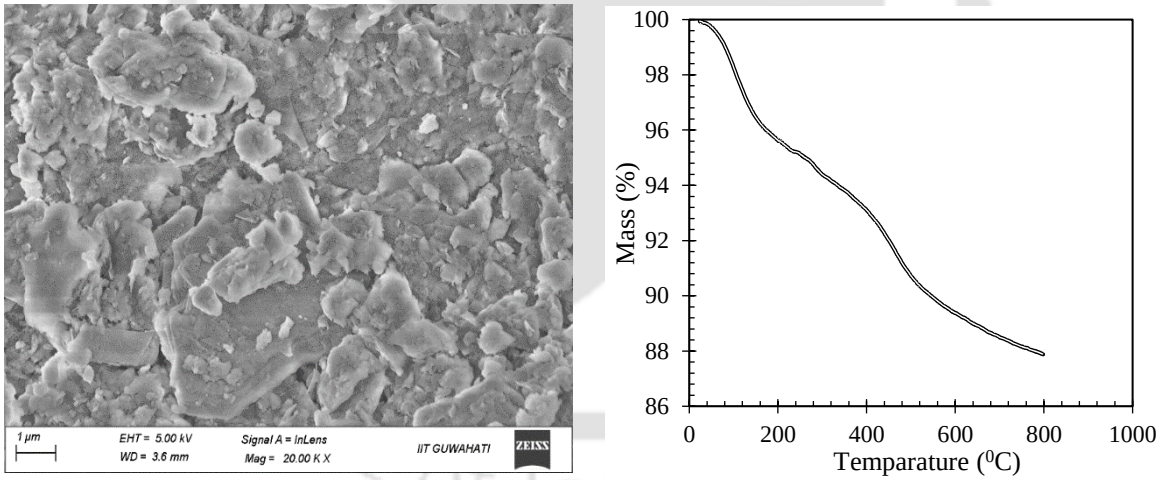

(a) (b)

Fig. 3.5. (a) FESEM image of BCS at 20000 x magnification; (b) TGA curve of BC soil.

In this test, a dry soil sample was placed into a crucible made of ceramic, and the temperature was raised at the level of 20°C/min from room temperature to 800°C. It was observed that there was a mass loss rate of around 12.1% at 800°C, as shown in Fig. 3.5(b). However, this TGA curve of BC soil was comparable with the TGA curve of sodium bentonite at maximum temperatures (Bandipally et al., 2018).

TH-3665_186104109

3.4. Tire fibre and its characterization

Tire fibres [Fig. 3.6(b)] used in this investigation of size 4.75 mm was passing and retained on a 2 mm sieve [Fig. 3.6(a)]. The water absorption capacity was found to be 3.57% as per ASTM D6270 (2008), and the specific gravity of tire fibres was determined as 1.15. These tire fibres were supplied from the local market and produced as a byproduct of waste tire treatment. The tire fibres adopted in this research exhibited an average diameter of around 2.6 mm and an average length of around 13.1 mm.

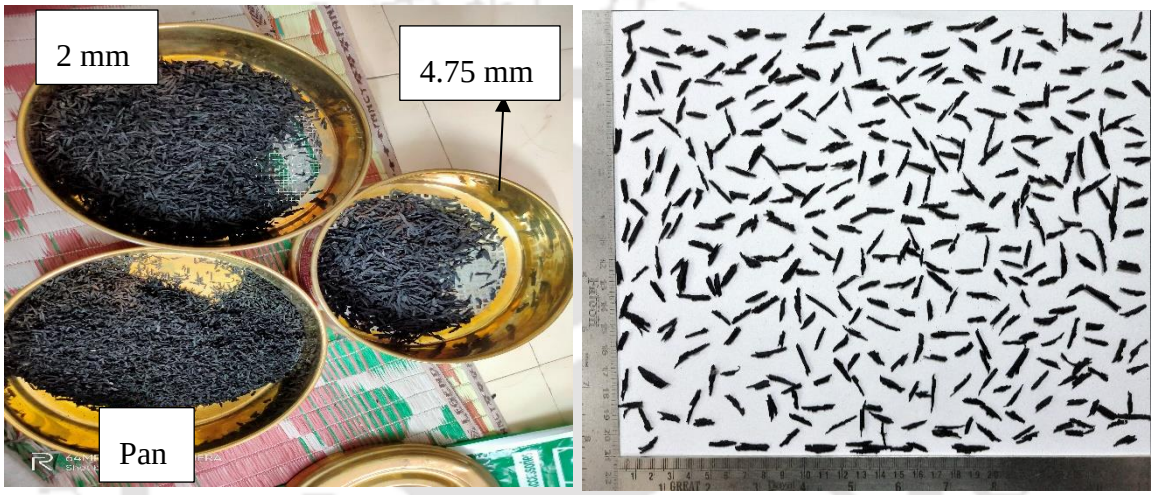

Fig. 3.6. Tire fibres used in this research.

EDX analysis was performed on single tire fibre as shown in Fig. 3.7(a), to determine the main elements present in the fibre. Different photographs were taken with respect to different locations marked in square boxes for identification of elements present in that particular location, shown in Fig. 3.7(a). Table 3.3 represents the elemental list of single tire fibre with respect to spectrum 1. FESEM analysis was carried out on single tire fibre, and the image is shown in Fig. 3.7(b). Uneven surface and micro cracks were observed from the FESEM output. The tire fibres are affixed to the soil because of the uneven surface, which mobilizes their tensile strength to form the ductile tire fibre-soil composite. The surface area of the fibre is intended to generate a more substantial interaction between the tire and the soil as a result of the uneven surface (Yadav and Tiwari 2017). Also, FTIR analysis was done on fibre to understand about the functional groups present in it. The FTIR plot was shown in Fig. 3.8(a), keeping the spectral range of 4000-400 cm^{-1} representing critical functional groups such as carbonyl groups (C-O stretching), carbon-carbon bond (C-C stretching), and hydro-carbon bond (C-H stretching). TGA analysis was performed on waste tire fibres at the heating

TH-3665_186104109

level of 20°C/min ranging from room temperature to 800°C, and the plot is shown in Fig. 3.8(b). A gradual mass loss rate (100 to 84.6%) was observed from ambient temperature to 370°C. However, an exponential mass loss rate (84.6 to 3.81%) was observed from 370°C to 608°C, as depicted in Fig. 3.8(b).

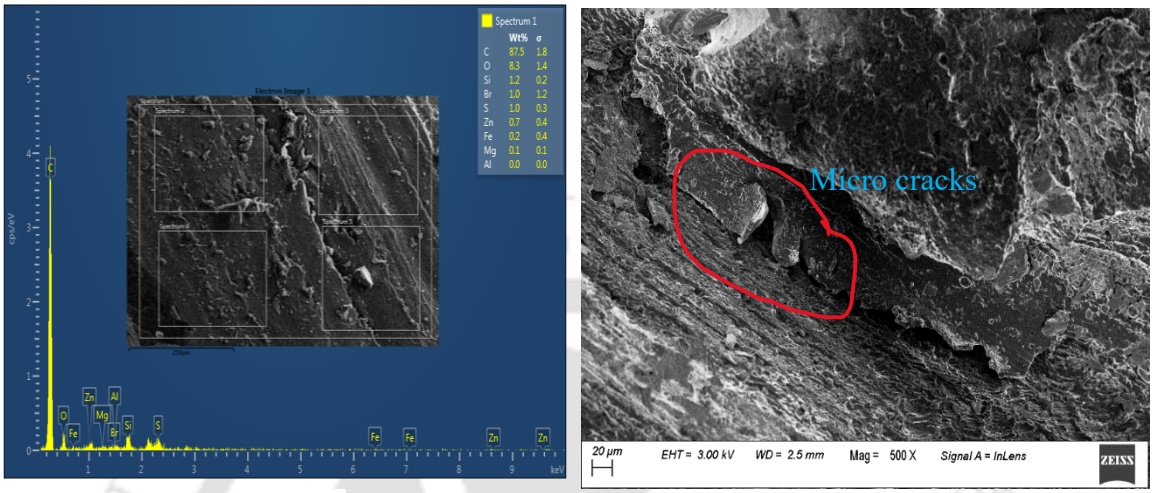

(a) (b)

Fig. 3.7. (a) EDX analysis of tire fibre; (b) FESEM analysis of tire fibre.

Table 3.3. Elemental analysis of single tire fibre

Element	Percentage
Carbon (C)	87.5
Oxygen (O)	8.3
Silicon (Si)	1.2
Bromine (B)	1.0
Zinc (Zn)	0.7
Iron (Fe)	0.2
Magnesium (Mg)	0.1

TH-3665_186104109

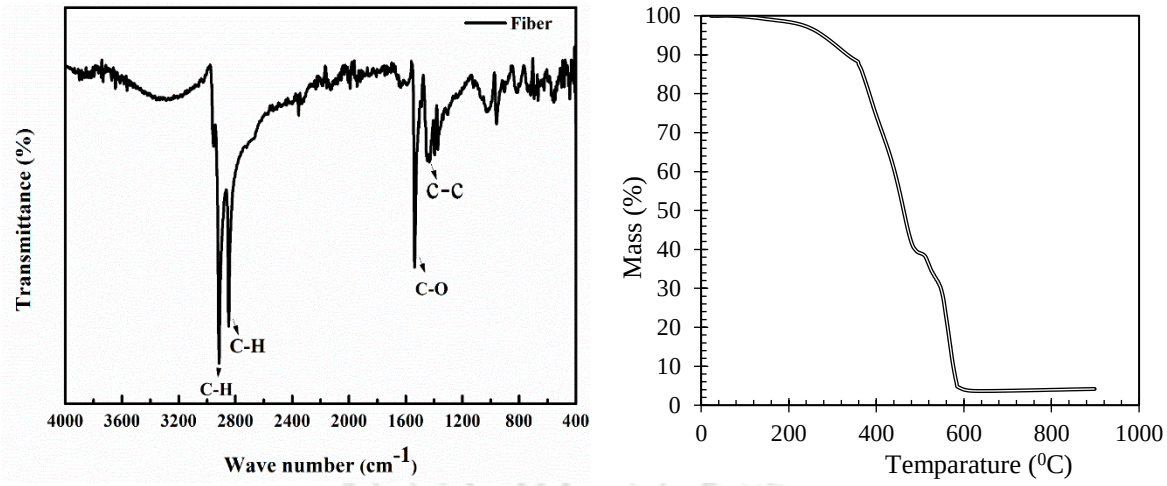

(a) (b)

Fig. 3.8. (a) FTIR analysis of tire fibre; (b) TGA analysis of tire fibre.

3.5. Permeant solutions

In this research, inorganic salts, heavy metals, and synthetic leachates were chosen as permeant liquids in order to test the barrier material in severe conditions. A detailed description of the permeant solution type, concentration, and preparation is mentioned in the section below.

3.5.1. Inorganic salt solutions

A substantial quantity of municipal solid waste, which is disposed of in landfills, contains cations such as Ca^{2+} and Na^{+} (Mishra et al., 2005). Therefore, monovalent (NaCl) and divalent ($CaCl_2$) salts were employed in this study. The salt solutions were prepared by dissolving the salts (i.e. NaCl and $CaCl_2$) in one litre of deionized (DI) water. The concentrations of the solutions used in these investigations were 0 (DI water), 0.1, and 1N, as indicated by the previously cited literature (Mishra et al., 2005; Dutta and Mishra, 2015; Jadda and Bag, 2020; Rout and Singh, 2020). The chemicals were acquired from Merck Life Science, Mumbai, India, and possess a purity level exceeding 99%.

3.5.2. Heavy metal solutions

Lead [Pb (II)], cadmium [Cd (II)], and hexavalent chromium [Cr (VI)] were considered for this study because these are the most common heavy metals identified in landfill leachate, according to prior investigations (Prudent et al., 1996; Chalermyanont et al., 2009; Sobti and

TH-3665_186104109

Singh, 2019; Fan et al., 2020). The requisite quantities of cadmium nitrate tetrahydrate [$Cd(NO_3)_2.4H_2O$], lead nitrate [$Pb(NO_3)_2$], and potassium dichromate [$K_2Cr_2O_7$] were dissolved in DI water to produce metal stock solutions. The needed concentrations of standard metal solutions were achieved by dissolving stock metal solutions in one litre of DI water. Based on previous research (Glatstein and Francisca, 2015; Dutta and Mishra, 2016b; Li et al., 2017; Gupt et al., 2020; Yang et al., 2021), the concentrations of metal solutions in the current investigation varied from 100 to 1,000 ppm in order to examine the worst-case scenario. The chemicals utilized in this work had purity levels above 99% and were purchased from Merk Life Science Private Limited, Mumbai. The molecular weights for cadmium nitrate tetrahydrate, lead nitrate and potassium dichromate were 308.47 g/mol, 331.20 g/mol, and 294.19 g/mol, respectively. The electrical conductivity (EC) of 1000 ppm stock solutions of Pb(II), Cd(II), and Cr(VI) was recorded as 1.3 mS/cm, 2.1 mS/cm, and 2.7 mS/cm, respectively. Similarly, the pH values of these 1000 ppm solutions were recorded as 4.74, 5.30, and 4.23, respectively, for the same order of metals.

3.5.3. Synthetic leachates

The initial focus of this research was on the impact of individual salt/heavy metal permeants on the engineering behaviour of barrier material as a result of salt/heavy metal permeants, which varied in concentration from low to extreme. However, leachate constitutes numerous other heavy metals, salts, biological spices and microbes in field conditions. Therefore, it is essential to examine the barrier material under leachate conditions. In this instance, we attempted to replicate the leachate effect by utilizing the salts and heavy metal concentrations present at the highest levels in leachates, which are referred to as synthetic leachates. However, it is challenging to replicate absolute actual field conditions, so we endeavour to create a laboratory-scale study that closely resembles real field investigations of the leachates. These synthetic leachates were prepared by reviewing past literature surveys.

In this work, two leachates, synthetic MSW leachate and fly ash leachate, were considered due to their familiarity and impact on the environment and human health. Additionally, prior research has indicated that fly ash leachate had a significantly greater impact on hydraulic behaviour than sewage sediment leachate and paper mill leachate (Ray et al., 2022(b)). Therefore, this research was focused on fly ash synthetic leachate to examine the worst-case scenario. The compositions of both leachates are mentioned in Tables 3.4 and 3.5 and prepared by dissolving the required amount of salts in 1 L DI water. The pH and electrical

TH-3665_186104109

conductivity (EC) of DI water are 6.64 and 3µS/cm, respectively. Synthetic MSW leachate contained Ca, Mg, and Fe as leading salts, whereas fly ash leachate was abundant in Zn, Pb, and Cu. The pH values of the synthetic municipal solid waste (MSW) and fly ash leachates were found to be 4.71 and 3.68, respectively, indicating that both leachates are acidic. The electrical conductivity (EC) values for these leachates were recorded at 22 mS/cm for the MSW leachate and 38 mS/cm for the fly ash leachate, suggesting that both leachates contain a high concentration of dissolved ions.

Table 3.4. Composition of synthetic MSW leachate

Constituents	Salts used	Concentration (mg/L)	References
Ca (II)	$CaCl_2$	3324.0	Tatsi and Zouboulis, (2002); Ray et al., (2021(a))
Mg (II)	$MgCl_2.6H_2O$	443.0	
Fe (II)	$FeCl_3$	160.0	
Zn (II)	$Zn(NO_3)_2.6H_2O$	36.0	
Mn (II)	$MnSO_4.H_2O$	16.2	
Ni (II)	$NiCl_2.6H_2O$	7.8	
Cd (II)	$Cd(NO_3)_2.4H_2O$	6.5	
Cu (II)	$CuCl_2.2H_2O$	6.0	
Pb (II)	$Pb(NO_3)_2$	2.1	

Table 3.5. Composition of synthetic MSW leachate

Constituents	Salts used	Concentration (mg/L)	References
Zn (II)	$Zn(NO_3)_2.6H_2O$	13044.0	Li et al., (2007); Ray et al., (2022(b))
Pb (II)	$Pb(NO_3)_2$	3655.3	
Cu (II)	$CuCl_2.2H_2O$	886.2	
Cd (II)	$Cd(NO_3)_2.4H_2O$	123.8	
Ni (II)	$NiCl_2.6H_2O$	26.9	

TH-3665_186104109

3.6. Preparation of BC soil-tire fibre mix

In this study, BC soil was mixed with 5, 10, and 15% of waste tire fibre by their dry weight. The concentration levels of fibres were chosen based on the past literature survey (Srivastava et al., 2014; Tajdini et al., 2016; Mukherjee and Mishra, 2019). Tire fibres comprise a compound that includes styrene-butadiene, polyisoprene, polybutadiene, and elastomers (Trouzine et al., 2012). However, fibres utilized in this study were produced from waste tire retreading operations, which would be useful in geotechnical and geoenvironmental applications.

Usually, tire fibres are light in weight due to their low specific gravity and tangle together. Therefore, proper care was taken while mixing of various concentrations of fibres with BC soil to maintain uniform distribution throughout the work. After the uniform distribution of fibres into BC soil (Fig. 3.9), the samples were mixed with varying water contents and stored in a moisture control desiccator for one day to attain moisture equilibrium. The compaction parameters of the samples were subsequently determined following the completion of moisture equilibrium. However, the testing methodology section provided a comprehensive description of the compaction test procedure. The theoretical specific gravity of each mix was determined as per the following equation;

$$G_c = \frac{M_s + M_t}{\left(\frac{M_s}{G_s}\right) + \left(\frac{M_t}{G_t}\right)} \quad \text{(Trouzine et al., 2012)} \tag{3.1}$$

Where M_s = Mass of soil; M_t = Mass of tire fibre; G_s = Specific gravity of soil;

G_t = Specific gravity of tire fibre; G_c = Specific gravity of soil-fibre composite.

TH-3665_186104109

Fig. 3.9. BC soil-tire fibre mix.

It could be seen that the soil-fibre composite's specific gravity decreased as the fibre content increased, a phenomenon that had been observed by a few other researchers in the past (Trouzine et al., 2012; Soltani et al., 2019).

3.7. Testing Methodology

In this section, the testing procedures of swelling pressures, swelling potentials, consolidation, and unconfined compressive strength were explained in detailed. However brief description was given about other methodologies like compaction characteristics, consistency limits, and free swell index as well.

3.7.1. Free swell index determination

The Free swell index (FSI) of BC soil was calculated as per IS 2720-40 (BIS 1977). Before performing the experiment, the soil sample was kept in the oven dry for 24 h at 105 °C. Then, two oven-dried BC soil samples weighing 10 g each were picked and poured into two 100 ml graduated cylinders separately. One cylinder was filled with a non-polar solution (kerosene) in which the BC soil would not swell, while the other was filled with DI water in which the BC soil swells to its full extent. After filling the necessary liquids to a volume of 100 ml, the entrapped air was removed by shaking the cylinders, and then the cylinders were left for 24 hours with a foil cover on top to achieve an equilibrium volume condition.

The FSI of BC soil was computed using the following formula;

TH-3665_186104109

$$\text{FSI (\%)} = \frac{V_{DI} - V_K}{V_K} \times 100 \quad (3.2)$$

Where V_{DI} = The amount of soil sample seen in the graduated cylinder with DI water

V_K = The amount of soil sample seen in the graduated cylinder with kerosene

The same procedure was repeated with different metal bulk solutions to determine BC soil's FSI.

3.7.2. Atterberg limits determination

The Atterberg limits (LL and PL) of BC soil with DI water and various heavy metal solutions were determined using the ASTM D4318, (2010). In this experiment, nearly 200g of oven dried 425 micron passing BC soil was initially taken and mixed with some quantity of DI water and mixed well with the help of a spatula, then placed that well-mixed slurry sample into a polyethene cover and tied it. This polyethene sample cover was put in a desiccator for 24 hrs to acquire an equilibrium state. After 24 hours, the sample was taken out of the desiccator and tested according to the codal procedure. A similar approach was followed for BC soil mixed with various metal concentrations of lead and cadmium. In addition, the plastic limit of BC soil with various metal solutions was tested by taking 20 g BC soil samples according to the code as mentioned above.

3.7.3. Compaction properties determination

Standard proctor tests for optimum moisture content (OMC) and maximum dry density (MDD) values of soil-fibre mixes were carried out in accordance with ASTM D698 (2012). The soil sample was initially mixed at a specific water content before being placed in a desiccator for one day to achieve moisture equilibrium in the compaction methodology. Later, the soil was compacted into three layers in a mould using a rammer that was dropped from a height of 305 mm and given 25 blows (for each layer). Then some amount of soil was taken from each layer for water content determination. This process was repeated for six different water contents to determine the relationship between dry density and water content of BC soil. The same methodology has been followed for remaining soil-fibre mixtures also. The findings of the compaction tests were used to prepare the samples for the consolidation and UCS testings.

TH-3665_186104109

3.7.4. Swelling potentials and swelling pressures determination

BC soil-tire fibre mixtures were subjected to oedometer tests to evaluate their swelling, hydraulic conductivity, and compressibility. Indirect measurement of hydraulic conductivity from oedometer tests offers some advantages over other permeability tests. The benefits of oedometer tests are like applying vertical loadings, which would simulate the field conditions, measuring swelling heights, and determining hydraulic conductivity values with respect to various stresses. However, this testing has its own disadvantages as well, like leakage problems and trimming of field samples. Therefore, proper care should be taken while fitting setup and performing experiments. However, it was a widely popular testing method used by many researchers in the past (Mesri and Olson, 1971; Sridharan et al., 1986; Sridharan and Nagaraj, 2004; Sivapullaiah et al., 2005; Cetin et al., 2006; Mukherjee and Mishra 2019 (a&b)). Fig. 3.11 illustrates the consolidation testing arrangement along with the consolidation ring.

The swelling potential (Spo) and swelling pressure (SPr) of fibre-mixed BC soil smaples were evaluated using the consolidometer method specified in ASTM D2435 (2010). For this, all samples were prepared at MDD and OMC conditions of fibre-mixed BC soil samples (5, 10, and 15%) with DI water. Then samples were transferred to polyethene covers and stored in a moisture-regulated desiccator for 24hrs to maintain an equilibrium state. Later, samples were compacted statically in the consolidation ring of dia 6 cm and height 1.5 cm. Then the consolidation ring was placed in the cell to provide double drainage conditions with the help of porous stones. Finally, the complete assembly was put on the consolidation stand, and then the sample was allowed to expand by inundating it with the relevant saturating fluid for a seating pressure of 4.9 kPa. Here, swelling values corresponding to respective timings were recorded using a sensitive dial gauge till minor changes in values were noticed.

The SPo of fibre-mixed BC Soil samples was computed after the completion of the swelling stage using the following formula.

$$\text{SPo (\%)} = \frac{\Delta H}{H_i} \times 100 \tag{3.3}$$

Where, ΔH = Final rise in the sample height; H_i = Initial height of the sample

TH-3665_186104109

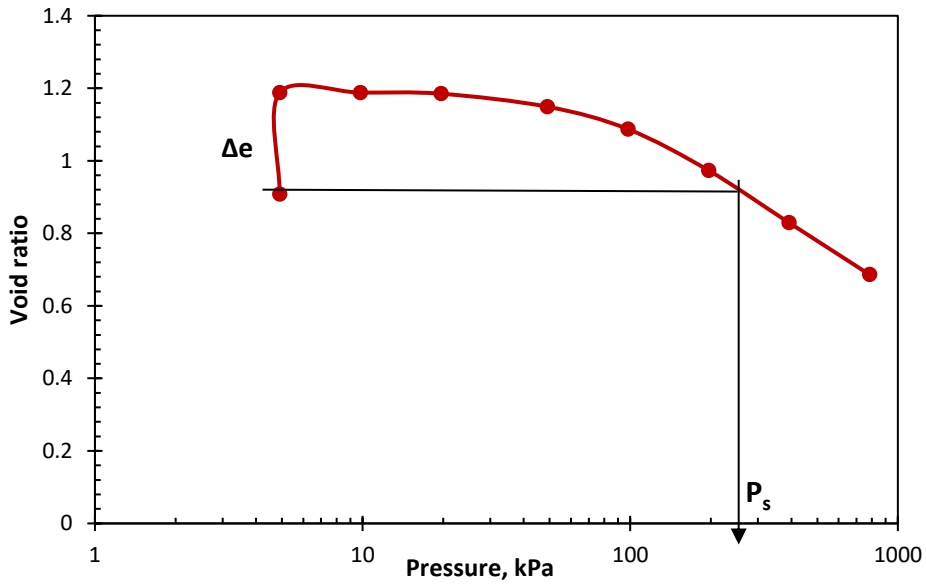

Fig. 3.10. Determination of swelling pressure and swelling potential.

The SPr of fibre-mixed BC soil samples can be estimated using the consolidation test after increasing the consolidation pressure gradually from 9.8 to 784.5 kPa after the swelling stage. The method described by Sridharan and Gurtug (2004) is used to determine the SPr of BC soil with various saturating liquids at varied concentrations. The point Ps represents the swelling pressure and is determined from the compression curve (*e*-log *p* plot) as shown in Fig. 3.10.

3.7.5. Hydraulic conductivity (*k*) determination

All fibre-mixed BC soil samples *k* was assessed by continuing the loading in a progressive way (4.9 to 9.8 kPa, 9.8 to 19.6 kPa up to 784.5 kPa) as mentioned in ASTM D2435 (2010) after the ending of the swelling stage. The variation in the sample's thickness was computed using the sensitive dial gauge.

The void ratio difference of each sample after applying load was computed using the following equation;

$$\Delta e = \frac{\Delta H(1 + e_0)}{H_0} \tag{3.4}$$

Where,

e_0 = Initial void ratio and H_0 = Initial height of the sample

Δe = Change in void ratio, and ΔH = Change in thickness

TH-3665_186104109

The coefficient of consolidation (c_v) was found using the data obtained from the time-settlement curve (Fig. 3.12) as per Taylor (1948) as per the following formula;

$$c_v = \frac{D^2.\ T_v}{t_{90}} \tag{3.5}$$

Where, D = Double drainage (H/2); T_v = Time factor

t_{90} = Time to complete for 90% consolidation (obtained from settlement curve)

The sample's volume change coefficient (m_v) was determined as follows:

$$m_v = -\frac{\Delta e}{(1 + e_0)} . \Delta p' \tag{3.6}$$

Where, $\Delta p'$ = Change in load

The sample's k was found (Terzaghi, 1943) with the help of the following calculation:

$$k = m_v . c_v . \gamma_w \tag{3.7}$$

Where, γ_w is the unit weight of the pore fluid

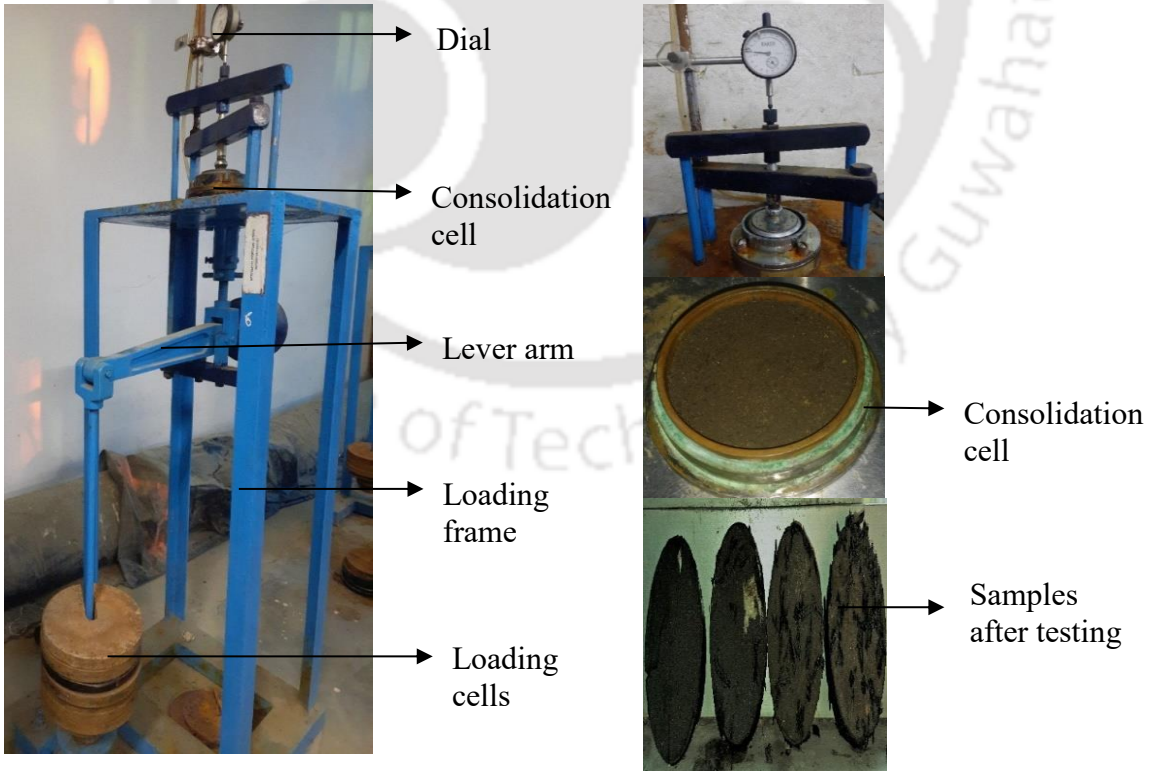

Fig. 3.11. Consolidation testing set up.

TH-3665_186104109

The samples' compression index (C_c) was calculated using the slope of the straight-line part of the virgin void ratio-pressure (e– log P) curve.

$$C_c = \frac{e_p - e_q}{log\frac{P_p}{P_q}} \tag{3.8}$$

Where e_p and e_q = Void ratios equivalent to the consolidation pressures of P_q and P_q at p^{th} and q^{th} steps of loading, respectively.

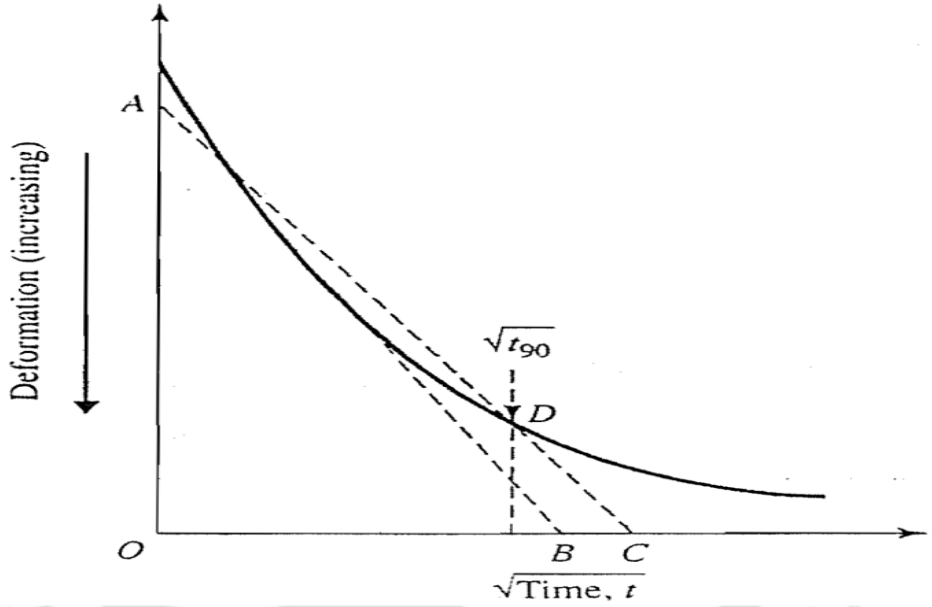

Figure 3.12. Taylor square root-of time fitting method (Taylor, 1948)

3.7.6. Unconfined compression strength (UCS) estimation

The UCS test of fibre mixed BC soil samples was carried out according to ASTM D2166 (2013). Fibre-mixed soil samples were mixed with DI water and various permeants at soil-fibre compaction conditions of DI water. The soil samples were prepared at a diameter of 38 mm and height of 76 mm to replicate the undrained condition, and tests were done under a constant strain rate (1.25 mm/min). Three UCS soil samples were examined for each composition to achieve better reliability. The peak load per unit area obtained, or the load per unit area at 15% axial strain, which occurred first during the test, was considered the UCS value of the particular sample. The UCS of fibre treated soil samples was calculated by the following equation.

TH-3665_186104109

$$S_u = \frac{P}{A_c} \tag{3.9}$$

Where P = Applied load in kN

A_c= Average cross-sectional area in mm^2 = $\frac{A_i}{(1-\epsilon_a)}$

Where A_i = Initial average cross-sectional area of the sample in mm^2

ϵ_a = Axial strain in percentage = $\frac{\Delta l}{l} \times 100$

Δl = Change in Length of the sample in mm, l = Initial length of the sample in mm.

The Fig. 3.13 shows the UCS testing equipment along with the soil sample.

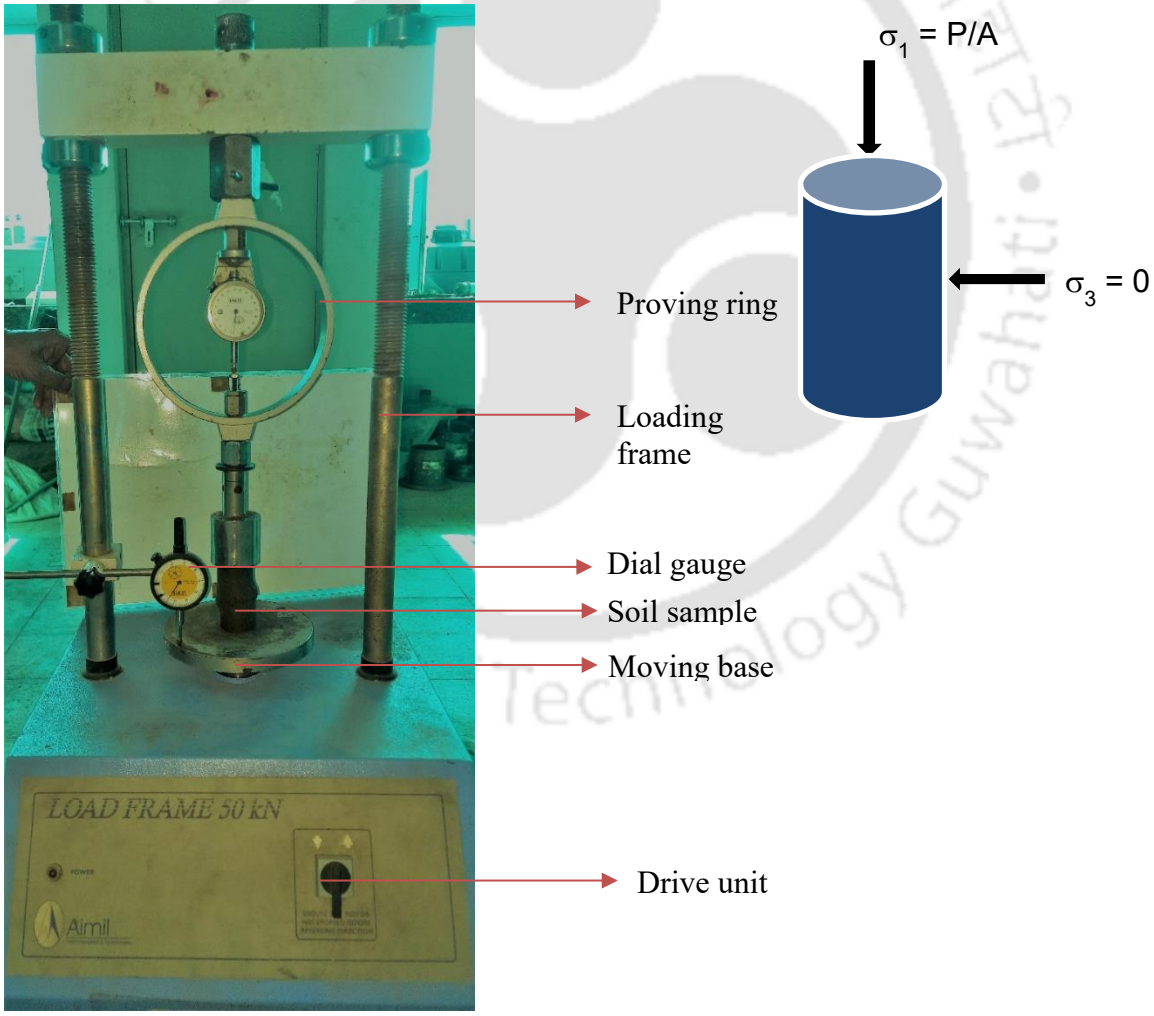

Fig. 3.13. UCS testing set up.

TH-3665_186104109

CHAPTER 4

INFLUENCE OF TIRE FIBRE ON THE BEHAVIOUR OF BC SOIL

4.1. Introduction

h lower vertical swell height. The time taken for initial and primary swelling decreases significantly as the fibre content increases, according to time-swelling plots. This swelling height and time for initial and primary swelling stages decreased more when In general, expansive soils are preferable soils for barrier applications in landfills due to their prominent swelling tendency, sorption capacity, and low permeable characteristics. However, these expansive soils tend to have high shrinkage characteristics during dry conditions, leading to the experience of desiccation cracks (Mishra et al., 2008; Divya et al., 2014). These desiccation cracks threaten the liner's stability and purpose by passing or leaking leachate into the groundwater system. In the past, many researchers investigated this issue and found a solution by adding fibres into expansive soils, which would produce tensile strength to soils and arrest this cracking phenomenon. Miller and Rifai (2004) used medium plasticity clay, with a liquid limit of 40, reinforced with polypropylene fibres (0.2 to 1%) as a barrier material and found a reduction in the crack intensity factor with the increase of fibres inclusion. Harianto et al. (2008) used compacted Akaboku clay (liquid limit of 162) added with polypropylene (PP) fibres (0.2 to 1.2 % by dry weight) as a cover material in landfill systems and found an increment in shrinkage limit and reduction in volumetric strains and crack intensity factors with the rise in the inclusion of fibre. Tang et al. (2012) also tested the cracking pattern of locally available low-plasticity clayey soil (liquid limit of 37) mixed with PP fibres (0.05 to 0.8% by dry mass) for barrier applications and found a significant reduction in widths and lengths of cracks with the increase in fibre content. Chaduvula et al. (2017) examined expansive clay (liquid limit of 87) reinforced with polyester fibres (0.25 to 0.75% by dry weight) of three various lengths (15, 30, and 50 mm) for barrier systems in landfills. They found optimum results regarding cracking pattern behavior was at 0.5% of fibre content with 15 mm length. However, the usage of these traditional fibres in expansive soils is neither economical nor provides the solution to environmental problems. For this reason, some scholars shifted their focus toward the usage of waste materials in the

TH-3665_186104109

geoenvironmental field recently, which would provide solutions to both engineering and environmental challenges. Especially, the usage of waste tire derivatives like chips, shreds, buffings, and fibres in both geotechnical and geoenvironmental applications has been given much attention due to the generation and hazardous consequences of waste tires, which were discussed in a detailed way in Chapter 2.

As the primary emphasis is on barrier application in landfill systems, there have been few investigations on using tire for barrier application. Cokca and Yilmaz (2004) used a flyash-bentonite mixture added with rubber content (1-10% by weight) for liner application and determined that a significant reduction in unconfined compressive strength and swell pressures and a significant rise in hydraulic conductivity values with the addition of rubber content. Jigheh et al. (2014) investigated the shrinkage behavior of two cohesive soils (liquid limits of 33 and 61) mixed with tire chips (10, 20, and 30% by weight) and found that a decrement in the crack depth and crack intensity factor and an increment in crack reduction percentage. Narani et al. (2020) investigated sodium bentonite (liquid limit of 415) and tire fibre (1-4% by dry mass) mix for landfill clay liner application by examining swelling, strength, shrinkage, and permeability behaviors and found a considerable reduction in swelling potentials, volumetric shrinkage, and cracking behavior and a noticeable rise in split tensile strength and permeability values up to 4% fibre content. Similarly, Mukherjee and Mishra (2021) focused on the usage of sand-bentonite (70:30) mixture added with tire fibres (5-15%) for liner layer material and found that rate of consolidation and permeability values increased and shrinkage strains decreased significantly upto 15% fibre content. Therefore, it is confirmed from the literature that the addition of tire fibre content significantly reduces the shrinkage potential, which would positive sign for barrier application. However, an alteration in other important properties like swelling and hydraulic conductivity was also noticed. Also, it is evident that many investigations have been focused on the use of bentonite-tire mix as liner material because of bentonite's expansive tendency. Since bentonite is scarce in India, this study aims to use black cotton (BC) soil (rich in montmorillonite) tyre fibre mix as a barrier material. BC soil is naturally available expansive soil, which has covered many parts of the Indian land. However, there is not much detailed investigation available on BC soil-tire fibre mix from the barrier application point of view. It is very important to understand the compressibility, hydraulic, swelling, and strength characteristics of liner material after adding additives to it.

TH-3665_186104109

This chapter provides detailed test results of fibre-soil composites, which would explain the impact of waste tire fibre content on the engineering behaviour of BC soil. Standard proctor compaction test, one-dimensional consolidation test, and unconfined compressive strength test were conducted on BC soil mixed with various proportions of tire fibre content (5, 10, and 15%) by dry weight.

4.2. Test Result and Discussion

4.2.1. Compaction characteristics

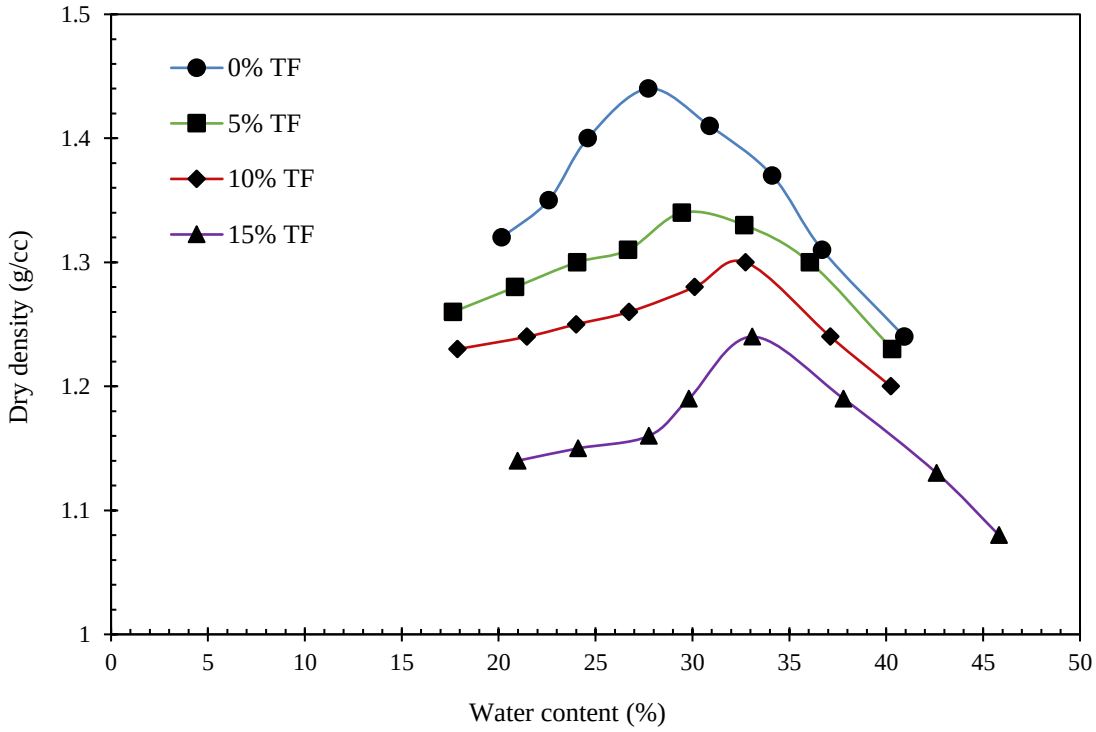

Fig. 4.1. Compaction curves for BC soil-tire fibre mixes.

A series of Standard Proctor tests were conducted on soil-fibre mixes for the determination of compaction parameters such as maximum dry density (MDD) and optimum moisture content (OMC) as per ASTM D698 (2012). The plot in Fig. 4.1. represents the compaction curve of the samples with various proportions of tire fibres. The results show a reduction in the MDD and an increment in the OMC with the addition of the fibre. The MDD of the BC soil reduces from 1.44 g/cc to 1.34, 1.30, and 1.24 g/cc by adding 5, 10, and 15% tire fibres, respectively. The elasticity response of tire fibres causes a loss in compaction efficiency, which may be the reason for the decrease in dry densities of tire-fibre mixes. The specific gravity of tire fibre (i.e 1.15) is considerably smaller than that for the BC soil (i.e 2.59), and

TH-3665_186104109

this lower specific gravity may also lead to a reduction in MDD of soil-fibre composites (Yadav and Tiwari, 2017; Mukherjee and Mishra, 2021). The OMC of BC soil increases from 27.7 to 30.0, 32.7, and 33.1% with tire fibres at 5, 10, and 15%, respectively. A higher water content is required to mobilise the soil-tire fibre composite to compact to a denser state resulting in an increase in the OMC values. Similar trends were observed by Cabalar et al. (2014), who obtained an increase in the OMC values after adding 5 to 15% tire buffings into clayey soil of a liquid limit of 49.5 %.

4.2.2. Time-swelling relationship

Swelling behaviour of fibre-mixed BC soil with DI water is shown in Fig. 4.3, representing the relationship between the time and swelling height. The plot exhibits a swelling behaviour in the S-shape curve irrespective of the fibre content in three different phases, named as initial, primary, and secondary swelling (Rao et al., 2006; Ye et al., 2014; Mishra et al., 2015), as shown in Fig. 4.2. The swelling starts slowly in the initial swelling stage, increases rapidly in the primary swelling stage, and finally achieves an asymptotic value in the last stage for all the soil-tire fibre composites, as displayed in Fig. 4.3. The swelling height of BC soil in de-ionized water as a permeant liquid was 3.13 mm under a pressure of 5 kPa as seating load, and it decreased to 2.20, 1.48, and 0.93 mm with the increasing the tire fibre content to 5, 10, and 15%, respectively. Identical results was observed by Mukherjee and Mishra (2019(a)) after the inclusion of tire fibres into sand-bentonite mixtures. The interaction of soil-tire fibre restricts the tensile forces developed due to the swelling phenomenon, causing less swelling for the inclusion of more fibre content. The time and percentage of swells for soil-fibre mixtures are determined by using lines as shown in Fig. 4.2. The details of time and swelling percentage with respect to each individual stage are mentioned in Table 4.1. It is observed that both time and percentage swells were decreased with the increase in the fibre content in each stage of swelling. The percentage of total swelling also observed that a minimum amount of swelling (13.39%) occurred in the initial swelling stage, followed by a significant amount of swelling (74.14%) in the primary swelling stage for the pure BC soil with DI water as per data mentioned in Table 4.1.

TH-3665_186104109

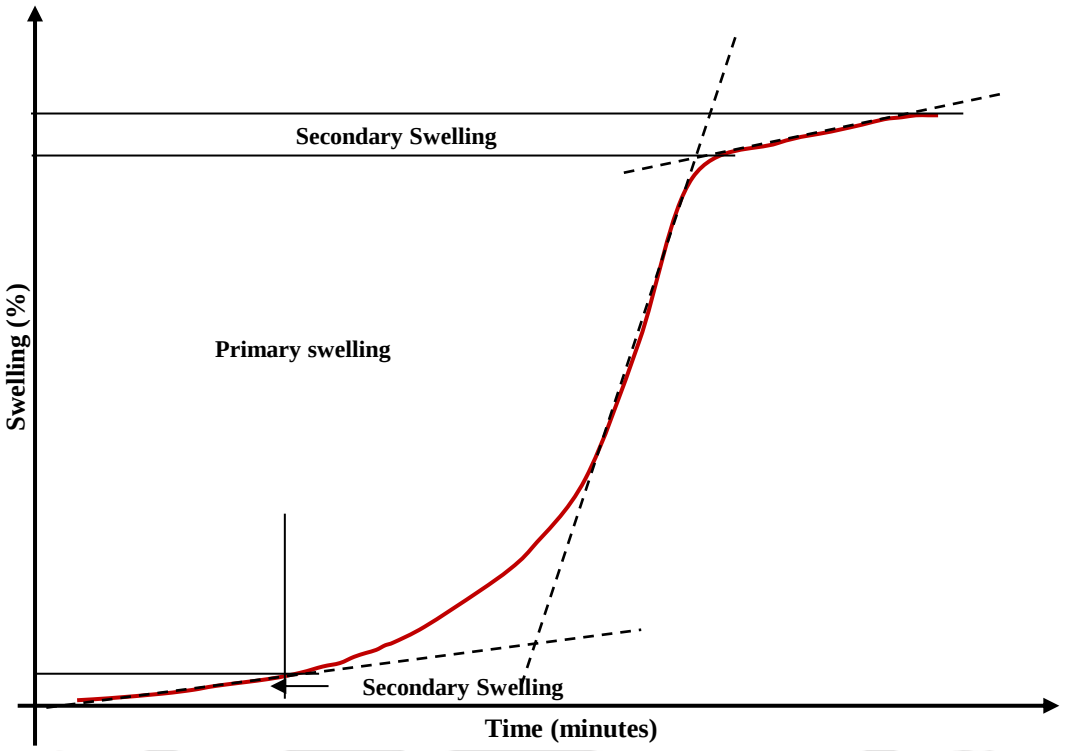

Fig. 4.2. Representation of swelling stages from swelling curve (S-curve).

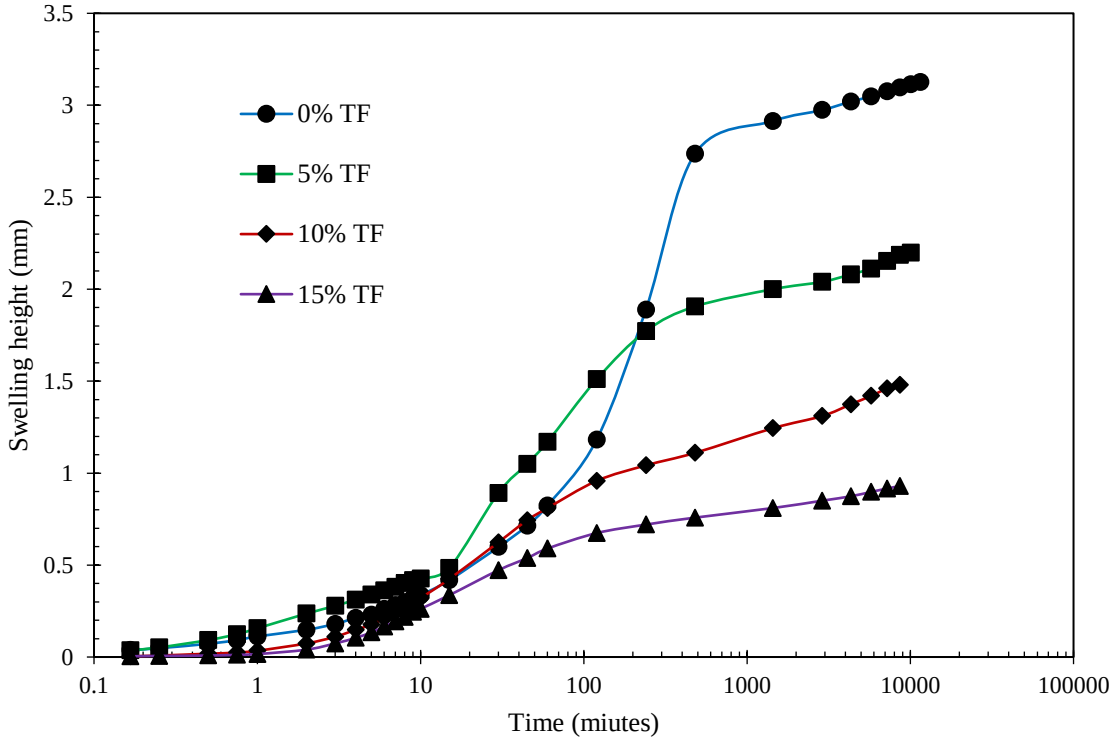

Fig. 4.3. Time-swell plot of fibre-mixed BC soil with DI water.

A similar trend was observed for BC soil mixed with tire fibre in various proportions. However, the amount of total swelling percentage that occurred in the initial swelling stage

TH-3665_186104109

was relatively less and took place quickly compared to pure soil due to the addition of fibre to the soil. The macrostructure of the samples causes the initial swelling phenomenon, whereas the microstructure of the samples causes the primary and secondary swelling phenomena (Mishra et al., 2015; Soltani et al., 2019).

Table 4.1. Time and percent swells of fibre-mixed BC soil with DI water

Tire fibre content (%)	Initial swelling		Primary swelling		Secondary swelling		Total swelling	
	Time (min)	% Swell	Time (min)	% Swell	Time (min)	% Swell	Time (min)	% Swell
0	15	2.79	465	15.45	11040	2.6	11520	20.84
5	9	2.79	471	9.92	9600	1.94	10080	14.65
10	5	1.17	395	6.13	8240	2.57	8640	9.87
15	4	0.69	296	4.21	6900	1.21	7200	6.20

4.2.3. Swelling pressures and Swelling potentials

In general, expansive soil possessing high swelling pressures and swelling potentials exhibits a higher water tightness and self-sealing characteristics, which are quite essential for barrier applications (Bucher and Vonmoos, 1989; Tang et al., 2019). Swelling potential is the amount of swelling that occurred in a sample that has been saturated with DI water or salt permeant under a seating pressure of 5 kPa, while swelling pressure is the pressure needed to compressed a swollen specimen under similar saturated conditions and seating pressure to its original volume (Sridharan et al., 1986; Dutta and Mishra, 2015). All the swelling pressure values of the specimens are determined by compacting the soil-tire mixes at their corresponding OMC and MDD and saturating them with DI water under a seating load of 5 kPa.The swelling pressures and swelling potentials of BC soil with different fibre proportions are mentioned in Table 4.2. The reduction of BC soil's swelling pressures can be observed by the inclusion of tire fibre concentration ranging from 0 to 15%. Initially, the swelling pressure of pure BC soil was 520 kPa, and it decreased to 270, 180, and 140 kPa for 5, 10, and 15% fibre content, respectively, and the percentage of reduction was about

TH-3665_186104109

48.08, 65.38, and 73.08% for the same fibre content. The possible reasons for this reduction in the swelling pressures of fibre added soil are the tensile forces of fibres, which restricts the swelling pressures of soil, and drainage paths created by fibres because of their interface, which may lead to pore water pressure dissipation (Kalkan, 2013). The addition of non-swelling tire fibres with swelling clay content and some minor cavities in tire fibres could also be the other possible reasons for the reduction of swelling pressures (Yadav and Tiwari, 2017).

Table 4.2. Swelling pressures and swelling potentials fibre-mixed BC soil with DI water

Tire fibre content (%)	Swelling Pressure (kPa)	Swelling Potential (%)
0	520	20.84
5	270	14.65
10	180	9.87
15	140	6.20

The swelling potentials also decreased with the rise in tire fibre content from 0 to 15% as shown in Table 4.2. The swelling potential of pure BC soil with DI water was 20.84%, which had declined to 14.65, 9.87, and 6.20% with the inclusion of 5, 10, and 15% tire fibre content, respectively. The reduction in the swelling potential of BC soil was about 29.7%, 52.64%, and 70.25% for tire fibre concentrations of 5, 10, and 15%, respectively. The drop in swelling potential may be due to the friction and interlocking effect between the clay particles and fibres responsible for the development of tensile stresses (Soltani et al., 2019; Narani et al., 2020).

4.2.4. Swelling prediction using RH model

In this work, the swelling phenomena of BC with various concentrations of fibre were predicted by the rectangular hyperbola (RH) model, which was used by various researchers (Dakshinamurthy, 1978; Sridharan and Gurtug, 2004; Soltani et al., 2017). This model linearize the swelling phenomena and helps calculate each sample's ultimate swell by considering the time-swell curve as an RH and using the following equation.

TH-3665_186104109

$$\frac{t}{S} = b + at \tag{4.1}$$

Where, t and S are time (minutes) and percent swell (%), respectively

b and a are intercept and straight-line slope, respectively

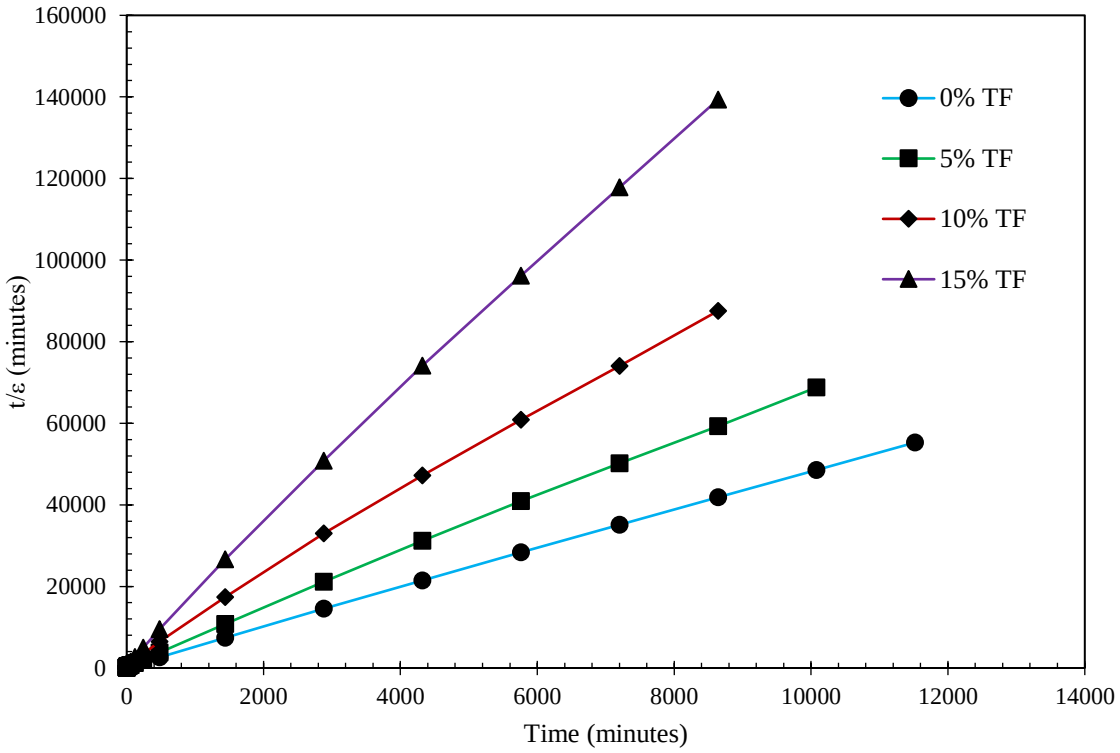

Fig. 4.4. Linearized representation of swelling potential data for BC soil-tire fibre mixes.

Here, BC soil-tire fibre mixes ultimate swelling was predicted using the rectangular hyperbola (RH) model (Eq. 4.1), and it was possible to establish a linear relationship between (t/S) and t from Eq. 4.1. As a result, the constant parameters (a and b) can be calculated using the traditional least squares approximation method. The linearised plot was shown in Fig. 4.4 for different tire fibre inclusion. It can be observed that the linear equation slope was increased for higher metal concentrations, and the R^2 value for all values was 0.999 as shown in Fig. 4.5. Therefore, rectangular hyperbola constants (b and a), predicted swelling (1/a) and measured swelling (%) were mentioned in Table 4.3 for BC soil at various fibre concentrations. These results show the relationship between observed and expected swelling, suggesting that the swelling data of BC soil-tire fibre samples can be properly assessed.

TH-3665_186104109

Table 4.3. Predicted swelling potentials (RH model) vs measured swelling potential values

Tire fibre content (%)	Hyperbolic parameters		Measured swell (%)	Predicted swell (%)
	a	b		
0	4.794	411.71	20.84	20.86
5	6.890	329.7	14.65	14.51
10	10.517	712.35	9.87	9.51
15	16.344	904.35	6.2	6.12

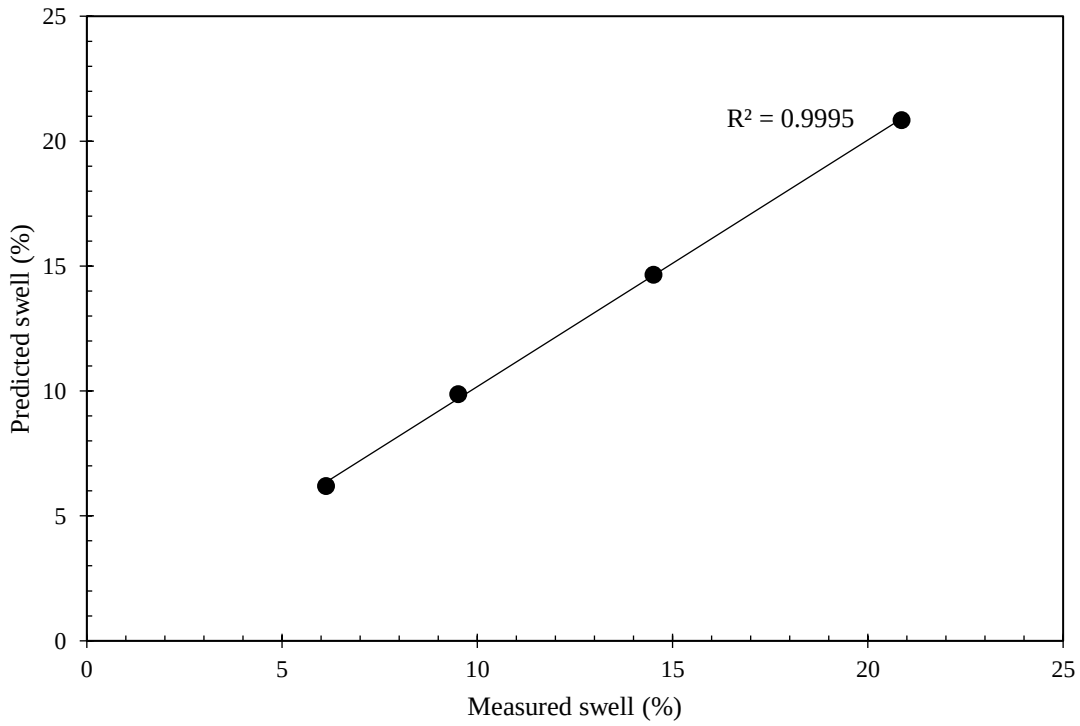

Fig. 4.5. Correlation between measured swell vs observed swell.

TH-3665_186104109

4.2.5. Coefficient of consolidation (c_v)

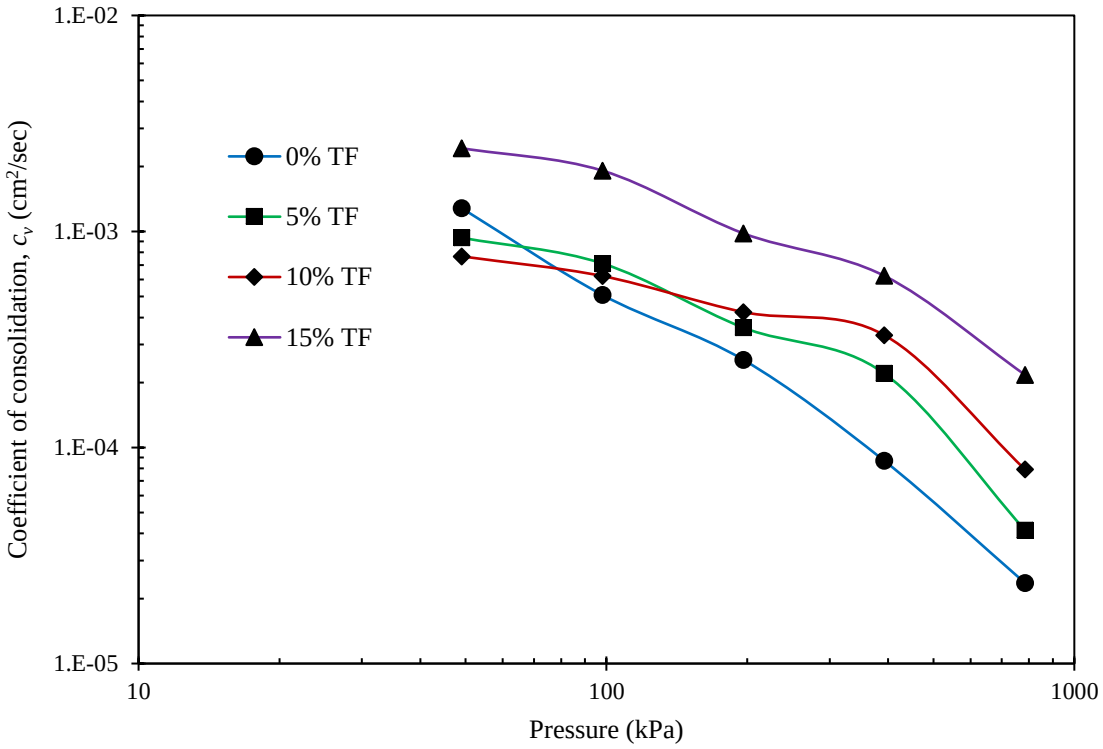

Fig. 4.6. Consolidation pressure vs coefficient of consolidation (c_v) plot for various fibre-mixed BC soil with DI water

The coefficient of consolidation (c_v) measures the rate at which a saturated soil sample consolidates in one dimension in response to an increase in consolidation pressure. This rate is directly influenced by the hydraulic conductivity of soil under compression (Terazaghi 1943). Therefore, the determination of c_v is important in finding settlement rate and hydraulic conductivity. The plot in Fig. 4.6 represents the coefficient of consolidation (c_v) values corresponding to different consolidation pressures for all fibre-mixed soil samples in the presence of DI water. It can be seen that there is a decrease in c_v values as the consolidation pressure increases for all samples, implying a slower rate of consolidation at higher consolidation pressures. For example, it was observed from Fig. 4.6 that the c_v values of pure BC soil were 1.28×10^{-3}, 0.51×10^{-3}, 0.25×10^{-3}, 8.7×10^{-5}, and 2.4×10^{-5} cm^2/s for a corresponding consolidation vertical pressures of 49.0, 98.1, 196.1, 392.3, and 784.5 kPa in the presence of DI water, respectively. A similar trend was noticed for all other samples as well, irrespective of fibre composition. Some researchers (Robinson and Allam, 1998; Dutta and Mishra, 2016(a); Ray et al., 2021(a)) observed a similar kind of behaviour for different types of bentonites. Reduction in void ratio may be the reason for this decrement in c_v values

TH-3665_186104109

at high pressures. For highly plastic soils, the DDL repulsive forces are mobilised, which acts against high external pressures and gives greater resistance to compression by clay particles moving closer together (Sridharan and Nagaraj, 2004). This phenomenon causes a reduction in DDL thickness and lower c_v values at higher consolidation pressures. Long-range attractive and repulsive forces regulate the compressibility of expansive soils in general. As the consolidation pressure rises, the clay plates become closer together, resulting in more repulsion between the plates, which prevents the sample from further consolidating, lowering the c_v values (Ray et al., 2021a). However, few of the researchers (Mishra et al., 2010; Thanh Duong and Van Hao, 2020) observed a reverse trend for the c_v values for bentonite-low swelling soil mixtures and stated the influence mechanical factors controlling the c_v, whereas, physicochemical factors play an essential role in pure expansive soils responsible for long-term attractive and repulsion forces (Sridharan and Rao, 1973; Dutta and Mishra, 2016((a)).

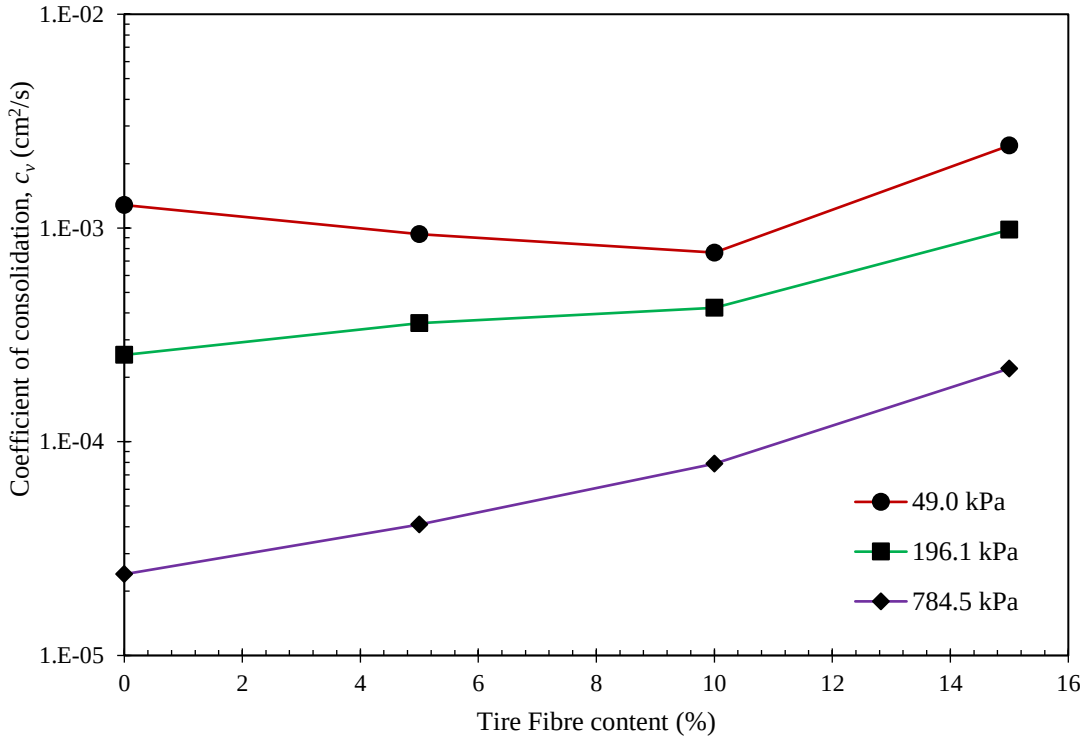

Fig. 4.7. Fibre content vs coefficient of consolidation plots with DI water at different consolidation pressures.

The plot in Fig. 4.7 shows the variation of c_v of BC soil mixed with 5, 10, and 15% of tire fibres under various pore fluids at different consolidation pressures (i.e. 49, 196.1, and 784.5 kPa). The plot shows an increase in the c_v values with the rise in fibre concentrations. Similar

TH-3665_186104109

kind of trend for different expansive soils was also observed by different researchers (Srivastava et al., 2014; Mukherjee and Mishra, 2019(b)). The plot in Fig 4.7 reveals that the c_v value of BC soil increased from 2.4 $\times 10^{-5}$ cm^2/s to 4.1 $\times 10^{-5}$ (1.7 times), 7.9 $\times 10^{-5}$ (3.29 times), and 22.0 $\times 10^{-5}$ cm^2/s (9.17 times) for 5, 10, and 15% of the tire fibre content, respectively with the DI water.

4.2.6. Time for 90% consolidation (t_{90})

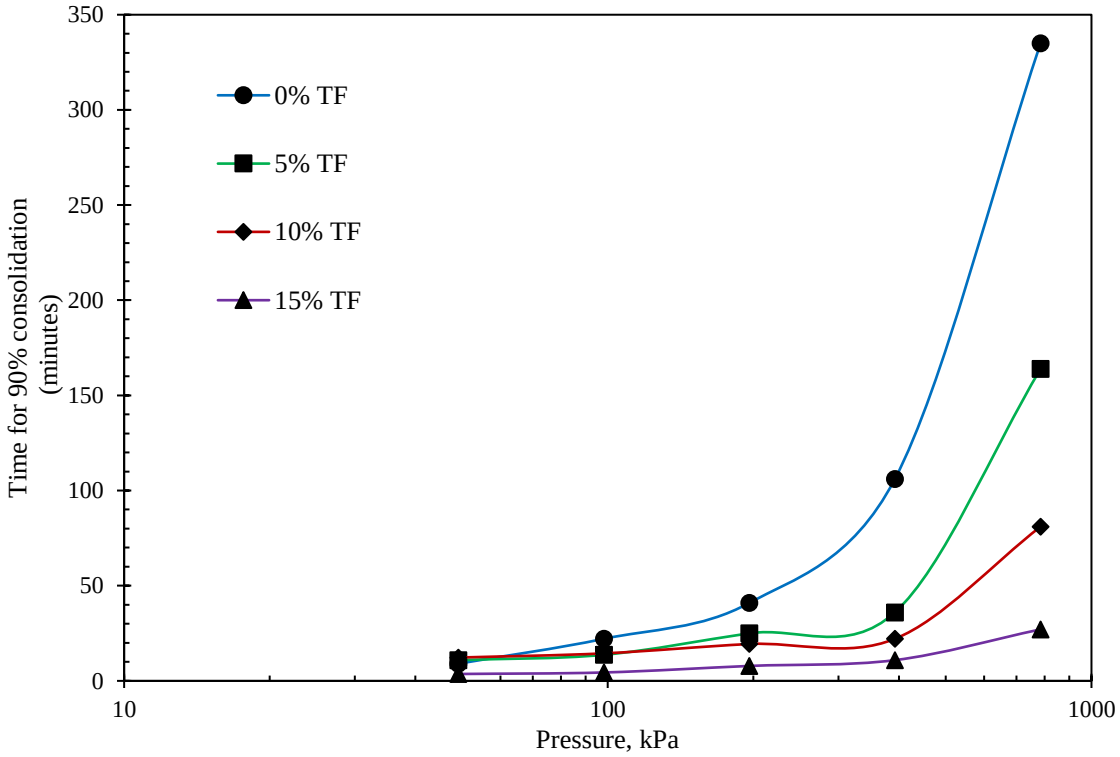

Fig. 4.8. Consolidation pressure vs time for 90% consolidation (t_{90}) plot for various fibre-mixed BC soil with DI water.

The time for 90% of consolidation (t_{90}) of a sample is the amount of time necessary to complete 90% of the consolidation under a particular consolidation pressure. The plot in Fig. 4.8 shows the variation in t_{90} values corresponding to different consolidation pressures of BC soil for different percentages of tire content in the presence of DI water. The plots show that as the consolidation pressure increases, the sample's t_{90} value increases. Similar observations for pure bentonites were also made by the other researchers (Dutta and Mishra, 2016(a); Ray et al., 2021(b)). The contact of clay plates at higher pressures may be the reason for this increment in t_{90} values of BC soil. At higher consolidation pressures, the clay plates come closer and repulsive forces act on negatively charged clay plates, thus inhibiting further movement resulting in a decrease in c_v values and an increase in t_{90} values of BC soil. The

TH-3665_186104109

plot in Fig. 4.8 depicts the t_{90} values for pure BC soil with DI water as the pore fluid. The plot shows that the t_{90} increased from 9 minutes to 22.09, 40.96, 106.09, and 334.89 minutes for the corresponding increase in the pressure from 49.0 kPa to 98.1, 196.1, 392.3, and 784.5 kPa, respectively.

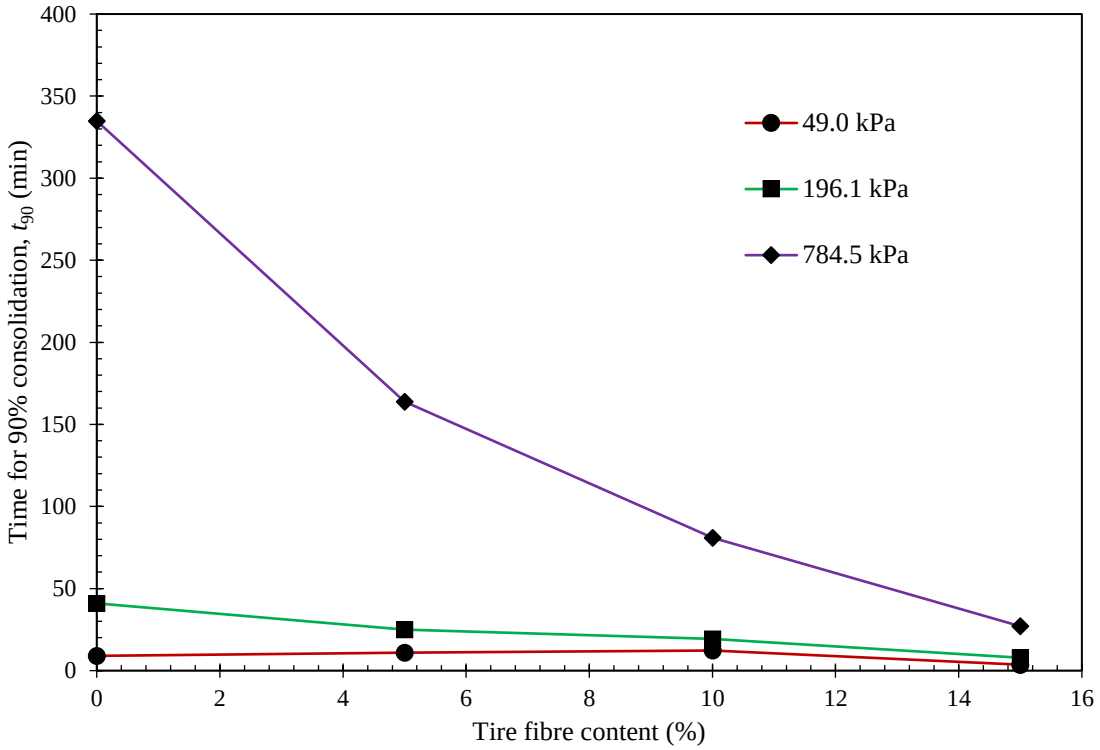

Fig. 4.9. Fibre content vs t_{90} plots with DI water at different consolidation pressures.

The plot in Fig 4.9 also explains the relation between the fibre content and t_{90} values with DI water at different consolidation pressures. The graph shows that when the fibre content increased from 0 to 15%, the t_{90} values declined. A similar kind of behavior was observed by Mistry et al. (2020) after conducting a consolidation study on expansive clay mixed with three different tire fibre content. The addition of tire fibres to soil creates some void spaces because of micro-cracks present in tire fibres. Whenever higher loads are applied to fibre-treated soil samples, there is a chance that the dissipation of pore water pressure through these voids (Kim and Kang, 2013) which leads to a faster consolidation. The plot in Fig. 4.9 shows that the t_{90} values of BC soil (DI water as pore fluid) decreased from 40.96 minutes to 25.00, 19.36, and 7.84 minutes with the 5, 10, and 15% fibre-soil mixes, respectively, under a consolidation pressure of 196.1 kPa. Similarly, at 784.5 kPa of consolidation pressure, the t_{90} value declined from 334.89 minutes to 163.84, 81, and 21.04 minutes for the 5, 10, and 15% of tire fibre content, respectively. The reduction in t_{90} values was about 51.08, 75.81, and 93.72% for 5, 10, and 15% of tire fibres under DI water at 784.5 kPa pressure.

TH-3665_186104109

4.2.7. Void ratio vs pressure (*e*-log *P*) relationship

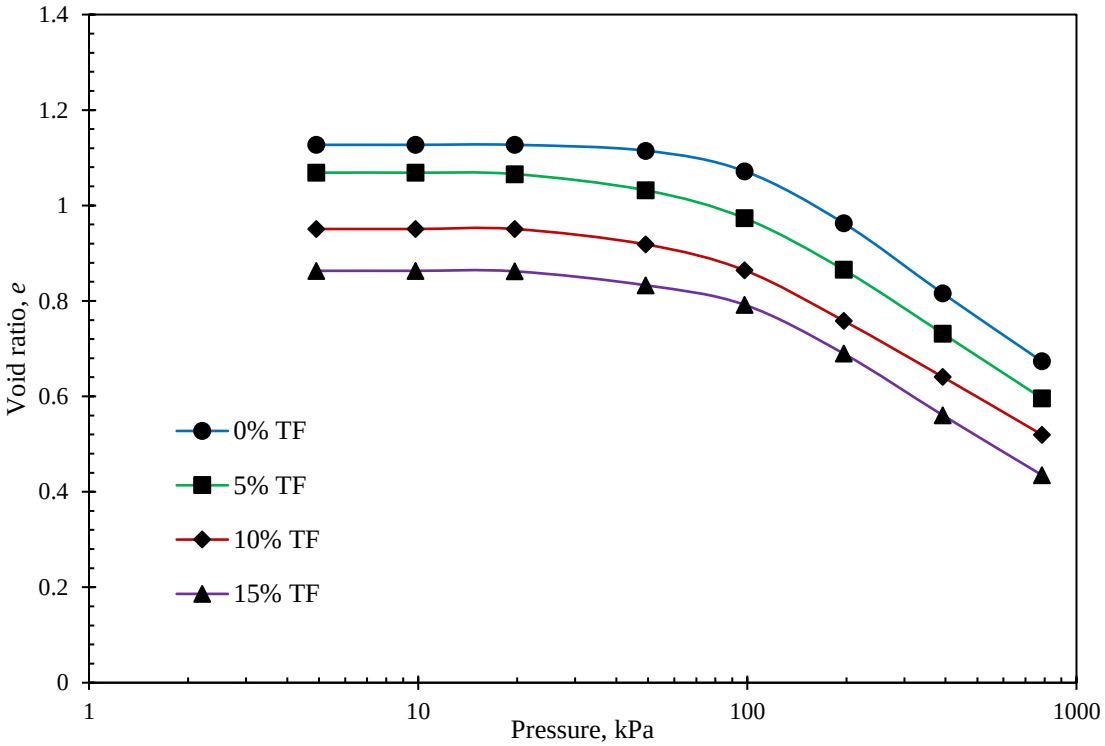

Fig. 4.10. Void ratio-pressure plots for various fibre-mixed BC soil with DI water.

The plot in Fig 4.10 shows the void ratio and pressure (*e*-log *P*) plots of all fibre-treated soils with DI water. The plot shows that the void ratios of all samples reduced as the consolidation pressures increased, irrespective of fibre content. For example, the void ratio of BC soil under a seating pressure of 5 kPa was 1.13 which was measured after completion of the swelling of the sample (at equilibrium void ratio). This void ratio declined significantly to 0.67 under the external pressure of 784.5 kPa. However, this reduction in the void ratios was less significant from 5 to 49.0 kPa of pressure range for all the samples, irrespective of fibre content. The void ratios of all the samples reduced slightly with the increase in fibre content at any given consolidation pressure, as depicted in Fig. 4.10. For example, the void ratio of pure BC soil was reduced from 1.1 to 0.97, 0.86, and 0.79 for 5, 10, and 15% fibre-mixed samples, respectively. Similarly, at the maximum consolidation pressure (i.e. at 784.5 kPa), this void ratio was changed from 0.67 to 0.60, 0.52, and 0.43 for a similar increase in the fibre content.

TH-3665_186104109

4.2.8. Compression index (C_c)

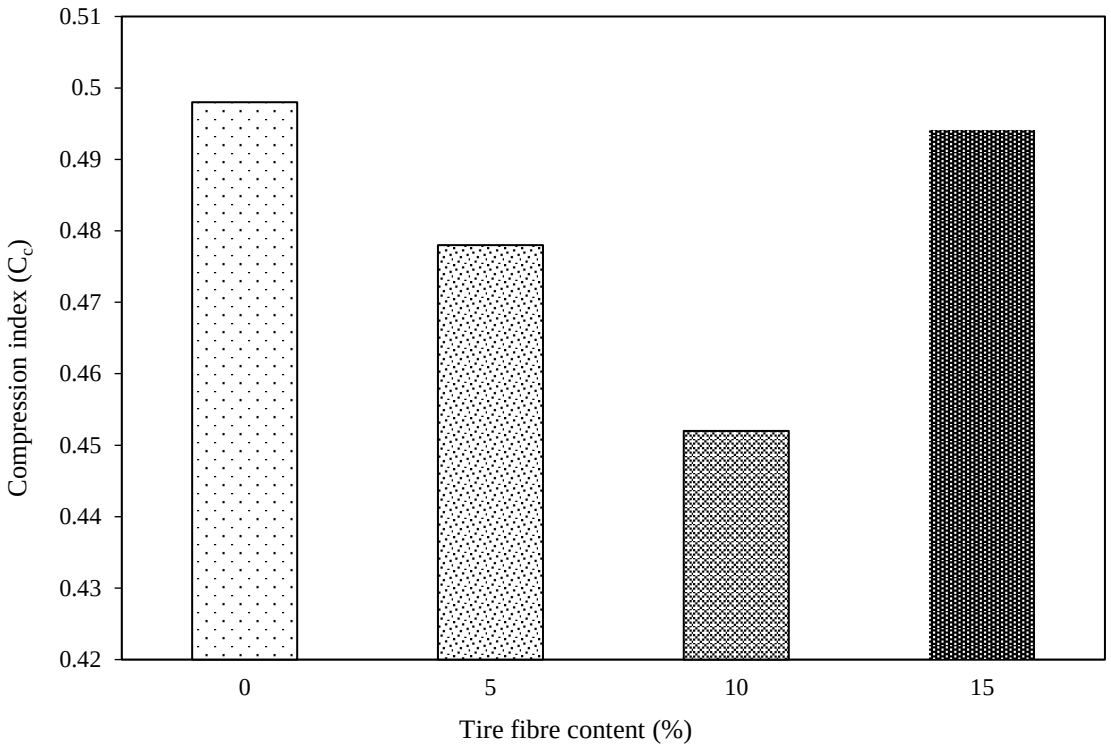

Fig. 4.11. Compression index of fibre-mixed BC soil with DI water.

The plot in Fig. 4.11 shows the compressibility behavior of fibre-mixed BC soil with DI water. The slope of the straight-line part of the *e*-log *P* curves was used to calculate the compression index for all the samples. The mechanical and physico-chemical properties of the soil have an effect on its compressibility behavior. Mechanical characteristics of soil particles, such as rolling, sliding, bending, and crushing, are affected by particle-to-particle contact (Bolt, 1956; Mukherjee and Mishra, 2019(b)). The compression index of BC soil was decreased from 0.498 to 0.478 and 0.452 for an increase in the fibre content from 0 to 5 and 10%, respectively. Several researchers (Trouzine et al., 2012; Srivastava et al., 2014) made a similar kind of observation of a decrease in the void ratio of expansive soils due to the inclusion of fibres. A slight increase in the C_c value of 0.494 for 15% tire fibre mixed soil can be due to the elastic behavior of tire fibre due to tire-to-tire interaction.

4.2.9. Hydraulic conductivity (*k*)

One of the most crucial factors to meet before being employed as a landfill liner is the soil's hydraulic conductivity (*k*). Many environmental organizations and researchers have recommended that landfill liners should have a minimum *k* value of 10^{-7}cm/s (USEPA 1988; Benson et al., 1999; Hauser et al. 2001). In this research work, the standard oedometer

TH-3665_186104109

apparatus was used to assess the impact of consolidation stresses on the hydraulic conductivity of BC soil under the influence of fibre content.

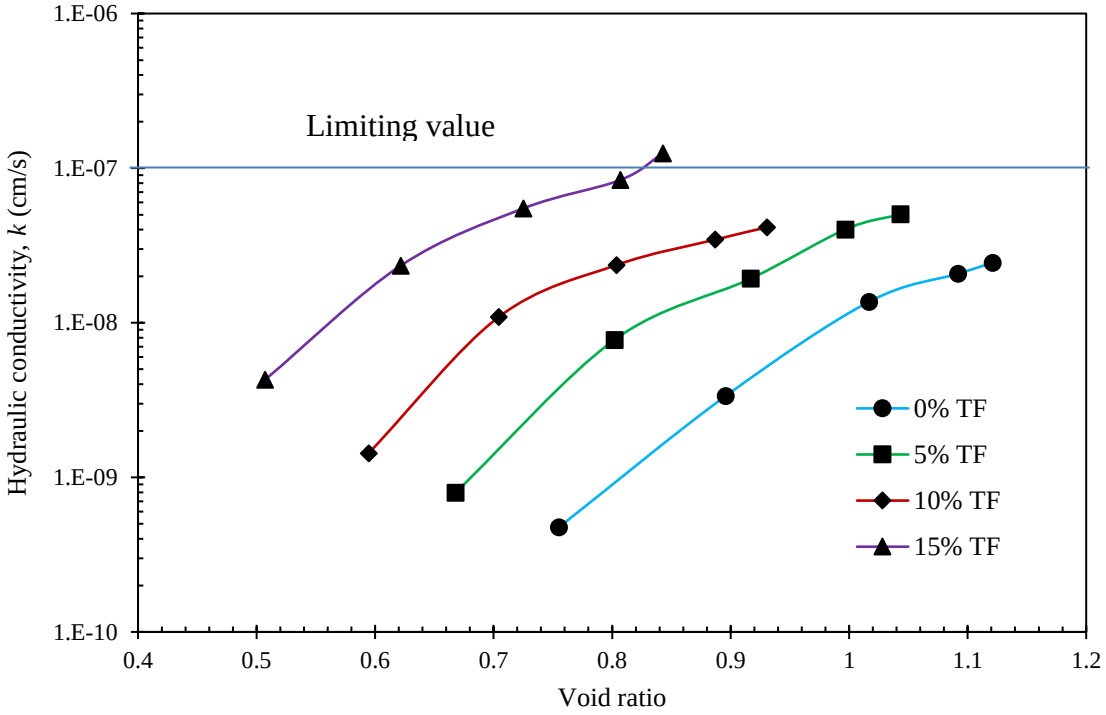

Fig. 4.12. Hydraulic conductivity vs void ratio plots for various fibre-mixed BC soil with DI water.

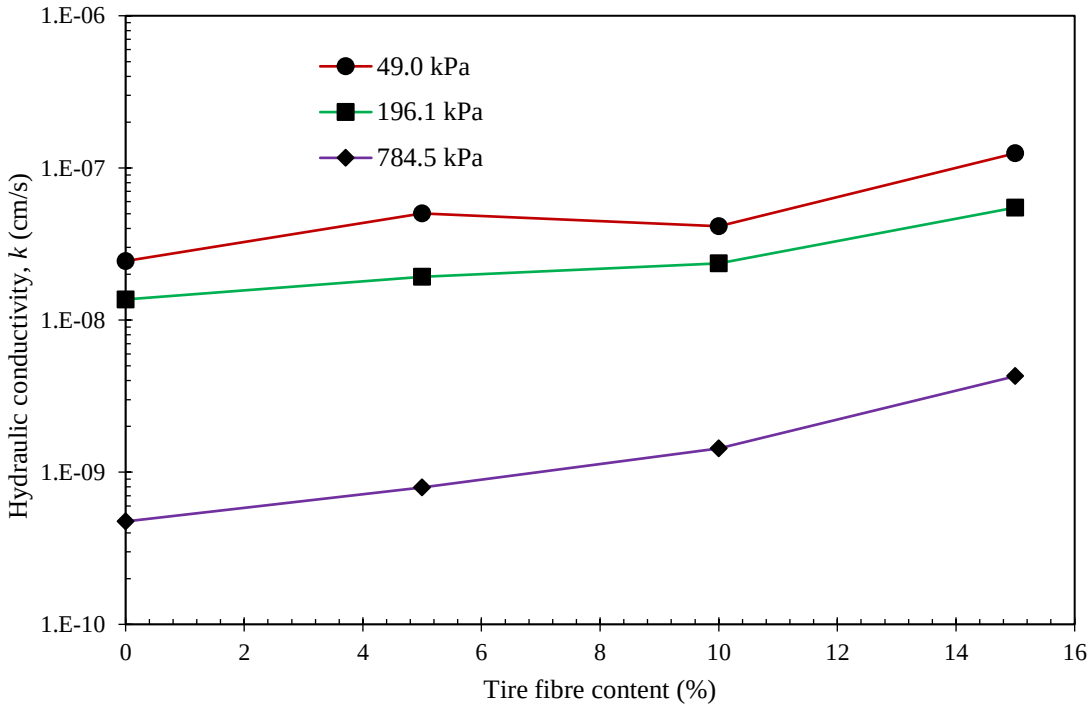

Fig. 4.13. Hydraulic conductivity vs consolidation pressure plots for various fibre-mixed BC soil with DI water.

TH-3665_186104109

The variation in *k* values of BC soil with the addition of tire content was displayed in Fig. 4.12. It was observed that there was a significant rise in *k* values with the inclusion of tire fibre content as shown in plots. For example, at a void ratio of 0.8, the hydraulic conductivity of BC soil was increased from 1.49×10^{-9} cm/s to 5.13×10^{-9}, 1.00×10^{-8}, and 8.26×10^{-8} cm/s due to the inclusion of 5, 10, and 15% of tire fibre content, respectively. This hike in *k* was nearly about 4.5, 8.8, and 72.4 times for 5, 10, and 15% fibre-soil mixes, respectively compared to BC soil without any fibre. The formation of additional drainage channels due to tire fibre may be the reason for this increment in the hydraulic conductivity of BC soil (Mukherjee and Mishra, 2019(a)). Some other researchers also had observed a higher hydraulic conductivity due to an increment in the fibre content (Cetin et al., 2006; Kalkan, 2013; Narani et al., 2020). However, lower *k* values were observed at high consolidation pressures irrespective of the fibre content, as depicted in Fig. 4.13. For example, the *k* value of pure BC soil at 49.0 kPa was reported as 2.44×10^{-8} cm/s, which was decreased to 4.75×10^{-10} cm/s (51.4 times) at the external consolidation pressure of 784.5 kPa. For 5% tire-fibre mix, the *k* value vas reported as 5.03×10^{-8} cm/s, which was reduced to 7.95×10^{-10} cm/s (63.3 times) at the same consolidation pressure difference. Similarly, this reduction in *k* values was about 29.0 times and 29.2 times for 10 and 15% fibre-soil mixes, respectively, at the same difference in consolidation pressures. The obvious reason behind this decrement in *k* values at higher consolidation pressures was the slower rate of consolidation at higher pressures.

4.2.10. Unconfined compressive strength (UCS)

The UCS tests were conducted on the different soil samples and the stress-strain behavior of fibre-mixed BC soil prepared at their respective OMC-MDD conditions as shown in Fig. 4.14. As per ASTM D2166 (2013), the UCS value of BC soil would be considered as peak load or load value corresponding to 15% axial strain, whichever occurred first during the test. The results showed that the UCS value of BC soil samples reduces with the corresponding addition in the tire fibre content from 0 to 15%. Table 4.4 summarises the peak strengths and corresponding peak strains of all fibre-mixed BC soil samples. Initially, the UCS value of BC soil without tire in the presence of DI water is 594.2 kPa; this value decreases to 370.2 (37.7% reduction), 232.6 (60.9 % reduction), and 166.5 kPa (72.0% reduction) for 5, 10,

TH-3665_186104109

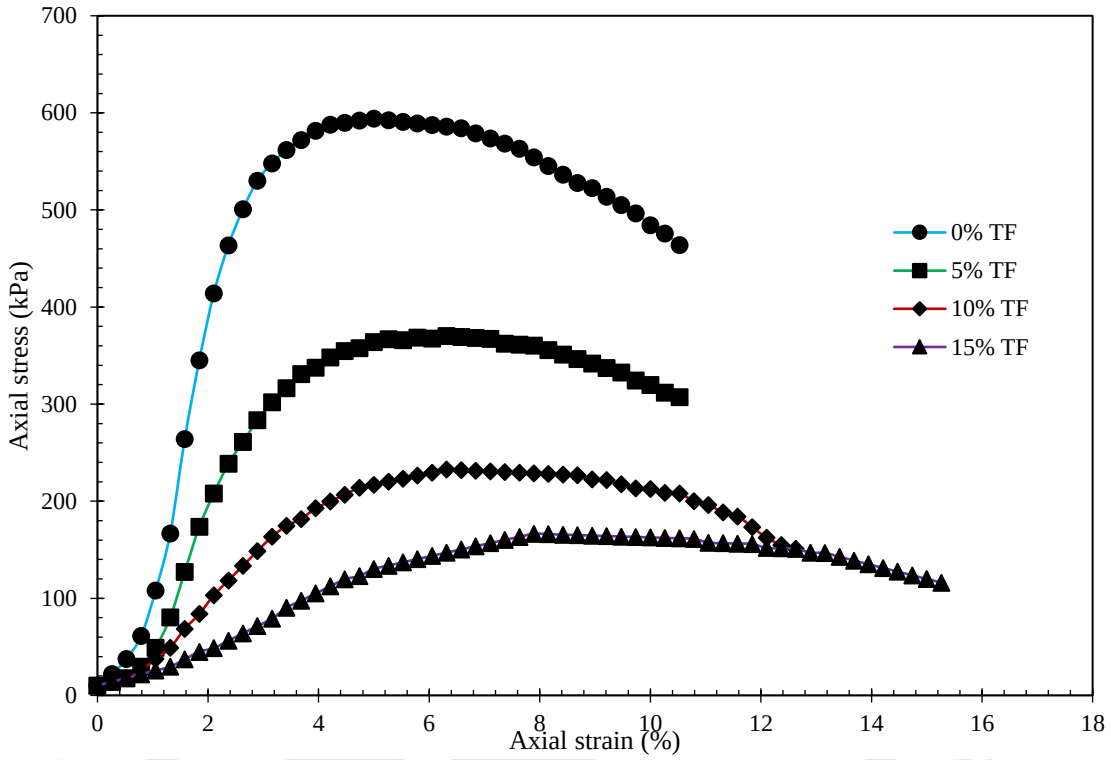

Fig. 4.14. UCS of fibre-mixed BC soil with DI water.

Table 4.4. Peak strength and peak strain values of fibre-mixed BC soil with DI water

Tire fibre content (%)	Peak strength (kPa)	Peak strain (%)
0	594.2	5.00
5	370.2	6.32
10	232.6	6.32
15	166.5	7.89

and 15% fibre content, respectively. Generally, high clay content in the sample leads to the development of pore water pressure, which is responsible for the strength increment. The strength reduction with an increase in fibre content is due to the bonding between clay content and tire fibres, which leads to pore water pressure dissipation. From the Fig. 4.14 it was observed that the axial stress of BC soil (DI water permeant) reaches its peak value very fast at lower axial strain (5.0%). In contrast, these axial strains increase to 6.3, 6.3, and 7.9% for corresponding peak strengths of 5, 10, and 15% fibres with the DI water, respectively,

TH-3665_186104109

indicating that the soil-fibre mixes display the ductile behaviour due to elastic nature of tire fibres. Here the percentage of increment in peak strains is 26.0, 26.0, and 58.0% for 5, 10, and 15% tire content, respectively, than 0% (pure BC soil) tire content. Jafari and Ashari (2012) and Cabalar et al. (2014) observed similar trends by testing the geotechnical properties of clayey samples with the incorporation of tire content. The initial slope of the stress-strain curve for pure BC soil looks steeper than that of all soil-tire fibre mix samples, and the reason behind this is the low secant Young's modulus of tire fibres owing to their flexible nature (Cokca and Yilmaz, 2004). The shear strength of compacted soils used in liner and cover systems must be adequate (≥ 200 kPa), as stated by Daniel and Wu (1993). It can be identified that this limiting value did not satisfy the liner material requirement for the 15% fibre-soil mix. The typical failure mode of fibre-mixed BC soil samples is shown in Fig.4.15. Bulging failure mode was observed for samples which are mixed with tire fibre content up to 5%. Both bulging and shear failure modes are observed with all 10% fibre-treated soil samples. However, shear failure mode is predominant in all 15% fibre-mixed soil samples.

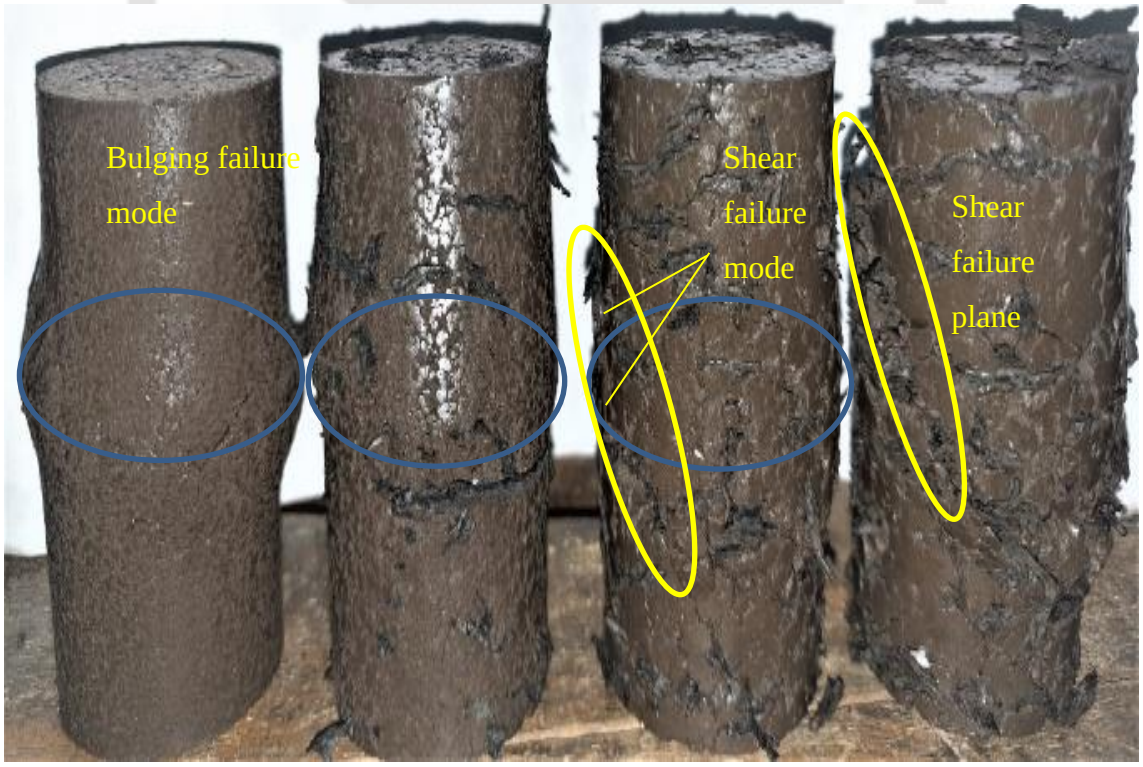

Fig. 4.15. Typical failure pattern of fibre-mixed samples (0, 5, 10, and 15%) after UCS testing.

TH-3665_186104109

4.3. Summary

In this chapter detailed investigation has been done on the engineering properties of BC soil-tire fibre (5, 10, and 15% by dry weight) mix for barrier application in landfill systems. A series of laboratory experiments performed on BC soil-tire fibre samples to determine compaction characteristics, swelling properties, consolidation parameters, hydraulic behavior, and shear strength response. The following are the summary points of this chapter.

- The incorporation of tire fibre in the BC soil resulted in a considerable reduction in MDD, while the BC soil's OMC increased.
- In comparison to pure BC soil, fibre-mixed samples showed mucfibre-mixed samples were saturated with salt permeants.
- As per RH modeling of swelling data, an appropriate correlation was found between measured swell and predicted swell.
- With the addition of fibre content, swelling pressures and swelling potentials of BC soil were reduced significantly. For 15% fibre content this reduction percentage of swelling pressures and swelling potentials was nearly about 73.1 and 70.2%, respectively.
- Coefficient of consolidation (c_v) values increased with the rise in fibre content, thereby time taken for 90% consolidation (t_{90}) values decreased prominently at the higher fibre content.
- The void ratios of BC soil reduced for the rise in fibre content from 5 to 15%.
- The compression indices of BC soil decreased with the increase in fibre content by up to 10%. However, a marginal increment in compression index value for 15% fibre content incorporation.
- High hydraulic conductivity values were reported at lower consolidation pressures than high pressures. The incorporation of tire fibre in the BC soil resulted in a considerable hike in hydraulic conductivity values. This hike was around 4.5 times, 8.8 times, and 72.4times for the waste tire fraction of 5, 10, and 15%, respectively at the void ratio of 0.8
- However, all *k* values fell within the limits except for 15% composition at 49.0 kPa consolidation pressure.
- From UCS tests, it can be observed that a reduction in strength values of BC soil with an increase in the fibre content. The result showed an improvement in ductile

TH-3665_186104109

behaviour of soil due to the addition of fibre content. However, for 15% fibre composition, the UCS values were reported as less than 200 kPa.

भारतीय प्रौद्योगिकी संस्थान गुवाहाटी • Indian Institute of Technology Guwahati •

TH-3665_186104109

CHAPTER 5

INFLUENCE OF SALT PERMEANTS ON THE BEHAVIOUR OF FIBRE-MIXED BC SOIL

5.1. Introduction

The main purpose of this research is to study the suitability of waste fibre-mixed BC soil in the presence of salts as a clay liner material. Despite the fact that fibres could impede the tendency to shrink/crack behaviour, the attack of chemicals poses an additional critical threat to barrier materials, as it would significantly affect their properties. Chemicals in landfill leachate reduces the thickness of the diffuse double layer (DDL), which could be the reason for a rise in hydraulic conductivity by multiple folds (Norrish and Quirk, 1954; Madsen and Mitchell, 1989). Hence, it is essential to evaluate the chemicals' effects on barrier materials prior to recommend for the use as a liner material. Typically, clay liners in landfills are exposed to substantial concentrations of inorganic salt solutions (Mishra et al., 2005; Li et al., 2008; Xu et al., 2018). Consequently, this issue has garnered significant attention from researchers, prompting them to concentrate on the testing of barrier materials under various permeants, and scholars in the past have explored the interaction of barrier material-salt solutions. Many of the researchers (Shackelford et al., 2000; Mishra et al., 2005; Shirazi et al., 2011; Dutta and Mishra, 2015; Zhang et al., 2016; Xu et al., 2018; Song et., 2024) have focused on the influence of salt concentrations on bentonites, soil-bentonites, and sand-bentonite mixtures for landfill liner use. Few researchers (Lee and Shackelford, 2005; Mishra et al., 2009; Dutta and Mishra 2016(a); Jadda et al., 2020) observed a dependency of swelling, strength, and permeability properties on the mineralogical parameters of bentonite. Limited studies (Maio et al., 2004 Arasan and Yetımoglu, 2008; Nguyen et al., 2013; Rao et al., 2013) are available on natural soils and their engineering behaviour in the presence of salt solutions in the past and observed significant changes in hydromechanical properties of high plasticity soils. Low plasticity soils, however, exhibited an opposite trend in the variation of index and engineering properties with inorganic salt solutions.

A review of the past literature suggested a considerable influence of salt type and concentrations on clayey soils. There have been limited investigations that concentrate on clay-salt interactions beyond bentonites and sand/soil-bentonite composites. Therefore, a

TH-3665_186104109

more thorough investigation is still required to determine the impact of monovalent and divalent salt concentrations on the engineering behaviour of natural clays such as black cotton (BC) soil. In addition, no research has been conducted in the past to investigate the consequences of concentrations of salt solutions on fibre-soil mixtures, as BC soil-fibre composite has been employed as a barrier material in landfills. Therefore, the primary objective of this work is to understand the index and engineering properties of BC soil under the influence of two (NaCl and $CaCl_2$) inorganic salt solutions at two different concentrations (0.1 and 1.0N) including DI water. Thereafter, this work carried forward by emphasizing the engineering properties of fibre-mixed BC soil samples under the same salt concentrations. The study examined engineering properties including swelling properties such as time-swelling relationship, swelling pressures, and swelling potentials, consolidation parameters such as coefficient of consolidation (c_v) and time for 90% consolidation (t_{90}), compressibility characteristics like void ratio-pressure (e-log P) relationships and compression indices (C_c), hydraulic conductivity (e-log k) properties, and axial stress-strain relationships and peak strength values by conducting unconfined compressive strength.

This chapter gives an insightful result regarding the behaviour of BC soil including index properties and engineering properties (swelling, consolidation, hydraulic conductivity, and shear strength) under the influence of inorganic salt concentrations. Also, it provides data on fibre-mixed soil inundated with various concentrations of inorganic salt permeants, which would be helpful to researchers and design engineers to get a comprehensive idea of fibre-BC soil usage for barrier applications.

5.2. Test Result and Discussion

5.2.1. Atterberg limits

Determining the Atterberg limits of soil will assist in identifying the plasticity characteristics of that particular soil. In addition, these results would be used to evaluate soil engineering characteristics, such as shear strength, compressibility, etc., in the field by correlating liquid limit, plastic limit, and plasticity index values individually or collectively (ASTM D4318, 2010; Haigh et al., 2013). The Atteberg limits of BC soil mixed with

TH-3665_186104109

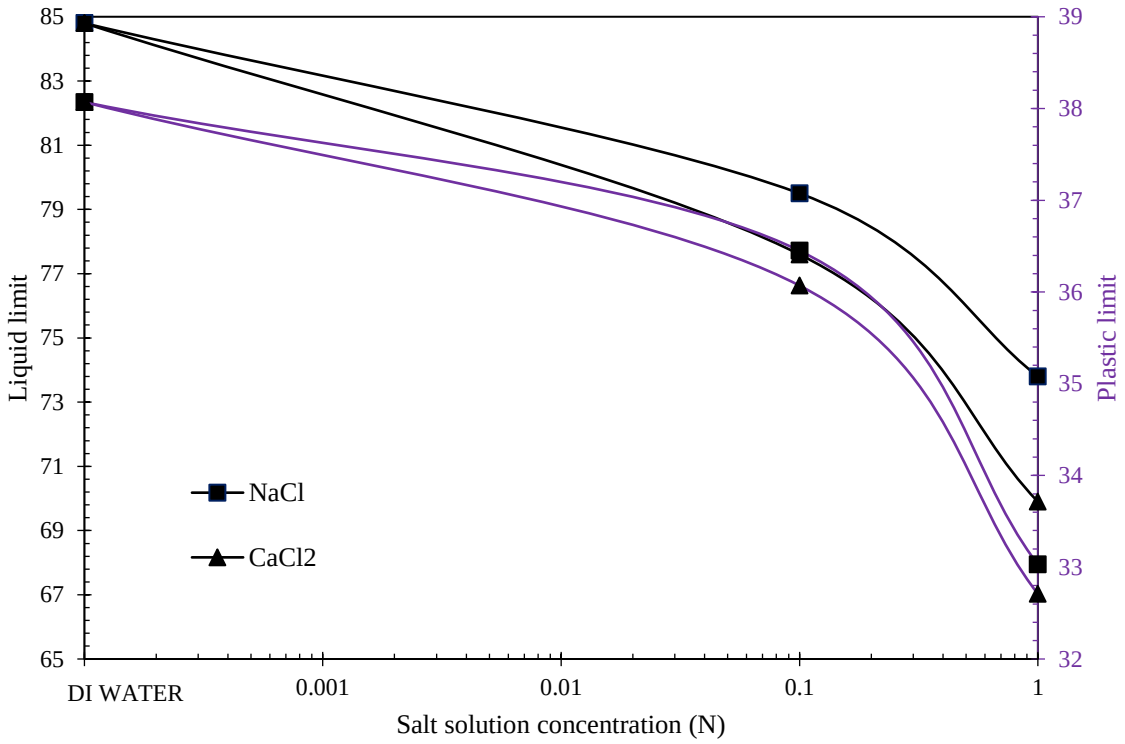

Fig. 5.1. Atterberg limits of BC soil with NaCl and $CaCl_2$ salt solutions.

different inorganic salt solutions are shown in Fig.5.1. The liquid limit (LL) of BC soil with DI water was found as 84.8%, as shown in Fig. 5.1. The LL was reduced by about 6.3 and 13% in presence of 0.1 and 1.0 N NaCl solution, respectively. However, for a rise in cation valency, this reduction in LL was more predominant. The reduction in LL was about 8.5 and 17.6% with 0.1 and 1.0 N $CaCl_2$ solution, respectively, compared to DI water. The lower inter-particle distance between the clay particles may be the reason for this reduction in LL at higher concentrations and the cation valency of salt solutions (Sivapullaiah and Sridharan, 1985). At lower inter-particle distances, the clay particles tend to move freely, resulting in lower LL values at higher concentrations and cation valency. A similar kind of behavior was observed for the plastic limit (PL) and plasticity index (PI) of BC soil with the same type and concentration of salt solution. Similar kind of behavior was observed for bentonite and sand-bentonite mixtures in the presence of various concentrations and types of the salt in the past (Mishra et al., 2009; Shirazi et al. 2011; Dutta and Mishra, 2015; Jadda and Bag, 2020; Rout and Singh 2020).

The variation of the plastic limit (PL) of BC soil with different inorganic salt solutions is shown in Fig. 5.1. The PL of soil is primarily controlled by the factors such as the fraction of coarse content, diffuse double layer (DDL) thickness, and clays fabric (Sivapullaiah et al., 1996). As shown in Fig. 5.1. the PL of BC soil with DI water was reported as 38.07% and

TH-3665_186104109

reduced to 36.45 and 33.03% with 0.1 and 1.0 N NaCl solutions, respectively. Similarly, for the $CaCl_2$ solution, these PL values were reported as 36.07 and 32.71% with 0.1 and 1.0N concentrations, respectively. The percentage reduction in PL values was marginal which is about 4.3 and 13.2% at 0.1 and 1.0 N of NaCl salt solution compared to DI water. This reduction was about 5.3 and 14.1% at similar concentrations of $CaCl_2$ salt solutions. The plasticity index (PI) is the difference between the liquid limit and plastic limit, which would signify the water content at which soil sample deforms plastically. The PI values also followed a similar trend of LL and PL for all the samples.

5.2.2. Free swell index (FSI)

The Free swelling index (FSI) results give an understanding of the swelling capacity of a soil under non-loading conditions. The free swelling behavior of BC soil under the influence of different salts is shown in Fig. 5.2. According to the obtained results, the FSI of BC soil decreased as the concentration of salt solution increased. FSI of BC soil with DI water was 196%, and it decreased to 171 and 141% for 0.1 and 1.0 N NaCl solution, respectively. For an increase in the cation valency, i.e. Ca^{2+} from Na^{+}, a higher reduction in FSI was observed. For the divalent salt solution $CaCl_2$, the FSI was decreased from 196 to 155 and 132% with 0.1 and 1.0 N concentrations, respectively. The swelling takes place in expansive soils due to inner-crystalline and osmotic or double-layer swelling (Zhang et al., 1995). Whenever a solution of high concentrations is added to soil, a significant decrease in double-layer swelling occurs, leading to a reduction in FSI values. This reduction in double-layer swelling would be more dominant for the presence of divalent cation in the solution than the monovalent cation (Mishra et al., 2009). The findings of this study revealed that FSI values were reduced by 12.8 and 28.1% at 0.1 and 1.0N NaCl solutions, respectively, compared to DI water. This reduction was 20.9 and 32.7% for the same concentration of $CaCl_2$ solution compared to DI water. Also, after pouring soil into measuring cylinders, quick settlement of clay particles in less time was observed with both NaCl and $CaCl_2$ solutions at 1.0 N concentration compared with DI water indicating flocculation tendency of the soil at higher concentration. A linear relationship was observed between LL and FSI with all concentrations of inorganic salt solutions as shown in Fig. 5.3. The plot in Fig. 5.3 indicates that with the increase in the LL, the FSI of the soil also increases.

TH-3665_186104109

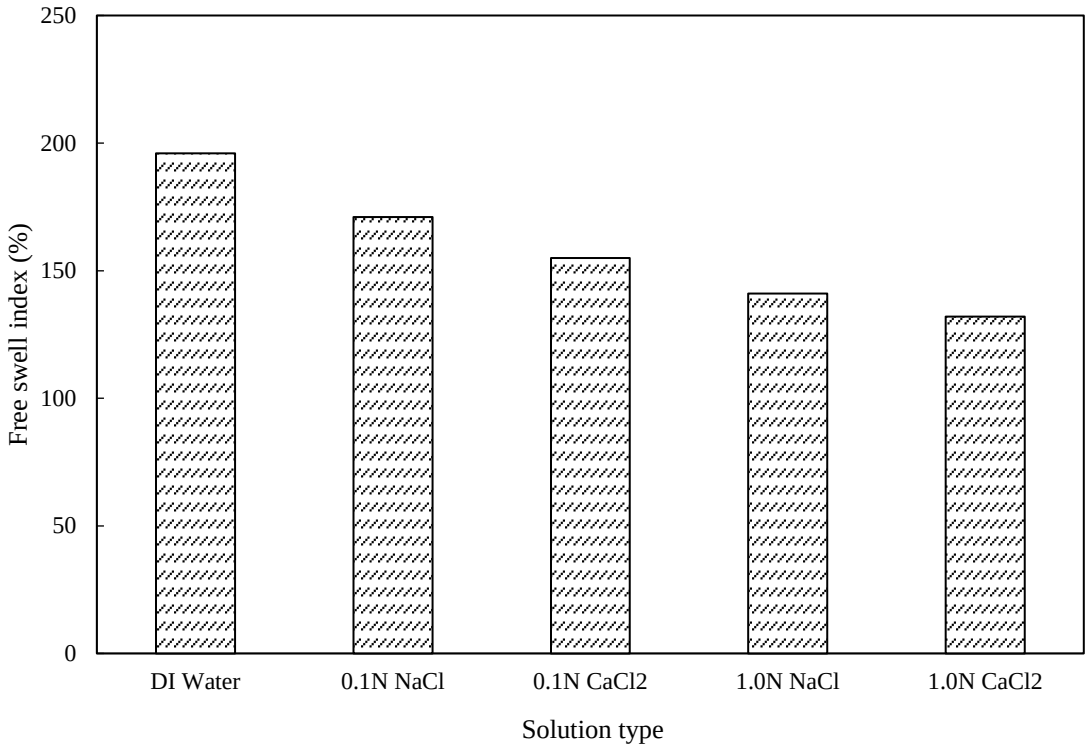

Fig. 5.2. Free swelling index (FSI) of BC soil with NaCl and $CaCl_2$ salt solutions.

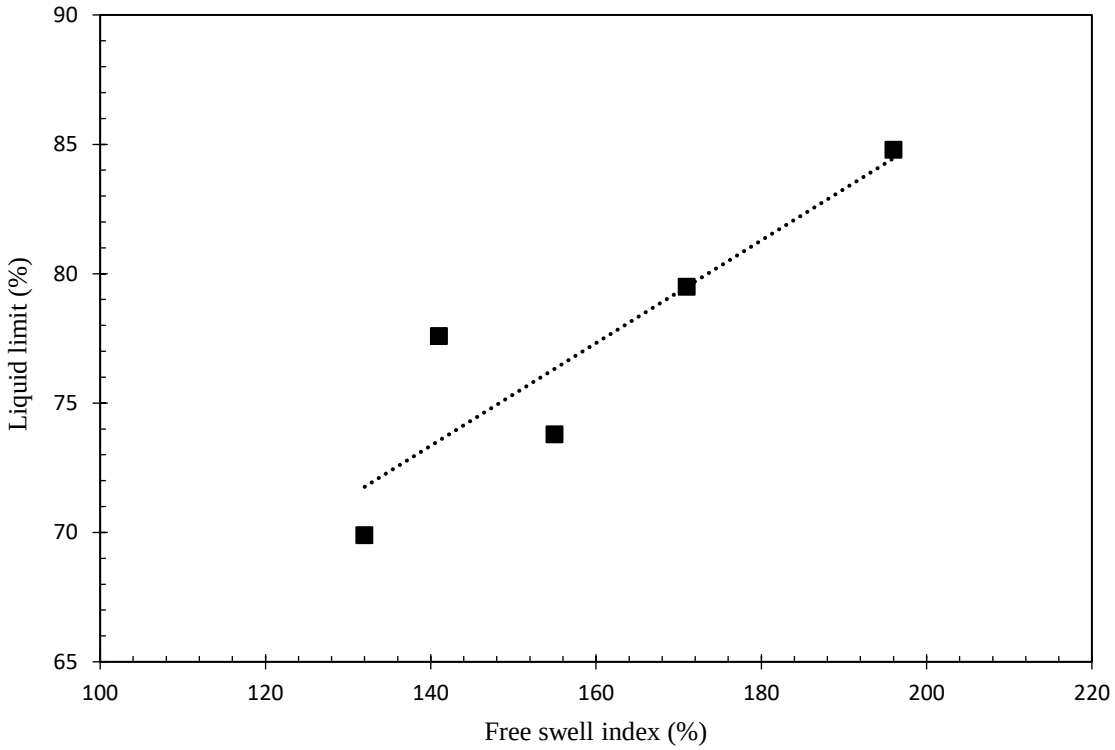

Fig. 5.3. Liquid limit versus FSI of BC soil with salts of various concentrations solutions

TH-3665_186104109

5.2.3. Time-swelling relationship

Swelling plots for fibre-mixed BC soil in the presence of different permeant fluids are shown in Figs. 5.4 to 5.7, representing a relationship between the time and swelling height. All the plots exhibit a swelling behaviour defined by a S-shaped curve with three different distinct stages (i.e. initial, primary, and secondary swelling stages), irrespective of the fibre content or permeant liquid. The increase in the height due to the swelling of the sample with 0% tire fibre (TF) (i.e. pure BC soil) was recorded as 3.13 mm, as shown in Fig. 5.4. This increase in the swelling height was reduced significantly to 2.4 and 2.1 mm with 0.1 and 1.0 N of NaCl permeant solutions, respectively. Similar trend for the BC soil was also observed with NaCl permeants as depicted in Fig 5.4. It is observed that there was a further decline in the swelling heights with divalent pore permeants compared to the monovalent permeants at the same order of concentration levels. As displayed in Fig. 5.4, the increase in the swelling height of BC soil was recorded as 1.80 and 1.61 mm with 0.1 and 1.0N $CaCl_2$ permeants, respectively. Dutta and Mishra (2015) also focused on the swelling behavior of bentonites in the presence of monovalent and divalent inorganic pore fluids and observed a similar kind of declining trend with divalent pore fluid concentrations than with the monovalent concentrations. Since the thickness of DDL thickness depends inversely on the electrolyte concentration and cation valency, an increase in these factors reduces the DDL thickness and, consequently, the swelling of the sample. Moreover, the swelling heights of all fibre-mixed BC soil samples (i.e. 5, 10, and 15% of tire fibre) under various concentrations of salt permeants exhibited a comparable trend to that of the 0% tire fibre sample, irrespective of the fibre content. For the samples with 5% of tire fibre, the swelling height was reduced from 2.2 mm (DI water) to 1.56 and 1.20 mm with 0.1 and 1.0 N NaCl permeants, respectively. For the $CaCl_2$ solution, the swelling values for identical concentrations were reported as 1.36 and 1.06 mm with 0.1 and 1.0 N of $CaCl_2$ permeants, respectively. Similarly, for 10% tire fibre samples, these heights were reduced from 1.48 to 1.21 and 0.96 mm with NaCl permeants, and 0.99 and 0.83 mm with $CaCl_2$ permeants at the same order of concentrations, respectively. Similarly, for samples with 15% tire fibre content and at the same order of concentrations, the swelling height was declined from 0.93 with DI water to 0.87 and 0.68 mm with NaCl permeants and 0.79 and 0.37 mm with $CaCl_2$ permeants, respectively. Therefore, it can be concluded that the presence of salt significantly influences the swelling tendency of all fibre-mixed BC soil samples, showing the importance of investigating the salt permeant's influences for liner applications.

TH-3665_186104109

Time vs percentage of swell that occurred in each swelling stage (i.e. initial, primary, and secondary) with respect to all the fibre-mixed BC samples under inorganic salt permeants is tabulated in Tables 5.1 to 5.4. Irrespective of fibre content, the amount of time taken for completion of each swelling stage was reduced with the rise in the concentration of pore fluid. For example, from Table 5.1, the time taken to complete the initial, primary, and secondary swelling stages under DI water was 15, 465, and 11040 minutes, respectively. However, these values were recorded as 10, 230, and 2640 minutes for the 1N concentration of NaCl solution for the same order of swelling stages, respectively. This reduction was more significant with the $CaCl_2$ solution than the NaCl. For 1.0 N of $CaCl_2$ solution, the order of reported time values for each swelling stage was 5, 235, and 2260 minutes, respectively. A prolonged duration is required to complete secondary swell, which may be due to the influence of adsorption-desorption reactions on ionic diffusion (Rao et al., 2006). The contribution of the microstructure of compacted soil samples was the reason for the swelling that occurred in the primary and secondary stages. However, the details of the time taken to complete each swelling stage and the percentage of swell that occurred in that particular stage with respect to all fibre-mixed samples under various pore fluids were mentioned in Tables 5.2 to 5.4. The maximum amount of swelling occurred in the primary swelling stage for all soil samples, irrespective of fibre content, salt type, and concentration. The minimum amount of swelling occurred in the initial swelling stages, followed by the secondary swelling stages. For pure BC soil, the percentage of total swelling occurred between 12 to 15% for all samples, irrespective of pore fluid type and concentration in the initial swelling stage. However, this percentage of total swelling occurred less with Ca^{2+} pore fluid than with Na^{+} pore fluid with respect to fibre-mixed soil samples in the initial swelling stage. All the obtained swelling values of fibre-mixed samples under the influence of salt permeants were compared with the RH model and depicted in Figs. 5.8 to 5.11. It was observed from these plots that the slopes of all fibre-mixed samples inundated with water were increased with the increase in both concentration and valency of pore fluid, indicating a substantial reduction in residual swelling values with the permeation of inorganic salt solutions.

TH-3665_186104109

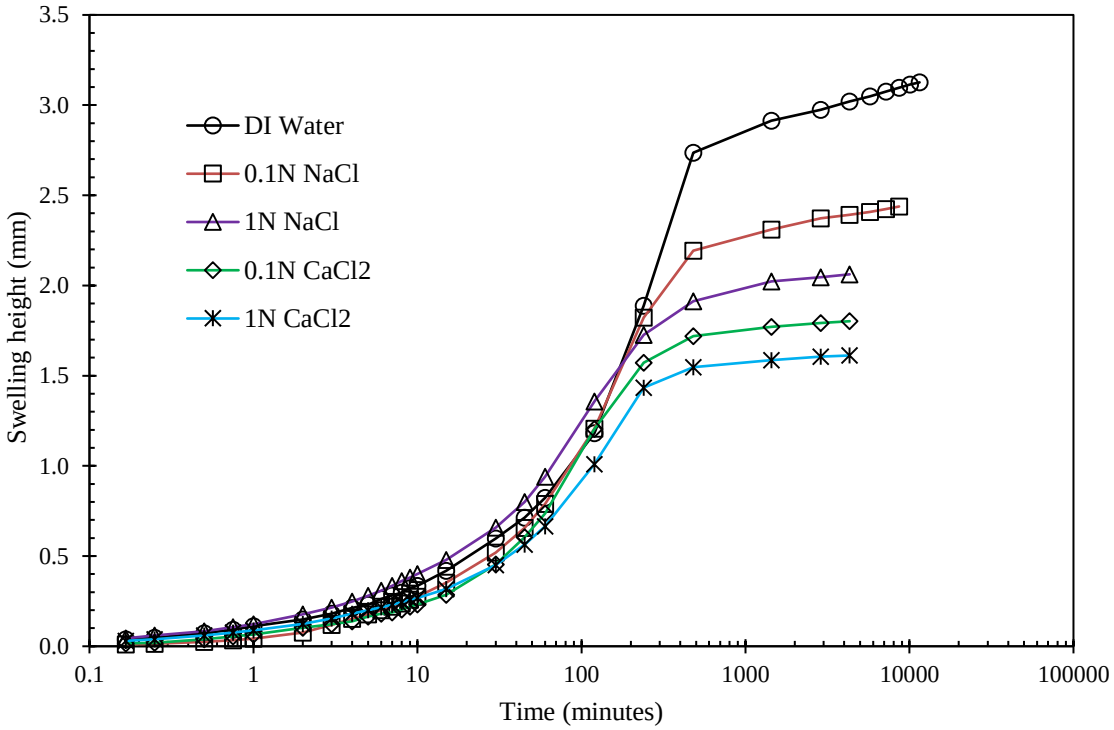

Fig. 5.4. Time-swelling plot of BC soil with NaCl and $CaCl_2$ salt permeants.

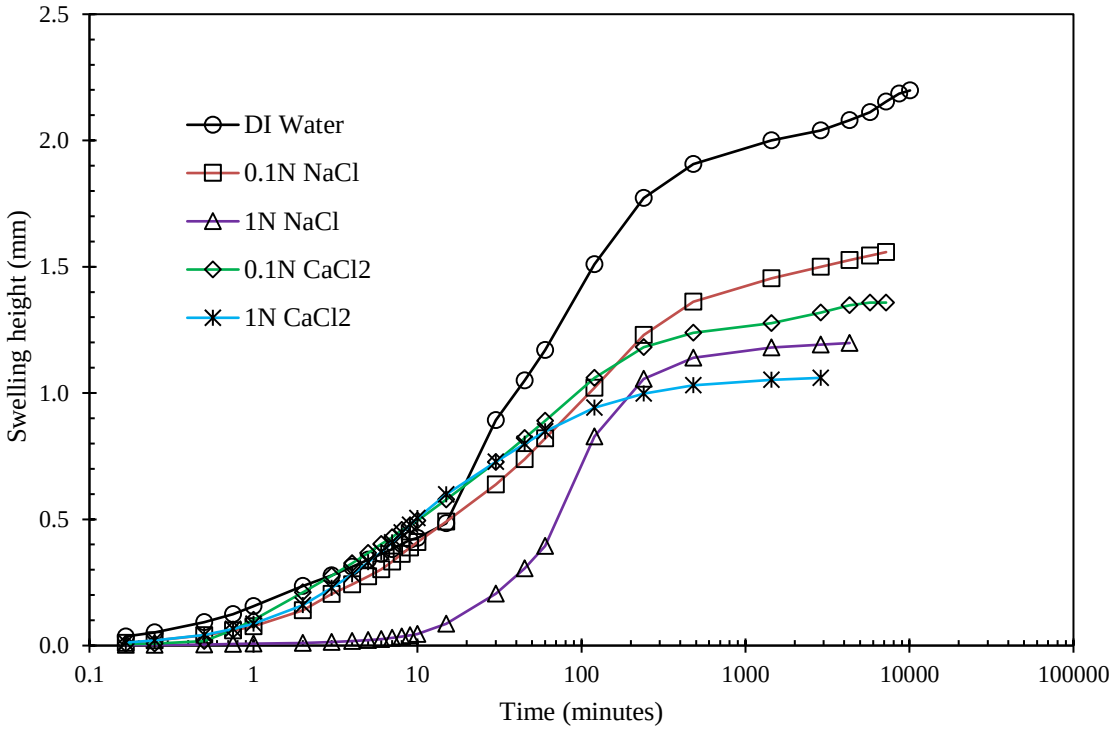

Fig. 5.5. Time-swelling plot of 5% fibre-mixed BC soil with NaCl and $CaCl_2$ salt permeants.

TH-3665_186104109

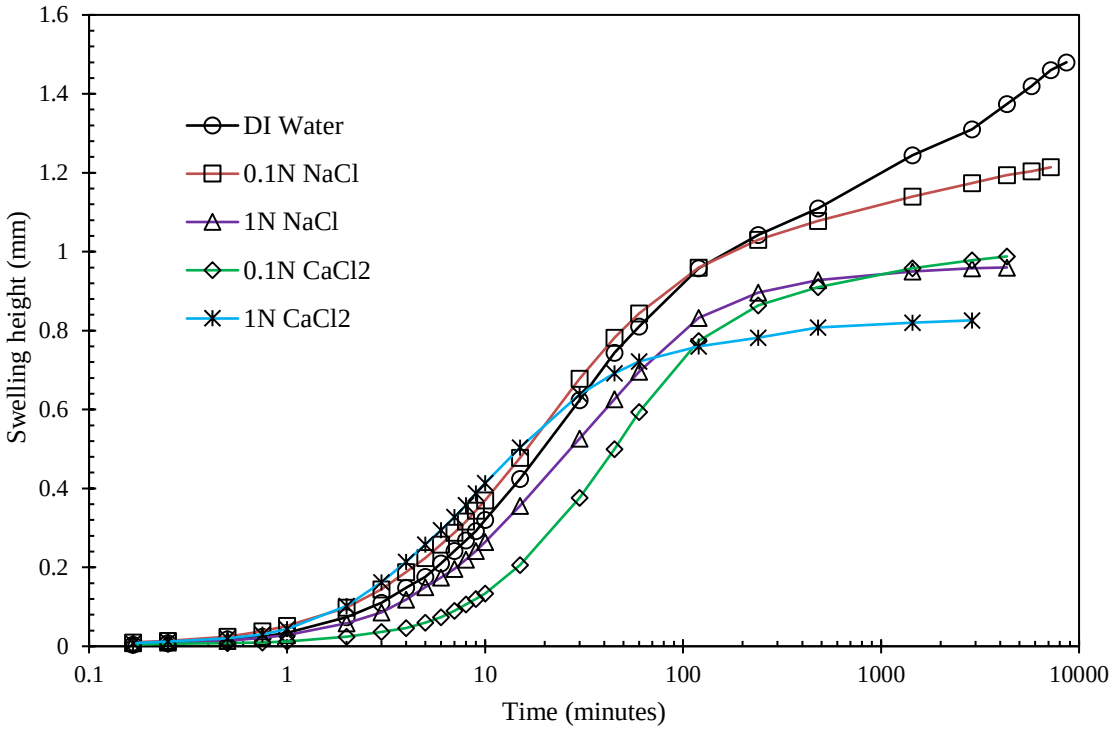

Fig. 5.6. Time-swelling plot of 10% fibre-mixed BC soil with NaCl and $CaCl_2$ salt permeants.

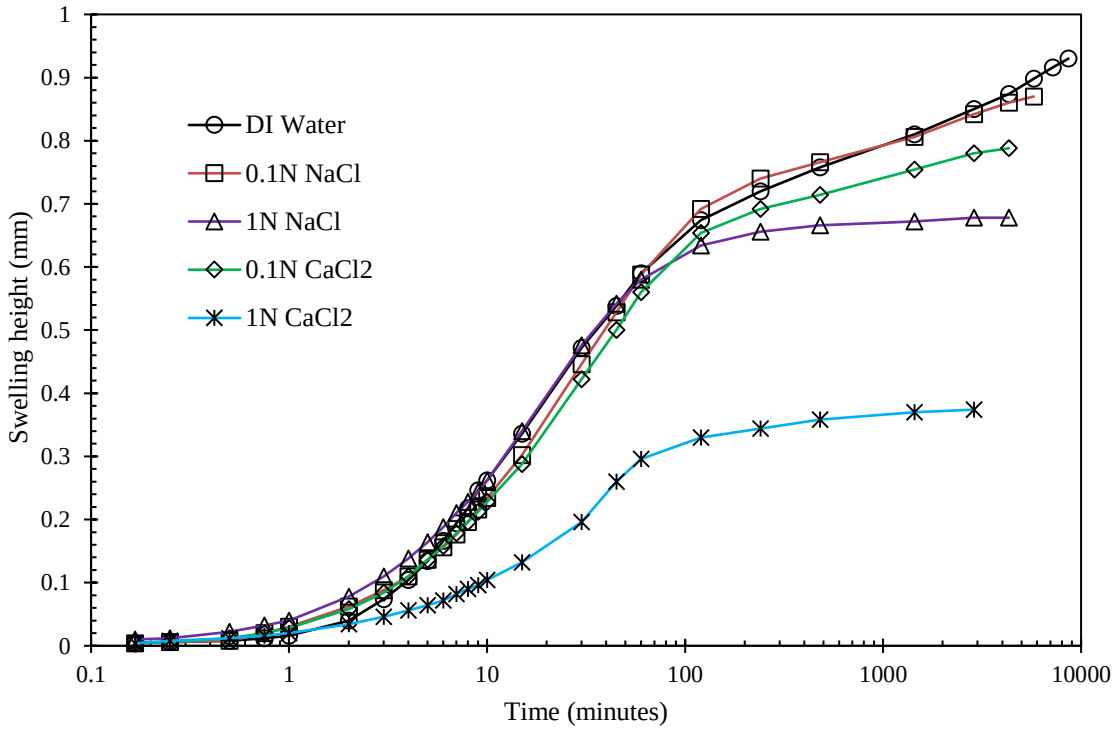

Fig. 5.7. Time-swelling plot of 15% fibre-mixed BC soil with NaCl and $CaCl_2$ salt permeants.

TH-3665_186104109

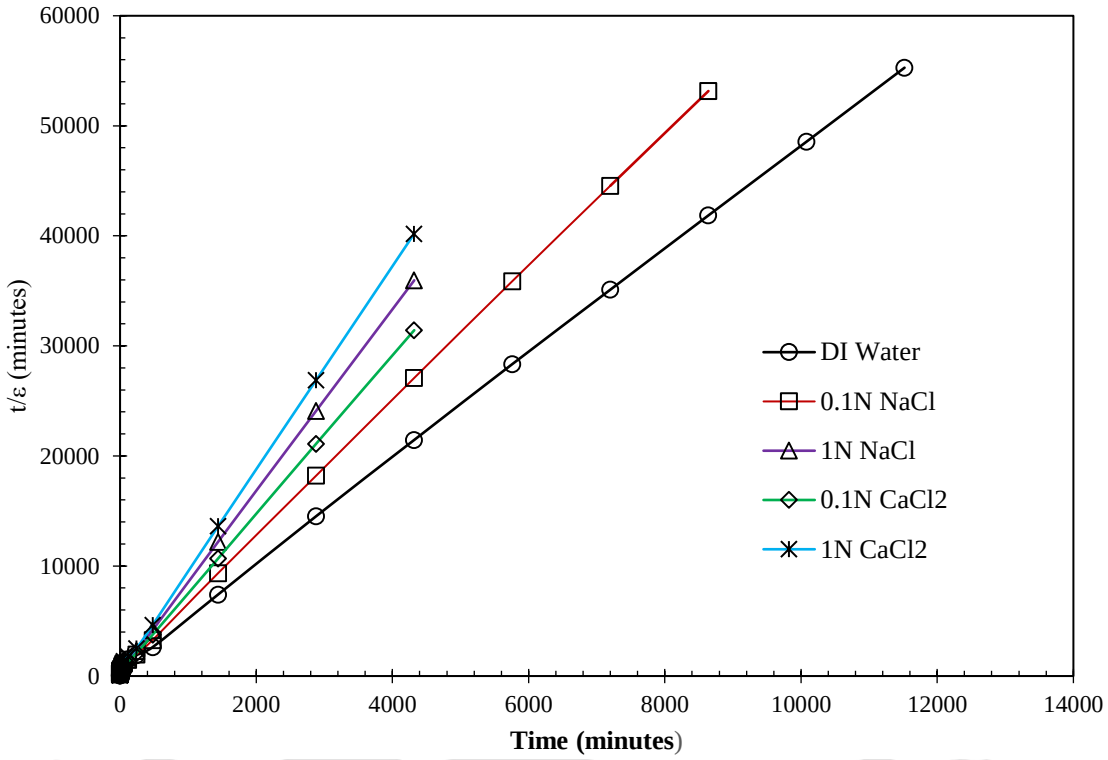

Fig. 5.8. Linearized representation of swelling potential data for BC soil under different salt permeants.

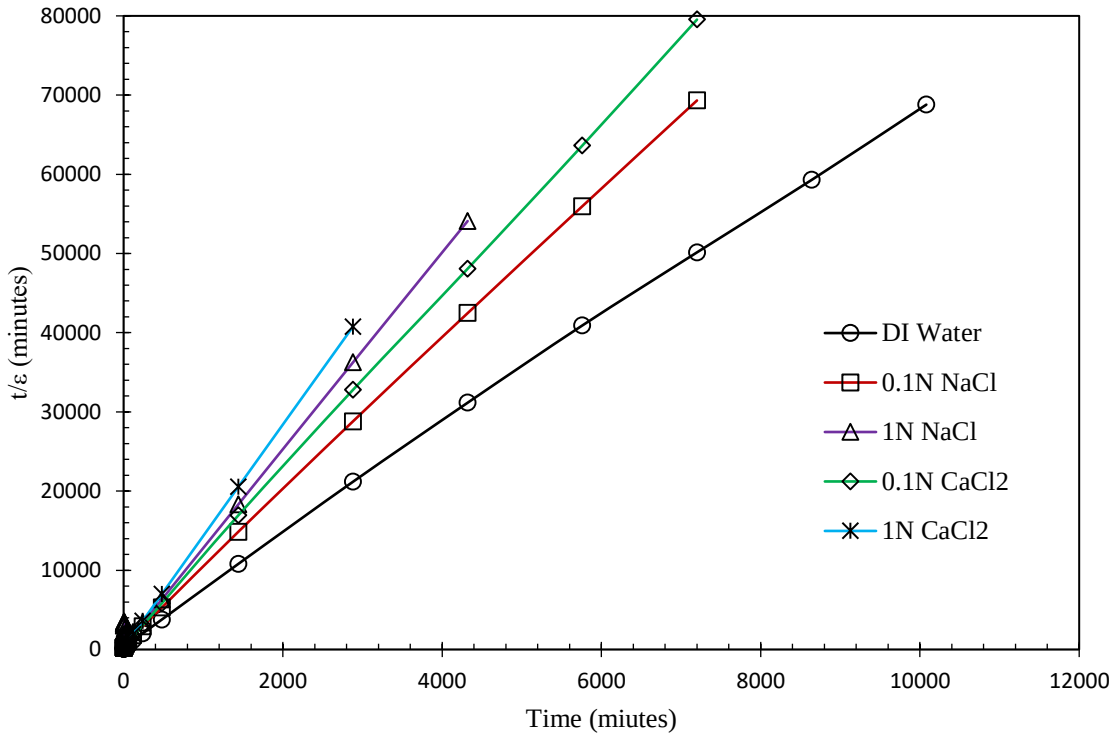

Fig. 5.9. Linearized representation of swelling potential data for 5% fibre-mixed BC soil under different salt permeants.

TH-3665_186104109

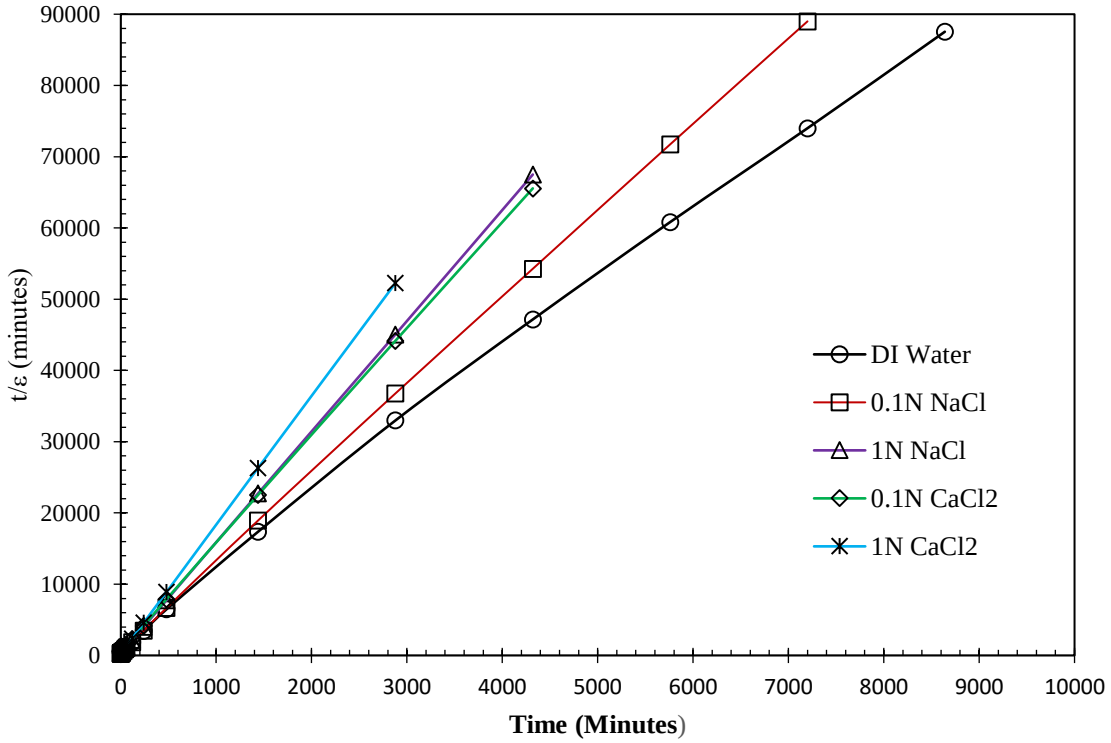

Fig. 5.10. Linearized representation of swelling potential data for 10% fibre-mixed BC soil under different salt permeants.

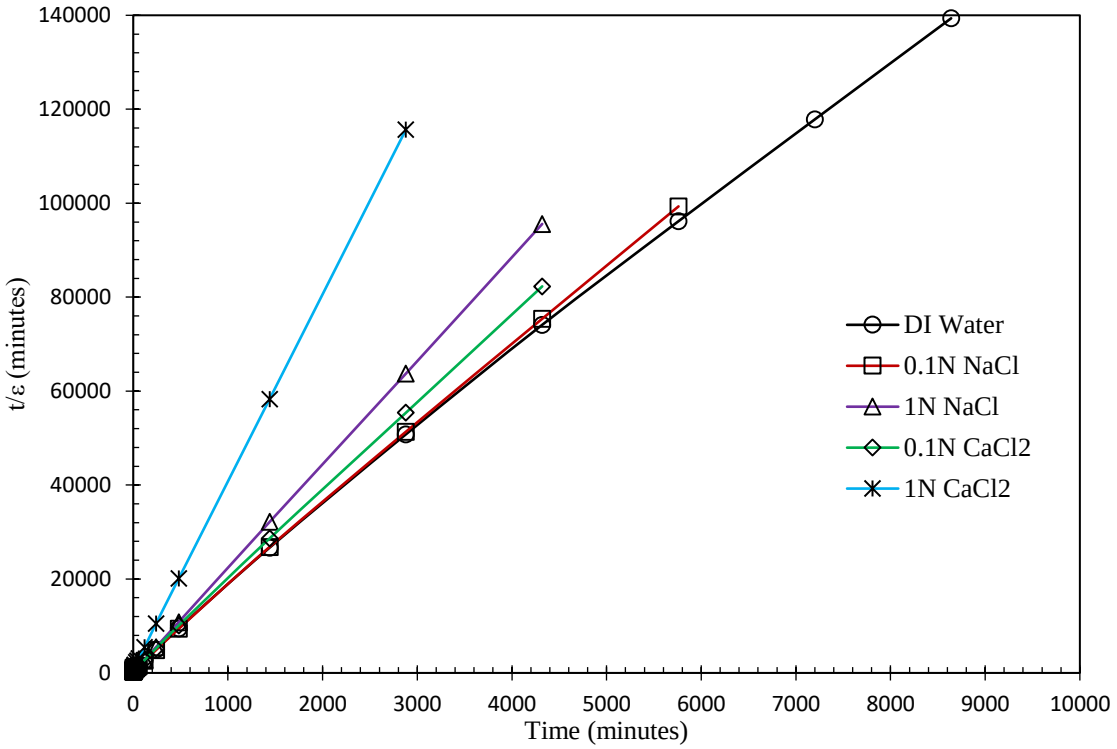

Fig. 5.11. Linearized representation of swelling potential data for 15% fibre-mixed BC soil under different salt permeants.

TH-3665_186104109

Table 5.1. Time and percent swells of pure BC soil with various salt permeant concentrations

Permeant type and concentration	Initial swelling		Primary swelling		Secondary swelling		Total swelling	
	Time (min)	% Swell	Time (min)	% Swell	Time (min)	% Swell	Time (min)	% Swell
DI Water	15	2.79	465	15.45	11040	2.6	11520	20.84
0.1 N NaCl	15	2.35	465	12.28	6720	1.53	7200	16.16
1.0 N NaCl	10	1.55	230	8.93	2640	1.47	2880	11.95
0.1 N $CaCl_2$	5	1.87	325	10.33	3940	1.35	4320	13.75
1.0 N $CaCl_2$	5	1.33	235	8.23	2260	1.14	2500	10.7

Table 5.2. Time and percent swell of 5% fibre-mixed BC soil with various salt permeant concentrations

Permeant type and concentration	Initial swelling		Primary swelling		Secondary swelling		Total swelling	
	Time (min)	% Swell	Time (min)	% Swell	Time (min)	% Swell	Time (min)	% Swell
DI Water	9	2.79	471	9.92	9600	1.94	10080	14.65
0.1N NaCl	7	2.21	473	6.87	6720	1.31	7200	10.39
1.0 N NaCl	10	0.31	230	6.73	2640	0.91	2880	7.95
0.1 N $CaCl_2$	0.5	0.12	239.5	7.76	4260	1.17	4500	9.05
1.0 N $CaCl_2$	0.5	0.28	119.5	6.00	1880	0.79	2000	7.07

TH-3665_186104109

Table 5.3. Time and percent swells of 10% fibre-mixed BC soil with various salt permeant concentrations

Permeant type and concentration	Initial swelling		Primary swelling		Secondary swelling		Total swelling	
	Time (min)	% Swell	Time (min)	% Swell	Time (min)	% Swell	Time (min)	% Swell
DI Water	5	1.17	395	6.13	8240	2.57	8640	9.87
0.1N NaCl	3	0.96	237	5.91	5520	1.16	5760	8.03
1.0 N NaCl	3	0.57	117	4.98	2080	0.84	2200	6.39
0.1 N $CaCl_2$	3	0.24	237	5.52	4080	0.83	4320	6.59
1.0 N $CaCl_2$	0.75	0.20	59.25	4.61	1840	0.69	1900	5.50

Table 5.4. Time and percent swells of 15% fibre-mixed BC soil with various salt permeant concentrations

Permeant type and concentration	Initial swelling		Primary swelling		Secondary swelling		Total swelling	
	Time (min)	% Swell	Time (min)	% Swell	Time (min)	% Swell	Time (min)	% Swell
DI Water	4	0.69	296	4.21	6900	1.21	7200	6.20
0.1N NaCl	3	0.59	177	4.21	5580	1.00	5760	5.80
1.0 N NaCl	2	0.52	88	3.58	2010	0.41	2100	4.51
0.1 N $CaCl_2$	1	0.19	119	4.17	3380	0.84	3500	5.20
1.0 N $CaCl_2$	0.75	0.11	59.25	1.86	1840	0.52	1900	2.49

TH-3665_186104109

5.2.4. Swelling pressures and swelling potentials

For engineered barrier applications, a highly expansive clays are preferred as barrier material due to their self-healing nature and high swelling capacity. Swelling pressure is an important factor in the selection of liner material for landfill application (Dutta and Mishra, 2015). The data in Table 5.5 summarizes the details of swelling pressure values of all fibre-mixed soil samples under various concentrations of saturating liquids. The swelling pressures of BC soil decreased from 520 kPa to 270, 180, and 140 kPa due to the inclusion of 5, 10, and 15% tire fibre, respectively. The discussion regarding swelling pressures of BC soil-tire fibre interaction was explained in Chapter 4. Swelling pressure results are highly dependent on the density state, salinity, and main type of adsorbed cation (Herbert et al., 2008). In this study, all samples were compacted to their OMC and MDD conditions in DI water. A significant influence of inorganic salt of various concentrations on the fibre-mixed BC soil could be observed from the data in Table 5.5. It is observed from the data that there is a considerable reduction in swelling pressure values with the increase in both concentration and valency of pore fluid. For a fibre content of 0, 5, 10, and 15%, the percentage swell pressure reduction with 0.1N NaCl permeant solution was 19.23, 25.93, 16.67, and 36.43%, respectively, compared to soil-fibre samples with saturating liquid as DI water. Similarly, when the concentration of NaCl permeant increases from 0.1 to 1.0 N for the same soil-tire fibre content ratio, the percentage decrease in swell pressures became 28.85, 33.33, 45.56, and 48.50 %, respectively. Previously, many researchers focused on swelling pressures of bentonites permeated with inorganic salt concentrations and found a significant reduction in swelling pressures (Zhu et al., 2013; Dutta and Mishra, 2015; Jadda et al., 2020). However, a few researchers observed a reverse trend with less swelling soils such as kaolinite and medium compressibility (CI) clays (Sivapullaiah and Manju, 2005; Arsan et al., 2010). Chemicals reduced the thickness of the DDL, leading to a contraction of the soil skeleton and a reduction in repulsive forces, thus facilitating the flocculation tendency of clay particles, which ultimately resulted in a granular or gritty texture, leading to the reporting of low swell pressures (Bowders and Daniel, 1987). This reduction in swelling pressures was increased more for the similar concentration of $CaCl_2$ solution used compared to NaCl solution i.e. 21.15, 27.78, 22.22, and 40.71% for 0.1N $CaCl_2$ solution, and 36.84, 40.74, 56.67, and 50.71% for 1N $CaCl_2$ solution with the same soil-fibre mixtures.

TH-3665_186104109

The swelling potentials of all fibre-mixed soil samples permeated with monovalent and divalent pore fluids at different concentrations are tabulated in Table 5.6. The swelling potential values of BC soil with 0, 5, 10, and 15% tire fibre incorporation were reported as 20.84, 16.65, 9.87, and 6.20%, respectively. All swelling potential values were reduced with salt concentrations, irrespective of tire fibre content. For example, the swelling potentials of 0, 5, 10, and 15% fibre-mixed samples with 0.1N NaCl permeant were calculated as 16.25, 10.39, 8.09, and 5.80%, respectively. Compared to DI water, the percentage reduction in these swelling potentials was about 22.02, 37.60, 18.03, and 6.45% with the same order of fibre content, respectively. Similarly, this reduction was nearly about 34.02, 45.65, 33.23, and 15.32% with 0.1N $CaCl_2$ permeant. The swelling potentials are decreased with an increase in the salt (NaCl and $CaCl_2$) concentrations from 0.1 to 1N as shown in Table 5.6. However, much reduction was observed for the $CaCl_2$ permeant compared to the NaCl permeant of the same concentration. The reduction percentage was about 27.10% for a 15% soil-tire mixture with 1N NaCl, which is increased to 59.84% with 1N $CaCl_2$ permeant. Electrical repulsive forces weaken when salt diffuses from the storage salt solution, which makes the clay particles closer together and the void ratio reduces, which leads to an osmotic consolidation. The infiltration of salt permeants diminishes the electrostatic repulsive forces between the montmorillonite minerals of BC soil, resulting in a thinning of the DDL (He et al., 2020) Higher concentration and cation valency reduce DDL thickness furthermore, which is responsible for swelling potentials reduction (Dutta and Mishra, 2015; Xiang et al., 2020). Therefore, it is clear that the influence of inorganic salt permeants was significant on the swelling tendencies of all fibre-mixed BC soil samples. The data in Table 5.7 compares the measured swelling potentials and predicted swelling potentials from the RH model. The hyperbolic parameters of each equation with respect to all samples are also tabulated in Table 5.7. The comparison showed the accuracy of all measured swelling values since no significant variation was observed between measured and predicted swelling potentials. This RH model was perfectly fitting for all permeated fibre-mixed soil samples, irrespective of salt concentration and cation type. Few researchers in the past (Nagaraj et al., 2010; Soltani et al., 2017) adopted this model to understand the swelling behaviour of stabilized expansive soils. A good correlation could be seen in between these two swelling tendencies as shown in Fig. 5.12.

TH-3665_186104109

Table 5.5. Swelling pressures of fibre-mixed BC soil with various salt permeant concentrations

Permeant type and concentration	Swelling pressure (kPa)			
	0% TF	5% TF	10% TF	15% TF
DI Water	520	270	180	140
0.1 N NaCl	420 (19.2%)	200 (25.9%)	150 (16.7%)	89 (36.4%)
1.0 N NaCl	370 (28.8%)	180 (33.3%)	98 (45.5%)	72 (48.6%)
0.1 N $CaCl_2$	410 (21.1%)	195 (27.7%)	140 (22.2%)	83 (40.7%)
1.0 N $CaCl_2$	330 (36.5%)	160 (40.7%)	78 (56.7%)	69 (50.7%)

* Values in brackets represent the percentage of reduction in swelling pressure of fibre-mixed samples under various salt permeants compared to DI water

Table 5.6. Swelling potentials of fibre-mixed BC soil with various salt permeant concentrations

Permeant type and concentration	Swelling potential (%)			
	0% TF	5% TF	10% TF	15% TF
DI Water	20.84	16.65	9.87	6.20
0.1 N NaCl	16.25 (22.0%)	10.39 (37.6%)	8.09 (18.0%)	5.80 (6.5%)
1.0 N NaCl	12.01 (42.4%)	7.99 (52.0%)	6.40 (35.1%)	4.52 (27.1)
0.1 N $CaCl_2$	13.75 (34.0%)	9.05 (45.6%)	6.59 (33.2%)	5.25 (15.3%)
1.0 N $CaCl_2$	10.75 (48.4%)	7.07 (57.5%)	5.51 (44.2%)	2.49 (59.8%)

* Values in brackets represent the percentage of reduction in swelling potential of fibre-mixed samples under various salt permeants compared to DI water

TH-3665_186104109

Table 5.7. Predicted swelling potentials (RH model) vs measured swelling potential values of fibre-mixed samples under various salt permeant concentrations

Tire fibre content (%)	Permeant type and concentration	Hyperbolic parameters		Measured swell (%)	Predicted swell (%)
		a	b		
0	DI Water	4.7941	411.71	20.84	20.86
	0.1N NaCl	6.1234	470.94	16.25	16.34
	1.0 N NaCl	8.2201	423.91	12.01	12.17
	0.1 N $CaCl_2$	7.2254	264.83	13.75	13.85
	1.0N $CaCl_2$	9.215	373.73	10.75	10.86
5	DI Water	6.89	329.7	14.65	14.52
	0.1N NaCl	9.6591	362.76	10.39	10.36
	1.0 N NaCl	11.838	2241.3	7.99	8.45
	0.1N $CaCl_2$	11.039	306.43	9.05	9.06
	1.0 N $CaCl_2$	14.102	178.71	7.07	7.1
10	DI Water	10.292	712.35	9.87	9.72
	0.1N NaCl	12.396	372.41	8.09	8.07
	1.0 N NaCl	15.519	409.46	6.40	6.45
	0.1 N $CaCl_2$	14.972	920.62	6.59	6.68
	1.0 N $CaCl_2$	18.076	234.86	5.51	5.54

TH-3665_186104109

Tire fibre content (%)	Permeant type and concentration	Hyperbolic parameters		Measured swell (%)	Predicted swell (%)
		a	b		
15	DI Water	16.344	904.35	6.11	6.12
	0.1N NaCl	17.287	626.66	5.73	5.79
	1.0N NaCl	22.04	307.47	4.52	4.54
	0.1N $CaCl_2$	19.003	549.98	5.25	5.27
	1.0N $CaCl_2$	39.876	849.88	2.49	2.51

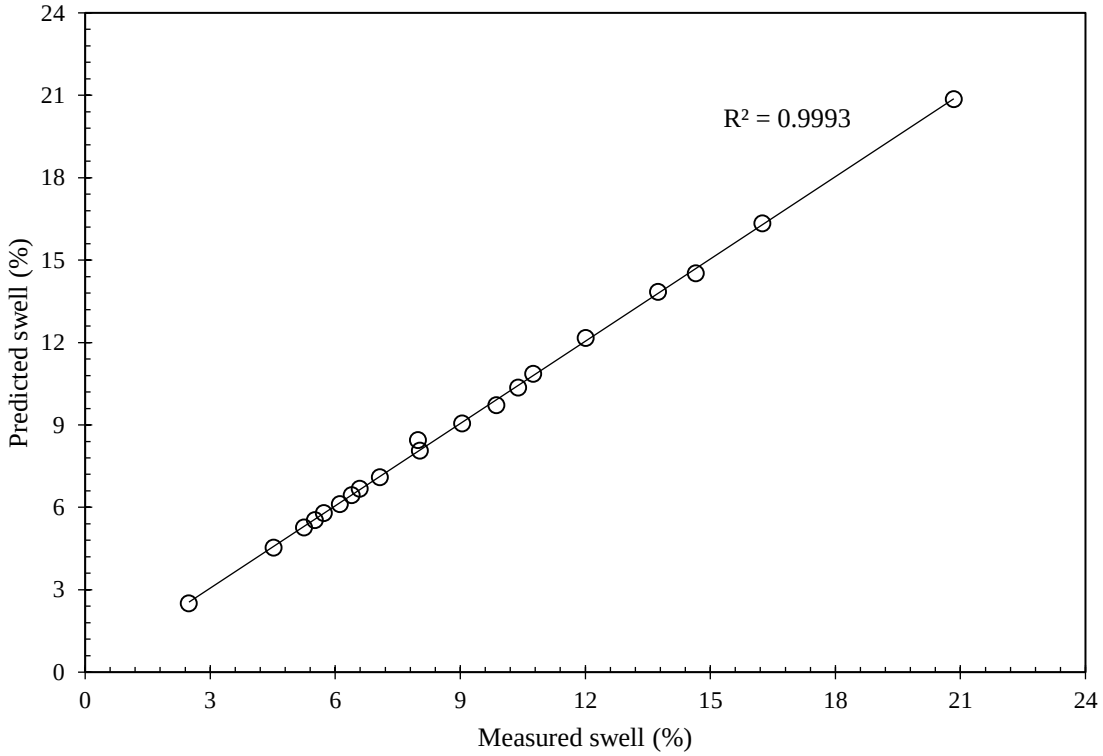

Fig. 5.12. Correlation between measured swell vs predicted swell of all fibre-mixed samples under various salt permeant concentrations.

TH-3665_186104109

5.2.5. Coefficient of consolidation (c_v)

Coefficient of consolidation (c_v) is a measure of the rate of consolidation of a soil sample and is reliant upon the rate at which water is expelled out from the compacted sample for a given load increment. A higher or faster rate of consolidation results in a higher c_v value. The coefficients of consolidation values were determined with the help of t_{90} values determined at various consolidation pressure increments, i.e. 49.0 to 98.1, 98.1 to 196.1 kPa etc. Coefficient of consolidation versus pressure plots for fibre-mixed soil samples permeated with various concentrations of salt permeants was displayed in Figs. 5.13 to 5.16. Irrespective of salt permeant type and concentration, all the samples exhibited lower c_v values at higher consolidation pressures. At a high consolidation pressures, clay particles come closer together due to high surcharge load, which would reduce the interparticle distance and lead to densification of the soil sample. A gradual increment in c_v values of fibre-mixed BC soil was observed in the presence of salt solutions as pore fluids. For example, from Fig. 5.13, the c_v values of pure BC soil are 1.28×10^{-3}, 0.51×10^{-3}, 0.25×10^{-3}, 8.7×10^{-5}, and 2.4×10^{-5} cm^2/s for a corresponding consolidation vertical pressures of 49.0, 98.1, 196.1, 392.2, and 784.5 kPa in the presence of DI water, respectively. For the same order of consolidation pressures, the c_v values of pure BC soil increased to 2.47×10^{-3} (1.93 times), 1.68×10^{-3} (3.29 times), 1.09×10^{-3} (4.36 times), 0.60×10^{-3} (6.9 times), and 0.26×10^{-3} cm^2/s (10.83 times) under 1.0 N NaCl as a pore fluid. This increment in c_v values becomes 6.26, 5.75, 6.52, 10.0, and 17.5 times for the same concentration of $CaCl_2$ pore fluid compared to DI water under the same consolidation pressures. Therefore, it can be concluded that the c_v values increased with an increase in both salt concentration and cation valency.

The plot in Fig. 5.17 shows the variation of c_v values of BC soil mixed with 5, 10, and 15% of tire fibres under various pore fluids at the maximum consolidation pressure of 784.5 kPa. In comparison to DI water at the same consolidation pressure, these values increased to 0.71×10^{-4} (2.96 times), 1.5×10^{-4} (3.66 times), 2.3×10^{-4} (2.91 times), and 9.9×10^{-4} cm^2/s (4.5 times) for 0, 5, 10, and 15% of tire fibre content, respectively under 0.1N NaCl as a pore fluid. At the same pressure, this increment was 10.83, 15.61, 15.06, and 33.27 times for BC soil samples with a tire fibre of 0, 5, 10, and 15%, respectively, under 1.0 N NaCl as a pore fluid. Similarly, for 0.1N $CaCl_2$ pore fluid, this increment was 4.83, 7.22, 7.59, and 8.04 times with the same tire fibre content. Similarly, it was increased by 17.50, 21.46, 18.99, and

TH-3665_186104109

47.73 times in the presence of 1.0 N $CaCl_2$ compared to DI water for the same tire fibre content. Therefore, irrespective of tire fibre content, inorganic salt permeants were found to be affecting BC soil's consolidation rate considerably at high concentrations and cation valency. This rise in c_v values with respect to other lower consolidation pressures also followed a similar kind of trend irrespective of tire fibre content, as depicted in Figs. 5.13 to 5.16. However, it can be clearly seen that there is a significant change in c_v values of fibre-mixed BC soil in the presence of salt permeants.

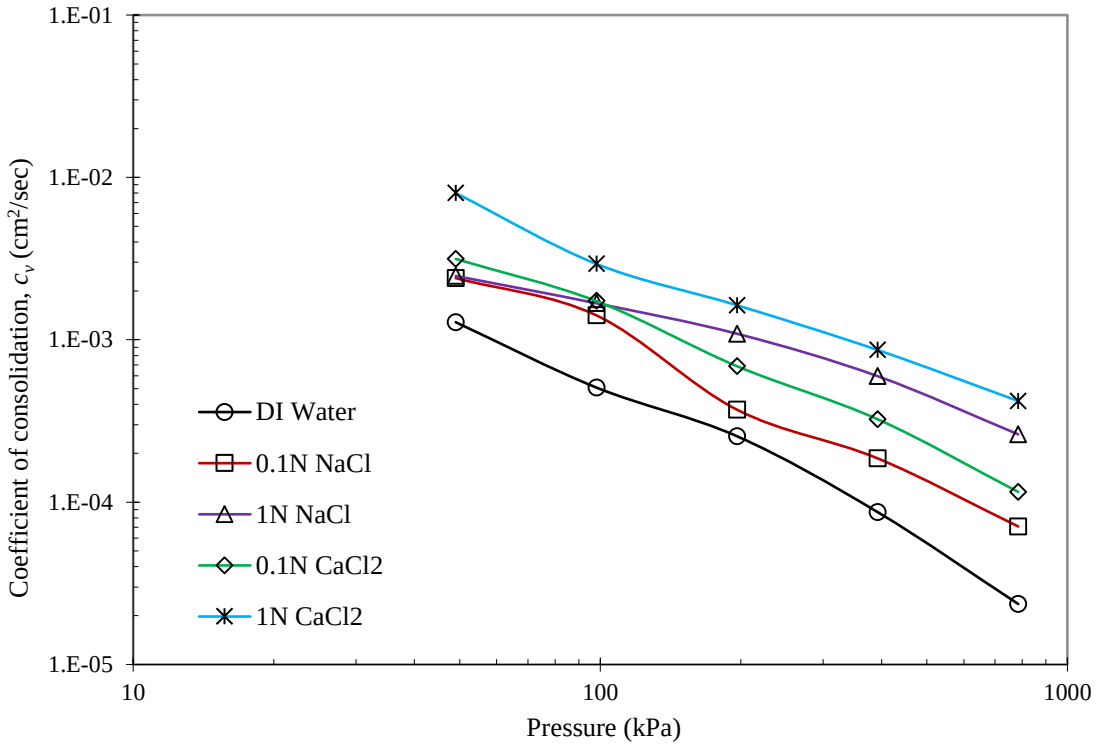

Fig. 5.13. Consolidation pressure vs coefficient of consolidation (c_v) plots for pure BC soil with various concentrations of salt permeants

TH-3665_186104109

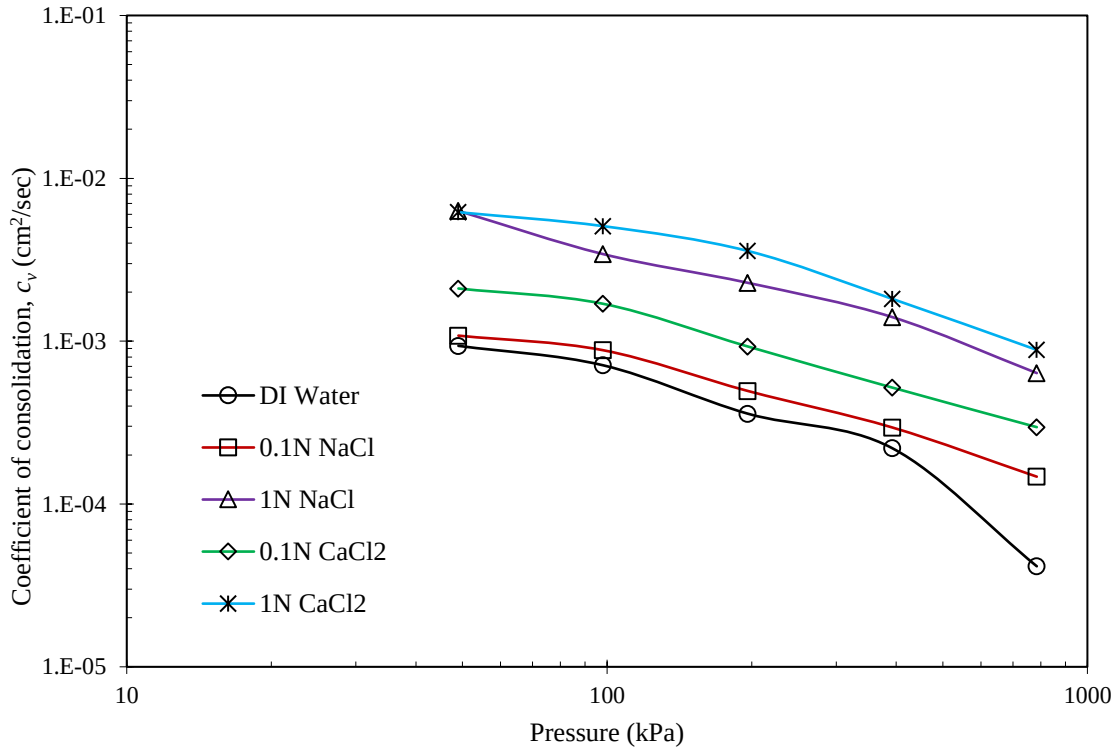

Fig. 5.14. Consolidation pressure vs coefficient of consolidation (c_v) plots for 5% fibre-mixed BC soil with various concentrations of salt permeants

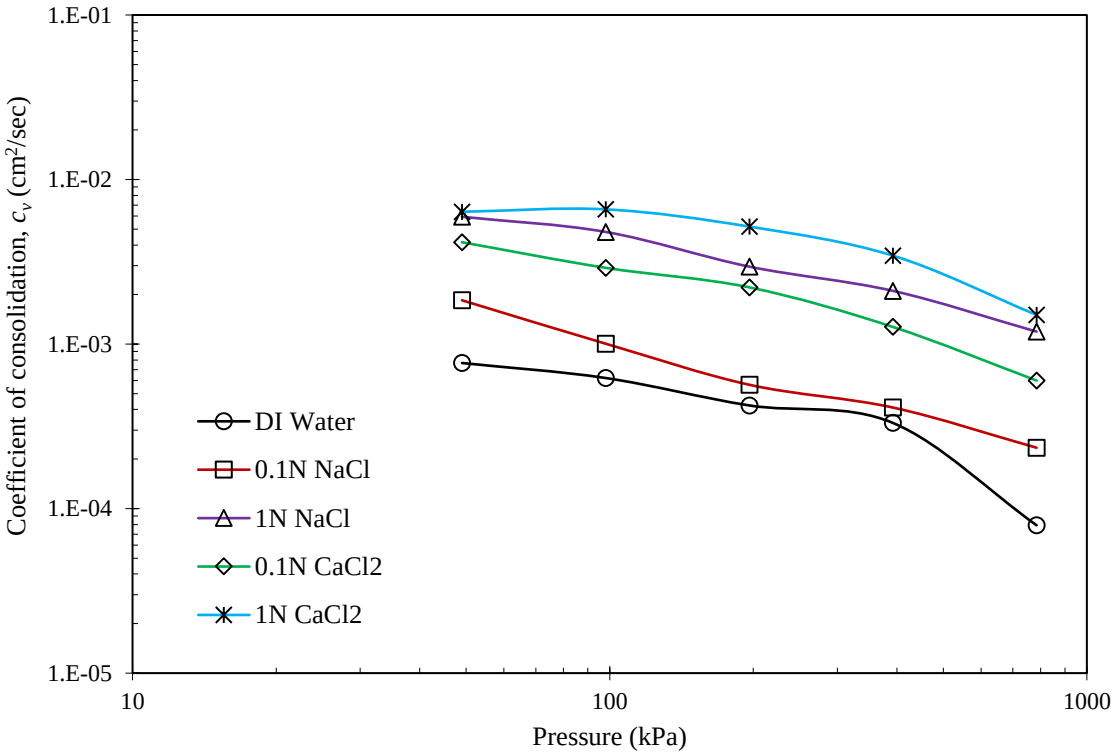

Fig. 5.15. Consolidation pressure vs coefficient of consolidation (c_v) plots for 10% fibre-mixed BC soil with various concentrations of salt permeant

TH-3665_186104109

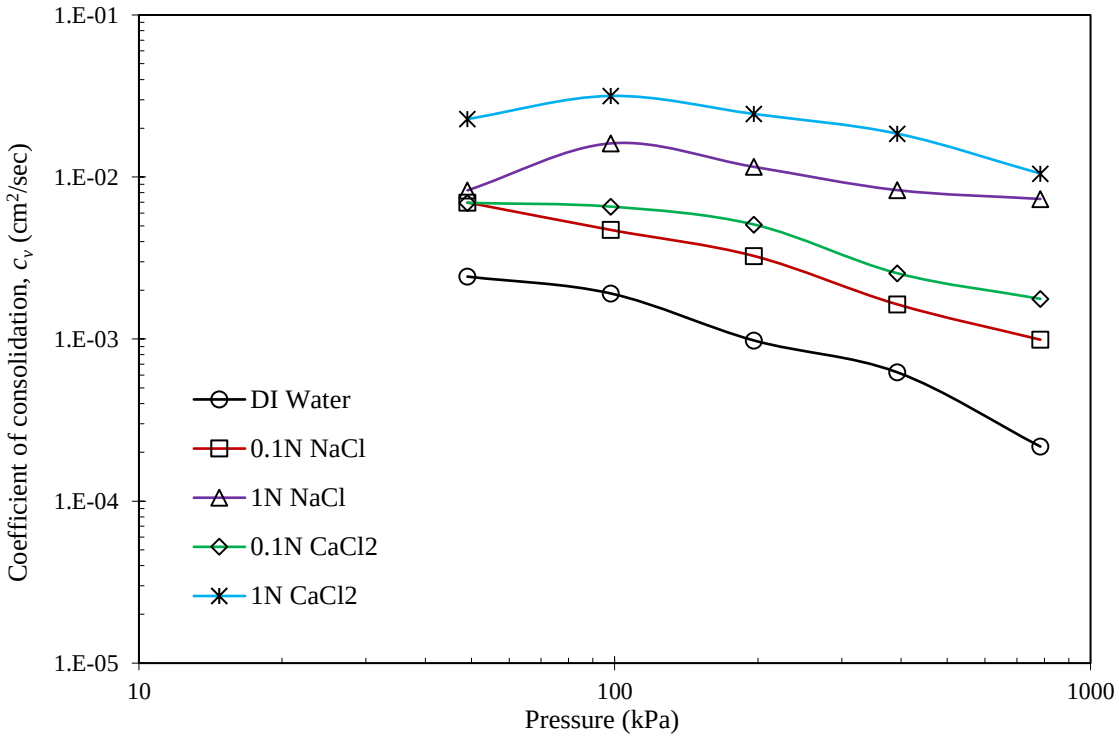

Fig. 5.16. Consolidation pressure vs coefficient of consolidation (c_v) plots for 15% fibre-mixed BC soil with various concentrations of salt permeant.

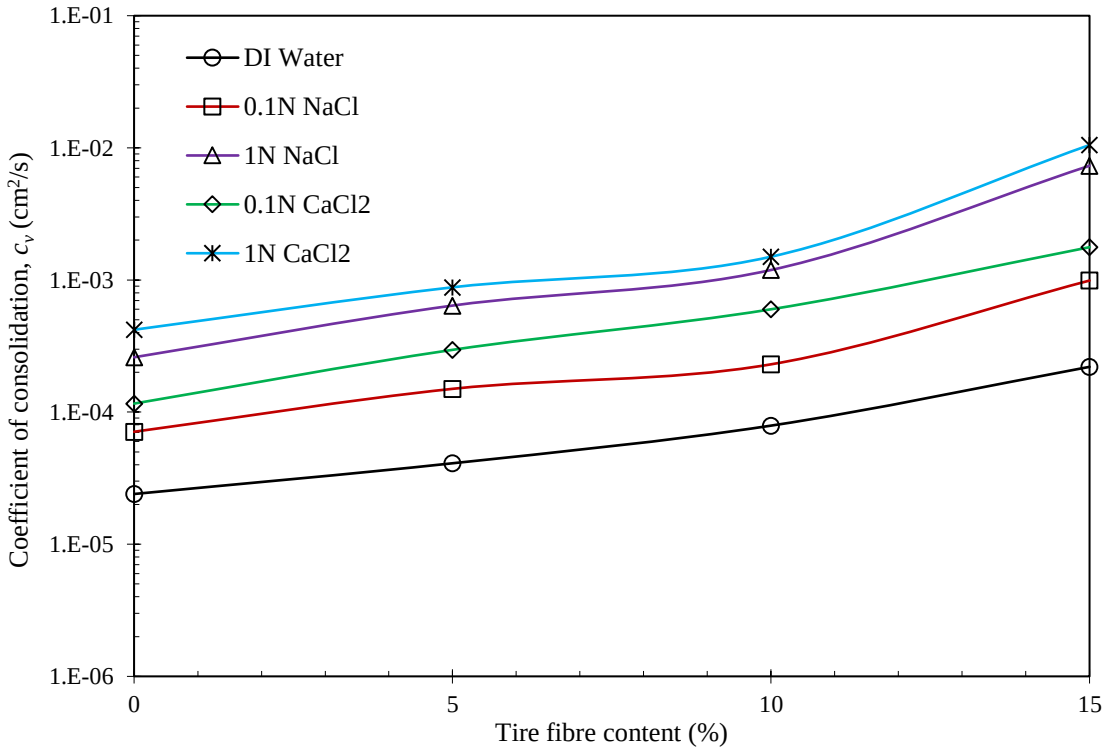

Fig. 5.17. Fibre content vs coefficient of consolidation plot with various salt permeant concentrations at a consolidation pressure of 784.5 kPa.

TH-3665_186104109

5.2.6. Time for 90% consolidation (t_{90})

The plot in Figs. 5.18 to 5.21 show the variation in t_{90} values corresponding to different consolidation pressures of BC soil for different percentages of tire content with various permeant solutions. The plots show that as the consolidation pressure increases, the sample's t_{90} value increases with for all salt permeants. Similar observations for pure bentonites was also observed by other researchers (Dutta and Mishra, 2016(a); Ray et al., 2021(a)). The plot in Fig. 5.18 shows that the t_{90} values of the BC soil in the presence DI water as a pore fluid increased from 9 minutes to 22.09, 40.96, 106.09, and 334.89 minutes due to a corresponding increase in the pressure from 49.0 kPa to 98.1, 196.1, 392.3, and 784.5 kPa, respectively. The decreased in the t_{90} values in the presence of $CaCl_2$ in comparison to similar concentrations of NaCl solution for the same consolidation pressures as shown in Fig. 5.18. In order to gain a more comprehensive comprehension of the t_{90} behaviour of fibre-mixed permeated soil samples, a comparison was done for a particular consolidation pressure of 784.5 kPa. The plot in Fig. 5.22 represents the variation of t_{90} values for the fibre-mixed BC soil in the presence of salt permeants at a consolidation pressure of 784.5 kPa. From Fig. 5.22, it can be noticed that the t_{90} values of BC soil decreased from 334.89 minutes to 104.04, 27.04, 63.20, and 16.81 minutes for a change in the pore fluid permeants from DI water to 0.1N NaCl, 1N NaCl, 0.1N $CaCl_2$, and 1N $CaCl_2$ solutions, respectively with a corresponding reduction in t_{90} values of 68.93, 91.92, 81.13, and 94.98% compared to DI water. The decrease in the inter-particle repulsion due to the presence of salts can be attributed to this variation in t_{90} values.

The plot in Fig. 5.22 also explains the relation between the fibre content and t_{90} values in the presence of various pore fluids at a consolidation pressure of 784.5 kPa. From the Fig. 5.22 it can be seen that the t_{90} values for BC soil (DI water as pore fluid) decreased from 334.89 minutes to 163.84, 81, and 21.04 minutes for an increase in the tire content from 0% to 5, 10, and 15%, respectively. The reasons for this decrement in t_{90} values with respect to tire fibre content was discussed in Chapter 4. However, the t_{90} values of fibre-mixed soil reduced significantly with salt permeants in comparison to DI water. At the same consolidation pressure, the t_{90} values were reported as 104.04, 43.56, 26.01, and 5.76 minutes for 0, 5, 10, and 15% tire content under 0.1N NaCl pore fluid, respectively. It can also be seen that with an increase in the concentration of the NaCl from 0.1 to 1.0N, the t_{90} values become 27.04, 10.24, 5.06, and 0.81 minutes for BC soil with 0, 5, 10, and 15% tire content, respectively.

TH-3665_186104109

From the plot it can also be seen that the t_{90} values decreases when the salt type changes from NaCl to $CaCl_2$. At the same consolidation pressure, these t_{90} values were reported as 63.20, 22.09, 10.89, and 3.24 minutes for 0.1N $CaCl_2$ and 16.81, 7.29, 4.00, and 0.56 minutes for 1.0 N $CaCl_2$ with a 0, 5, 10, and 15% fibre content, respectively. It can also be observed that the t_{90} value of 15% fibre-mixed soil with DI water is 27.04 minutes, and it decreased drastically to 0.81 minutes (97% reduction) for 1.0N NaCl solution and 0.56 minutes (97.93% reduction) for 1.0N $CaCl_2$ solution at 784.5kPa. The variation in t_{90} values of all fibre-mixed permeated BC soil samples with respect to remaining consolidation pressures could be observed in Figs. 5.18 to 5.21. From the plots it could be concluded that the concentration of pore fluid influences the t_{90} values of all fibre-mixed BC soil samples significantly. The formation of drainage paths due to fibres and the reduction in the DDL thickness due to salts lead to this substantial reduction in t_{90} values of BC soil.

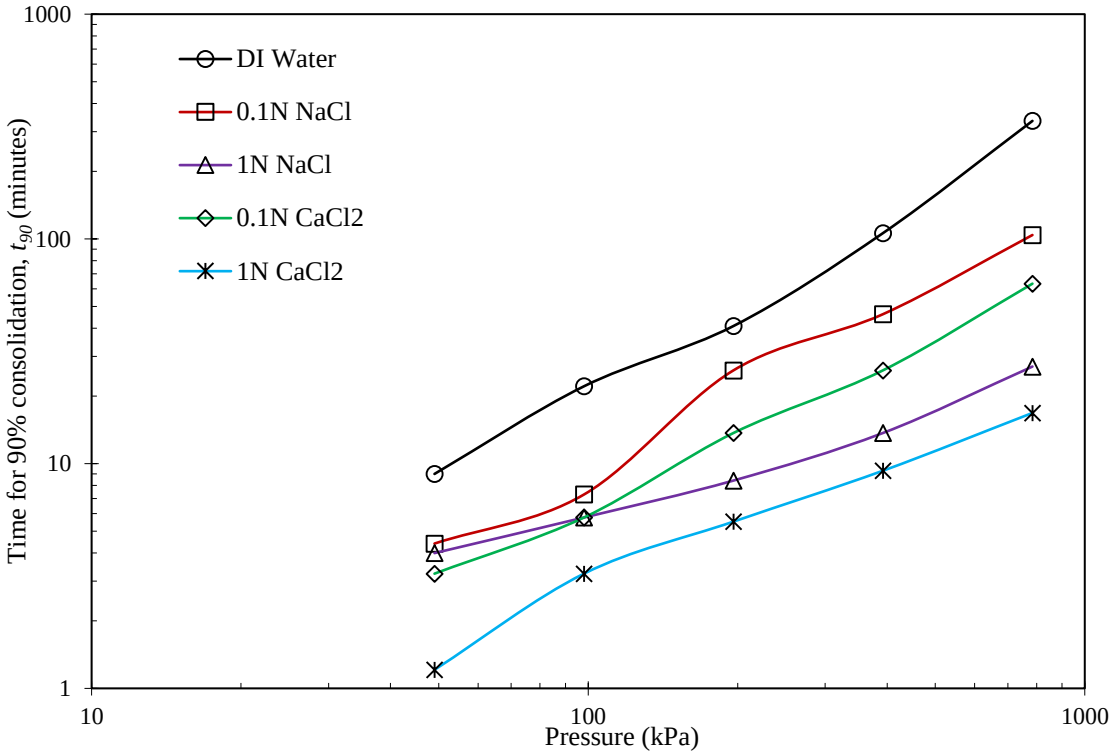

Fig. 5.18. Consolidation pressure vs time for 90% consolidation (t_{90}) plots for pure BC soil with various salt permeant concentrations

TH-3665_186104109

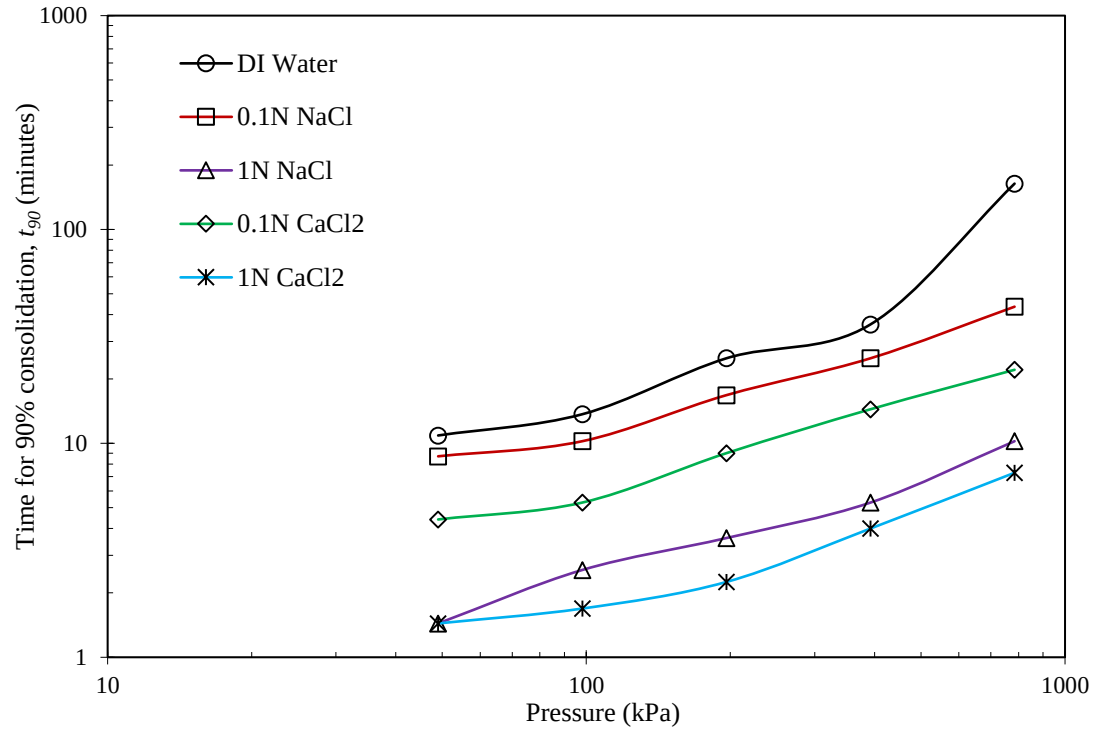

Fig. 5.19. Consolidation pressure vs time for 90% consolidation (t_{90}) plots for 5% fibre-mixed BC soil with various salt permeant concentrations.

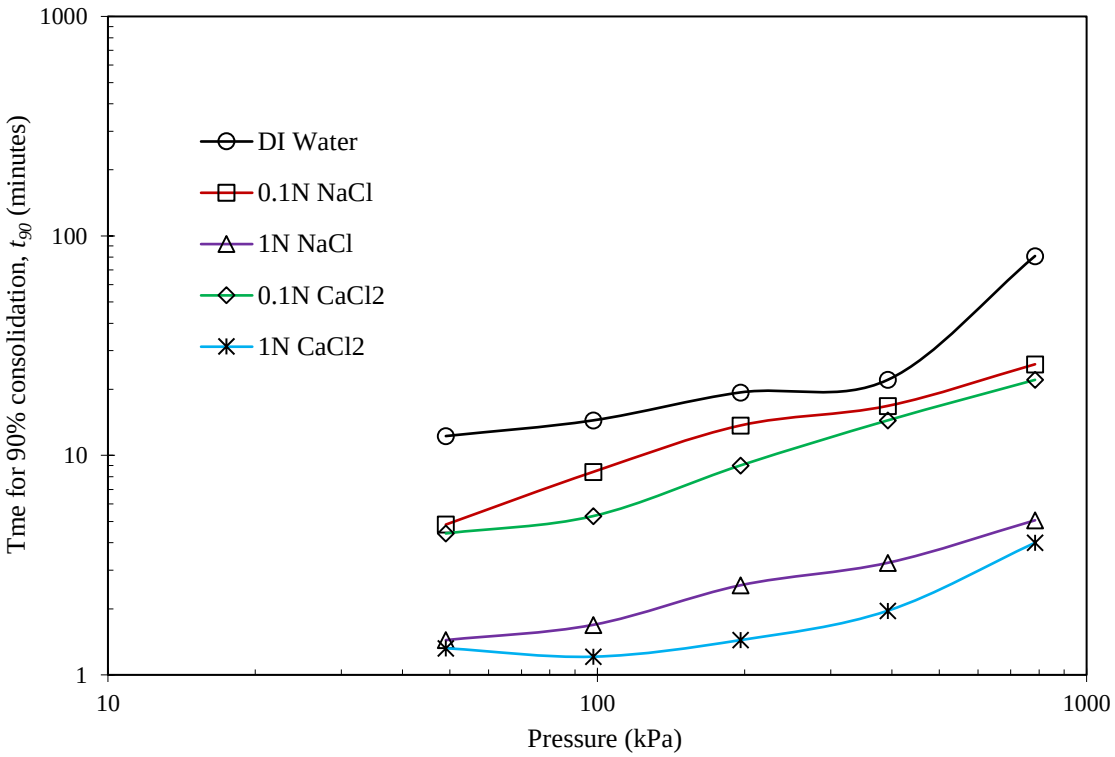

Fig. 5.20. Consolidation pressure vs time for 90% consolidation (t_{90}) plots for 10% fibre-mixed BC soil with various salt permeant concentrations.

TH-3665_186104109

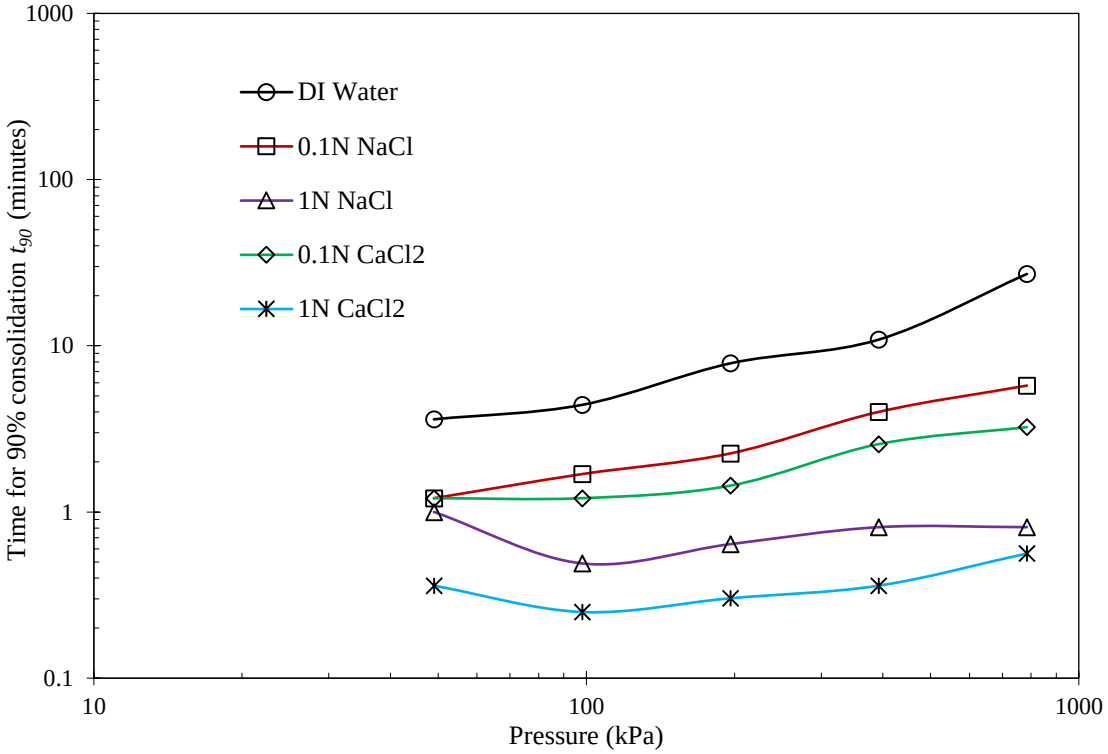

Fig. 5.21. Consolidation pressure vs time for 90% consolidation (t_{90}) plots for 15% fibre-mixed BC soil with various salt permeant concentrations.

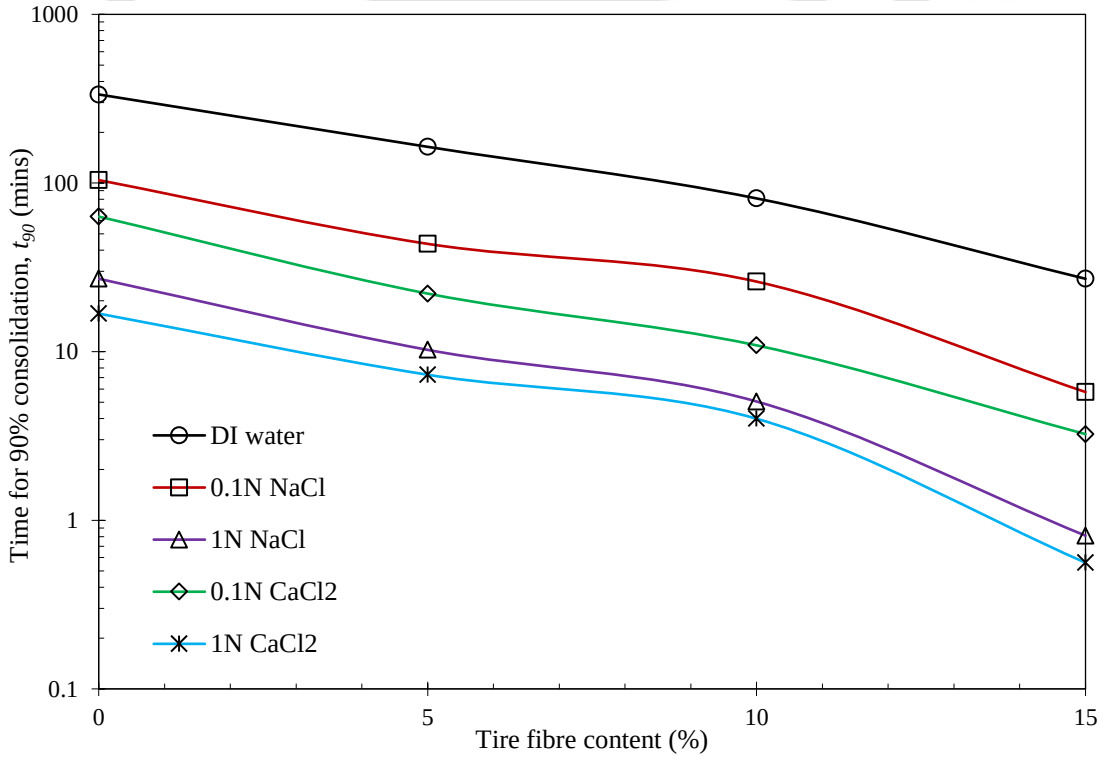

Fig. 5.22. Fibre content vs time for 90% consolidation (t_{90}) plot with various salt permeant concentrations at the consolidation pressure of 784.5 kPa.

TH-3665_186104109

5.2.7. Void ratio vs Pressure (*e*-log *P*) relationship

Consolidation tests were performed at different consolidation pressures on the fibre-mixed BC soil samples permeated with various concentrations of saturating liquids. The test results simulate the compressibility characteristics of soil samples at various overburden pressures which represents the weight of the overburden waste material. The plot in Figs. 5.23 to 5.26 show the *e*-log *P* relationship of all the fibre-mixed soils under various saturating pore fluids. The void ratios of all samples reduced as the consolidation pressures increased regardless of fibre content and pore fluid type and concentration. The plot in Figs 5.23 to 5.26 depicts a reduction in the void ratio for all the samples in the presence of salt as pore fluids. This reduction in the void ratio with the increase in the pore fluid concentrations is due to a decrease in interparticle repulsive forces between clay particles caused by cation migration into the montmorillonite interlayer (Bolt, 1956; Sridharan et al., 1986). This reduction in the void ratio was higher with an increase in the salt concentration and cation valency. For example, from Fig. 5.23, it can be noticed that the void ratio of pure BC soil in DI water at a consolidation pressure of 49.0 kPa was 1.11, which was decreased marginally to 1.04, 0.99, 1.03, and 0.98 for 0.1N NaCl, 1N NaCl, 0.1N $CaCl_2$, and 1N $CaCl_2$ salt permeants, respectively. However, at a higher overburden pressure of 784.5 kPa, the corresponding void ratios were reported as 0.67, 0.64, 0.63, 0.65, and 0.63 for the same order of salt permeant type and concentration, respectively indicating a marginal reduction in the void ratio in the presence of salt at higher pressure. Ye et al. (2014) and Jadda and Bag (2020) also observed similar behaviour for pure bentonites for monovalent and divalent salt permeants.

A slight reduction in void ratios with the inclusion of fibre can be seen in Figs 5.23 to 5.26. A detailed discussion on the BC soil-fibre compressibility behaviour is made in Chapter 4. The effect of salts on the void ratio of fibre-mixed soils can also be observed in Figs 5.23 to 5.26. The plots show that the void ratios of all fibre-mixed soils decrease with the salt permeants as pore fluids compared to DI water. This reduction was more with a rise in the concentration of the same salt type. It can be seen from Fig. 5.24 that the void ratio for 5% fibre-mixed BC soil was decreased from 1.03 to 0.94 and 0.92 with an increase in the concentration from 0 (DI water) to 0.1N NaCl and 1N NaCl, at a consolidation pressure of 49.0 kPa, respectively. For an increase in the cation valency from Na^+ to Ca^{2+}, this reduction in void ratio becomes 0.94 and 0.90 for 0.1N $CaCl_2$ and 1N $CaCl_2$ at the same consolidation pressure, respectively. Similar behaviour was observed for the remaining soil-fibre mixes also. However, at high consolidation pressures no particular pattern was observed.

TH-3665_186104109

4.2.8. Compression index (C_c)

The plot in Fig. 5.27 shows the compressibility behaviour of fibre-mixed BC soil in the presence of different pore fluids. The slope of the straight-line portion of the *e*-log *P* curves was used to calculate the compression index for all the samples. In addition to the mechanical properties, the physio-chemical properties are the main factors influencing the compressibility behaviour of an expansive soil such as BC soil (Bolt, 1956; Dutta and Mishra, 2016a; Thanh Duong and Van Hao 2020). The compression index (C_c) of BC soil was decreased from 0.478 and 0.432 with 0.1 and 1.0 N of NaCl permeant. to 0.465 and 0.422 with 0.1 and 1.0 N concentrations of $CaCl_2$, respectively. The particle orientation becomes more flocculated at higher concentrations, preventing the settlement and lowering the Cc value (Dutta and Mishra, 2016a). Similar observations were made with all fibre-mixed soil samples with the same pore fluid concentrations. For example, for 5% tire content, the C_c value decreased from 0.450 (DI water) to 0.404 and 0.339 for 1N NaCl and 1N $CaCl_2$ pore fluids, respectively. However, at 0.1N of NaCl concentration, a very marginal difference was observed compared to DI water. Similarly, for 10% fibre-mixed soils the C_c value was decreased from 0.391 (DI water) to 0.362 (7.42% reduction) and 0.318 (18.67% reduction) with 1.0 N NaCl and $CaCl_2$ salt permeants, respectively. Finally, for 15% fibre-mixed soils the C_c value was decreased from 0.429 (DI water) to 0.370 (13.75% reduction) and 0.322 (24.94% reduction) with the same order of permeant type and concentration, respectively.

TH-3665_186104109

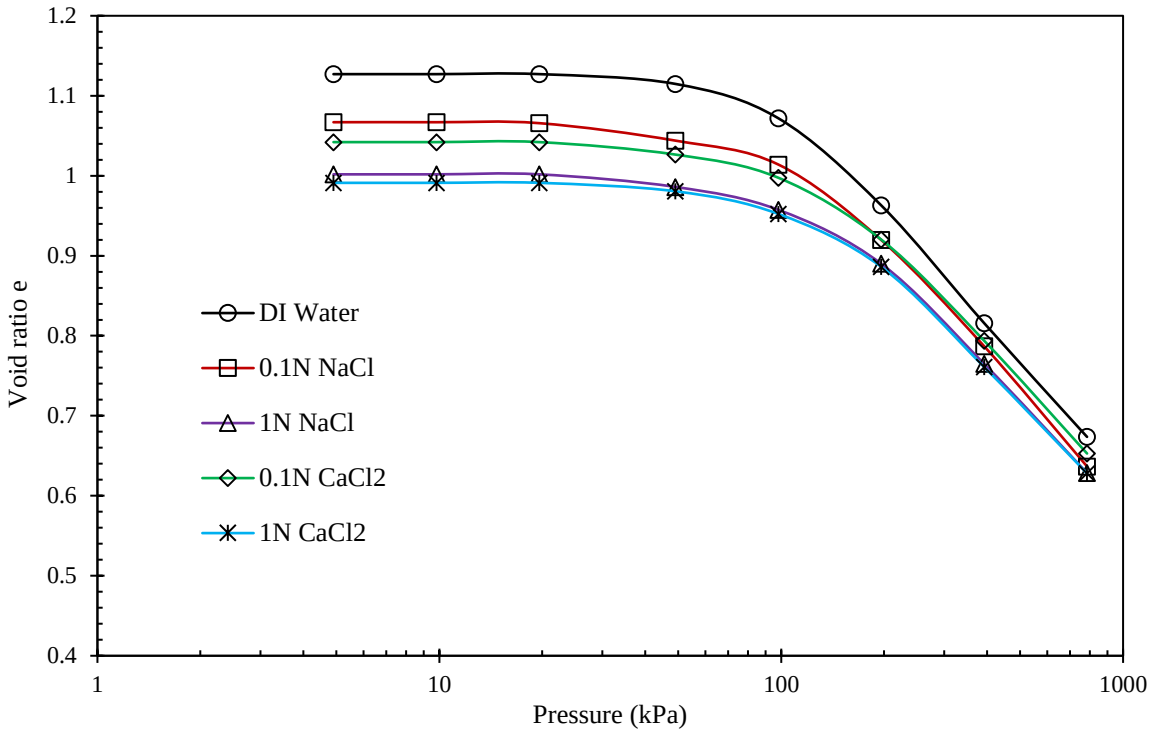

Fig. 5.23. Void ratio (*e*) vs consolidation pressure (*P*) plots for pure BC soil with various salt permeant concentrations.

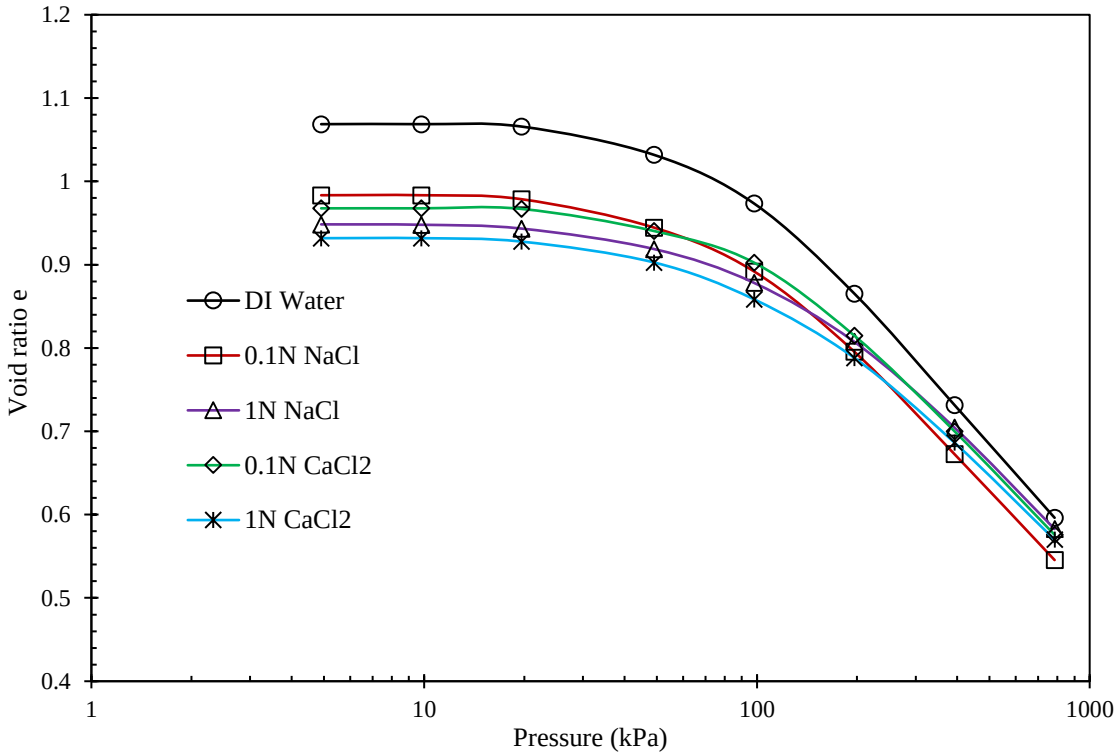

Fig. 5.24. Void ratio (*e*) vs consolidation pressure (*P*) plots for 5% fibre-mixed BC soil with various salt permeant concentrations.

TH-3665_186104109

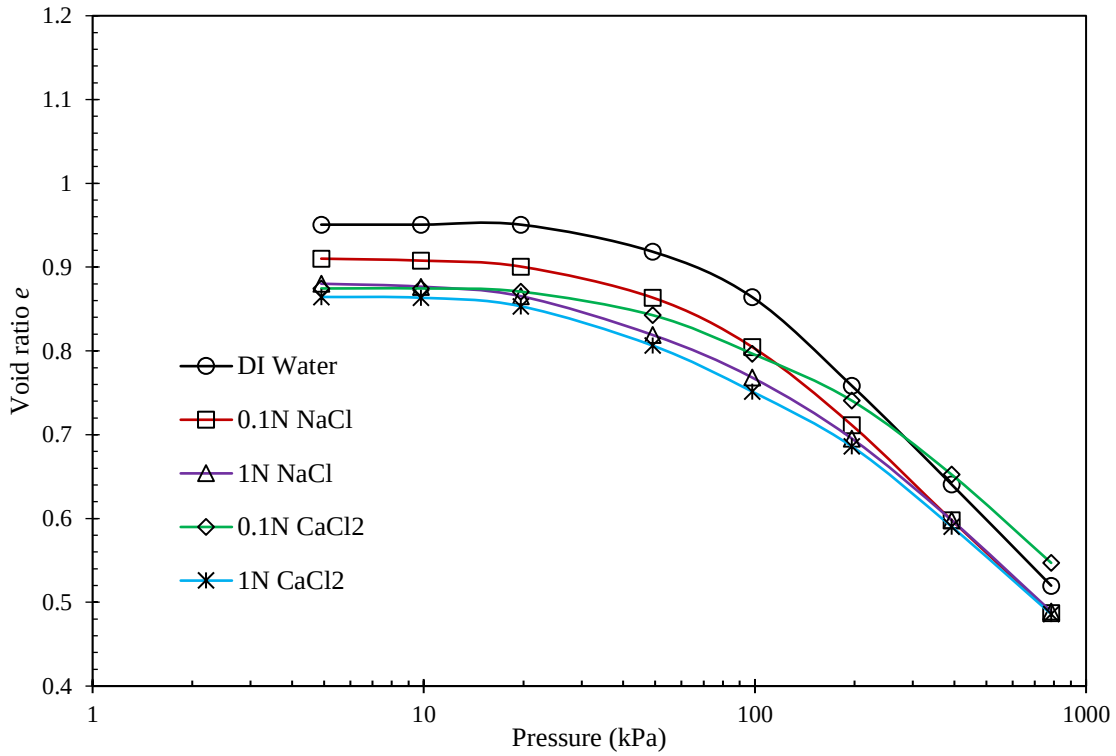

Fig. 5.25. Void ratio (*e*) vs consolidation pressure (*P*) plots for 10% fibre-mixed BC soil with various salt permeant concentrations.

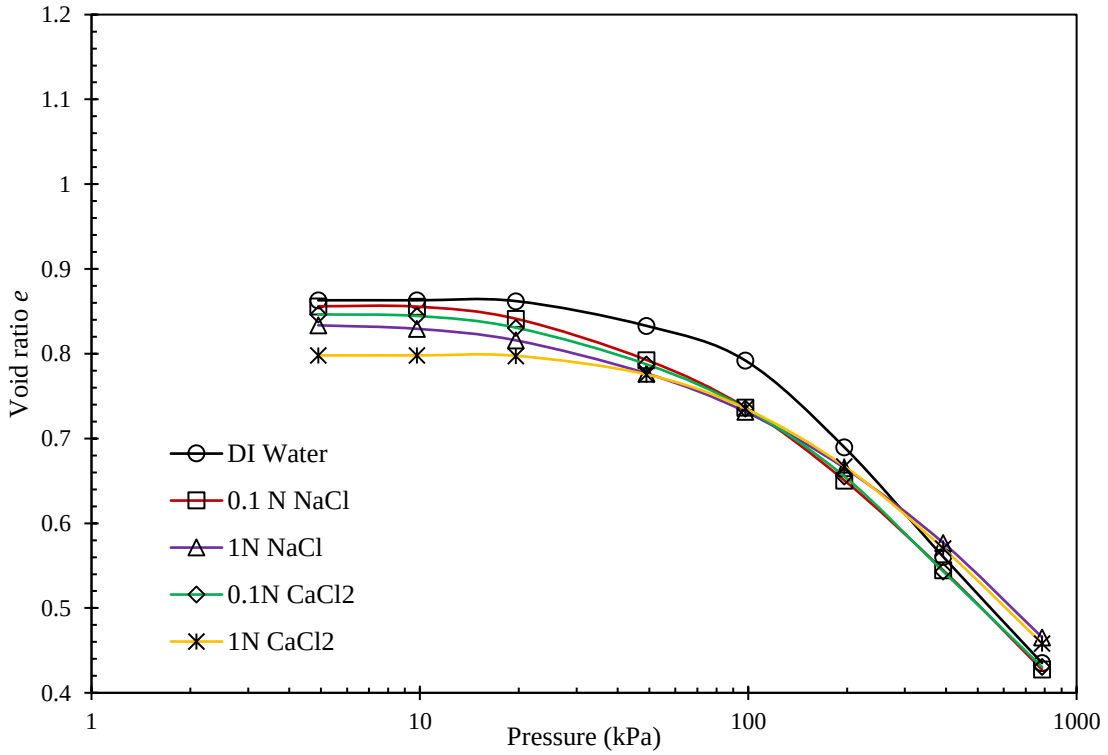

Fig. 5.26. Void ratio (*e*) vs consolidation pressure (*P*) plots for 15% fibre-mixed BC soil with various salt permeant concentrations.

TH-3665_186104109

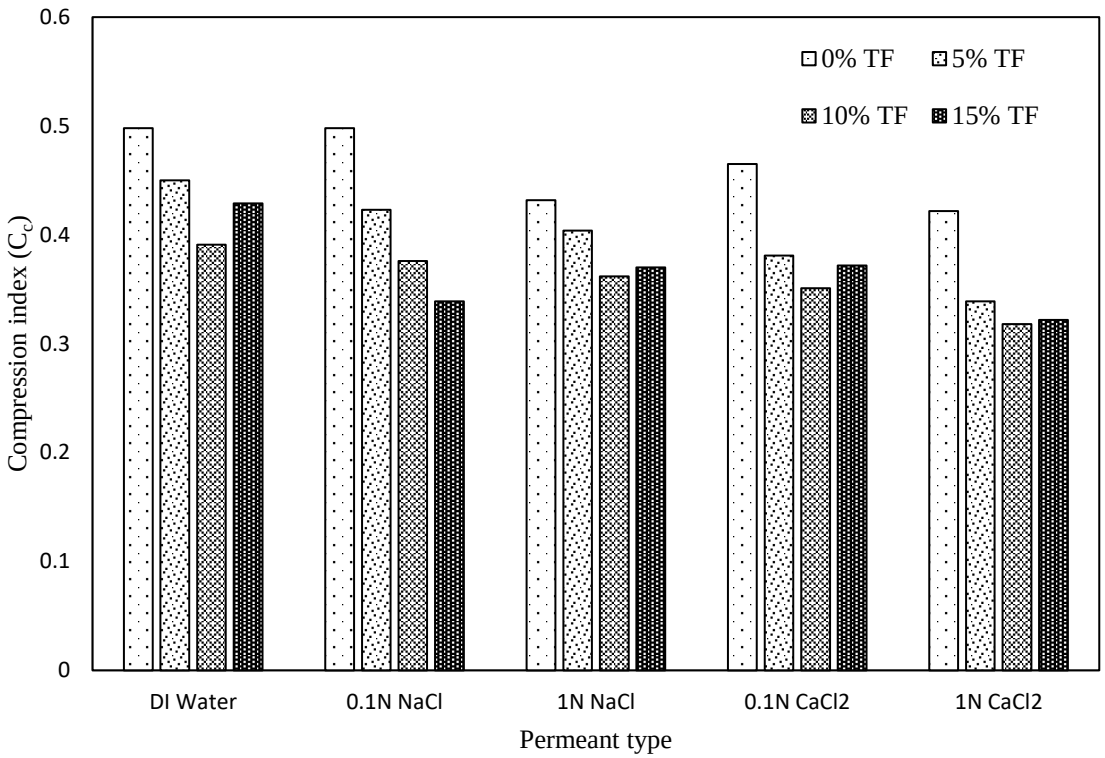

Fig. 5.27. Compression index (C_c) of fibre-mixed BC soil with various salt permeant concentrations.

5.2.9. Hydraulic conductivity (*k*)

Hydraulic characteristics is one of the most highly sought-after parameters when dealing with the geotechnical barrier materials. Hydraulic conductivity values were evaluated with respect to different overburden pressures, which simulate field conditions by performing a sequence of consolidation studies on fibre-mixed BC soil samples. The recommended/limiting values of hydraulic conductivity for barrier materials, including landfill covers and landfill liners, are 10^{-5} cm/sec and 10^{-7} cm/sec, respectively (USEPA, 1988; Hauser et al., 2001). All the soil samples used in this investigation were prepared by compacting them at the OMC and MDD conditions of DI water of the appropriate tire fibre composition. It was observed that all sample's *k* values decreased with the reduction in void ratio, irrespective of the fibre content, pore fluid type, and amount of concentration, as depicted in Figs. 5.28 to 5.31. The hydraulic conductivity increased significantly as the concentration of tire fibre content increased, as previously discussed in Chapter 4. The hydraulic conductivity values of all fibre-mixed soil samples with respect to three different overburden pressures, i.e. 49.0, 196.1 and 784.5 kPa, in the presence of various pore fluids are tabulated in Tables 5.8 to 5.11. The data shows a significant reduction in *k* values with the increase in the overburden pressure for all the soil samples. At high consolidation

TH-3665_186104109

pressures, the available pore space for water to travel decreases as the void ratio decreases resulting in a decrease in the hydraulic conductivity. For example, the hydraulic conductivity value of pure BC soil in DI water was reported as 2.44×10^{-8} cm/s at 49.0 kPa of overburden pressure. This value decreased to 1.37×10^{-8} (1.78 times) and 4.75×10^{-10} cm/s (51.37 times) at 196.1 and 784.5 kPa overburden pressures, respectively. In a similar way, the hydraulic conductivity values of pure BC soil under various pore fluids also decreased significantly at lower consolidation pressures compared to higher consolidation pressures, as shown in Table 5.8.

The hydraulic conductivity values corresponding to different void ratios in the presence of various salt solutions of different concentrations are shown in Figs. 5.28 to 5.31. It can be evident from the plots that the hydraulic conductivity value of BC soil increased with an increase in salt concentration, irrespective of fibre content. This increase in the hydraulic conductivity value was more pronounced at high salt concentrations. The water present in the pore space between the soil particles is both mobile and immobile in nature. The mobile water in the pores of BC soil is normally free to move under gravity, but the immobile water is bound to the clay surface. A decrease in the diffuse double layer (DDL) thickness with the increase in the salt concentration causes a rise in the hydraulic conductivity (k). The proportion of immobile water in the pore reduces as the DDL thickness is reduced, causing an increase in the k value. Shariatmadari et al. (2011) and Dutta and Mishra (2015) found similar results for different bentonites and concluded that flow channels become more open as DDL thickness decreases, resulting in an increase in the k. The increase in the k was more significant for a higher cation valency (i.e. Ca^{2+}) in comparison to a lower cationic valence (i.e. Na^{+}). The variation in k values with respect to different overburden pressures for all fibre-mixed samples is tabulated in Tables 5.9 to 5.11. The k value corresponding to a void ratio of 0.75 was determined and compared. The plot in Fig. 5.32 represents the relation between the k value and salt solutions of different concentrations at a void ratio of 0.75 for the BC soil treated with a fibre content from 0 to 15%. The plot in Fig. 5.32 shows that the k for BC soil was increased from 4.93×10^{-10} cm/s (DI water) to 9.04×10^{-9} (18.34 times) and 1.11×10^{-8} cm/s (22.52 times) for an increase in the concentrations of solutions to 1.0 N NaCl and $CaCl_2$, respectively. At a void ratio of 0.75, the k for 5% fibre-treated soil was increased from 2.83×10^{-9} cm/s (DI water) to 4.19×10^{-8} (14.81 times) and 6.39×10^{-8} cm/s (22.58 times) for 1N NaCl and 1N $CaCl_2$, respectively. Similarly, for the BC soil with 10% tire fibre, this increase was 26.0 times and 49.0 times in comparison to DI water for 1N NaCl and 1N $CaCl_2$,

TH-3665_186104109

respectively. Similarly, for the samples with 15% tire fibre, the corresponding increase in the *k* value was 9.36 and 18.21 times in comparison to the *k* value for DI water. For all the samples, a lower values *k* was observed at lower concentrations of salt permeants was observed compared to the higher concentrations. The reduction in DDL thickness due to cations present in salts is the reason for this increment in the *k* values of the soil samples. It was also observed that the *k* values were increased due to the addition of the fibre to the BC soil. The results also indicated that the *k* values were exceeded the limiting values for 1N of $CaCl_2$ and NaCl for the samples with the 5 and 10% fibre at a higher void ratio. However, with a decrease in the void ratio brought the *k* values within the permissible limit. On the contrary, the *k* values for the BC soil with 15% fibre content for 1N $CaCl_2$ and NaCl solutions were found to be higher than the permissible value of 10^{-7} cm/sec for all the void ratios. The morphological structure of BC soil after permeation of salt solutions was observed by performing FESEM analysis and results are shown in Fig. 5.33. High concentrations of inorganic salt permeants showed aggregation of clay particles by neutralizing surface charges with cations of salt concentrations. The formation of flow channels at high concentrations is evident, leading to increased hydraulic conductivity values, as illustrated in Fig. 5.33.

Table 5.8. Hydraulic conductivity vs consolidation pressure values for pure BC soil with various salt permeant concentrations

Permeant type and concentration	**Hydraulic conductivity (cm/s)**		
	49.0 kPa	**196.1 kPa**	**784.5 kPa**
DI Water	2.44×10^{-8}	1.37×10^{-8}	4.75×10^{-10}
0.1 N NaCl	8.28×10^{-8}	1.71×10^{-8}	1.46×10^{-9}
1.0 N NaCl	6.35×10^{-8}	3.68×10^{-8}	4.96×10^{-9}
0.1 N $CaCl_2$	7.84×10^{-8}	2.61×10^{-8}	2.23×10^{-9}
1.0 N $CaCl_2$	1.39×10^{-7}	5.43×10^{-8}	7.43×10^{-9}

TH-3665_186104109

Table 5.9. Hydraulic conductivity vs consolidation pressure values for 5% fibre-mixed BC soil with various salt permeant concentrations

Permeant type and concentration	Hydraulic conductivity (cm/s)		
	49.0 kPa	**196.1 kPa**	**784.5 kPa**
DI Water	5.03×10^{-8}	1.93×10^{-8}	7.95×10^{-10}
0.1 N NaCl	6.08×10^{-8}	2.47×10^{-8}	2.75×10^{-9}
1.0 N NaCl	2.60×10^{-7}	8.44×10^{-8}	1.12×10^{-8}
0.1 N $CaCl_2$	9.26×10^{-8}	4.19×10^{-8}	5.32×10^{-9}
1.0 N $CaCl_2$	2.63×10^{-7}	1.33×10^{-7}	1.50×10^{-8}

Table 5.10. Hydraulic conductivity vs consolidation pressure values for 10% fibre-mixed BC soil with various salt permeant concentrations

Permeant type and concentration	Hydraulic conductivity (cm/s)		
	49.0 kPa	**196.1 kPa**	**784.5 kPa**
DI Water	4.14×10^{-8}	2.36×10^{-8}	1.43×10^{-9}
0.1 N NaCl	1.17×10^{-7}	2.87×10^{-8}	3.99×10^{-9}
1.0 N NaCl	4.81×10^{-7}	1.19×10^{-7}	1.99×10^{-8}
0.1 N $CaCl_2$	2.04×10^{-7}	6.77×10^{-8}	9.40×10^{-9}
1.0 N $CaCl_2$	5.27×10^{-7}	1.90×10^{-7}	2.42×10^{-8}

TH-3665_186104109

Table 5.11. Hydraulic conductivity vs consolidation pressure values for 15% fibre-mixed soil with various salt permeant concentrations

Permeant type and concentration	Hydraulic conductivity (cm/s)		
	49.0 kPa	**196.1 kPa**	**784.5 kPa**
DI Water	1.25×10^{-7}	5.49×10^{-8}	4.28×10^{-9}
0.1 N NaCl	6.02×10^{-7}	1.58×10^{-7}	1.84×10^{-8}
1.0 N NaCl	5.82×10^{-7}	4.33×10^{-7}	1.27×10^{-7}
0.1 N $CaCl_2$	5.35×10^{-7}	2.31×10^{-7}	3.17×10^{-8}
1.0 N $CaCl_2$	9.12×10^{-7}	9.43×10^{-7}	1.84×10^{-7}

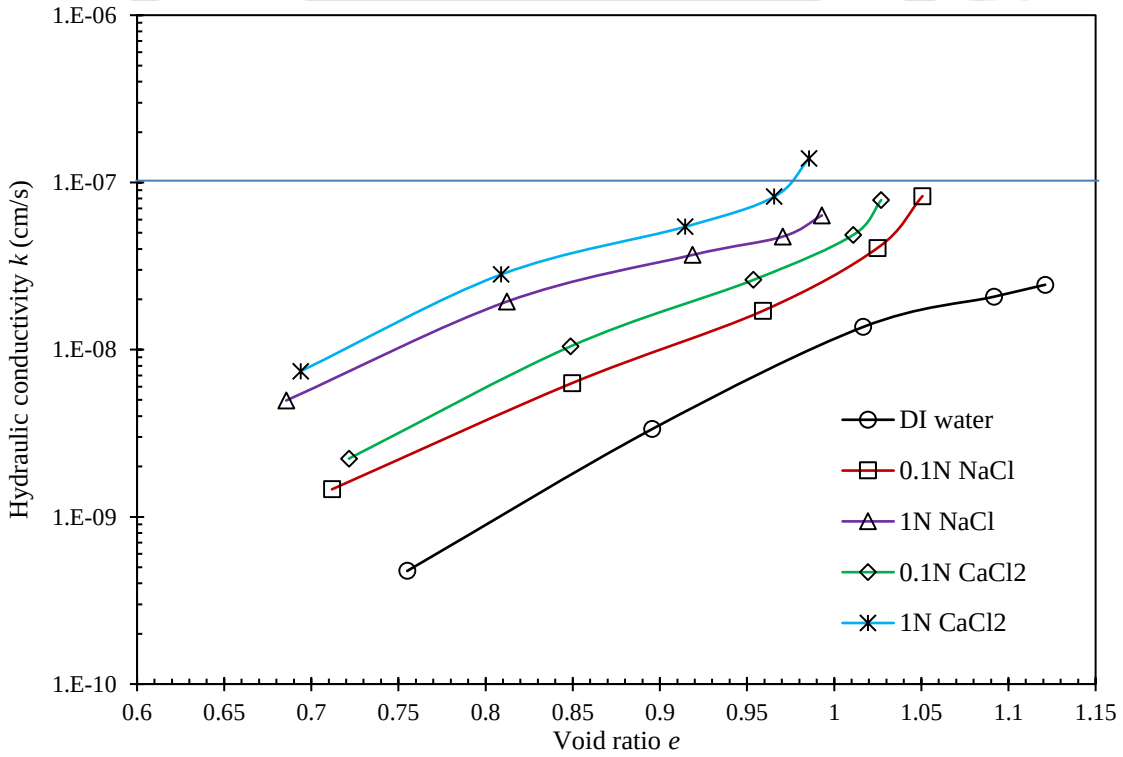

Fig. 5.28. Hydraulic conductivity vs void ratio plots for pure BC soil with various salt permeant concentrations

TH-3665_186104109

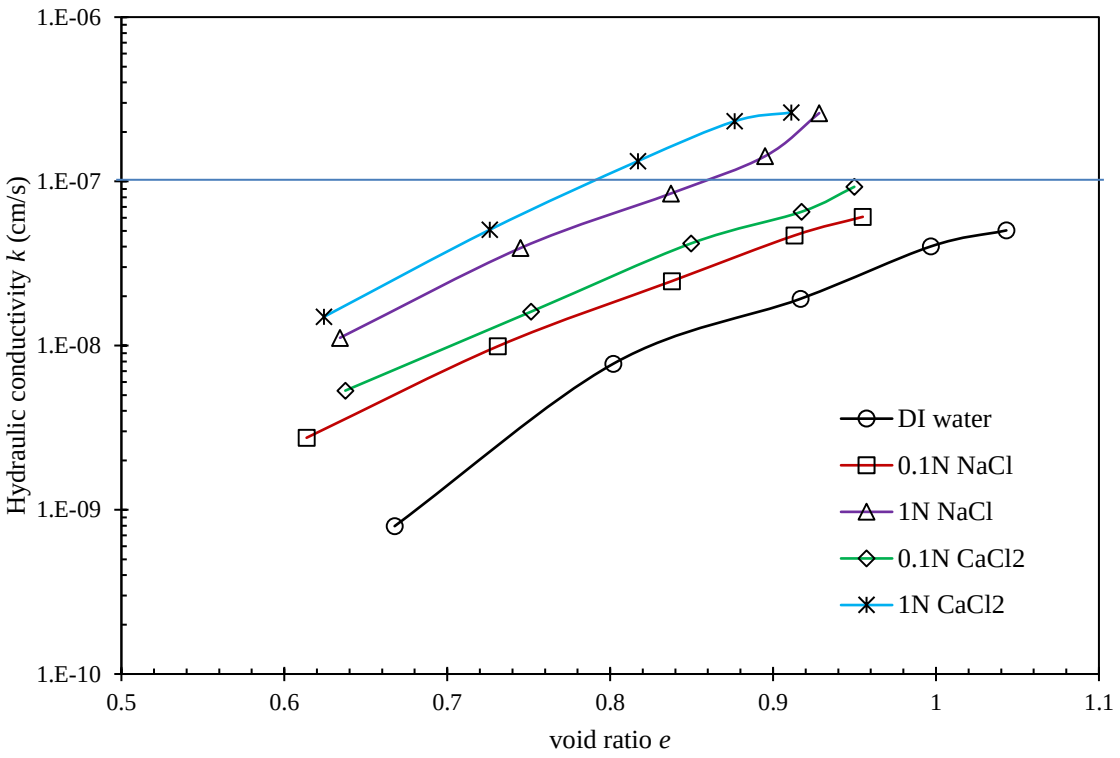

Fig. 5.29. Hydraulic conductivity vs void ratio plots for 5% fibre-mixed BC soil with various salt permeant concentrations.

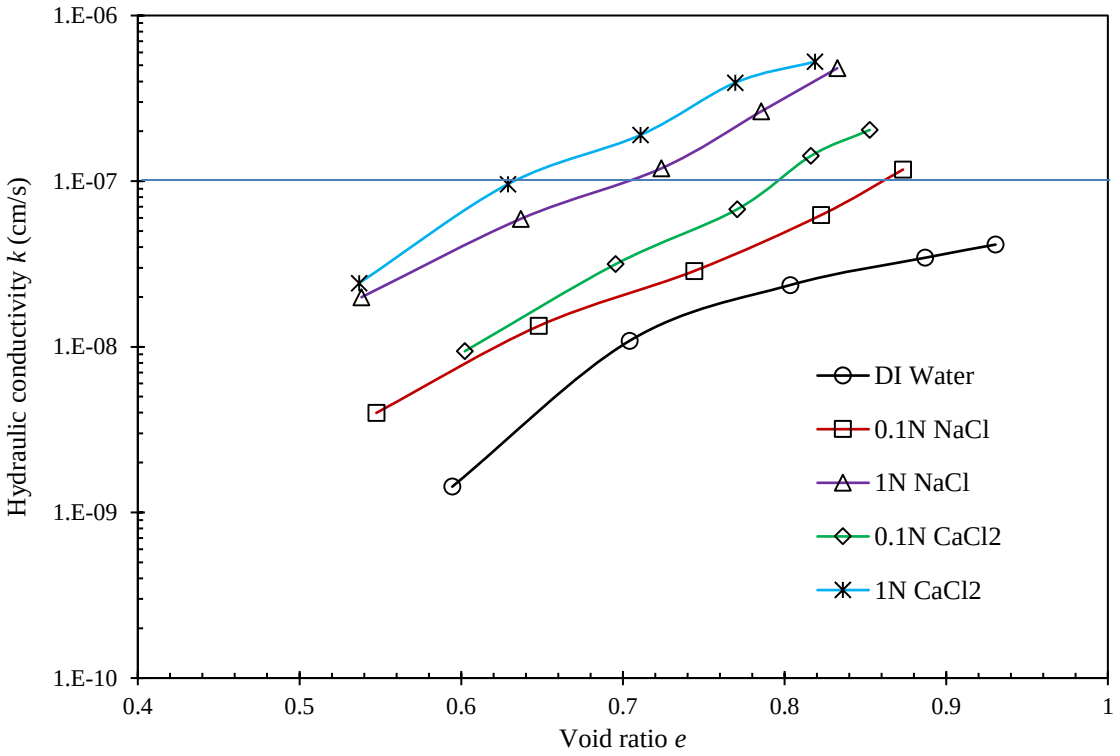

Fig. 5.30. Hydraulic conductivity vs void ratio plots for 10% fibre-mixed BC soil with various salt permeant concentrations

TH-3665_186104109

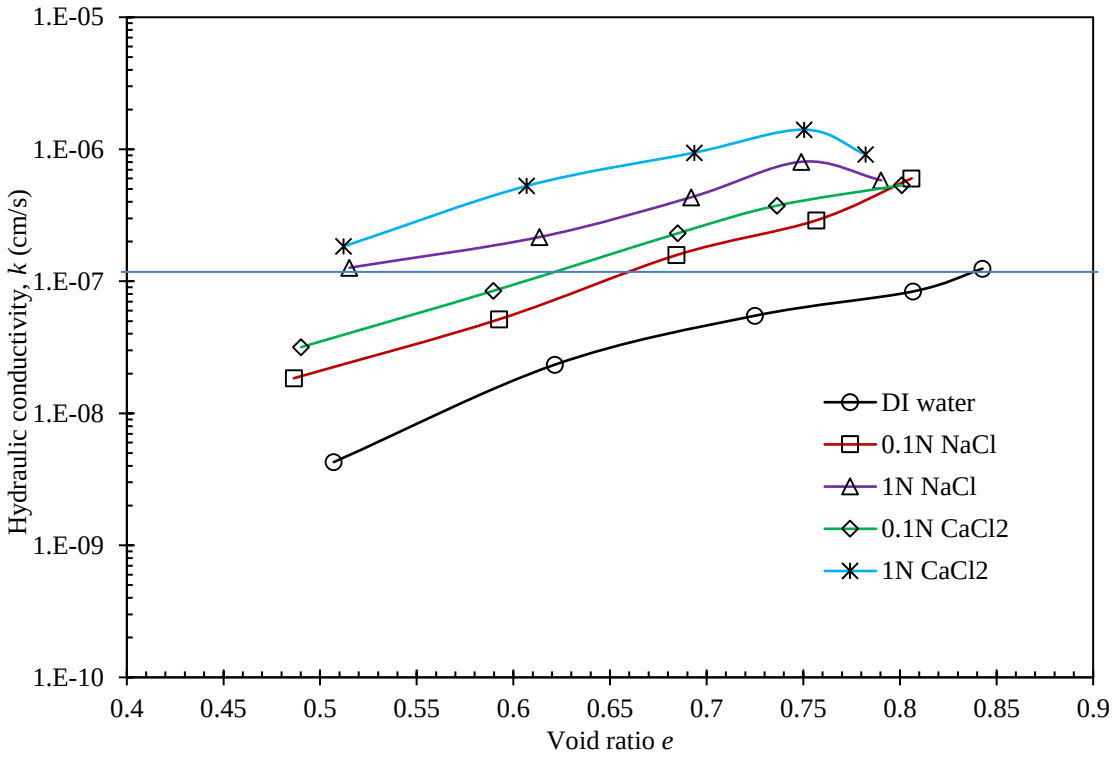

Fig. 5.31. Hydraulic conductivity vs void ratio plots for 15% fibre-mixed BC soil with various salt permeant concentrations.

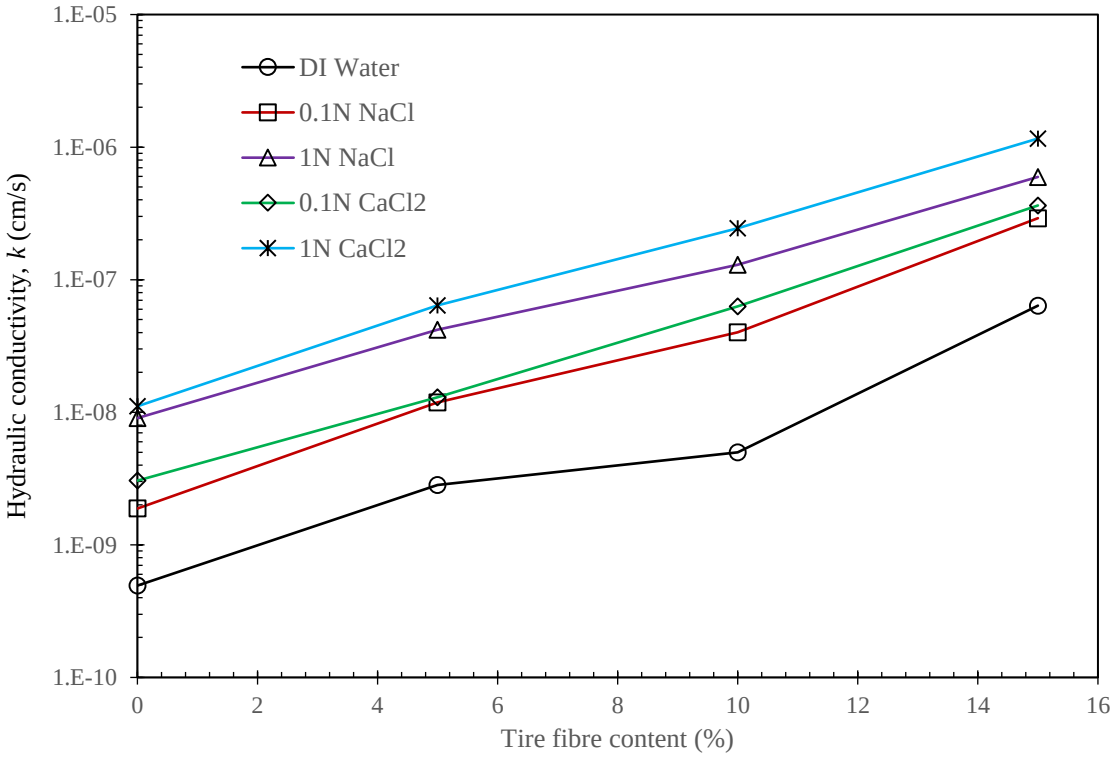

Fig. 5.32. Fibre content vs Hydraulic conductivity plots for fibre-mixed BC soil with various salt permeant concentrations at the void ratio of 0.75.

TH-3665_186104109

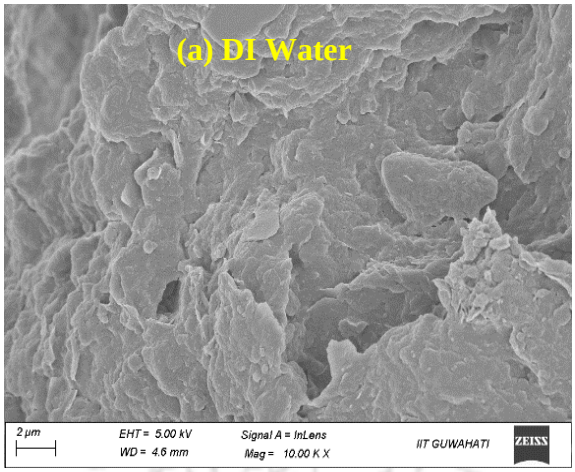

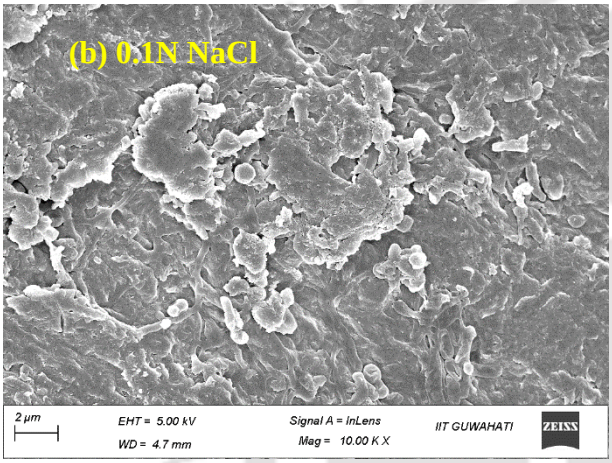

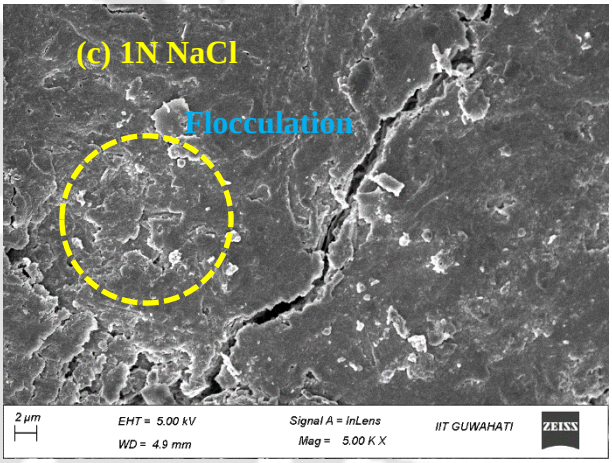

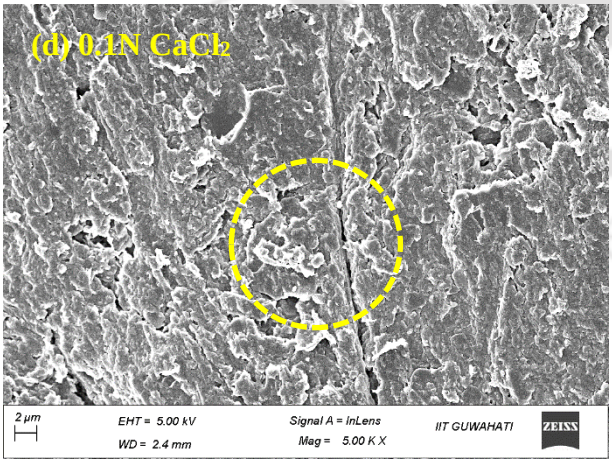

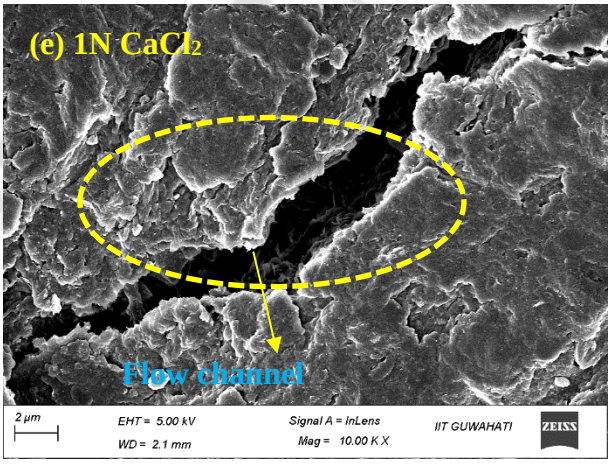

Fig. 5.33. FESEM images of BC soil with various salt permeant concentrations after completion of consolidation tests.

TH-3665_186104109

5.2.10. Unconfined compressive strength (UCS) characteristics

The stress-strain curves of fibre-mixed BC soil samples obtained from the UCS test under inorganic salt permeants are depicted in Figs. 5.34 to 5.37. All the samples with NaCl and $CaCl_2$ permeants in this study were prepared at the OMC-MDD of DI water only because, in the field condition, leachate would come in contact with the clay liner compacted at OMC-MDD of water itself. The result shows the UCS of fibre mixed soil with 0.1N NaCl permeant decreases from 585.6 with 0% fibre to 330.2, 233.7 and 157.8 kPa for the fibre content of 5, 10, and 15%, respectively. The corresponding peak strains were 3.9, 5.0, 7.4, and 8.7% for the 0, 5, 10 and 15% of fibre content, respectively. The UCS and corresponding peak strain value for different fibre content in the presence of various permeants are listed in Tables 5.12 and 5.13, respectively. The data in the Tables 5.12 and 5.13 shows a negligible reduction in peak strength values of all samples with 0.1N NaCl compared to DI water. The cause for the strength reduction in the presence of salt permeant is attributed to the decrement in the density of soil samples as the samples were compacted at MDD of DI water. The percentage reduction in UCS values of fibre mixed BC soil with 1N NaCl permeant is approximately 8.1, 6.2, 6.7, and 15.8% with 0, 5, 10, and 15%, respectively, compared to DI water. The high salt concentration contributes to the reduction of interparticle cohesion, which causes a marginal decrease in UCS values (Rout and Singh, 2020). The corresponding peak strains with 1N NaCl permeant were recorded as 4.2, 5.0, 6.6, and 8.4% with for the 0.5. 10 and 15% of fibre content. A slight reduction in peak strains for 10 and 15% fibre mixed soil samples is noticed with 1N NaCl than 0.1N NaCl permeant. However, a furthermore strength reduction is observed when divalent cations permeant liquid ($CaCl_2$) is used for the same concentration and fibre content. The percentage reduction in peak strength values at 1N $CaCl_2$ permeant is around 11.7, 16.0, 11.4, and 17.5% with 0, 5, 10, and 15% tIre content, respectively, compared to DI water. However, the change in peak strains with 1N $CaCl_2$ is negligible. Rout and Singh (2020) also observed lower peak strength values with trivalent and divalent permeants than monovalent permeants at higher salt concentrations. They stated This reduction in peak strength values with greater cation valency permeant than with lower cation valency permeant was attributed to a possible decrease in DDL thickness at high salt concentrations.

TH-3665_186104109

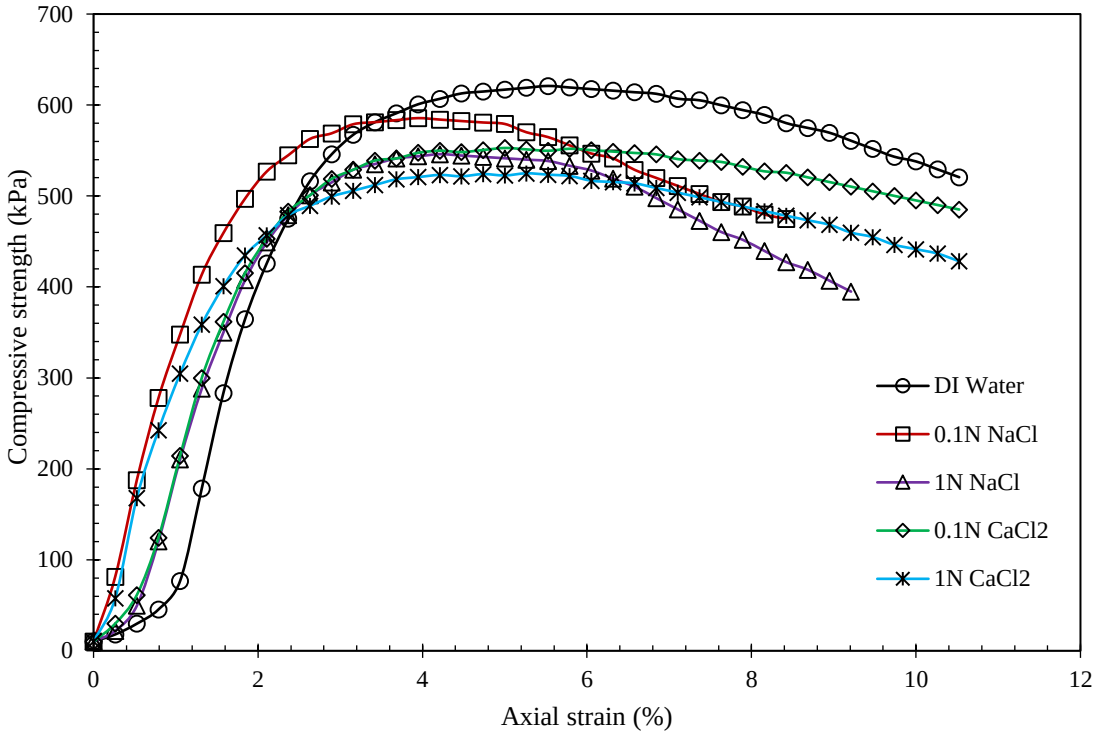

Fig. 5.34. Axial stress vs axial strain curves for pure BC soil with various salt permeant concentrations.

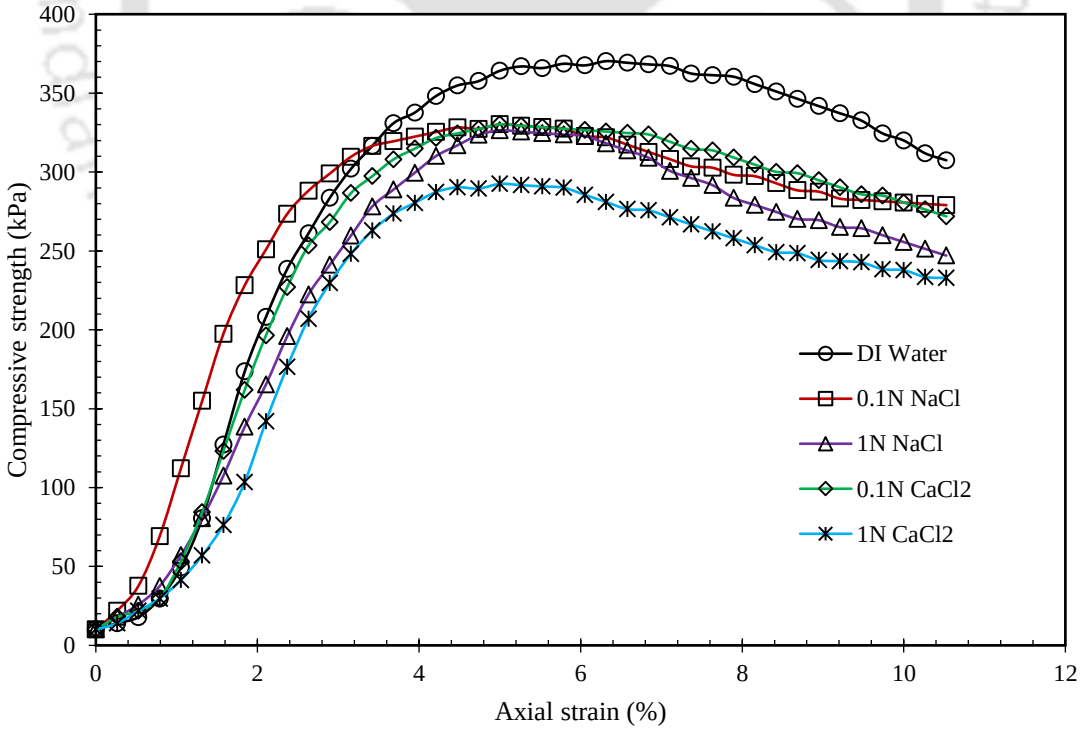

Fig. 5.35. Axial stress vs axial strain curves for 5% fibre-mixed BC soil with various salt permeant concentrations.

TH-3665_186104109

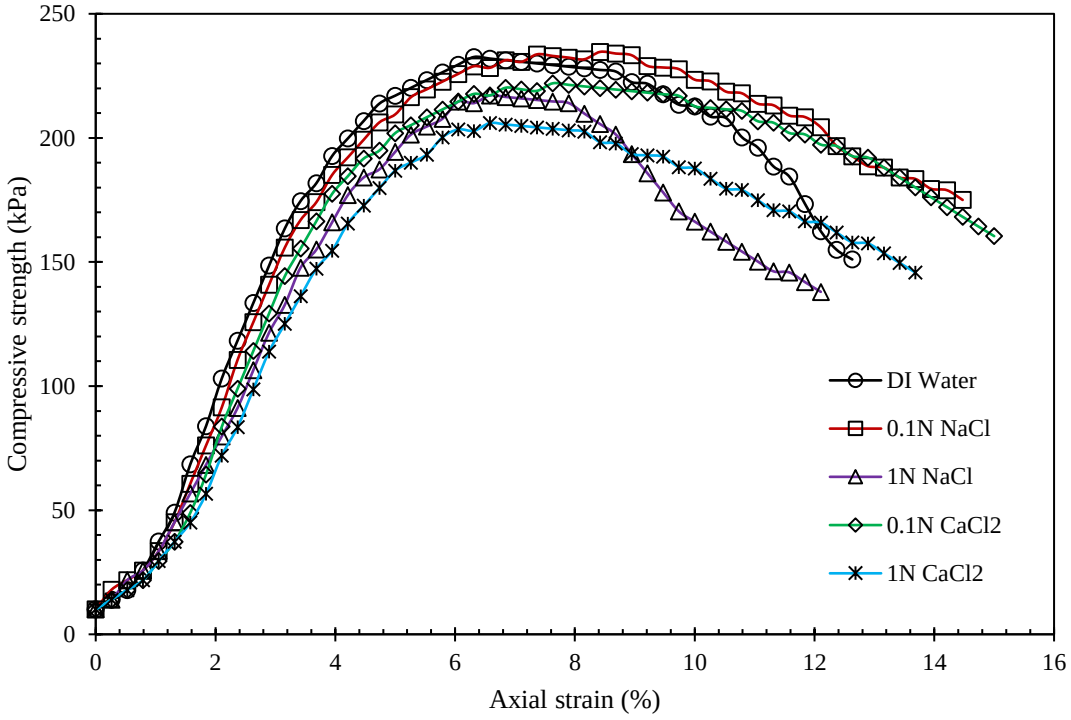

Fig. 5.36. Axial stress vs axial strain curves for 10% fibre-mixed BC soil with various salt permeant concentrations.

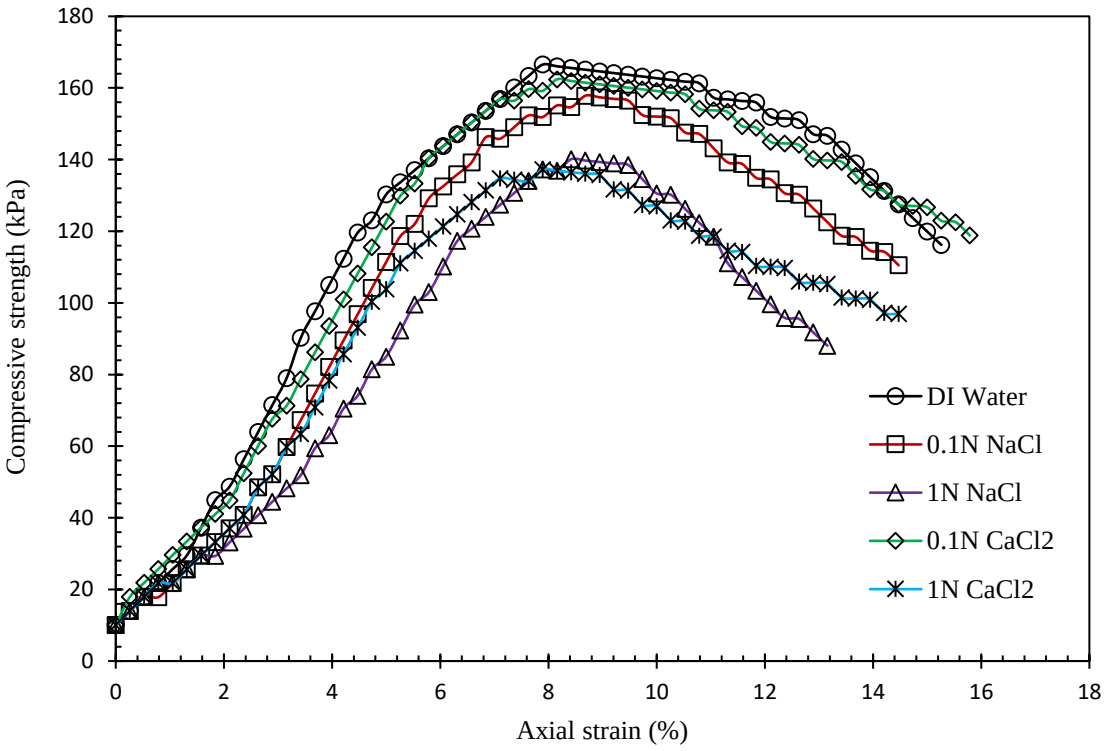

Fig. 5.37. Axial stress vs axial strain curves for 15% fibre-mixed BC soil with various salt permeant concentrations.

TH-3665_186104109

Table 5.12. Peak strength values of fibre-mixed BC soil with various salt permeant concentrations

Permeant type and concentration	Peak strength (kPa)			
	0% TF	5% TF	10% TF	15% TF
DI Water	594.2	370.2	232.6	166.5
0.1N NaCl	585.6 (1.4%)	330.2 (10.8%)	233.7	157.8 (5.2%)
1.0N NaCl	545.9 (8.1%)	326.4 (11.8%)	217.1 (6.7%)	140.1 (15.8%)
0.1N $CaCl_2$	552.7 (7.0%)	328.4 (11.3%)	222.0 (4.5%)	162.4 (2.5%)
1.0N $CaCl_2$	524.9 (11.7%)	292.5 (21.0%)	206.0 (11.4%)	137.3 (17.5%)

* Values in brackets represent the percentage of reduction in peak strength of fibre-mixed samples under various salt permeants compared to DI water

Table 5.13. Peak strain values of fibre-mixed BC soil with various salt permeant concentrations

Permeant type and concentration	Peak strain (%)			
	0% TF	5% TF	10% TF	15% TF
DI Water	5.00	6.32	6.32	7.89
0.1N NaCl	3.95	5.00	7.37	8.68
1.0N NaCl	4.21	5.00	6.58	8.42
0.1N $CaCl_2$	5.00	5.53	7.63	8.16
1.0N $CaCl_2$	5.26	5.00	6.58	7.89

TH-3665_186104109

5.3. Summary

This investigation was done to understand the influence of inorganic salt concentrations on the engineering beahviour of fibre-mixed BC soils for barrier application in landfills. Initially, this study was aimed at the investigation of monovalent and divalent salts on index properties and engineering properties of pure BC soil. Then, engineering properties like swelling, consolidation, compressibility, hydraulic, and strength characteristics of BC soil mixed with waste tire fibres were added from 5 to 15% by dry weight. The results obtained from several laboratory tests are summarized below.

- Atterberg limits and free swell values of BC soil showed a declining trend with both monovalent and divalent inorganic salt solutions.
- Results showed a substantial reduction in swelling heights of all fibre-mixed BC soil samples under salt permeants, irrespective of fibre content. This reduction was more with divalent permeants than monovalent permeants at the same concentration.
- It was observed from test results that the maximum amount of swelling occurs in the primary swelling stage irrespective of salt type for all fibre-mixed samples. However, this percentage of swelling that occurred in each swelling stage was reduced by salt permeants.
- This study revealed that the influence of inorganic salt concentrations on swelling pressures and swelling potentials was significant. All fibre-mixed BC soils showed a declining trend in both swelling pressures and swelling potentials with the rise in concentrations of salt permeants. The suppression of DDL thickness increased more with the increase in the concentration of salt solutions led this reduction in swelling pressures.
- The swelling test results were compared with the rectangular hyperbola method. A good correlation was observed between measured and predicted swelling potentials.
- The test results showed that with the rise in consolidation pressure, the c_v values decreased significantly for all fibre-mixed BC soil samples. At any consolidation pressure, these c_v values were with the rise in salt concentration and cation valency, irrespective of fibre content.
- Time for 90% consolidation values reduced significantly at higher concentrations for all fibre-mixed samples.

TH-3665_186104109

- The void ratio-pressure relationship results showed a drop in the void ratio of each sample with the rise in concentration and valency of the salt solution.
- The C_c of the sample decreased with rising salt permeant concentration due to the reduced DDL thickness, causing clay particles to flocculate and resist settlement, resulting in a lower C_c value.
- The hydraulic conductivity values of all fibre-mixed samples increased significantly at both 0.1 and 1.0N concentrations of both monovalent and divalent salt permeants. At any consolidation pressure, the 15% fibre-mixed BC soil exceeded the limiting value for barrier material when subjected to 1.0N monovalent and divalent permeants.
- The higher hydraulic conductivity of pure BC soil under DI water was reported as 2.44×10^{-8} cm/s, and this value becomes 1.46×10^{-6} cm/s for 15% fibre-mixed soil under 1N $CaCl_2$ salt permeant.
- The UCS results observed a marginal reduction in strength values with the increase in the concentration of salt permeants for all samples, irrespective of fibre content. A slight increment in peak strains was observed for all samples at higher concentrations of salt permeants.

TH-3665_186104109

CHAPTER 6

INFLUENCE OF HEAVY METAL CONCENTRATIONS ON THE BEHAVIOUR OF FIBRE-MIXED BC SOIL

6.1. Introduction

Expansive soils are an excellent choice for geoenvironmental applications due to their swelling and impermeable properties, which uphold the leachate and avoid groundwater pollution. In recent decades, the usage of bentonites and sand-bentonite mixtures as liners has become prevalent due to their feasibility. However, these materials are scarce and prohibitively expensive in India. Black cotton (BC) soil was chosen as an alternative clay liner for this research due to its abundance in India and its mineralogical composition. Substantial proportions of this municipal solid trash are accountable for producing various heavy metal substances through commercial, domestic, and industrial processes (Long et al., 2011; Dutta and Mishra, 2016(b); Wang et al., 2017). Thus, these toxic wastes necessitate a systematic strategy for their disposal; otherwise, inappropriate management poses serious threats to the geo-environment (biosphere, lithosphere, and hydrosphere) and human life (Rahman and Singh, 2019). These metal concentrations decrease liner material's efficiency, leading to leachate percolating into the ground and polluting the groundwater, adversely affecting human health. Lead, cadmium, and chromium are the significant metals present in the landfill from the observed literature survey, which alters the liner parameters.

Earlier, many studies have concentrated on the behaviour of landfill materials in the presence of toxic heavy metals, as these metal concentrations have a harmful influence on human life and the environment (Li and Li, 2001; Chalermyanont et al., 2009; Saha and Sanyal, 2010; Li et al., 2015; Mohammed et al., 2016; Dutta and Mishra, 2016b; Li et al., 2017; Taheri et al., 2018; Moghal et al., 2020; Yang et al., 2021; Ray et al., 2022a), which were thoroughly discussed in Chapter 2. Based on the above literature survey, lead, cadmium, and hexavalent chromium are three hazardous metals commonly found in leachate and wastewater, and selected for this examination. The sources and implications of these heavy metals were already discussed in Chapter 2.

TH-3665_186104109

It is clear from the previous literature that many investigators are attentive to adsorption studies on soils in order to determine the soil's metal retention capacity. However, this available geotechnical research for the liner layer is also limited to bentonites only. Therefore, no study has been done on the influence of heavy metals on the engineering performance of black cotton soil (BC) soil as a liner base material. Hence, the first objective of this study is to examine the index properties (free swell index and Atterberg limits), engineering properties (swelling, hydraulic conductivity, and shear strength), and microstructural behaviour of BC soil with three distinct concentrations (100, 500, and 1000 ppm) of three hazardous heavy metal permeants (lead, cadmium, and hexavalent chromium) to replicate the impact of heavy metal leachate in landfills. Also, it is essential to comprehend the volume change behaviour of liner material, as it has the potential to cause abrupt failures in landfill systems through differential settlement due to overburden pressure. Therefore, it is necessary to understand the consolidation behaviour, such as the coefficient of consolidation and time for 90% consolidation, and compressibility characteristics, such as void ratio-pressure relationship and compression index. Hence, the influence of heavy metal concentrations on BC soil's consolidation and compressibility properties should be examined in detail.

Also, shrinkage is a threatening concern for expansive soils that would eventually lead to groundwater pollution by leaking leachate through desiccation cracks. Therefore fibre reinforcement is a better approach that would control the shrinkage phenomenon, as studied by many researchers discussed in Chapter 2. In this study, waste tire fibres at three different concentrations (5, 10, and 15% by dry weight) were adopted as mixing material into BC soil for barrier application due to the substantial generation of waste tires and their implications on the environment and society. Therefore, the second objective of this study was to investigate the impact of these heavy metal concentrations ranging from 100 to 1000 on engineering properties such as swelling, strength, consolidation, compressibility, and hydraulic conductivity of all fibre-mixed (5, 10, and 15%) soil samples. Several laboratory tests were conducted to obtain these objectives, and the detailed results are given below.

TH-3665_186104109

6.2. Test Result and Discussion

6.2.1. Atterberg limits

Atterberg limits such as liquid limit (LL), Plastic limit (PL), and plasticity index (PI) are important index properties, which would help in the determination or estimation of engineering properties. The variation in Atterberg limits of BC soil with various concentrations of metal solutions was depicted in Fig. 6.1. The liquid limit of BC soil was marginally decreased from 84.8 (DI water) to 83.5 % for 100 ppm lead solution, which is a negligible reduction of approximately 1.5%. With cadmium solution, this liquid limit value was dropped to 82.2% for the same metal concentration, which is a 3.1% reduction compared to DI water. This reduction in liquid limit was more prominent for high metal concentrations. For example, the LL of BC soil at 1000 ppm lead solution was determined as 76.5%, which declined by about 9.8% compared with DI water. Similarly, this reduction was determined as 11.6% and 14.9% for similar concentrations with cadmium and hexavalent chromium metal solutions, respectively. Past studies carried out by various researchers (Du et al., 2015; Muththalib and Baudet, 2019; Nasab and Keykha, 2020; Ray et al., 2022a) also observed a lower liquid limit values with higher lead concentrations for bentonites, sand-bentonites, and soil-bentonite samples. This decrease in liquid limit may be attributed to the contraction of DDL thickness imposed by the cations prevalent in metal solutions (Mesri and Olson, 1971; Sridharan et al., 1986). High metal concentrations induce the reduction in inter-particle distance of clay particles that causes free movement in clay particles, contributing to the drop in liquid limit values (Warkentin, 1961; Sridharan and Prakash, 1998).

The PL of BC soil with different metal bulk solutions was displayed in Fig. 6.1. At higher metal concentrations, BC soil's PL dropped marginally, which can be observed in Fig.6.1. In this case, the PL of BC soil was 38.1% with DI water but reduced to 37.0, 36.4, and 35.9% with 1000 ppm lead, cadmium, and hexavalent chromium solutions, respectively. However, this reduction was very marginal at lower metal concentrations. Nasab and Keykha (2020) and Amiri et al. (2022) also noticed comparable trends with bentonite and natural marl soil, respectively. Furthermore, the PI of BC soil also followed an identical pattern of LL results, as plotted in Fig. 6.1.

TH-3665_186104109

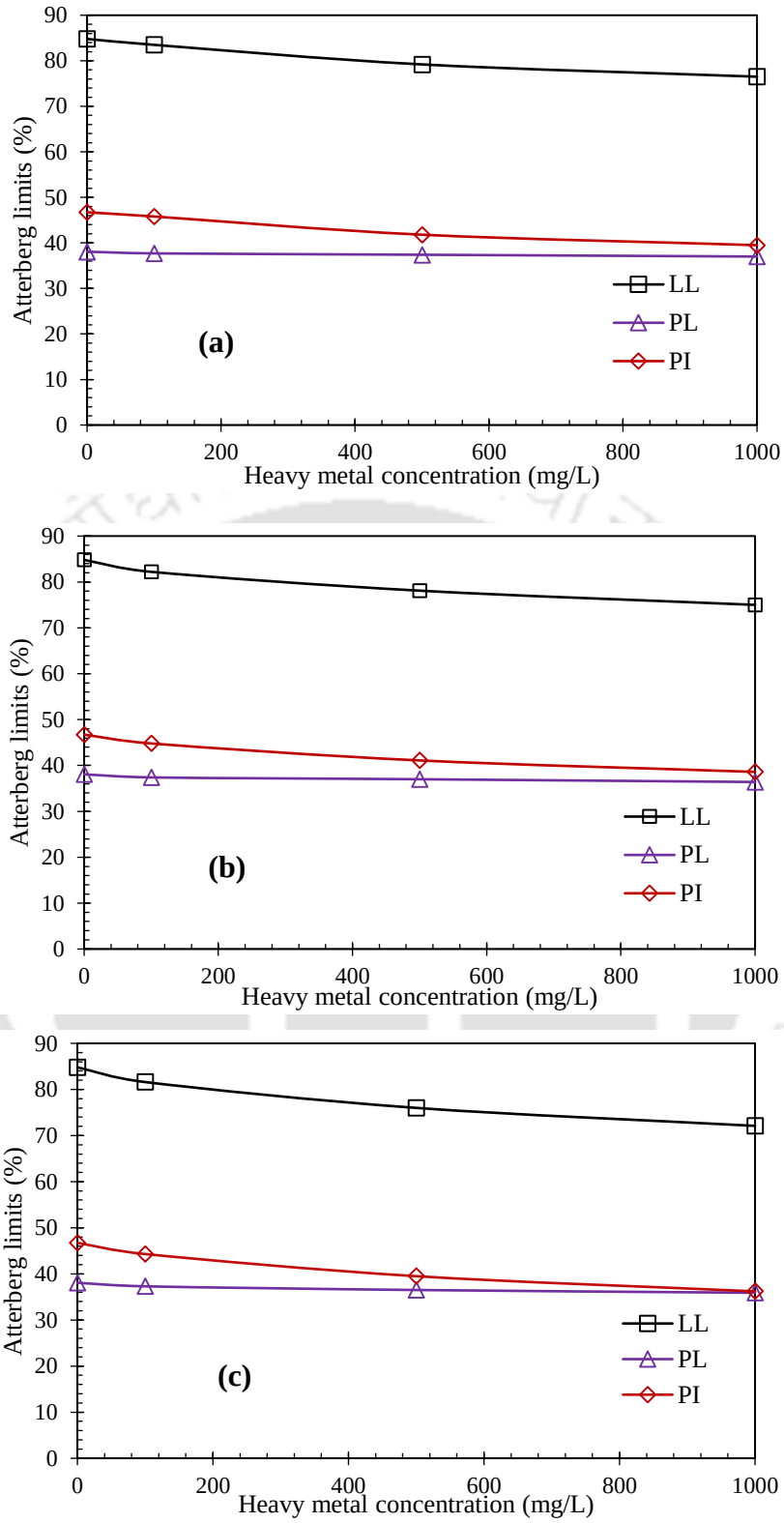

Fig.6.1. Atterberg limits of BC soil with heavy metal solutions: (a) Lead; (b) Cadmium; (c) Hexavalent chromium.

TH-3665_186104109

6.2.2. Free swell index (FSI)

The influence of lead, cadmium, and hexavalent chromium metal solutions on the FSI behaviour of BC soil is represented in Fig. 6.2. The FSI of BC soil with DI water was determined to be 196%, as shown in Fig. 6.2, and a decrease in FSI values was observed when metal concentration increased, regardless of metal solution type. The FSI of BC soil was reduced slightly for 100 ppm lead solution and reported as 189%, which decreased nearly 3.6% compared to DI water. The decrement in the diffuse double layer occurs when BC soil interacts with the metal solution instead of DI water, leading to reduced FSI values. These FSI values were 162 and 143% for 500 and 1000 ppm of lead solutions, respectively; whereas, the decrement was around 17.3 and 27.0% as compared to DI water for the same order. Similarly, the FSI values of BC soil with cadmium solutions were 182, 152, and 133% at 100, 500, and 1000 ppm concentrations, respectively, with a reduction of about 7.1%, 22.4%, and 32.1% compared to DI water for the same order of metal concentration. A comparison between cadmium and lead shows that the BC soil in the presence of cadmium solutions exhibits lower FSI values than lead solutions of the same concentration, as shown in Fig. 6.2. Furthermore, compared to lead solutions, this reduction percentage was 3.7, 6.17, and 7.0 % for 100, 500, and 1000 ppm concentrations of cadmium solutions, respectively. This difference in the FSI values was due to the different degree of impact of various heavy metals to the diffuse double layer thickness. A higher impact to the diffuse double layer thickness results in a lesser swelling which allows the permeant to flow more easily through clay, posing a threat to the engineering behaviour of the liner.

However, the free swelling behavior of BC soil was observed with an anionic heavy metal solution [Cr(VI)] which was prepared from potassium dichromate ($K_2Cr_2O_7$) salt. It was observed that a significant reduction in FSI value of BC soil compared to lead and cadmium solutions. The FSI of BC soil was reported as 170% (13.27% reduction compared to DI water) with 100 ppm hexavalent chromium solution, as displayed in Fig. 6.2. It is evident that significant reduction was observed even at lower concentrations of hexavalent chromium solutions compared to other cationic heavy metal solutions. However, this percentage in reduction of FSI was about 27.0 and 34.7% at 500 and 1000 ppm hexavalent chromium solutions, respectively, in comparison to DI water. Thus, it is noticeable that metal concentrations would influence BC soil's free swelling behaviour. The higher valency may be attributed to this reduction of the free swell with these hexavalent chromium solutions.

TH-3665_186104109

Here, the clay in the measurement cylinder was entirely dispersed and submerged in the metal bulk solutions, causing the clay structure to be disregarded for FSI reduction. So this reduction in FSI relies on the hydrophilicity behavior of BC soil. At higher metal concentrations, the hydrophilicity of BC soil will occur less due to the drop in diffuse double-layer thickness. This allows permeant to flow more easily through clay, posing a threat to the engineering behaviour of the liner. Thus, it is noticeable that metal concentrations would influence BC soil's free swelling behaviour. Furthermore, the relationship between LL and FSI is shown in Fig. 6.3, at which LL was reducing steadily with the drop in FSI values, irrespective of metal solution and concentration.

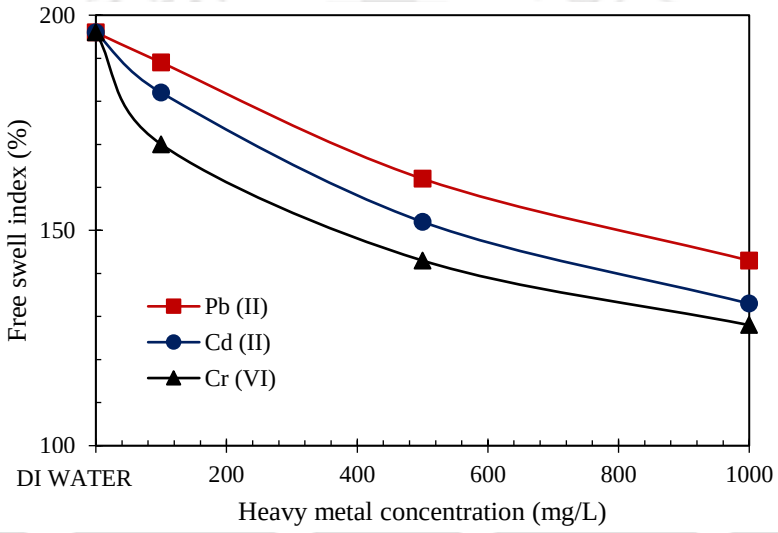

Fig. 6.2. Free swelling index of BC soil with cationic and anionic heavy metal solutions

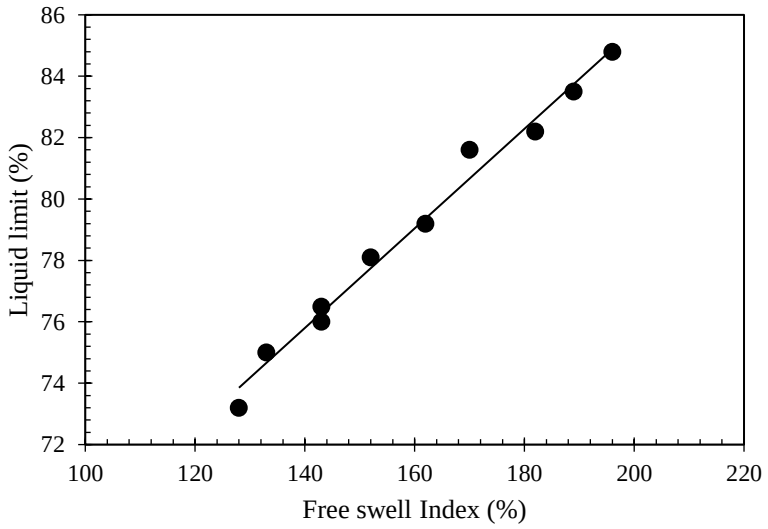

Fig. 6.3. Relationship between liquid limit versus FSI of BC soil

TH-3665_186104109

6.2.3. Time vs swelling behaviour

Time vs swelling plots of BC soil at different heavy metal permeant concentrations are displayed in Fig. 6.4. Regardless of heavy metal type and concentrations, the phenomenon of swelling was observed in S-shaped curves in three distinct stages (i.e., initial, primary, and secondary) for all specimens. Previous research also observed similar behavior after saturating bentonites and clays with a range of inorganic salt solutions (Rao et al., 2006; Mishra et al., 2015; Ye et al., 2015; Chen et al., 2017). As depicted in Fig. 6.4, the plot indicate a reduction in swelling heights in response to an increase in heavy metal concentrations. The increase in swelling height was 3.13 mm after inundating with DI water, which was dropped to 2.9, 2.61, and 2.27 mm for 100, 500, and 1000 ppm lead permeants, respectively, as depicted in Fig. 6.4 (a). Previously, Dutta and Mishra (2016(b)) and Ray et al. (2021(b)) also got this decrement trend after permeating bentonites with heavy metals and leachates, respectively. The permeated metal solution diminishes the repulsive forces between clay particles, and the DDL of BC soil becomes thinner, which may contribute to this decline in swelling height (He et al., 2020). However, with cadmium permeants, the reduction in swelling heights was slightly higher compared to lead permeants as shown in Fig. 6.4 (b), and these values were reported as 2.63, 2.41, and 2.13 mm for 100, 500, and 1000 ppm, respectively. Furthermore, the highest reduction was observed with hexavalent chromium solutions as shown in Fig. 6.4 (c), and the swelling heights were recorded as 2.33, 1.83, and 1.77 mm for the same order of concentrations. Both higher valency and potassium ions present in the hexavalent chromium solutions are responsible for this significant reduction in swelling heights. Similarly, the time vs swelling behaviour of all fibre-mixed soil samples (5,10, and 15%) were shown in Figs. 6.5 to 6.7. All the plots exhibit a swelling behaviour in the S-shape curve irrespective of the fibre content and permeant liquid in three different stages. This study determined all fibre-treated BC soil's swell heights with three metal permeants, lead, cadmium, and hexavalent chromium at three different concentrations (100, 500, and 1000 ppm), which were illustrated in Figs. 6.5 to 6.7. It was found that all swelling heights were reduced marginally with lower permeant concentrations (100 ppm) and significantly changed with higher concentrations (1000 ppm) of metal permeants, irrespective of metal type. For example, 5% fibre-mixed soil's swelling height decreased from 2.20 mm to 2.01, 1.72, and 1.61 mm with 100, 500, and 1000 mm lead permeants, respectively, as shown in Fig. 6.5. Similarly, for the same fibre content and the same order of concentrations, this swelling

TH-3665_186104109

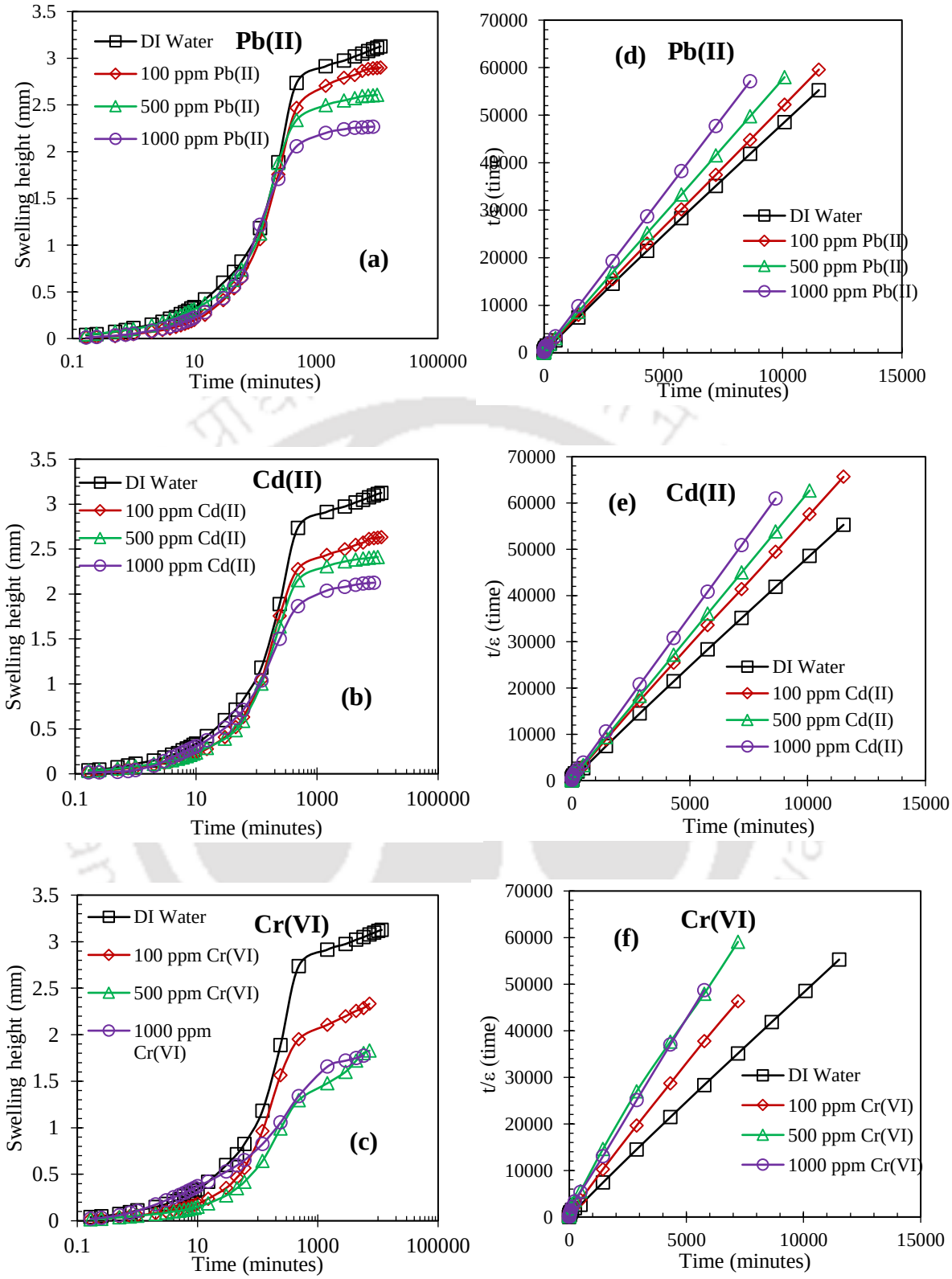

Figure 6.4. (a), (b), & (c) Time vs swelling relationship of pure BC soil with heavy metal permeants. (d), (e), and (f) Linear representation of swelling behavior of pure BC soil with RH model permeated with heavy metals.

TH-3665_186104109

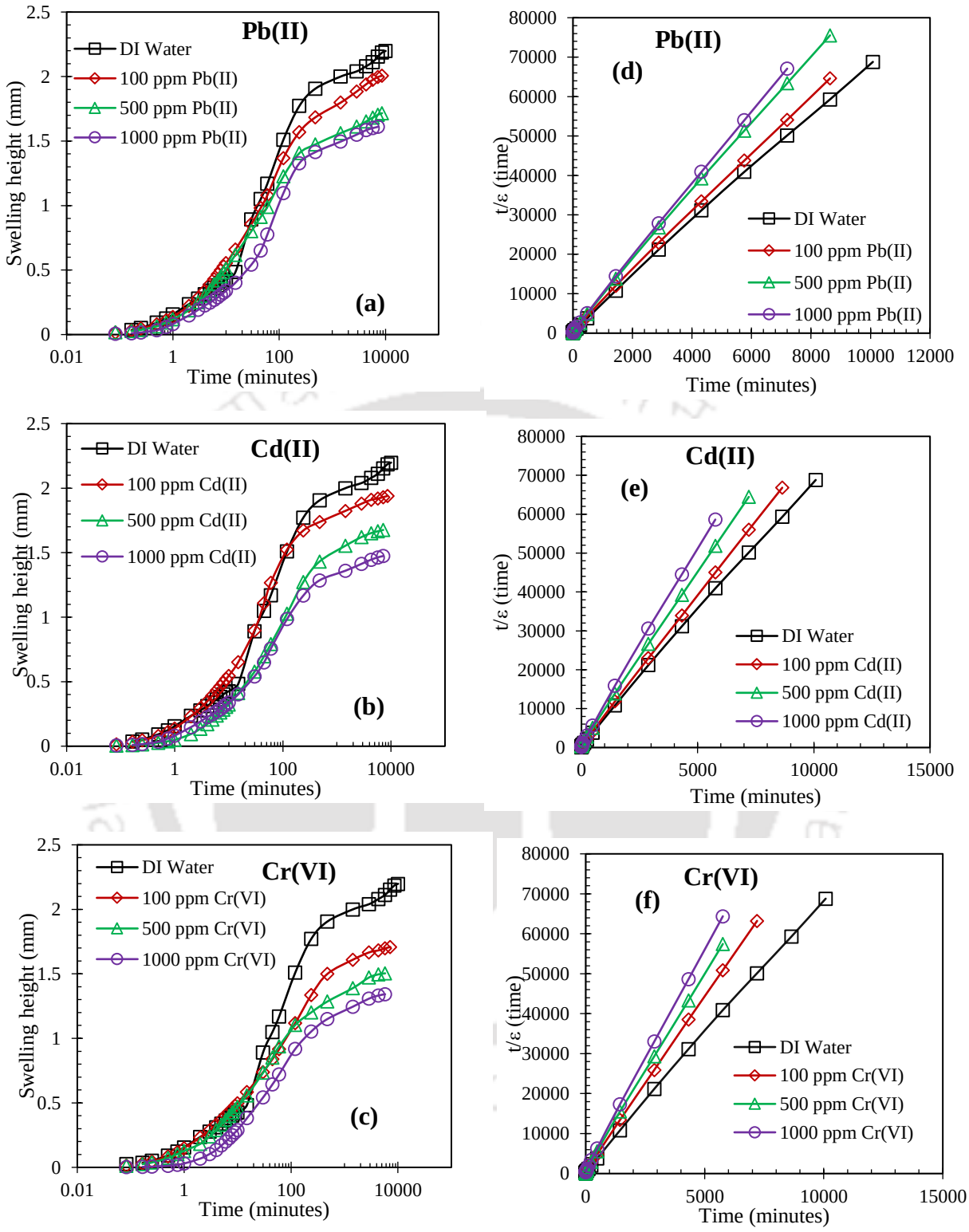

Figure 6.5. (a), (b), & (c) Time vs swelling relationship of 5 % fibre-mixed BC soil with heavy metal permeants. (d), (e), and (f) Linear representation of swelling behaviour of 5% fibre-mixed BC soil with RH model permeated with heavy metals.

TH-3665_186104109

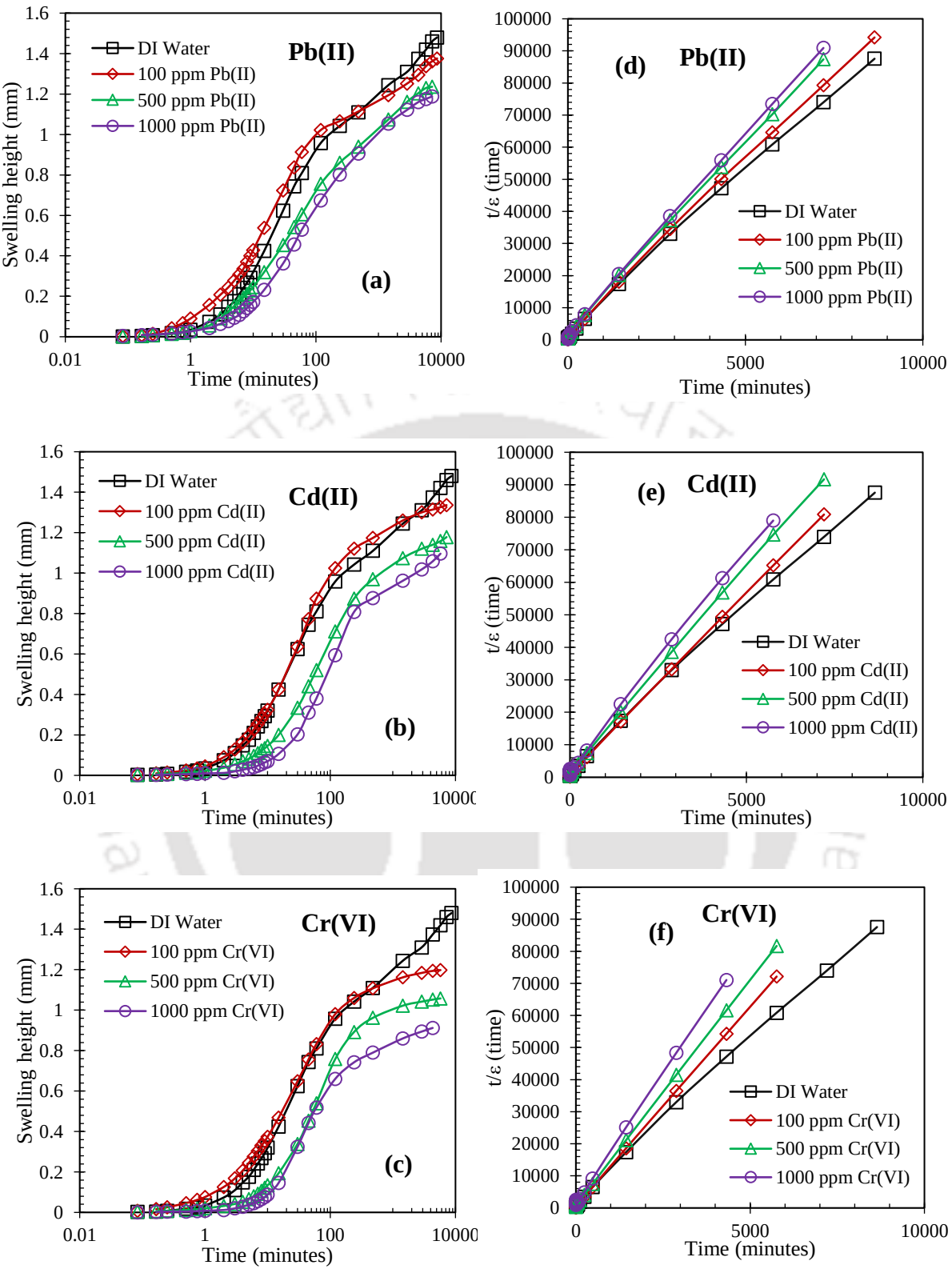

Figure 6.6. (a), (b), & (c) Time vs swelling relationship of 10 % fibre-mixed BC soil with heavy metal permeants. (d), (e), and (f) Linear representation of swelling behavior of 10% fibre-mixed BC soil with RH model permeated with heavy metals.

TH-3665_186104109

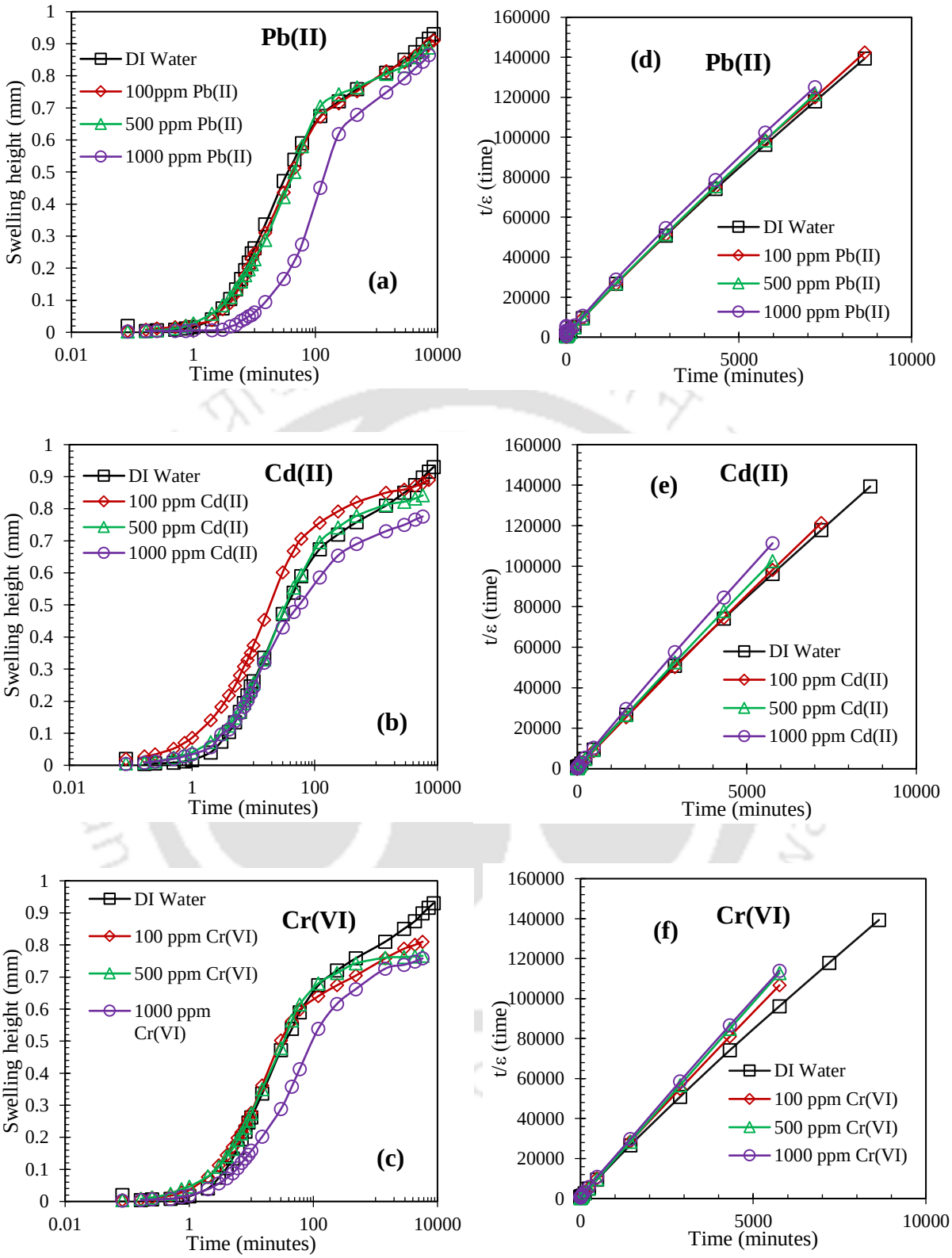

Figure 6.7. (a), (b), & (c) Time vs swelling relationship of 15% fibre-mixed BC soil with heavy metal permeants. (d), (e), and (f) Linear representation of swelling behavior of 15% fibre-mixed BC soil with RH model permeated with heavy metals.

TH-3665_186104109

height was decreased the same fibre content and the same order of concentrations, this swelling height was decreased to 1.94, 1.68, and 1.47 mm with cadmium permeants, and 1.71, 1.50, and 1.34 mm with hexavalent chromium permeants, respectively. For 10% fibre-mixed soil, these swelling heights were reduced from 1.48 mm to 1.38, 1.24, and 1.19 mm with 100, 500, and 1000 ppm lead permeants, respectively. Furthermore, these swelling heights were reduced to 1.34, 1.18, and 1.10 mm with cadmium permeants and 1.12, 1.06, and 0.91 mm with hexavalent permeants, respectively, at the same order of concentrations and for the fibre content. However, there was not much change in heights was observed with 15% fibre-mixed BC soil with metal permeants. The swelling height was reduced marginally from 0.93 mm to 0.91, 0.89, and 0.86 mm with 100, 500, and 1000 ppm lead permeants, respectively. These heights were reported as 0.89, 0.84, and 0.78 mm with 100, 500, and 1000 ppm cadmium permeants, respectively. Whereas, for the same order of hexavalent chromium permeant concentrations and fibre content, these heights reduced to 0.81, 0.77, and 0.76 mm, respectively. Therefore, it is evident that at higher concentrations, this reduction in swelling height was significant. However, with hexavalent chromium permeants, this reduction in swelling height was considerable at lower concentrations i.e. 100 ppm as well compared to lead and cadmium permeants.

The swelling that occurred in each stage was determined using tangent lines as prescribed by Sridharan and Gurtug (2004), Rao and Nagaraj et al. (2010). As listed in Table 6.1, for all BC soil samples, regardless of permeant metal type and concentration, the maximum swelling occurred in the primary swelling stage compared to the other two (initial and secondary) stages. The data in Table 6.1 shows almost 73 to 77% of total swelling occurred during the primary stage; while 10 to 14% occurred during each initial and secondary swelling phase with lead and cadmium permeants. However, around 61 to 71% of total swelling was observed in the primary swelling stage with hexavalent chromium permeants. The swelling process in expansive clays was primarily governed by inner crystalline and osmotic swelling mechanisms (Rao et al., 2013; Liu et al., 2018). Chen et al. (2017) examined the swelling behaviour of expansive bentonite under two inorganic salt fluids. They concluded that inner crystalline swelling was responsible for the original swelling, which is caused by the hydration of interlayer exchange cations, and then osmotic swelling or the double-layer swelling mechanism contributed to the secondary swelling. Furthermore, Rao et al. (2006) and Mishra et al. (2015) confirmed that the macrostructure of clay may contribute to the first stage (initial) of swelling, whilst the microstructure of clay may be

TH-3665_186104109

responsible for the subsequent two phases (primary and secondary) of swelling. However, BC soil's swelling took place in each stage, with corresponding timings for all permeants listed in Table 6.1. Time and swell percentage of BC soil recorded in each swelling stage were decreased for a rise in metal concentration, and this reduction was slightly greater for hexavalent permeants than lead and cadmium permeants. For example, the primary swelling time for DI water was determined to be approximately 465 minutes, but 1000 ppm lead, cadmium, and hexavalent chromium permeants were recorded as 428, 420, and 475 minutes, respectively, as mentioned in Table 6.1. However, the time required for hexavalent chromium permeants to reach asymptotic swelling value in the secondary stage was significantly less than that of lead and cadmium permeants. Similarly, the time and percent swelling that occurred in each swelling stage for all fibre-mixed soil samples (5, 10, and 15%) were reported in Tables 6.2, 6.3, and 6.4. Irrespective of fibre content proportion, heavy metal type, and concentration, a significant amount of swelling occurred in the primary swelling stage for all samples. The time required to reach asymptotic swelling was significantly reduced with hexavalent chromium compared to lead and cadmium permeants for all fibre-mixed soil samples. For example, the asymptotic time value with 5% fibre-mixed BC soil was decreased from 10080 mins to 7200, 5760, and 5760 minutes with 1000 ppm lead, cadmium, and hexavalent chromium permeants. For the same order and concentration of heavy metal permeants, this time value decreased from 8640 minutes to 7200, 5760, and 4320 minutes with 10% fibre-mixed BC soil, respectively. Whereas, this time values declined from 7200 to 5760 and 4000 for 1000 ppm cadmium and hexavalent chromium, respectively. No change in time values was observed with all concentrations of lead permeants at 15% fibre incorporation. However, not much change in asymptotic time values was observed at lower concentrations for all fibre contents, irrespective of heavy metal type and fibre content. Therefore, from the obtained results, it was evident that the amount of total swelling and time to reach asymptotic swell value were slightly more influenced by hexavalent chromium followed by cadmium and lead permeants for all fibre-mixed soil samples. Hence, it is important to consider metal permeants' influence as well before finalising the barrier material in landfill systems. Also, obtained swelling values of all fibre-mixed soil samples under various heavy metal permeants were compared with RH model as shown in Figs. 6.4 to 6.7. The rise in slope values was observed with the hike in the concentration of heavy metal permeant for all soil samples.

TH-3665_186104109

Table 6.1. Time and percent swells of pure BC soil with various heavy metal permeant concentrations

Permeant type and concentration	Initial swelling		Primary swelling		Secondary swelling		Total swelling	
	Time (min)	% Swell	Time (min)	% Swell	Time (min)	% Swell	Time (min)	% Swell
DI Water	15	2.79	465	15.45	11040	2.60	11520	20.84
100 ppm Pb(II)	15	1.69	465	15.04	11040	2.60	11520	19.33
500 ppm Pb(II)	13	2.07	437	13.93	9630	1.38	10080	17.38
1000 ppm Pb(II)	12	1.53	428	12.29	8160	1.30	8600	15.12
100 ppm Cd(II)	15	1.84	455	13.35	11050	2.36	11520	17.55
500 ppm Cd(II)	13	1.67	427	12.66	9600	1.75	10040	16.08
1000 ppm Cd(II)	10	2.04	420	10.93	8210	1.20	8640	14.17
100 ppm Cr(VI)	12	1.33	388	11.35	6850	2.87	7250	15.55
500 ppm Cr(VI)	10	1.00	380	8.3	6810	2.89	7200	12.19
1000 ppm Cr(VI)	5	1.73	475	7.18	5280	2.92	5760	11.83

TH-3665_186104109

Table 6.2. Time and percent swells of 5% fibre-mixed BC soil with various heavy metal permeant concentrations

Permeant type and concentration	Initial swelling		Primary swelling		Secondary swelling		Total swelling	
	Time (min)	% Swell	Time (min)	% Swell	Time (min)	% Swell	Time (min)	% Swell
DI Water	9	2.79	471	9.92	9600	1.94	10080	14.65
100 ppm Pb(II)	9	3.52	471	7.71	9600	2.14	10080	13.37
500 ppm Pb(II)	10	3.40	470	6.43	8160	1.61	8640	11.44
1000 ppm Pb(II)	10	2.27	290	6.92	6900	1.54	7200	10.73
100 ppm Cd(II)	8	3.29	392	8.21	8240	1.43	8640	12.93
500 ppm Cd(II)	10	2.16	390	7.24	6800	1.77	7200	11.17
1000 ppm Cd(II)	7	1.92	293	6.28	5460	1.63	5760	9.83
100 ppm Cr(VI)	2	1.55	478	8.45	6720	1.39	7200	11.39
500 ppm Cr(VI)	2	1.21	238	6.8	5520	2.02	5760	10.03
1000 ppm Cr(VI)	4	0.91	396	6.59	5360	1.45	5760	8.95

TH-3665_186104109

Table 6.3. Time and percent swells of 10% fibre-mixed BC soil with various heavy metal permeant concentrations

Permeant type and concentration	Initial swelling		Primary swelling		Secondary swelling		Total swelling	
	Time (min)	% Swell	Time (min)	% Swell	Time (min)	% Swell	Time (min)	% Swell
DI Water	5	1.17	395	6.13	8240	2.57	8640	9.87
100 ppm Pb(II)	5	1.85	475	5.58	8160	1.74	8640	9.17
500 ppm Pb(II)	5	1.01	395	4.99	6800	2.24	7200	8.24
1000 ppm Pb(II)	5	0.63	395	5.27	6800	2.02	7200	7.92
100 ppm Cd(II)	5	1.31	295	6.29	6900	1.31	7200	8.91
500 ppm Cd(II)	10	0.97	470	5.5	6720	1.38	7200	7.85
1000 ppm Cd(II)	10	0.47	290	5.13	5460	1.69	5760	7.29
100 ppm Cr(VI)	3	1.12	297	6.08	5460	0.79	5760	7.99
500 ppm Cr(VI)	6	0.53	234	5.42	4760	1.10	5000	7.05
1000 ppm Cr(VI)	5	0.25	195	4.55	4120	1.28	4320	6.08

TH-3665_186104109

Table 6.4. Time and percent swells of 15% fibre-mixed BC soil with various heavy metal permeant concentrations

Permeant type and concentration	Initial swelling		Primary swelling		Secondary swelling		Total swelling	
	Time (min)	% Swell	Time (min)	% Swell	Time (min)	% Swell	Time (min)	% Swell
DI Water	4	0.69	296	4.21	6900	1.21	7200	6.20
100 ppm Pb(II)	4	0.61	296	4.19	6900	1.27	7200	6.07
500 ppm Pb(II)	3	0.56	237	4.39	6960	0.97	7200	5.92
1000 ppm Pb(II)	9	0..36	231	3.76	6960	1.64	7200	5.76
100 ppm Cd(II)	2	0.93	198	4.27	7000	0.73	7200	5.93
500 ppm Cd(II)	2	0.48	198	3.22	5560	1.91	5760	5.61
1000 ppm Cd(II)	2	0.37	198	3.93	5560	0.87	5760	5.17
100 ppm Cr(VI)	2	0.51	198	3.99	5560	0.90	5760	5.40
500 ppm Cr(VI)	1	0.31	119	4.22	3880	0.58	4000	5.11
1000 ppm Cr(VI)	1	0.12	179	3.78	3880	1.15	4000	5.05

6.2.4. Swelling pressures and swelling potentials

The swelling pressures (SPr's) and swelling potentials (SPo's) of BC soil under different metal permeants were plotted in Tables 6.5 and 6.6. The SPr's of BC soil were diminished with a rise in the concentration of lead permeants as per Table 6.5. The SPr of BC soil with DI water was calculated as 520 kPa, which was dcreased to 495, 475, and 420 kPa for 100, 500, and 1000 ppm lead permeants, respectively. The percentage decrement in SPr was marginal (4.81%) for 100 ppm lead permeant than DI water, whereas, it was significant (19.23%) for 1000 ppm lead permeant. This trend was consistent with test results reported

TH-3665_186104109

by Dutta and Mishra (2016(b)) and Ray et al. (2022(a)) with bentonites with heavy metal permeants. This decrease in SPr's may be related to a decline in electrical DDL thickness that is inversely proportional to the metal concentration (Tripathy et al., 2004; Jadda and Bag, 2020). However, it was shown that the reduction in SPr was slightly more with cadmium in comparison to the lead permeants. Here, the SPr values for cadmium permeants were found to be 490 (5.77% reduction) and 395 kPa (24.04% reduction) for 100 and 1000 ppm concentrations, respectively. The maximum hike in SPr values was observed with anionic heavy metal permeant compared to both cationic heavy metal permeants as displayed in Table 6.5. The SPr value of BC soil was reported as 480, 410, and 365 kPa with 100, 500, and 1000 ppm hexavalent chromium concentrations, respectively. The reduction in SPr was about 7.69, 21.15, and 29.81%, respectively, compared to DI water. The valence and potassium ions present in chromium solutions are responsible for this significant reduction in SPr values of BC soil compared to cadmium and lead permeants. Similar kind of observations were made with all fibre-mixed soil samples as well, as shown in Table 6.5. Significant reductions in SPr values were observed at high concentrations, irrespective of fibre content. For example, at 5% fibre-mixed soil the percentage of reduction in SPr values was observed as 14.81, 16.67, and 22.22% with 1000 ppm lead, cadmium, and hexavalent chromium permeants, respectively, compared to DI water. For the similar order of concentrations, this reduction was about 11.11, 13.89, and 30.56% with 10% fibre-mixed soil. Similarly, the values of this reduction became 7.69, 23.08, and 36.15% with 15% fibre-mixed soil compared to DI water for the same order of heavy metal permeant type and concentration, respectively.

Swelling potentials of all fibre-mixed soil samples permeated with various heavy metal concentrations are shown in Table 6.6. All swelling potentials (SPo's) were diminished with the rise in the concentration of heavy metal permeants similar to the swelling pressures pattern. The SPo value of pure BC soil was decreased from 20.84% (DI water) to 15.12, 14.17, and 11.83 % with 1000 ppm lead, cadmium, and hexavalent chromium permeants, respectively. The percentage reduction in SPo values was about 27.45, 32.00, and 43.23%, respectively, compared to DI water. At higher metal concentrations, changes in interlayer cation are likely to affect the pore structure of clay, which may impact the swelling phenomenon that leads to a reduction in SPo of BC soil (Likos and Lu, 2006; Chen et al., 2017). A similar trend was observed with all fibre-mixed soil samples as well, displayed in Table 6.6. For 5% fibre-mixed soil samples, the percentage reduction in swelling percentage

TH-3665_186104109

was around 26.76, 32.90, and 38.91% with 1000 ppm lead, cadmium, and hexavalent chromium permeants, respectively. Similarly, this percentage reduction was about 19.76, 26.14, and 38.40% with 10% fibre-mixed BC soil and 7.10, 16.61, and 18.54% with 15% fibre-mixed samples, respectively, for the same order of metal type and concentration. Therefore, it is evident that the impact of heavy metal permeants on SPr and SPo tendencies is significant and considerable for all samples independent of fibre content.

Table 6.5. Swelling pressures of fibre-mixed BC soil with various salt permeant concentrations

Permeant type and concentration	Swelling pressure (kPa)			
	0% TF	5% TF	10% TF	15% TF
DI Water	520	270	180	140
100 ppm Pb(II)	495	265	175	140
500 ppm Pb(II)	475	240	165	135
1000 ppm Pb(II)	420	230	160	130
100 ppm Cd(II)	490	260	170	135
500 ppm Cd(II)	455	235	160	120
1000 ppm Cd(II)	395	225	155	110
100 ppm Cr(VI)	480	250	160	125
500 ppm Cr(VI)	410	235	155	110
1000 ppm Cr(VI)	365	210	125	93

TH-3665_186104109

Table 6.6. Swelling potentials of fibre-mixed BC soil with various heavy metal permeant concentrations

Permeant type and concentration	Swelling potential (%)			
	0% TF	5% TF	10% TF	15% TF
DI Water	20.84	14.65	9.87	6.20
100 ppm Pb(II)	19.33	13.37	9.17	6.07
500 ppm Pb(II)	17.38	11.44	8.24	5.92
1000 ppm Pb(II)	15.12	10.73	7.92	5.76
100 ppm Cd(II)	17.55	12.93	8.91	5.93
500 ppm Cd(II)	16.08	11.17	7.85	5.61
1000 ppm Cd(II)	14.17	9.83	7.29	5.17
100 ppm Cr(VI)	15.55	11.39	7.99	5.40
500 ppm Cr(VI)	12.19	10.03	7.05	5.11
1000 ppm Cr(VI)	11.83	8.95	6.08	5.05

Also, obtained swell potentials were compared with the rectangular hyperbola regression model to determine the ultimate predicted swell potential, and obtained fitting parameters (a and b), ultimate swell potential (1/a), and measure swelling potential values were mentioned in Tables 6.7 to 6.10 with respect to all fibre-mixed BC soil samples. Also, a plot was drawn between measured swell and predicted swell values shown in Fig. 6.8. The R^2 value is coming close to 1, which shows a good agreement between measured swell and predicted swell.

TH-3665_186104109

Table 6.7. Predicted swelling potentials (RH model) vs measured swelling potential values of BC soil samples under various heavy metal permeant concentrations

Permeant type and concentration	Hyperbolic parameters		Measured swell (%)	Predicted swell (%)
	a	b		
DI Water	4.796	396.52	20.84	20.85
100 ppm Pb(II)	5.123	605.99	19.33	19.52
500 ppm Pb(II)	5.720	374.76	17.38	17.48
1000 ppm Pb(II)	6.552	493.52	15.12	15.26
100 ppm Cd(II)	5.671	542.18	17.55	17.63
500 ppm Cd(II)	6.175	489.03	16.08	16.19
1000 ppm Cd(II)	7.013	442.43	14.17	14.26
100 ppm Cr(VI)	6.427	638.35	15.55	15.56
500 ppm Cr(VI)	8.260	963.44	12.19	12.12
1000 ppm Cr(VI)	8.458	444.06	11.83	11.82

TH-3665_186104109

Table 6.8. Predicted swelling potentials (RH model) vs measured swelling potential values of 5% fibre-mixed BC soil samples under various heavy metal permeant concentrations

Permeant type and concentration	**Hyperbolic parameters**		**Measured swell (%)**	**Predicted swell (%)**
	a	b		
DI Water	6.89	329.7	14.65	14.52
100 ppm Pb(II)	7.5191	295.05	13.37	13.30
500 ppm Pb(II)	8.808	312.34	11.44	11.35
1000 ppm Pb(II)	9.3268	383.12	10.73	10.72
100 ppm Cd(II)	7.7515	215.58	12.93	12.90
500 ppm Cd(II)	8.9399	440.34	11.17	11.18
1000 ppm Cd(II)	10.214	390.19	9.83	9.79
100 ppm Cr(VI)	8.7975	265.04	11.39	11.37
500 ppm Cr(VI)	9.9872	276.55	10.03	10.01
1000 ppm Cr(VI)	11.146	549.98	8.95	8.97

TH-3665_186104109

Table 6.9. Predicted swelling potentials (RH model) vs measured swelling potential values of 10% fibre-mixed BC soil samples under various heavy metal permeant concentrations

Permeant type and concentration	Hyperbolic parameters		Measured swell (%)	Predicted swell (%)
	a	b		
DI Water	10.517	712.35	9.87	9.51
100 ppm Pb(II)	11.045	483.95	9.17	9.05
500 ppm Pb(II)	12.159	747.74	8.24	8.22
1000 ppm Pb(II)	12.64	860.52	7.92	7.91
100 ppm Cd(II)	11.246	390.71	8.91	8.89
500 ppm Cd(II)	12.77	895.42	7.85	7.83
1000 ppm Cd(II)	13.637	1767.7	7.29	7.33
100 ppm Cr(VI)	12.505	273.25	7.99	8.00
500 ppm Cr(VI)	14.055	826.53	7.05	7.11
1000 ppm Cr(VI)	16.143	1534.00	6.08	6.19

TH-3665_186104109

Table 6.10. Predicted swelling potentials (RH model) vs measured swelling potential values of 15% fibre-mixed BC soil samples under various heavy metal permeant concentrations

Permeant type and concentration	Hyperbolic parameters		Measured swell (%)	Predicted swell (%)
	a	b		
DI Water	16.344	904.35	6.20	6.12
100 ppm Pb(II)	16.686	784.77	6.07	5.99
500 ppm Pb(II)	17.021	692.50	5.92	5.88
1000 ppm Pb(II)	17.300	2529.8	5.76	5.78
100 ppm Cd(II)	16.975	298.09	5.93	5.89
500 ppm Cd(II)	17.86	436.85	5.61	5.60
1000 ppm Cd(II)	19.413	553.12	5.17	5.15
100 ppm Cr(VI)	18.593	489.38	5.40	5.38
500 ppm Cr(VI)	19.539	334.27	5.11	5.12
1000 ppm Cr(VI)	19.774	865.97	5.05	5.06

TH-3665_186104109

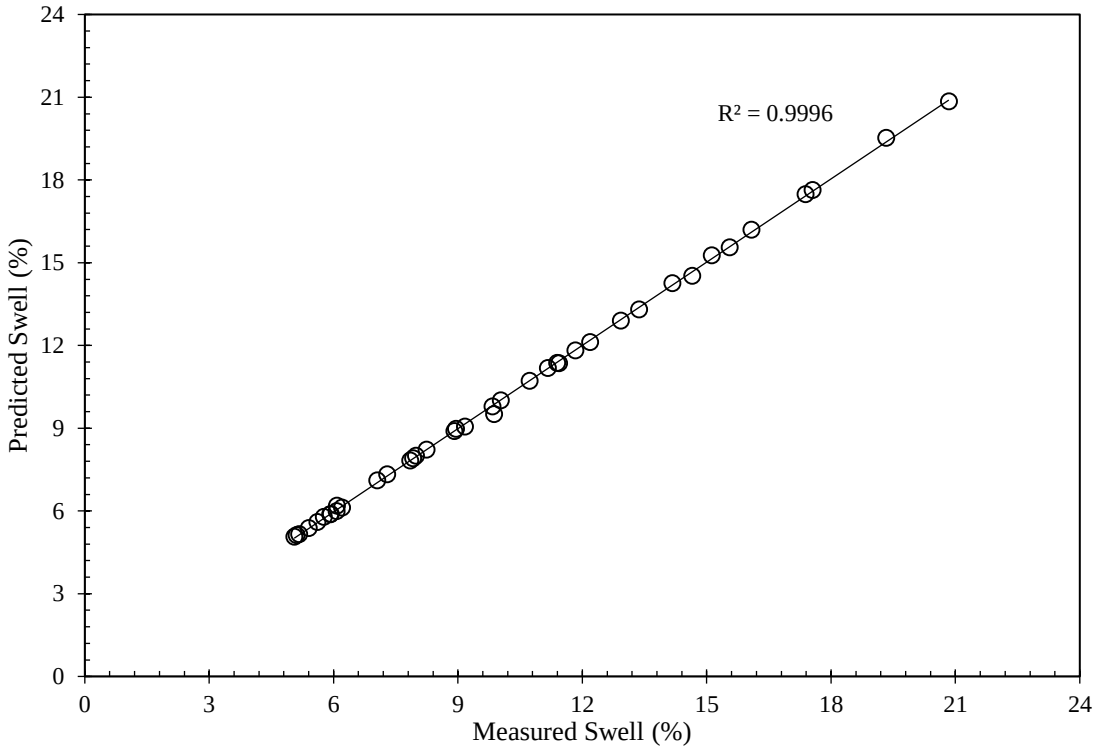

Fig. 6.8. Correlation between measured swell vs predicted swell of all fibre-mixed samples under various heavy metal permeant concentrations.

6.2.5. Coefficient of consolidation (c_v)

The plot in Figs. 6.9 to 6.12 show that the coefficient of consolidation (c_v) values of fibre-mixed BC soil samples with respect to different consolidation pressures (49.0, 98.1, 196.1, 392.3, and 784.5 kPa) permeated with two cationic (lead and cadmium) and one anionic (hexavalent chromium) heavy metal permeants ranging from 100, 500, and 1000 ppm concentrations. It is clear that the hike in c_v values with the rise in fibre content and permeant concentration, which indicates that the faster rate of consolidation as displayed in Figs. 6.9 to 6.12. The formation of drainage paths due to tire fibre content caused this significant hike in c_v values which were discussed in a detailed way in Chapter 4. In this chapter, the main objective is to understand the consolidation behaviour of all fibre-mixed samples inundated by various concentrations of heavy metal permeants. However, irrespective of permeant type and concentration c_v values were decreased with the increase in consolidation pressure as shown in Figs. 6.9 to 6.12. At higher consolidation pressures, particles come closer together causing the suppression of DDL thickness, which leads to the densification of the sample resulting in a reduction in c_v value (Mersi and Olson, 1971; Sridharan et al., 1986; Sridharan and Nagara, 2004). Also, c_v values are influenced by pore-fluid chemistry since pore-fluid chemistry is related to DDL thickness (Sridharan and Jayadeva, 1982; Dutta and Mishra

TH-3665_186104109

2016(a)). However, irrespective of consolidation pressure, c_v values increased with the increase in the concentration of heavy metal permeants. For example, from Figure 6.9, the c_v values of pure BC soil are 1.28×10^{-3}, 0.51×10^{-3}, 0.25×10^{-3}, 8.7×10^{-5}, and 2.4×10^{-5} cm^2/s for corresponding consolidation pressures of 49.0, 98.1, 196.1, 392.3, and 784.5 kPa in the presence of DI water. These values were increased to the variation 2.62×10^{-3}, 1.31×10^{-3}, 6.13×10^{-4}, 1.80×10^{-4}, and 7.71×10^{-5} cm^2/s with 1000 ppm lead concentrations, for the same order of consolidation pressures, respectively. However, these values increased furthermore with the same concentration of cadmium permeants at the same order of consolidation pressures. These c_v values were reported as 2.56×10^{-3}, 1.88×10^{-3}, 8.13×10^{-4}, 2.04×10^{-4}, and 8.98×10^{-5} cm^2/s with cadmium permeants. However, compared to cadmium and lead higher c_v values were reported with hexavalent chromium permeants. At 1000 ppm concentration, the c_v values of BC soil were recorded as 3.41×10^{-3}, 1.82×10^{-3}, 8.44×10^{-4}, 3.94×10^{-4}, and 1.68×10^{-4} cm^2/s, for the same order of consolidation pressures, respectively. The hike in c_v values was about 2.66, 3.57, 3.38, 4.53, and 7.00 times for the same order of consolidation pressures, respectively, with hexavalent chromium permeants. Therefore, it is evident that higher c_v values reported with hexavalent chromium followed cadmium and lead permeant with BC soil at constant permeant concentration and consolidation pressure, as depicted in Fig. 6.9. However, there was not much variation in c_v values was observed with lower concentration i.e 100 ppm with all three heavy metal permeants. Since DDL thickness is inversely proportional to electrolyte concentration and cation valency, resulting in the variation of c_v values of BC soil. However, it is important to understand the consolidation behaviour of all fibre-mixed samples under these heavy metal concentrations.

The coefficient of variation (c_v) values of all fibre-mixed BC soils were compared and depicted for a specific consolidation pressure of 784.5 kPa in order to enhance clarity, as demonstrated in Fig. 6.13. For example, the c_v value of 0% tire fibre-mixed BCS with DI water at 784.5 kPa was 2.36×10^{-5} cm^2/s, which was increased to 4.10×10^{-5}, 7.92×10^{-5}, and 2.17×10^{-4} cm^2/s for 5, 10, and 15% tire content, respectively. However, at 1000 ppm concentrations of lead, cadmium, and hexavalent chromium permeants, these values were reported as 1.20×10^{-4}, 1.70×10^{-4}, and 2.40×10^{-4} cm^2/s respectively, with 5% tire fibre-mixed BC soil at the same consolidation pressure of 784.5 kPa. This hike was about 2.93, 4.15, and 5.85 times compared to DI water with 5% fibre-mixed BC soil. At identical pressure and concentration conditions, these c_v values became 2.80×10^{-4} (3.53 times), 3.44

TH-3665_186104109

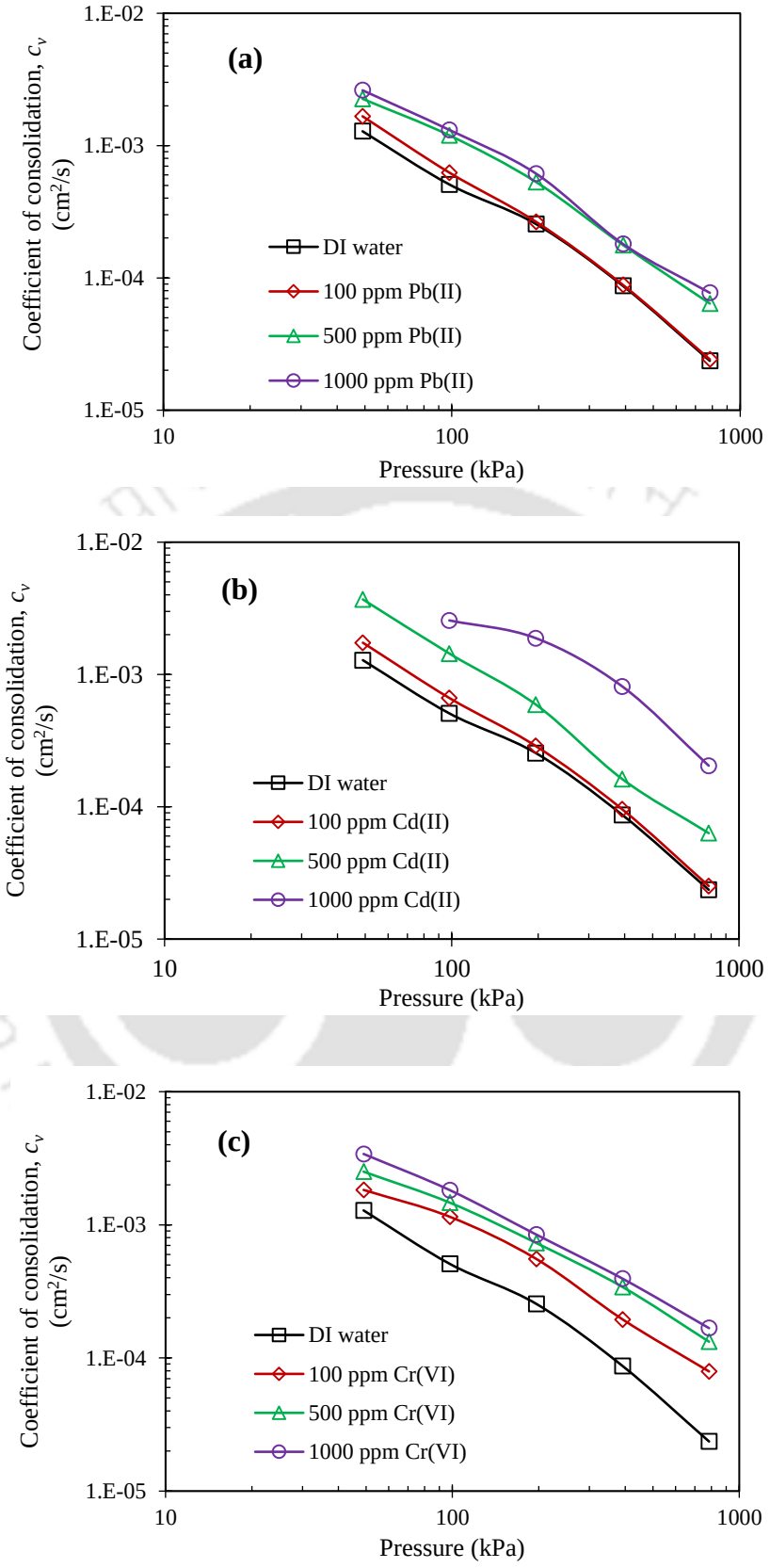

Fig.6.9. Coefficient of consolidation vs consolidation pressure plots of BC soil with heavy metal permeants: (a) Lead; (b) Cadmium; (c) Hexavalent chromium.

TH-3665_186104109

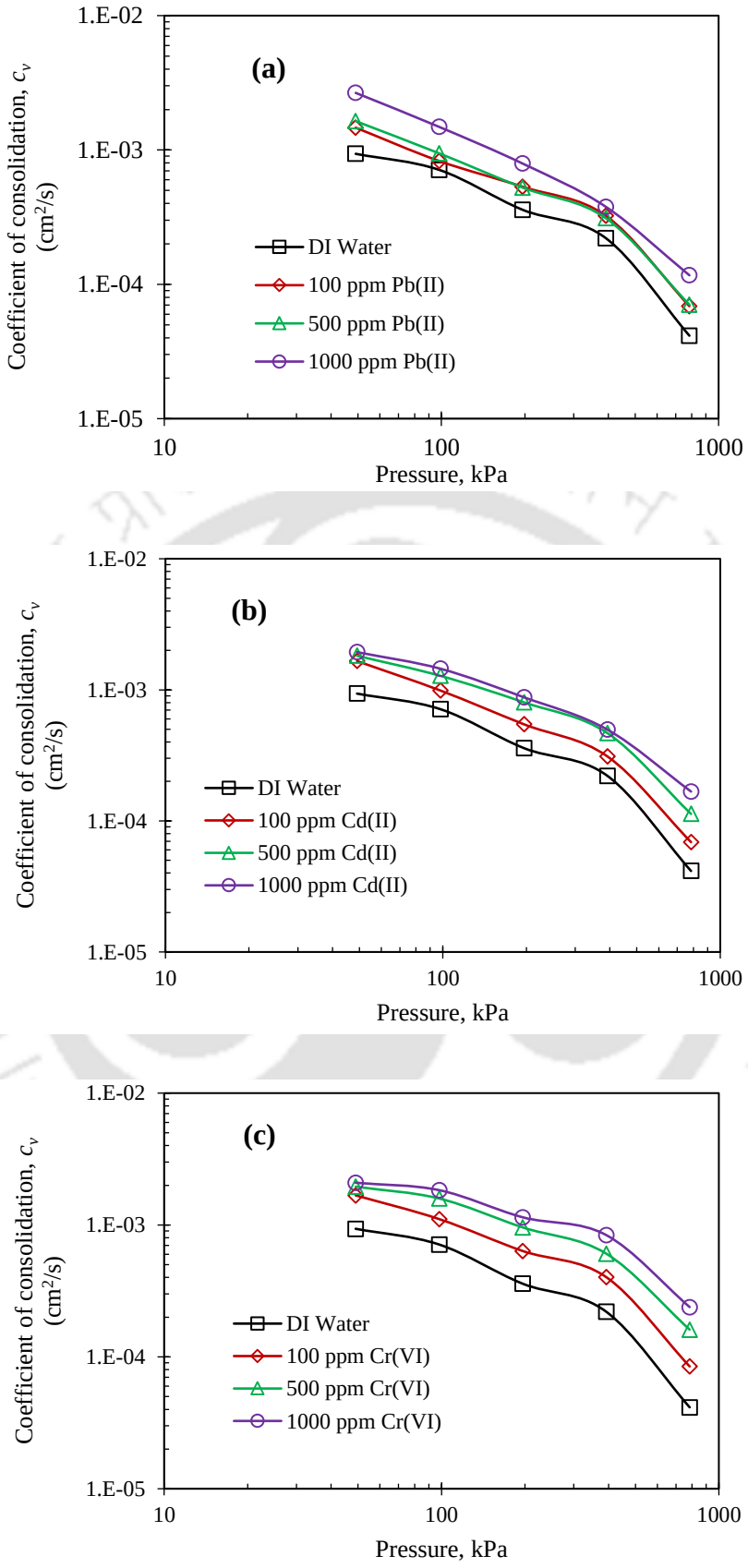

Fig.6.10. Coefficient of consolidation vs consolidation pressure plots of 5% fibre-mixed BC soil with heavy metal permeants: (a) Lead; (b) Cadmium; (c) Hexavalent chromium.

TH-3665_186104109

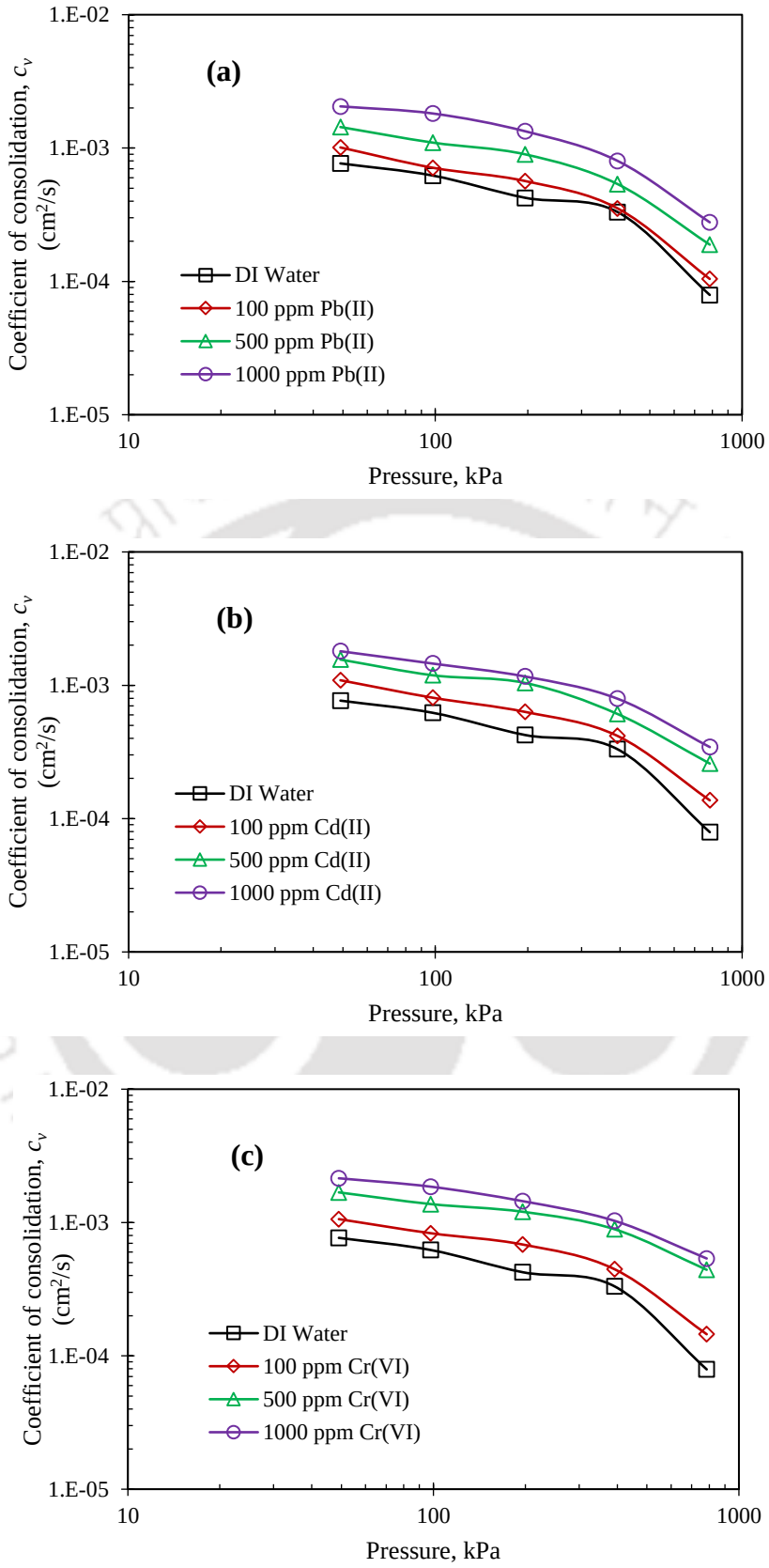

Fig.6.11. Coefficient of consolidation vs consolidation pressure plots of 10% fibre-mixed BC soil with heavy metal permeants: (a) Lead; (b) Cadmium; (c) Hexavalent chromium.

TH-3665_186104109

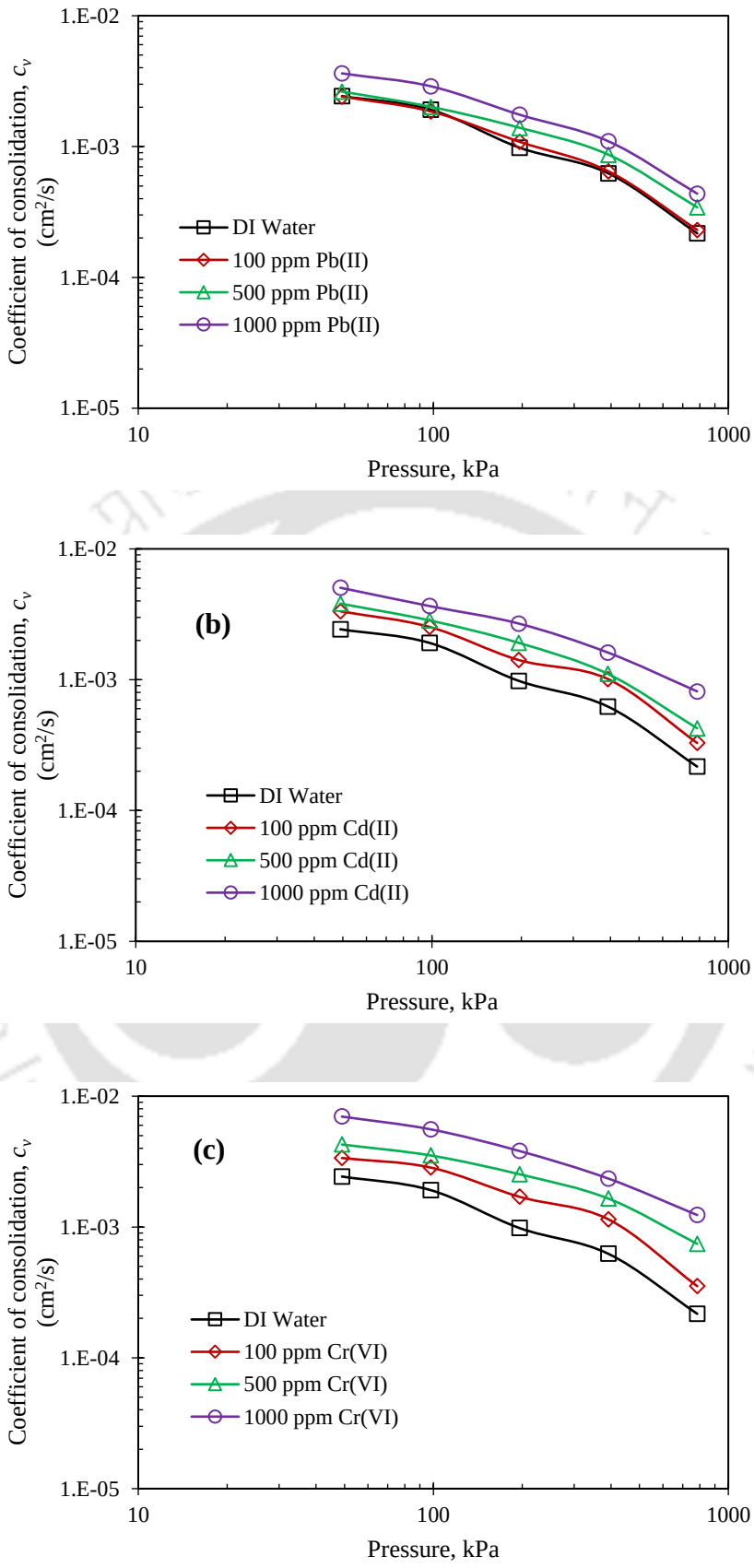

Fig.6.12. Coefficient of consolidation vs consolidation pressure plots of 15% fibre-mixed BC soil with heavy metal permeants: (a) Lead; (b) Cadmium; (c) Hexavalent chromium.

TH-3665_186104109

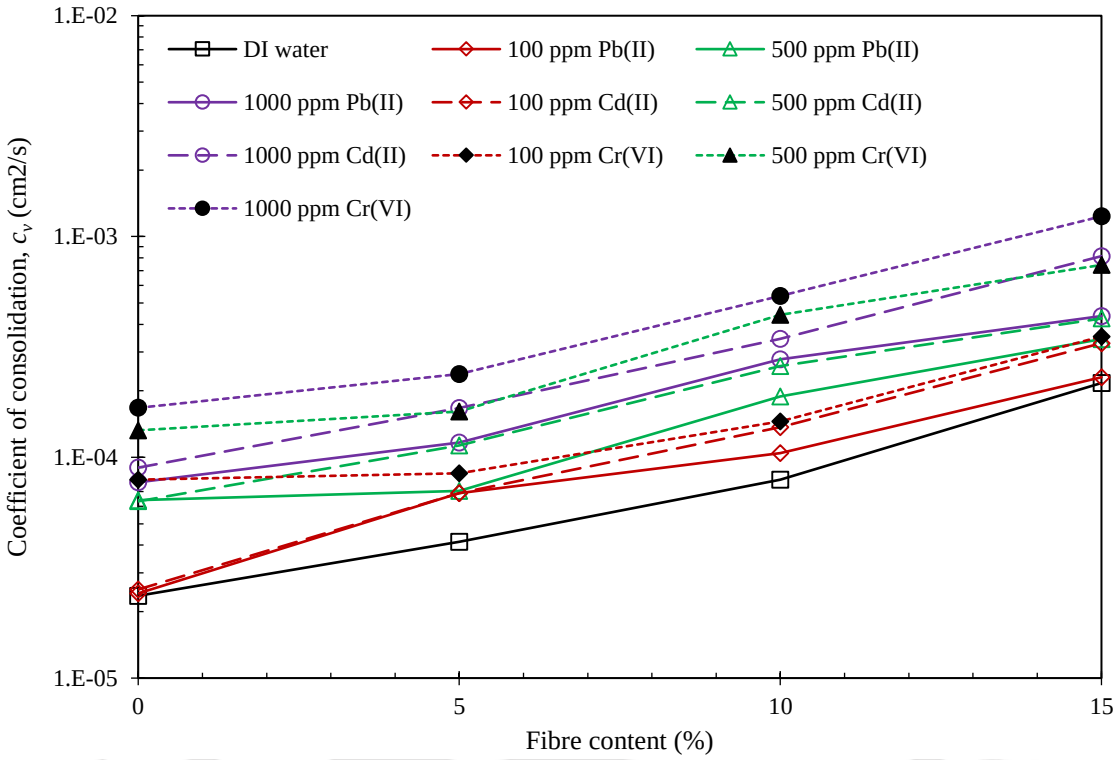

Fig. 6.13. Fibre content vs coefficient of consolidation plot with various heavy metal permeant concentrations at the consolidation pressure of 784.5 kPa.

$\times 10^{-4}$ (4.34 times), and 5.40×10^{-4} cm^2/s (6.82 times) for lead, cadmium, and hexavalent chromium permeants, respectively, with 10% tire fibre-mixed BC soil compared to DI water. Whereas for 15% tire fibre-mixed BC soil, these values were reported as 4.36×10^{-4} (2.01 times), 8.10×10^{-4} (3.73 times), and 1.23×10^{-3} cm^2/s (5.67 times) for the same pressure and similar metal concentrations. A similar kind of behaviour was observed with remaining consolidation pressures as well, shown in Figs. 6.9-6.12. However, this change/increment in c_v values was less pronounced at lower metal concentrations (i.e. 100 ppm). The findings unequivocally illustrate the substantial influence of heavy metal permeants on all fibre-mixed BC soil samples, demonstrating their consideration in the context of landfill barrier system applications.

6.2.6. Time for 90% consolidation (t_{90})

The plot in Figs. 6.14 to 6.17 demonstrate the correlation between the consolidation pressures (49.0 to 784.5 kPa) and the time required to achieve 90% of consolidation (t_{90}) for all fibre-mixed BC soil samples that were exposed to both cationic and anionic heavy metal permeants. The t_{90} values could not be determined at low consolidation stresses (below 49.0 kPa) due to the negligible settlement observed over time, despite the stress being

TH-3665_186104109

incrementally increased from 4.9 to 784.5 kPa. This is because the pore water is the primary absorber of the applied stress at reduced consolidation pressures. The load is transferred to the soil grains as the stress increases, resulting in the settlement, which leads to a proper settlement curve display from 49.0 kPa onwards. As the consolidation pressure increased, the time required to achieve 90% of consolidation also increased, regardless of fibre content and permeant type or concentration, as illustrated in Figs. 6.14 to 6.17. This phenomenon could be obviously expected due to the packed dense structure at higher consolidation stresses resulting in a slower rate of consolidation and low hydraulic conductivity values. These t_{90} values were observed to vary with the proportion of fibre content, type of metal permeant, and concentration of metal permeants, as depicted in Figs. 6.14 to 6.17. High fibre content caused low t_{90} values due to the quick dissipation of pore water pressure through micro-cracks of fibres and drainage paths, as discussed in Chapter 4. Therefore, a detailed discussion has been conducted in this chapter regarding the influence of heavy metal concentration on time to achieve 90% consolidation for all samples. The time taken for 90% consolidation for pure BC soil under DI water permeation was from 9.00, 22.09, 40.96, 106.09, and 334.89 minutes for the corresponding pressures 49.0, 98.1, 196.1, 392.3, and 784.5 kPa consolidation pressures, respectively. These values decreased marginally at lower concentrations of heavy metal permeants, and this reduction was significant at higher concentrations. For example, at the same consolidation pressures, these t_{90} values of pure BC soil were reported as 4.00, 7.84, 16.10, 49.00, and 100.00 minutes, respectively, with 1000 ppm lead solution permeation. These values were 4.00, 5.29, 11.56, 40.96, and 81.00 minutes with 1000 ppm cadmium solution permeation and 2.89, 5.29, 10.89, 2116, and 43.56 minutes with 1000 ppm hexavalent chromium solution permeation for the same sequence of consolidation pressures, respectively. The cations present in the lead and cadmium concentration lead to these lower t_{90} values at constant consolidation pressure and permeant concentration. The double K^+ ions and valency of chromium (VI) resulted in lower t_{90} values with hexavalent permeants significantly than lead and cadmium concentrations. A similar impact in t_{90} results was observed with all fibre-mixed BC soil samples as well, shown in Figs. 6.15-6.17. To facilitate a simpler comparison, the t_{90} values for all fibre-mixed samples at the maximum consolidation stress of 784.5 kPa are illustrated in Fig. 6.18. For example, the t_{90} value for 5% fibre-mixed BC soil was 163.84 minutes, which was reduced to 56.25, 39.69, and 28.09 minutes with 1000

TH-3665_186104109

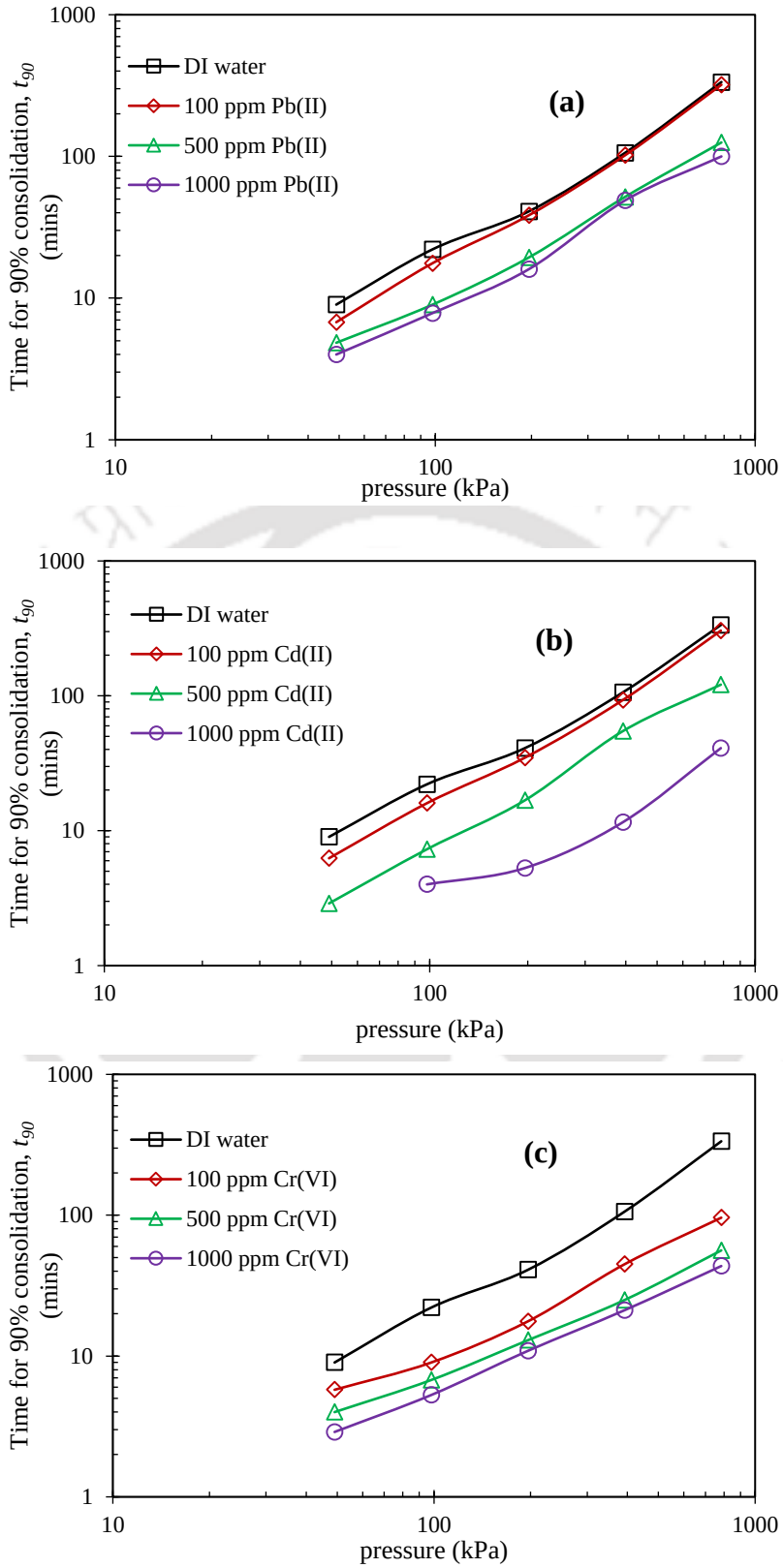

Fig.6.14. Time taken for 90% consolidation vs consolidation pressure plots of BC soil with heavy metal permeants: (a) Lead; (b) Cadmium; (c) Hexavalent chromium.

TH-3665_186104109

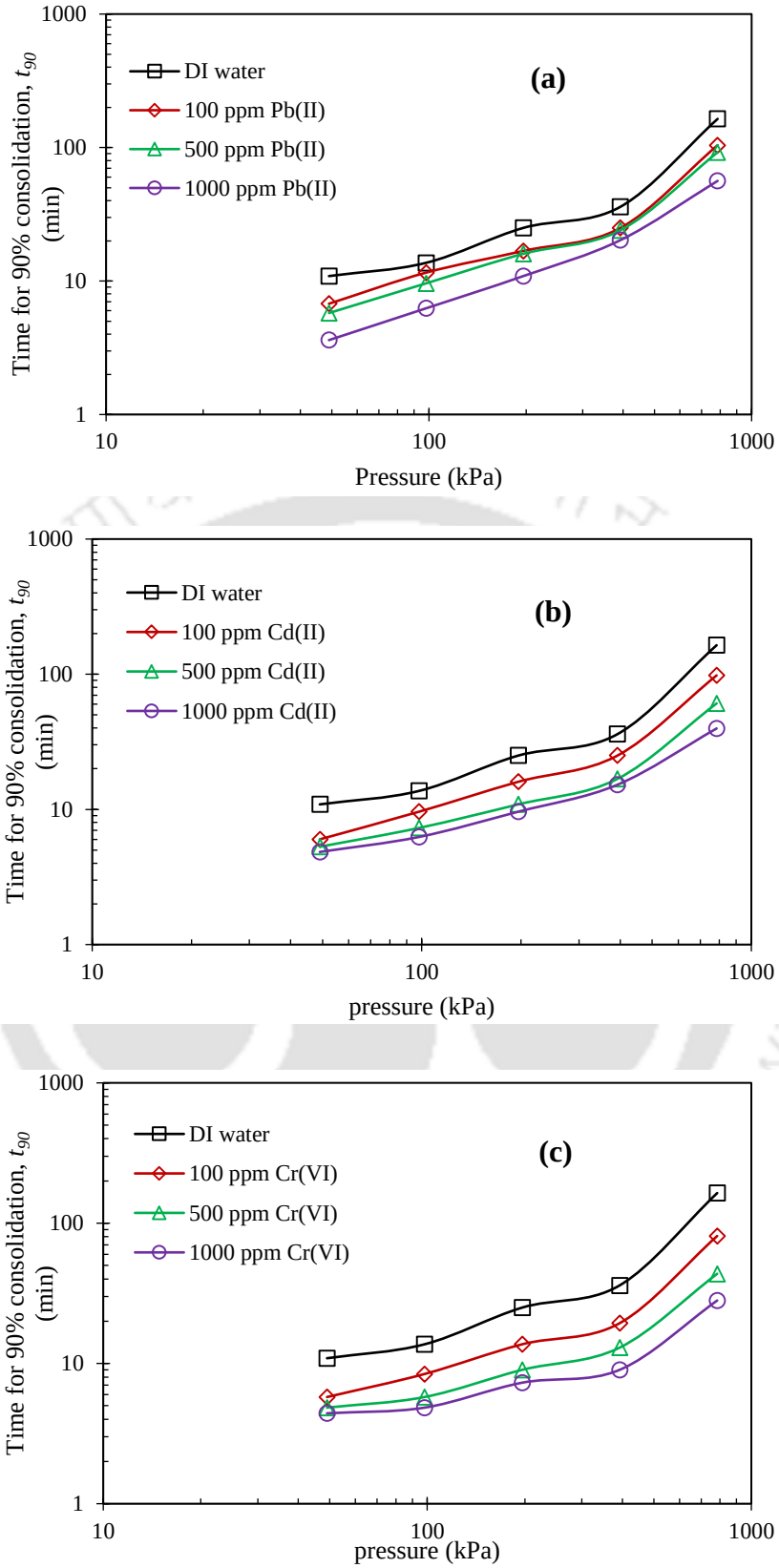

Fig.6.15. Time taken for 90% consolidation vs consolidation pressure plots of 5% fibre-mixed BC soil with heavy metal permeants: (a) Lead; (b) Cadmium; (c) Hexavalent chromium.

TH-3665_186104109

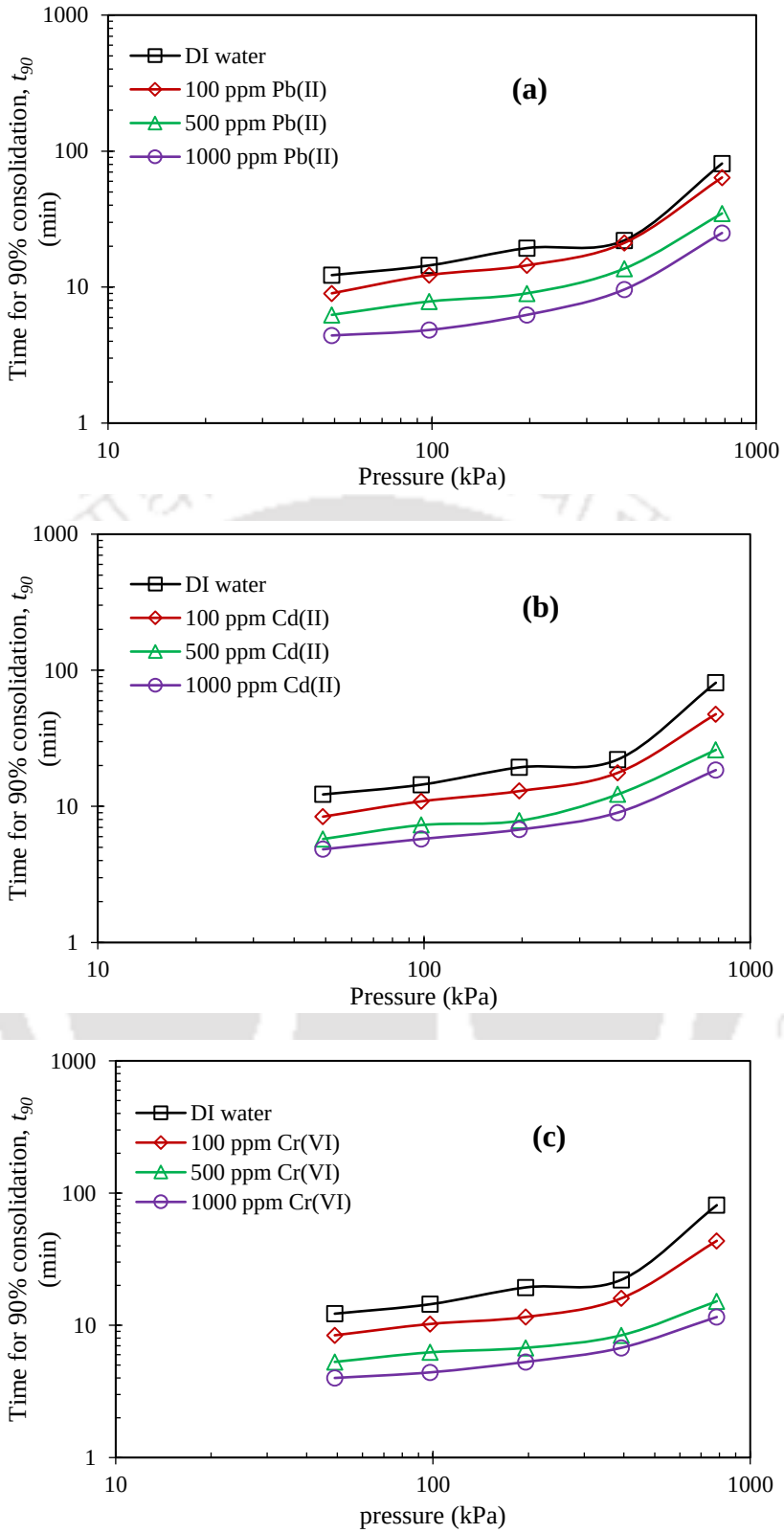

Fig.6.16. Time taken for 90% consolidation vs consolidation pressure plots of 10% fibre-mixed BC soil with heavy metal permeants: (a) Lead; (b) Cadmium; (c) Hexavalent chromium.

TH-3665_186104109

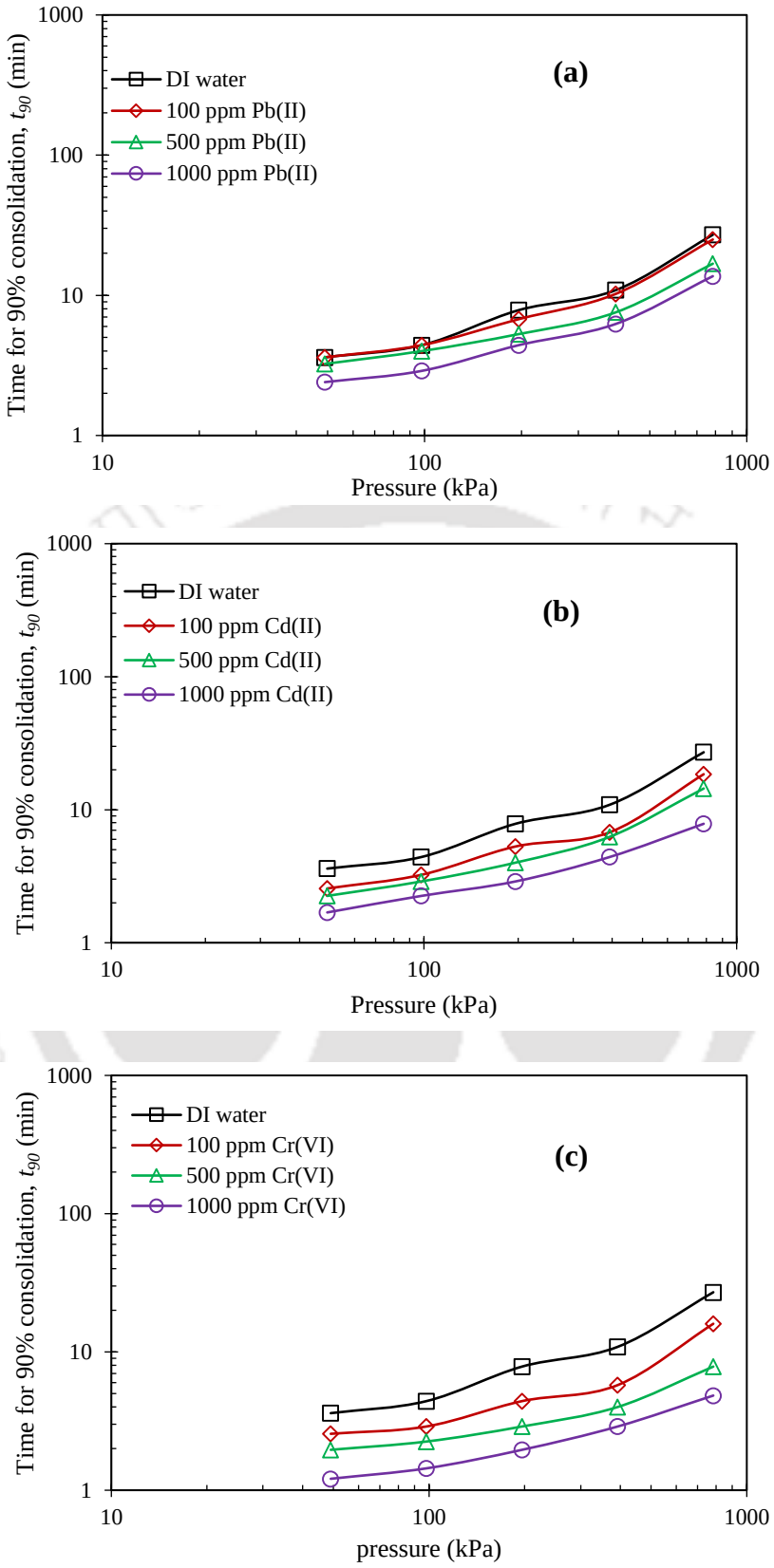

Fig.6.17. Time taken for 90% consolidation vs consolidation pressure plots of 15% fibre-mixed BC soil with heavy metal permeants: (a) Lead; (b) Cadmium; (c) Hexavalent chromium.

TH-3665_186104109

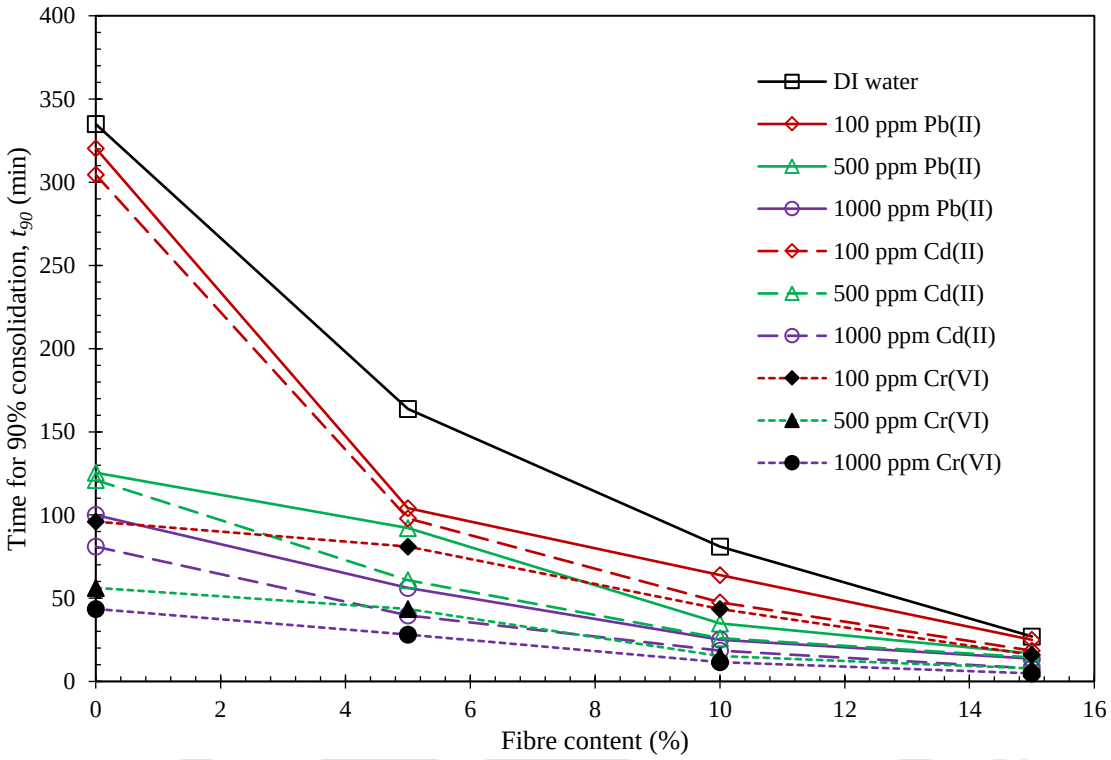

Fig. 6.18. Fibre content vs time for 90% consolidation (t_{90}) plot with various heavy metal permeant concentrations at the consolidation pressure of 784.5 kPa.

ppm lead, cadmium, and hexavalent chromium permeants, respectively. This reduction was about 65.6, 75.8, and 82.8% for the same concentration and order of metal permeants, respectively. For 10% fibre content, this reduction was about 69.1, 77.2, and 85.7% with 1000 ppm lead, cadmium, and hexavalent chromium concentrations, respectively, at the same consolidation stress. On the other hand, the reduction in 15% fibre-mixed BC soil was approximately 49.4, 71.0, and 82.1% for the same sequence of metal permeants and concentrations, respectively. Therefore, based on the obtained results, it can be concluded that a significant variation in t_{90} values of fibre-mixed BC soil was observed at prominent concentrations. However, this reduction is less influential at lower concentrations.

6.2.7. Void ratio vs Pressure (*e*-log *P*) relationship

The experimental data from the oedometer was utilised to illustrate the compression curves in a semilogarithmic plot for all fibre-mixed BC soil samples. The relationship between void ratio and consolidation pressure (*e*-log *P*) for all fibre-mixed (0 to 15%) samples permeated with various heavy metal concentrations ranging from 0 (DI water) to 1000 ppm was shown in Figs. 6.19 to 6.22. For all samples, the void ratios were decreased with the rise of consolidation pressures, irrespective of fibre content, permeant type, and concentration. The

TH-3665_186104109

compression behaviour of soil was usually controlled by mechanical and physiochemical properties (Bolt, 1956; Dutta and Mishra, 2016(a)). An increase in vertical consolidation pressure led to the dissipation of excess pore pressure and a decrease in void ratio, which is due to the development of a stiff soil layer. It was observed that a minimum change in void ratios for all fibre-mixed BC soil samples up to 98.1 kPa, irrespective of permeant type and concentration, as displayed in Figs. 6.19 to 6.22. However, it is evident that the void ratios of BC soil were influenced by fibre content, permeant type, and concentration. The void ratio-pressure relationships with respect to the inclusion of fibre content were discussed in Chapter 4. In this chapter, the focus is emphasized on the influence of heavy metal concentrations on pure BC soil and fibre-mixed BC soils. A marginal reduction in the void ratio of BC soil was observed with an increase in heavy metal concentrations, as shown in Fig. 6.19. For example, at 49.0 kPa consolidation pressure, the void ratio was decreased from 1.11 (with DI water) to 1.10, 1.02, and 0.99 with 100, 500, and 1000 ppm lead permeants, respectively. These void ratios were reported as 1.00 and 0.98 at 1000 ppm concentration of cadmium and hexavalent chromium concentrations, respectively. Earlier, Moghal et al. (2020) observed a similar trend with expansive soils under various concentrations of heavy metal solutions. Ray et al., (2021b) also observed this trend with bentonites under various heavy metal permeations. The attraction of cations to charged clay particles leading the suppression of DDL thickness, causing this decline in void ratios with the permeate heavy metal concentrations. Similarly, this drop in void ratio was noticed with all fibre-mixed samples as well, depicted in Figs 6.20 to 6.22. For example, with 5% fibre-mixed BC soil, the void ratio was dropped from 1.03 to 0.97, 0.93, and 0.92 with 1000 ppm lead, cadmium, and hexavalent chromium concentrations, respectively, at 49.0 kPa. Similarly, for 10% fibre-mixed soil composition, the void ratio reported from 0.93 to 0.84, 0.84, and 0.82 with the same order of heavy metal permeants and same consolidation pressure, respectively, at 1000 ppm concentration. These values changed from 0.83 to 0.78, 0.75, and 0.76 at the same consolidation pressure and identical order of heavy metal permeants and concentration, respectively. However, this change in void ratio at maximum consolidation pressure was marginal and negligible. Fibre-mixed samples were slightly more influenced by hexavalent chromium followed by cadmium and lead.

TH-3665_186104109

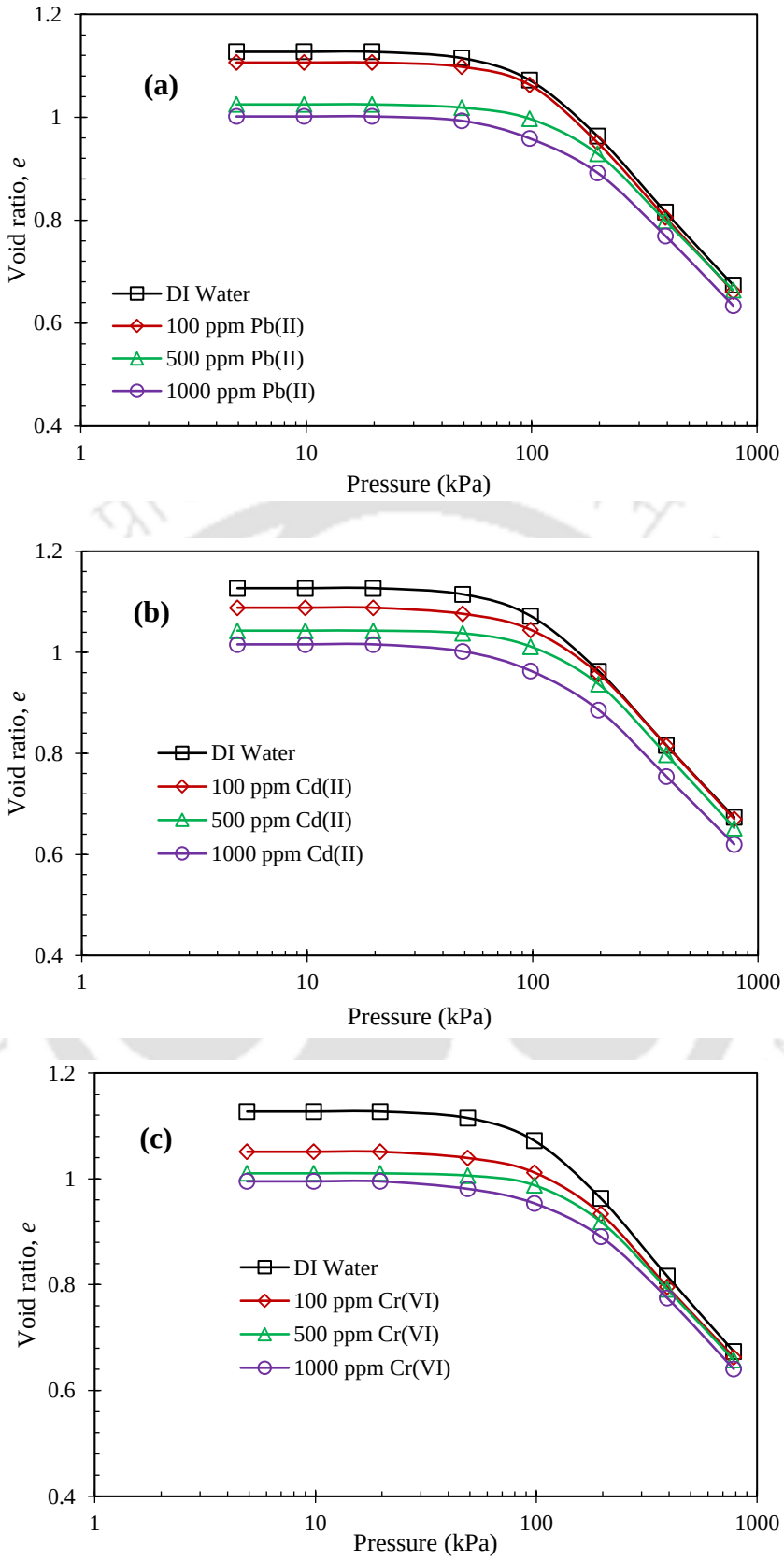

Fig. 6.19. Void ratio (*e*) vs consolidation pressure plots for pure BC soil with various heavy metal permeant concentrations: (a) Lead; (b) Cadmium; (c) Hexavalent chromium.

TH-3665_186104109

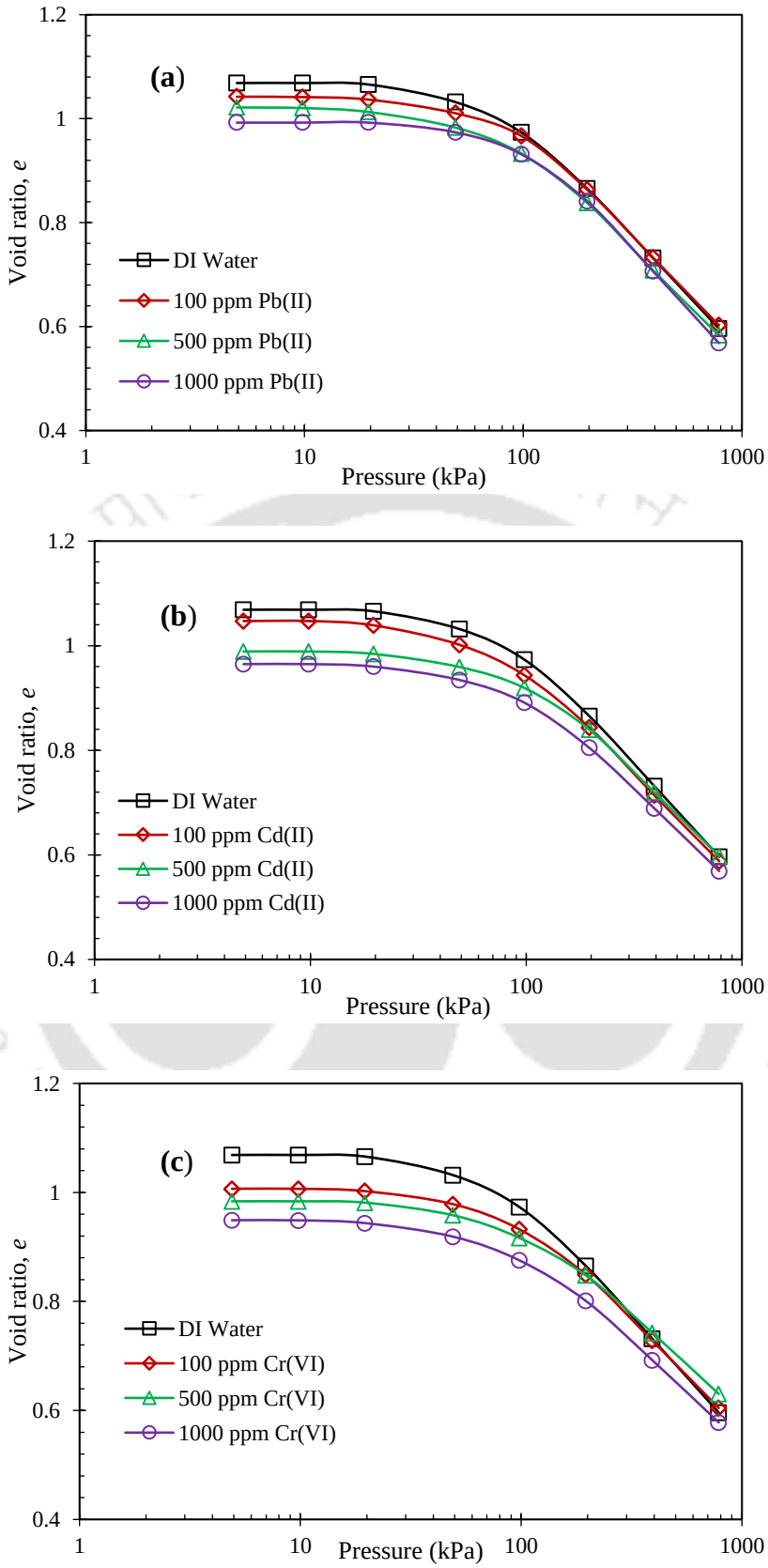

Fig. 6.20. Void ratio (*e*) vs consolidation pressure plots for 5% fibre-mixed BC soil with various heavy metal permeant concentrations: (a) Lead; (b) Cadmium; (c) Hexavalent chromium.

TH-3665_186104109

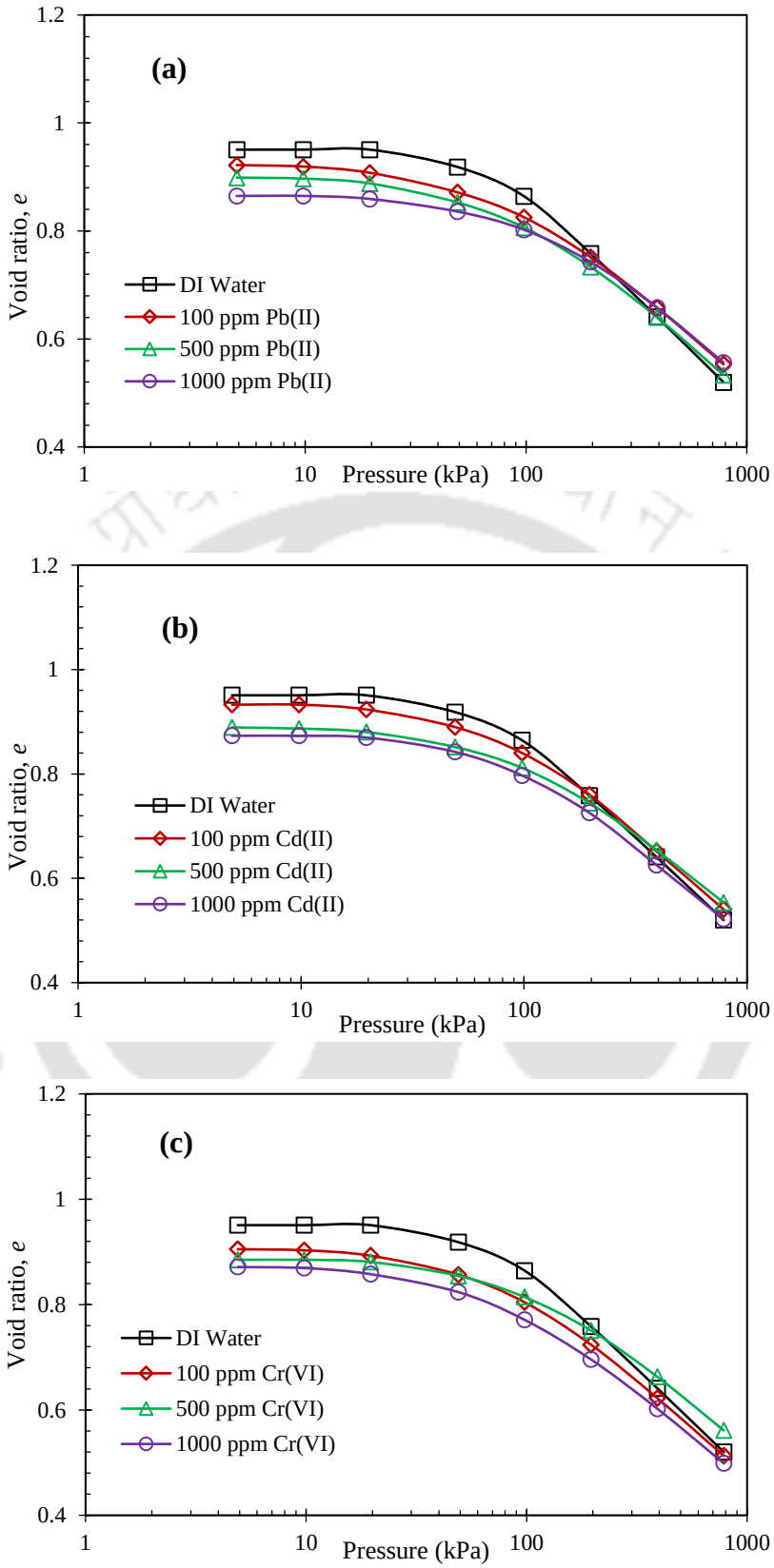

Fig. 6.21. Void ratio (*e*) vs consolidation pressure plots for 10% fibre-mixed BC soil with various heavy metal permeant concentrations: (a) Lead; (b) Cadmium; (c) Hexavalent chromium.

TH-3665_186104109

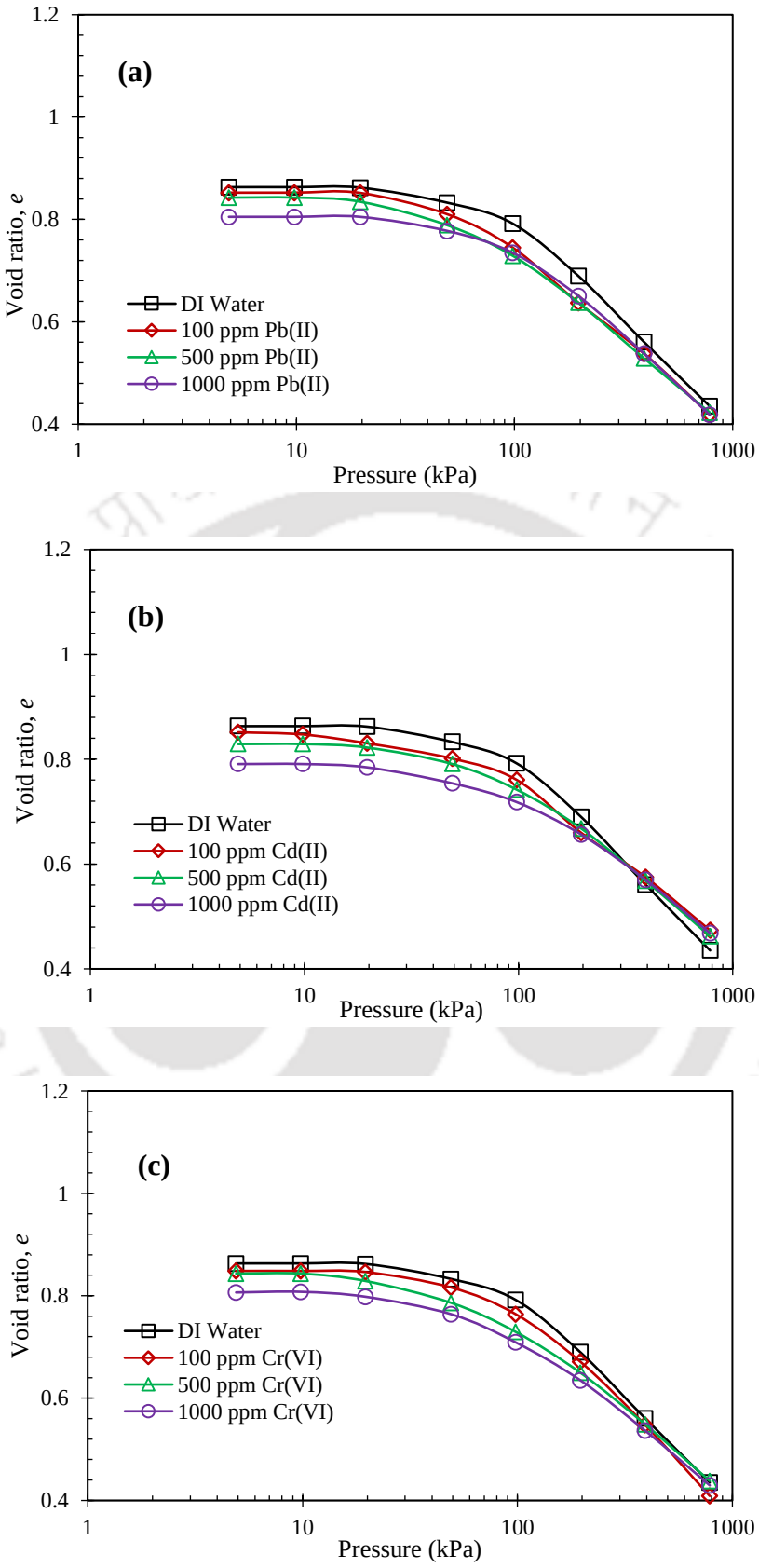

Fig. 6.22. Void ratio (*e*) vs consolidation pressure plots for 15% fibre-mixed BC soil with various heavy metal permeant concentrations: (a) Lead; (b) Cadmium; (c) Hexavalent chromium.

TH-3665_186104109

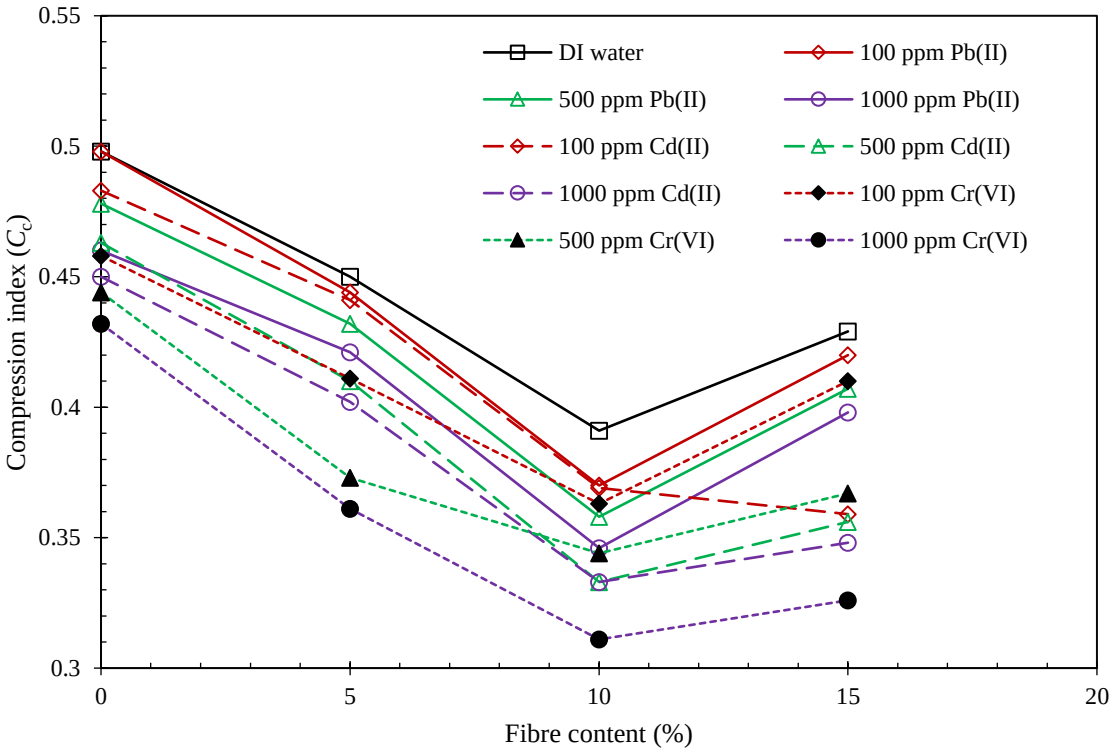

Fig. 6.23. Compression index (C_c) of fibre-mixed BC soil with various salt permeant concentrations.

6.2.8. Compression index (C_c)

All compressibility values of fibre-mixed BC soil samples were calculated by taking the slopes of straight-line portions of *e*-log *P* curves, depicted in Fig. 6.23. The impact of heavy metal permeants on compression indices of fibre-mixed BC soil was marginal, as observed from plots. The compression index (C_c) of BC soil was calculated as 0.498 with DI water permeation. The C_c values were reported as 0.498, 0.478, and 0.460 with 100, 500, and 1000 ppm lead permeations, respectively. It was clearly seen that no difference was observed in the C_c value at 100 ppm of lead solution. However, a slight change was observed with cadmium and hexavalent chromium permeant at lower concentrations. At 1000 ppm concentration, the C_c values were reported as 0.460 and 0.432 with cadmium and hexavalent chromium concentrations, respectively. A similar trend was observed across all samples, regardless of fibre content, as displayed in Fig. 6.23. For example, with 5% fibre-mixed BC soil, the C_c value was changed from 0.450 (DI water) to 0.421, 0.402, and 0.361 with 1000 ppm concentrations of lead, cadmium, and hexavalent chromium permeants, respectively. These values changed from 0.391 to 0.346, 0.333, and 0.311 with 10% fibre-mixed BC soil for a similar order of permeant types and concentration. Finally, these values were reduced from 0.429 to 0.398, 0.348, and 0.326 with 15% fibre-mixed BC soil in the same order of

TH-3665_186104109

metal permeants. However, the change in compression indices was less significant at lower concentrations of heavy metal permeants for all fibre-mixed soil samples.

6.2.9. Hydraulic conductivity (*k*)

Since hydraulic conductivity (*k*) is the most significant engineering property for the clay liners, a minimum *k* value of $\leq 10^{-7}$ cm/s has been recommended (USEPA, 1988; Kayabah, 1997; Chalermyanont et al., 2009). In this research work, the standard oedometer was used to assess the impact of consolidation stresses on all fibre-mixed BC soil samples under various heavy metal permeants, and *k* values were estimated for the corresponding consolidation stresses using the coefficient of consolidation and coefficient of volume change. The influence of both cationic (lead and cadmium) and anionic (hexavalent chromium) heavy metal permeants at the concentrations varying from 0 (DI water) to 1000 ppm on *k* values of fibre-mixed BC soils has been shown in the Figs. 6.24 to 6.27. It was noticed that the rise in *k* value is proportional to the rise in the concentration of tire fibre content irrespective of metal type and concentration for overburden pressures ranging from 49.0 to 784.5 kPa, as illustrated in Figs. 6.24 to 6.27. However, the possible reasons for the hike in the *k* values with the inclusion of tire fibre content were discussed in Chapter 4. Therefore, the focus has been emphasized on the impact of metal concentrations on the hydraulic characteristics of BC soil and fibre-mixed (5,10, and 15%) BC soil. The hydraulic conductivity values of all fibre-mixed BC soils with respect to various overburden pressures are listed in Table 6.11. A lower *k* value was observed at high consolidation pressures irrespective of permeant type, as shown in Table 6.11. For example, using DI water as permeant, the *k* value of BC soil at 49.0 kPa was reported as 2.44×10^{-8} cm/s, which was decreased to 4.75×10^{-10} cm/s (51.37 times) under an external consolidation pressure of 784.5 kPa. Similarly, at a similar increase in the consolidation pressure (i.e. from 49.03 to 784.53 kPa), this reduction in conductivity value with 100 and 1000 ppm lead permeants was about 45.90 and 25.21 times, respectively. Similarly, for the same increase in the pressure, it was 66.67 and 38.28 times with 100 and 1000 ppm cadmium permeants, respectively. This reduction was about 23.4 and 24.8 times, with 100 and 1000 ppm hexavalent chromium permeants, respectively, for the same range of consolidation pressures. A similar trend was observed with all fibre-mixed samples, as shown in Table 6.11. The variation in *k* values with respect to corresponding average void ratios was shown in Figs. 6.24 to 6.27. These higher consolidation pressures lead to a reduction in void ratios of samples by moving clay

TH-3665_186104109

particles to closer distances resulting in low *k* values. At 100 ppm concentrations, the fluctuation in *k* values was minimal for both lead, cadmium, and hexavalent chromium permeants, whereas it became prevalent at 1000 ppm concentrations.

The *k* values of all fibre-mixed BC soils under different metal concentrations were calculated at a specific void ratio of 0.75 and tabulated in Table 6.12 for easy comparison. At a void ratio of 0.75, the *k* value for DI water was determined to be 4.93×10^{-10} cm/s; Furthermore, this *k* value was increased to 5.68×10^{-10}, 1.19×10^{-9}, and 1.84×10^{-9} cm/s for 100, 500 and 1000 ppm lead permeants, respectively. Therefore, compared to DI water, the *k* value was raised by a factor of 1.15, 2.41, and 3.73 for the similar order of metal concentrations. Moreover, this difference in *k* values was more pronounced at higher void ratios. This increment trend at higher metal concentrations was comparable with earlier studies on bentonites and locally available soils (Chalermyanont et al., 2009; Li et al., 2015; Ray et al., 2022b). The lowering of repulsive forces at higher metal concentrations may account for larger *k* values by causing the DDL layer to contract (Sridharan and Jayadeva, 1982; Jadda and Bag, 2020). Due to the contraction of this DDL layer, clay particles become closer together, leading to a more significant aggregation, which results in a widening of flow channels and a corresponding rise in the *k* (Madsen and Vonmoos, 1989; Dutta and Mishra, 2015b; Amiri et al., 2022). As described in Table 6.12, this increment in *k* values was more pronounced for hexavalent chromium followed by cadmium permeants than for lead. The *k* values at the void ratio of 0.75 for 100, 500, and 1000 ppm cadmium were 6.85×10^{-10}, 1.88×10^{-9}, and 3.44×10^{-9} cm/s, and these values were reported as 2.19×10^{-9}, 3.10×10^{-9}, and 4.90×10^{-9} cm/s with the same order of concentrations of hexavalent chromium permeants, respectively. At 1000 ppm, *k* was 6.98 and 9.94 times higher than in DI water with cadmium and hexavalent chromium, respectively, which is a significant difference. Here the valency and cation concentration played key roles in the change in hydraulic conductivity values. Thus, it is apparent that high metal permeant concentrations significantly affect BC soil's hydraulic behaviour. Plot from the Figs. 6.25 to 6.27, it was evident that a significant hike in *k* values was observed with all fibre-mixed soils at high concentrations, irrespective of permeation metal type. All fibre-mixed sample's *k* values were compared at a particular void ratio of 0.75, as mentioned in Table 6.12.

TH-3665_186104109

Table 6.11. Hydraulic conductivity vs consolidation pressure values for fibre-mixed BC soil samples with various heavy metal permeant concentrations

Tire fibre content (%)	Permeant type and concentration (ppm)	Hydraulic conductivity (cm/s)		
		49.0 kPa	196.1 kPa	784.5 kPa
0	0 (DI Water)	2.44×10^{-8}	1.37×10^{-8}	4.75×10^{-10}
	Pb(II)-100	2.13×10^{-8}	1.41×10^{-8}	4.64×10^{-10}
	Pb(II)-500	2.24×10^{-8}	1.80×10^{-8}	1.20×10^{-9}
	Pb(II)-1000	3.53×10^{-8}	2.00×10^{-8}	1.40×10^{-9}
	Cd(II)-100	3.30×10^{-8}	1.20×10^{-8}	4.95×10^{-10}
	Cd(II)-500	3.05×10^{-8}	2.15×10^{-8}	1.35×10^{-9}
	Cd(II)-1000	5.78×10^{-8}	2.39×10^{-8}	1.51×10^{-9}
	Cr(VI)-100	3.51×10^{-8}	2.18×10^{-8}	1.50×10^{-9}
	Cr(VI)-500	1.77×10^{-8}	2.57×10^{-8}	2.54×10^{-9}
	Cr(VI)-1000	8.11×10^{-8}	2.75×10^{-8}	3.26×10^{-9}
5	0 (DI Water)	5.03×10^{-8}	1.90×10^{-8}	7.95×10^{-10}
	Pb(II)-100	6.19×10^{-8}	2.20×10^{-8}	1.10×10^{-9}
	Pb(II)-500	7.99×10^{-8}	2.50×10^{-8}	1.30×10^{-9}
	Pb(II)-1000	8.18×10^{-8}	3.60×10^{-8}	2.30×10^{-9}
	Cd(II)-100	9.89×10^{-8}	2.75×10^{-8}	1.24×10^{-9}
	Cd(II)-500	7.51×10^{-8}	3.27×10^{-8}	1.97×10^{-9}
	Cd(II)-1000	8.26×10^{-8}	3.93×10^{-8}	2.92×10^{-9}

TH-3665_186104109

Tire fibre content (%)	Permeant type and concentration (ppm)	Hydraulic conductivity (cm/s)		
		49.0 kPa	196.1 kPa	784.5 kPa
5	Cr(VI)-100	6.52×10^{-8}	2.70×10^{-8}	1.50×10^{-9}
	Cr(VI)-500	7.44×10^{-8}	3.40×10^{-8}	2.50×10^{-9}
	Cr(VI)-1000	8.73×10^{-8}	4.50×10^{-8}	4.00×10^{-9}
10	0 (DI Water)	4.14×10^{-8}	2.36×10^{-8}	1.43×10^{-9}
	Pb(II)-100	6.30×10^{-8}	2.25×10^{-8}	1.62×10^{-9}
	Pb(II)-500	8.79×10^{-8}	3.56×10^{-8}	3.01×10^{-9}
	Pb(II)-1000	8.49×10^{-8}	4.32×10^{-8}	4.17×10^{-9}
	Cd(II)-100	6.25×10^{-8}	2.68×10^{-8}	2.27×10^{-9}
	Cd(II)-500	7.79×10^{-8}	3.78×10^{-8}	3.84×10^{-9}
	Cd(II)-1000	8.68×10^{-8}	4.54×10^{-8}	5.38×10^{-9}
	Cr(VI)-100	6.59×10^{-8}	2.99×10^{-8}	2.40×10^{-9}
	Cr(VI)-500	7.69×10^{-8}	4.13×10^{-8}	6.63×10^{-9}
	Cr(VI)-1000	1.29×10^{-7}	6.03×10^{-8}	8.51×10^{-9}
15	0 (DI Water)	1.25×10^{-7}	5.49×10^{-8}	4.28×10^{-9}
	Pb(II)-100	1.77×10^{-7}	6.58×10^{-8}	4.36×10^{-9}
	Pb(II)-500	2.14×10^{-7}	7.24×10^{-8}	5.82×10^{-9}
	Pb(II)-1000	1.79×10^{-7}	8.36×10^{-8}	8.33×10^{-9}
	Cd(II)-100	1.74×10^{-7}	8.00×10^{-8}	5.20×10^{-9}

TH-3665_186104109

Tire fibre content (%)	Permeant type and concentration (ppm)	Hydraulic conductivity (cm/s)		
		49.0 kPa	196.1 kPa	784.5 kPa
5	Cd(II)-500	2.15×10^{-7}	8.00×10^{-8}	7.00×10^{-9}
	Cd(II)-1000	2.81×10^{-7}	9.50×10^{-8}	1.30×10^{-8}
	Cr(VI)-100	1.80×10^{-7}	8.78×10^{-8}	7.76×10^{-9}
	Cr(VI)-500	3.25×10^{-7}	1.16×10^{-7}	1.30×10^{-8}
	Cr(VI)-1000	4.31×10^{-7}	1.65×10^{-7}	2.11×10^{-8}

For example, the hydraulic conductivity value of 5% fibre-mixed BC soil was increased from 2.83×10^{-9} (DI water) to 9.53×10^{-9} (3.37 times), 1.14×10^{-8} (4.03 times), and 1.83×10^{-8} cm/s (6.45 times) with 1000 ppm lead, cadmium, and hexavalent chromium permeants, respectively, at a void ratio of 0.75. Similarly, with 10% fibre-mixed soil, this hike in *k* value was around 6.72, 10, and 13.74 times with the same order of permeants, respectively, at 1000 ppm concentration. Furthermore, at the same void ratio and similar order of metal permeants, this hike was about 2.17, 3.28, and 6.59 times, respectively, with 15% fibre-mixed BC soil. However lower hike in *k* values was observed at lower concentrations for all fibre-mixed samples. Therefore, the change in *k* value was almost independent of fibre content under all heavy metal permeations. Generation of multiple flow paths due to fibre content and the formation of widened flow channels due to high metal concentrations are the possible reasons for this hike in conductivity values of fibre-mixed soils after permeating with various heavy metal concentrations. Nevertheless, previous research has not investigated the impact of metal concentrations on tire fibre-mixed soils in order to compare the results. Thus, it is crucial to evaluate the impact of heavy metal permeants prior to selecting fibre-mixed soils as barrier applications in landfills. However, up to 10%fibre-mixed BC soil, all *k* values fell within the range of limiting values but 15% fibre-mixed soil samples exceeded the limiting value at lower overburden consolidation pressures. However, 15% fibre-mixed soil also met the liner criterion under 392.3 and 784.5 kPa overburden consolidation pressures.

TH-3665_186104109

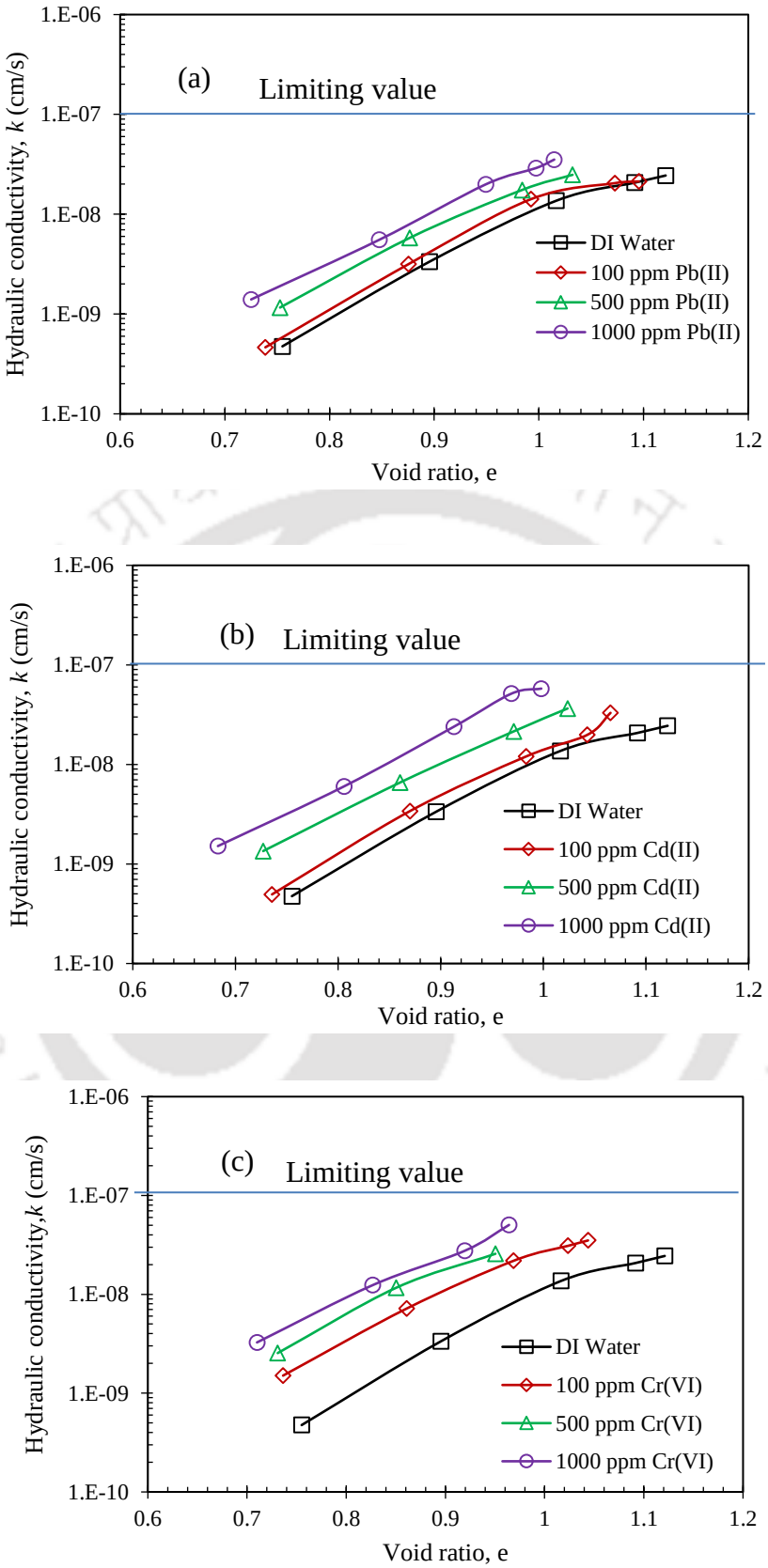

Fig. 6.24. Hydraulic conductivity vs void ratio plots for pure BC soil with various heavy metal permeant concentrations.

TH-3665_186104109

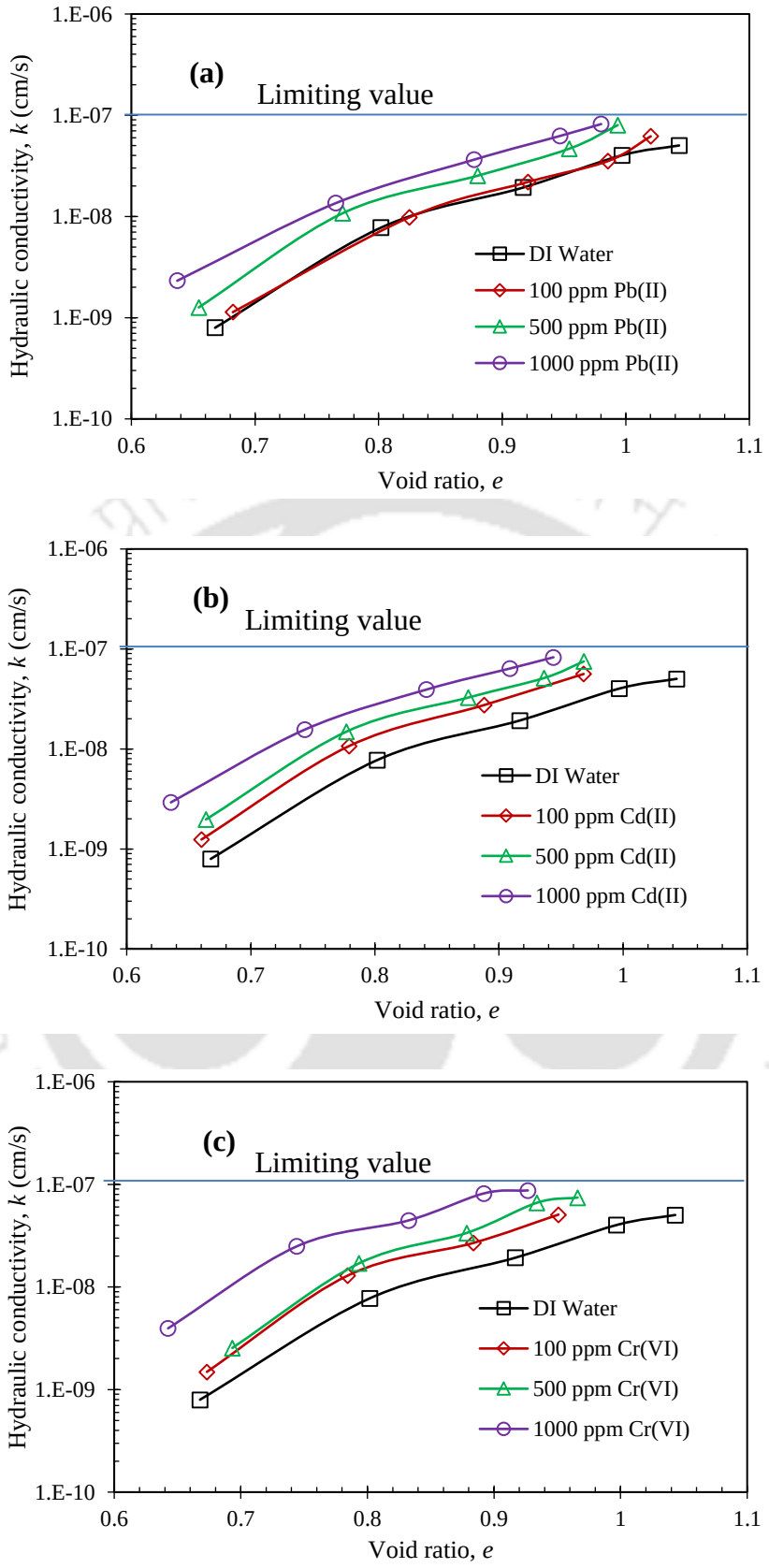

Fig. 6.25. Hydraulic conductivity vs void ratio plots for 5% fibre-mixed BC soil with various heavy metal permeant concentrations: (a) Lead; (b) Cadmium; (c) Hexavalent chromium.

TH-3665_186104109

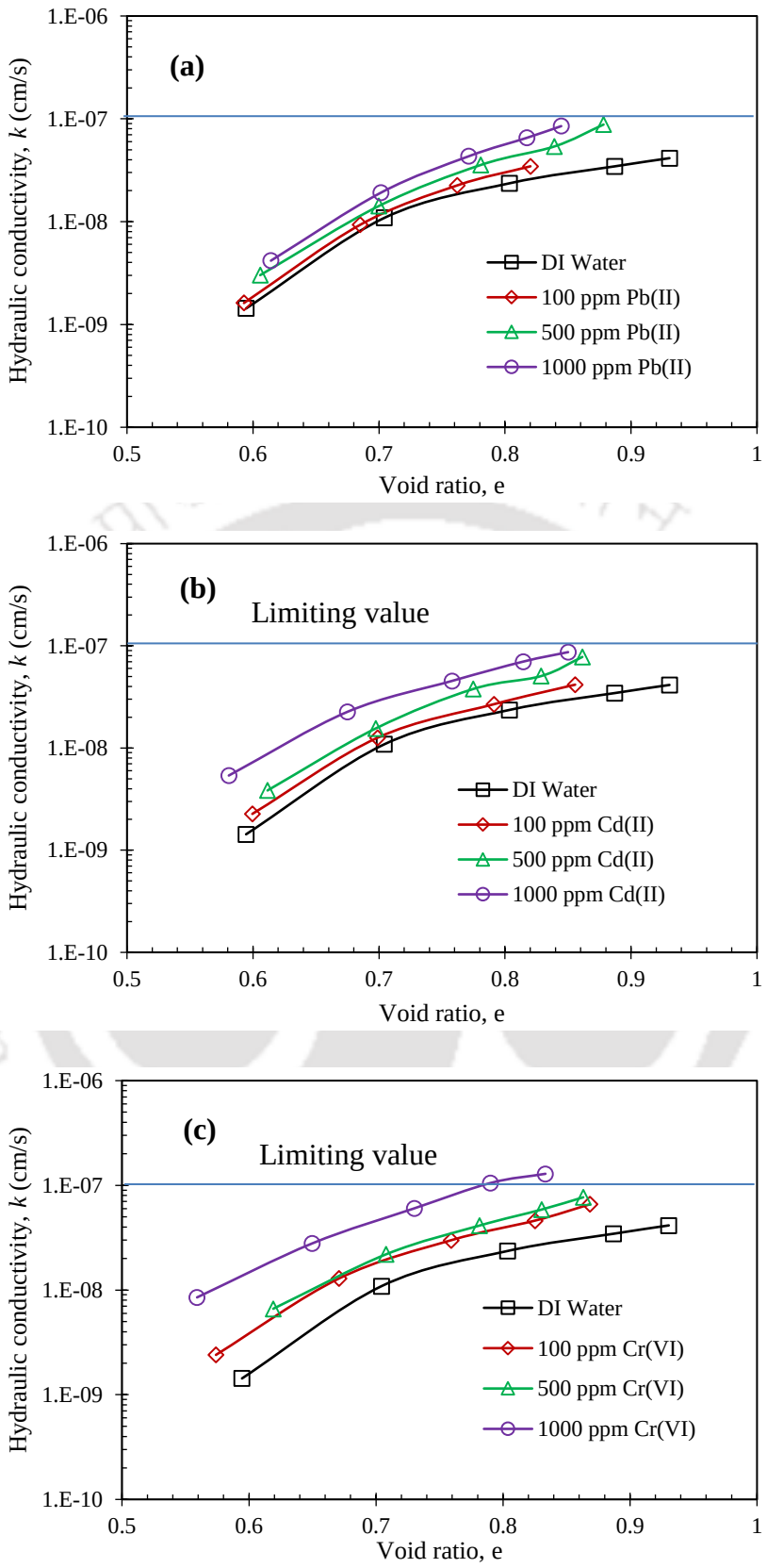

Fig. 6.26. Hydraulic conductivity vs void ratio plots for 10% fibre-mixed BC soil with various heavy metal permeant concentrations: (a) Lead; (b) Cadmium; (c) Hexavalent chromium.

TH-3665_186104109

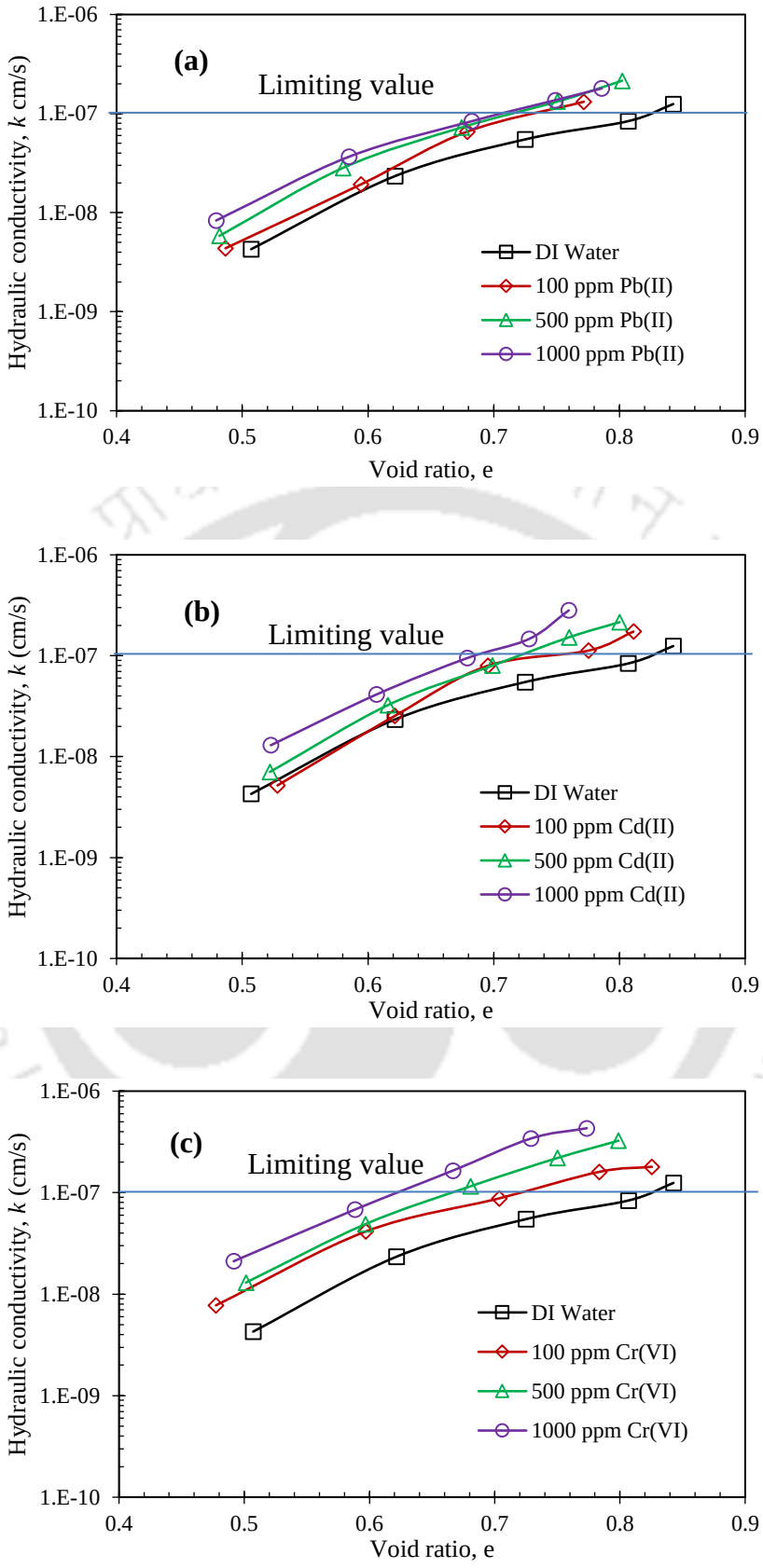

Fig. 6.27. Hydraulic conductivity vs void ratio plots for 15% fibre-mixed BC soil with various heavy metal permeant concentrations: (a) Lead; (b) Cadmium; (c) Hexavalent chromium.

TH-3665_186104109

Table 6.12. Hydraulic conductivity values of fibre-mixed BC soil (at e = 0.75) under various heavy metal permeants

Tire fibre content (%)	Metal concentration (ppm)	Hydraulic conductivity (cm/s)		
		Pb(II)	Cd(II)	Cr(VI)
0	0 (DI Water)	4.93×10^{-10}	4.93×10^{-10}	4.93×10^{-10}
	100	5.68×10^{-10}	6.85×10^{-10}	2.19×10^{-9}
	500	1.19×10^{-9}	1.88×10^{-9}	3.10×10^{-9}
	1000	1.84×10^{-9}	3.44×10^{-9}	4.90×10^{-9}
5	0 (DI Water)	2.83×10^{-9}	2.83×10^{-9}	2.83×10^{-9}
	100	3.23×10^{-9}	5.32×10^{-9}	5.63×10^{-9}
	500	5.99×10^{-9}	6.99×10^{-9}	7.23×10^{-9}
	1000	9.53×10^{-9}	1.14×10^{-8}	1.83×10^{-8}
10	0 (DI Water)	5.00×10^{-9}	5.00×10^{-9}	5.00×10^{-9}
	100	1.76×10^{-8}	1.93×10^{-8}	2.11×10^{-8}
	500	2.44×10^{-8}	2.58×10^{-8}	7.50×10^{-8}
	1000	3.36×10^{-8}	5.00×10^{-8}	6.87×10^{-8}
15	0 (DI Water)	6.37×10^{-8}	6.37×10^{-8}	6.37×10^{-8}
	100	9.48×10^{-8}	9.96×10^{-8}	1.15×10^{-7}
	500	1.36×10^{-7}	3.37×10^{-7}	2.76×10^{-7}
	1000	1.38×10^{-7}	2.09×10^{-7}	4.20×10^{-7}

TH-3665_186104109

6.2.10. FESEM behaviour

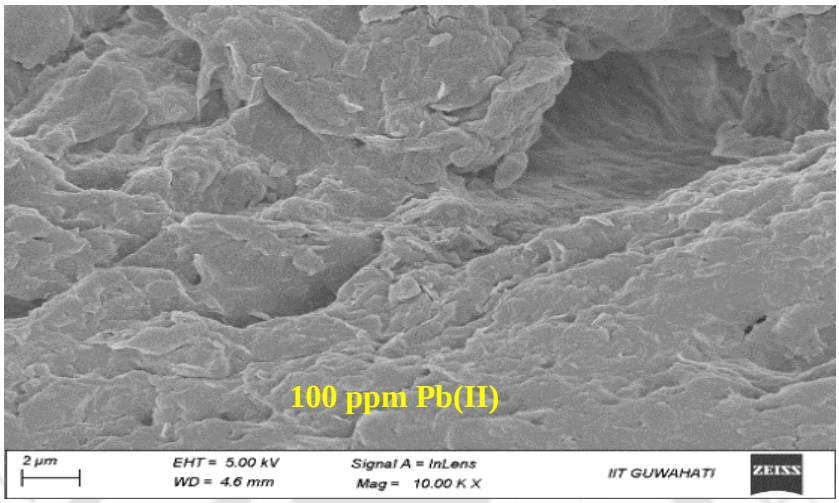

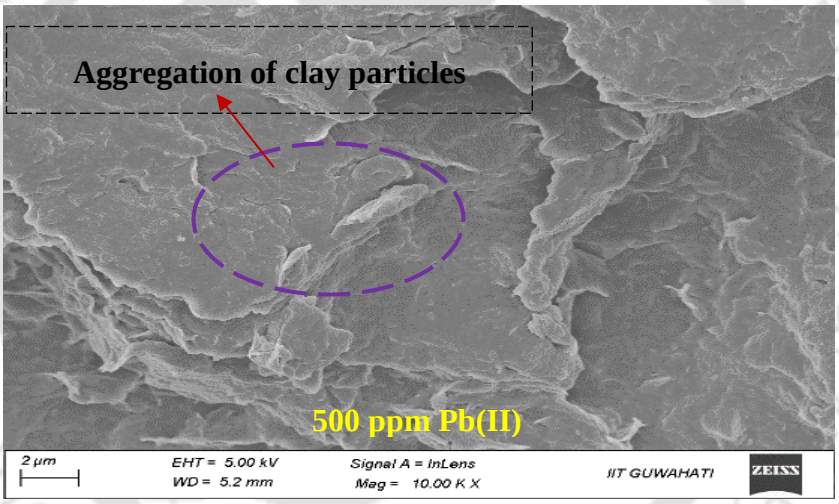

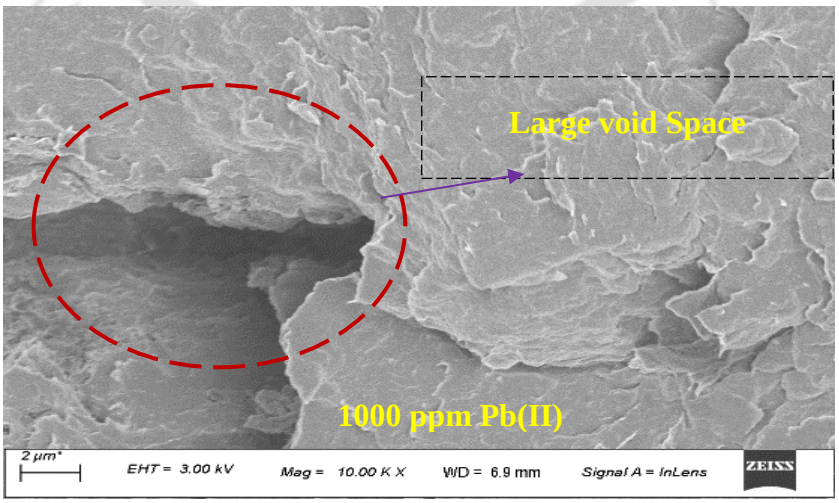

TH-3665_186104109

Fig. 6.28 FESEM images of BC soil with lead permeant concentrations.

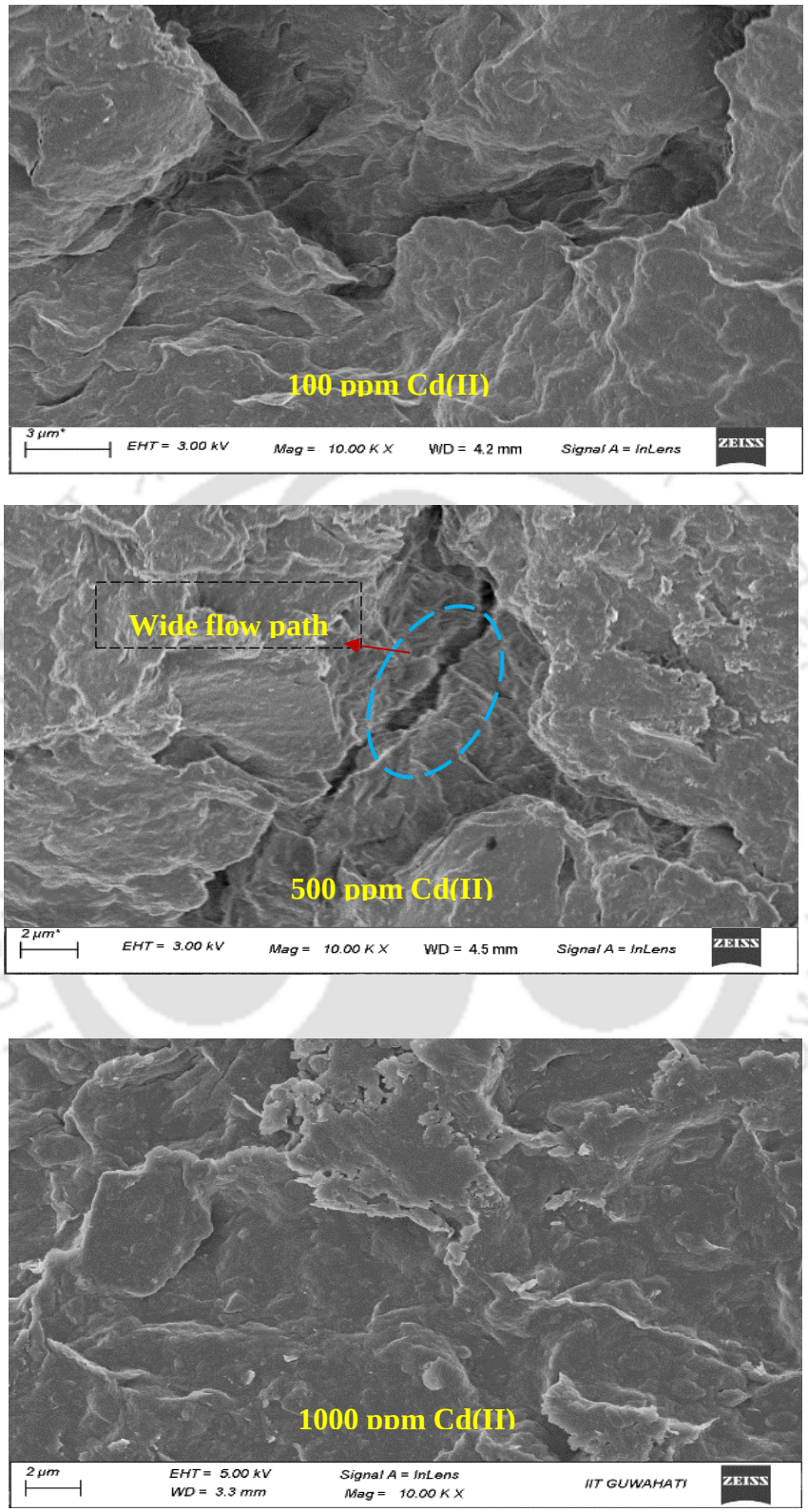

Fig. 6.29 FESEM images of BC soil with cadmium permeant concentrations.

TH-3665_186104109

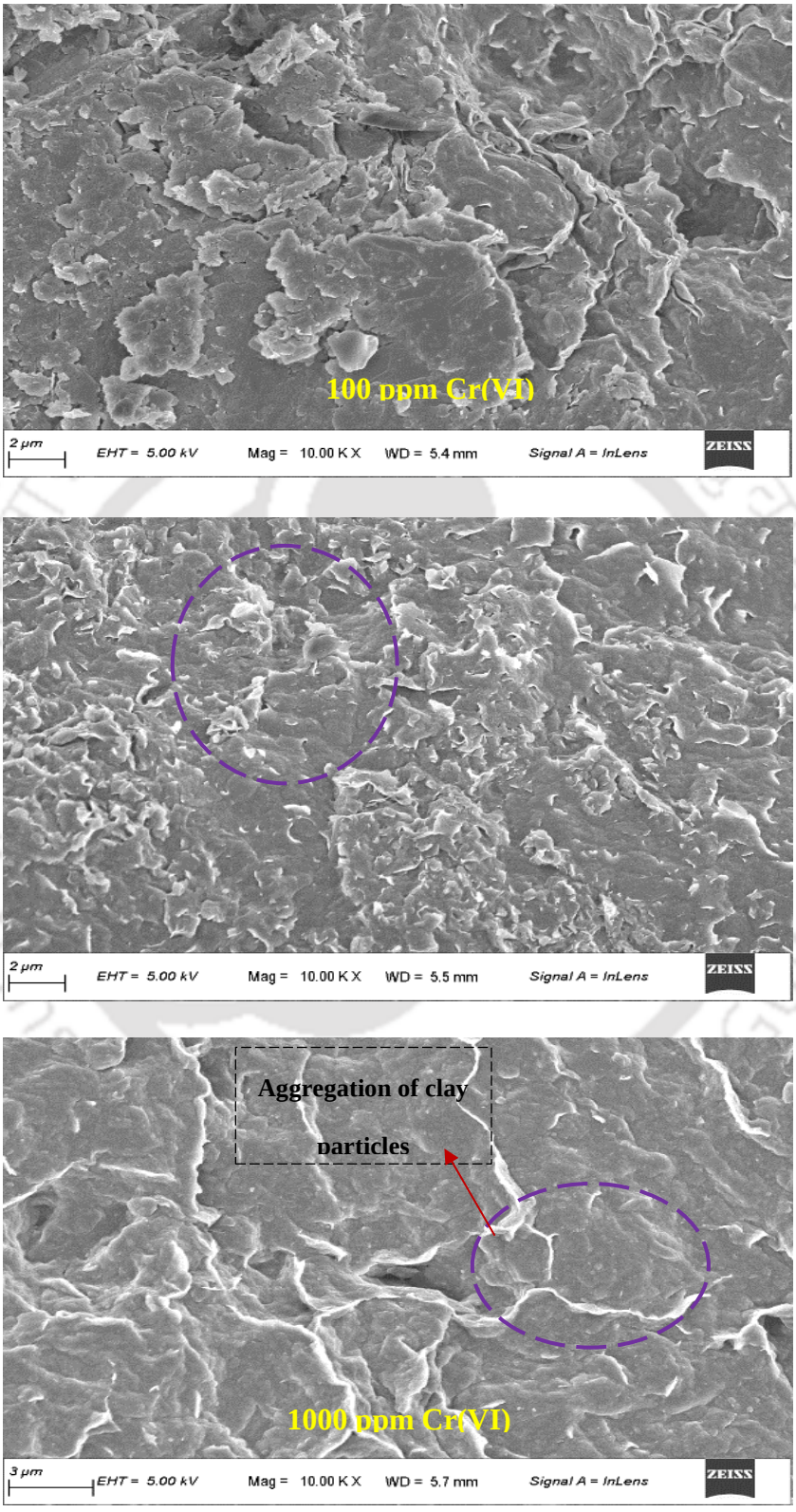

Fig. 6.30 FESEM images of BC soil with hexavalent chromium permeant concentrations.

TH-3665_186104109

The FESEM investigation was performed on BC soil samples that were saturated with various pore permeants and subjected to an overburden pressure of up to 784.5 kPa. Figures 6.28 to 6.30 illustrate the FESEM images of BC soil with lead, cadmium, and hexavalent chromium permeants; all images were captured at a magnification of 10,000 using the Sigma 300 field emission scanning electron microscope. As represented in Figs. 6.28 to 6.30, the interlayer spacing between clay particles was larger with lower heavy metal permeants (especially with lead and cadmium) than with higher concentration heavy metal permeants. However, it was noteworthy that greater repulsive forces were associated with these large interlayer spacings (Madsen and Vonmoos, 1989). In dry environments, the negative charges on the surfaces of clay particles can be neutralized by exchangeable Na^+ ions. After permeation with metal permeants, these Na^+ ions are replaced by heavy metal ions such as Pb^{2+}, Cd^{2+}, and Cr^{6+} due to the cation exchange process, resulting in a changing of soil fabric arrangements. Thereby, flocculated fabrics formed due to higher concentrations from dispersed conditions, leading to the formation of wide flow channels. Also, from Figs. 6.28-6.30, it was recognized that clay particles came together and formed larger aggregations for the higher concentration of metal permeants. Li et al. (2015) obtained this type of observation after passing a lead nitrate solution through Chinese clay. In addition, substantial void spaces were detected at higher concentrations, which led to an increase in *k* values.

6.2.11. Unconfined compressive strength (UCS)

The plot in Figs 6.31 to 6.34 illustrates the stress-strain behavior of all fibre-mixed BC soil in the presence of lead, cadmium, and hexavalent chromium metal permeants at 100, 500, and 1000 ppm concentrations. As per ASTM D2166 (2013), the UCS value of BC soil would be considered as peak load or load value corresponding to 15% of axial strain, whichever occurred first during the test. The plots show that the UCS values were decreased with the rise in fibre content from 0 to 15%. The discussion regarding UCS behaviour of clay-tire fibre interaction was done in Chapter 4. However, the focus of this chapter is the influence of metal type and concentration on each soil sample. Irrespective of metal type and concentration, all BC soil samples displayed steep stress-strain curves compared to fibre-mixed BC soil samples. From Fig. 6.13, it could be seen that the UCS value of BC soil with DI water was 594.2 kPa, which was slightly increased to 600.1, 637.9, and 643.3 kPa for 100, 500, and 1000 ppm lead permeants, respectively. This increase in UCS values of BCC

TH-3665_186104109

was around 1.0%, 7.3%, and 8.3% for the same order of lead permeant concentrations. This rise in the UCS value due to an increase in the concentration can be attributed to the reduction in the DDL thickness due to the presence of salt solution. As the salt concentration increases, the DDL thickness reduces, and it allows the particles to move to a closer spacing, thereby increasing the point-to-point contact between the soil particles. This leads to an increase in the effective or contact stress and formation of the flocculated structure, which increases the UCS value (Rout and Singh, 2020; Ray et al., 2022(a)). However, OMC-MDD conditions also contribute to this marginal variation in UCS values of BC soil. Because, in this study, all permeated samples (0, 5, 10, and 15%) were prepared at OMC and MDD conditions of DI water of respective composition. The peak strengths and peak strain values are also shown in Tables 6.13 and 6.14, and an insignificant difference was seen in peak strengths and corresponding peak strains for all lead permeants. As demonstrated in Table 6.13, peak strength values for cadmium permeants also significantly elevated with an increase in concentration from 100 to 1000 ppm. Here, the peak strength values of cadmium permeants were reported as 595.9, 613.1, and 626.7 kPa for 100, 500, and 1000 ppm concentrations, respectively. The strength enhancement percentage was nearly about 0.3, 3.2, and 5.5%, which was very marginal for the same order of concentrations. However, as seen in Table 6.13, cadmium permeants exhibited slightly lower peak strength than lead permeants. However, a reverse trend in peak strength values of BC soil was observed with hexavalent chromium permeants. The UCS values witnessed a small decline as the concentration of hexavalent chromium permeants increased from 0 (DI water) to 1000 ppm, as illustrated in Table 6.13. There was not much change in peak strain values of pure BC soil with respect to all heavy metal permeants, as shown in Table 6.14. However, this kind of trend was observed with inorganic salt concentrations as well. All fibre-mixed BC soil samples also exhibited a similar kind of trend i.e. enhanced strength values with lead and cadmium permeants and lower strength values with hexavalent chromium solutions irrespective of fibre content, as shown in Table 6.13. For example, with 5% fibre-mixed BC soil the UCS value was increased from 370.2 (DI water) to 393.7,416.1, and 432.2 kPa with 100, 500, and 1000 ppm lead solutions, respectively. This hike was around 6.3, 12.4, and 16.7% for the similar order of lead permeants, respectively, in comparison to DI water. This hike was around 12.4% with 1000 ppm cadmium concentration for the same fibre content, which is relatively less than lead permeant.

TH-3665_186104109

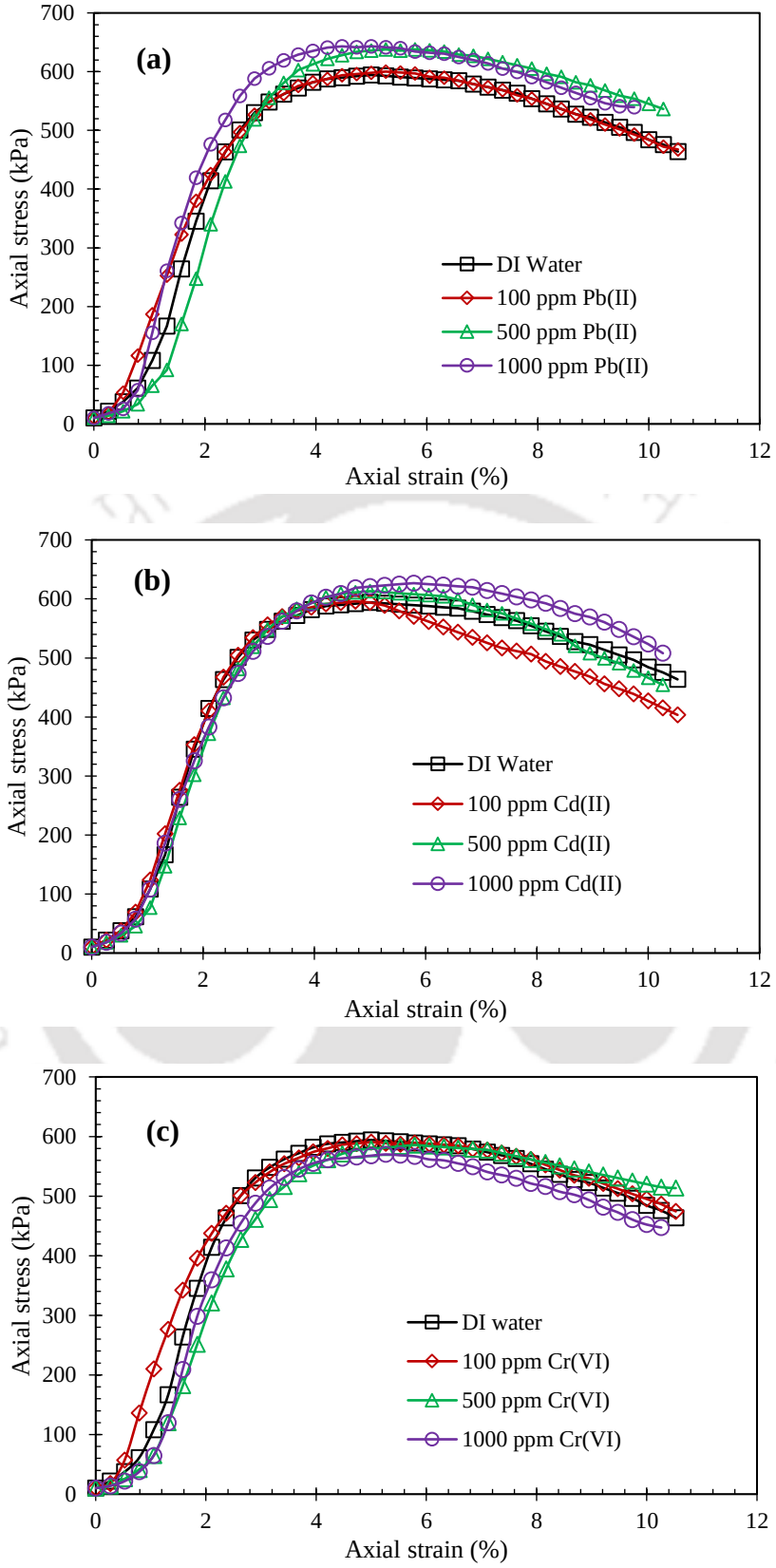

Fig. 6.31. Axial stress vs axial strain curves for pure BC soil with various heavy metal permeant concentrations: (a) Lead; (b) Cadmium; (c) Hexavalent chromium.

TH-3665_186104109

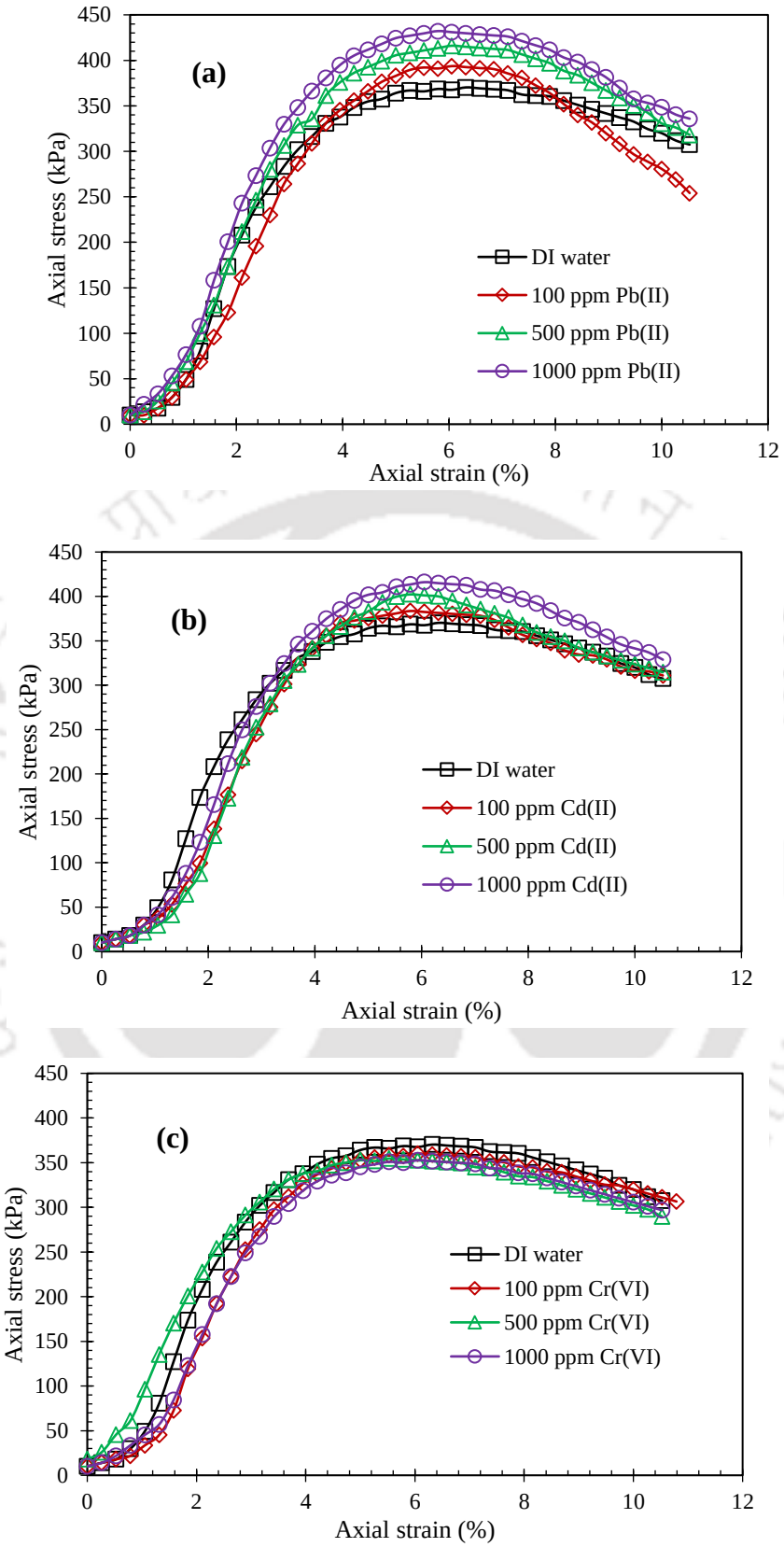

Fig. 6.32. Axial stress vs axial strain curves for 5% fibre-mixed BC soil with various heavy metal permeant concentrations: (a) Lead; (b) Cadmium; (c) Hexavalent chromium.

TH-3665_186104109

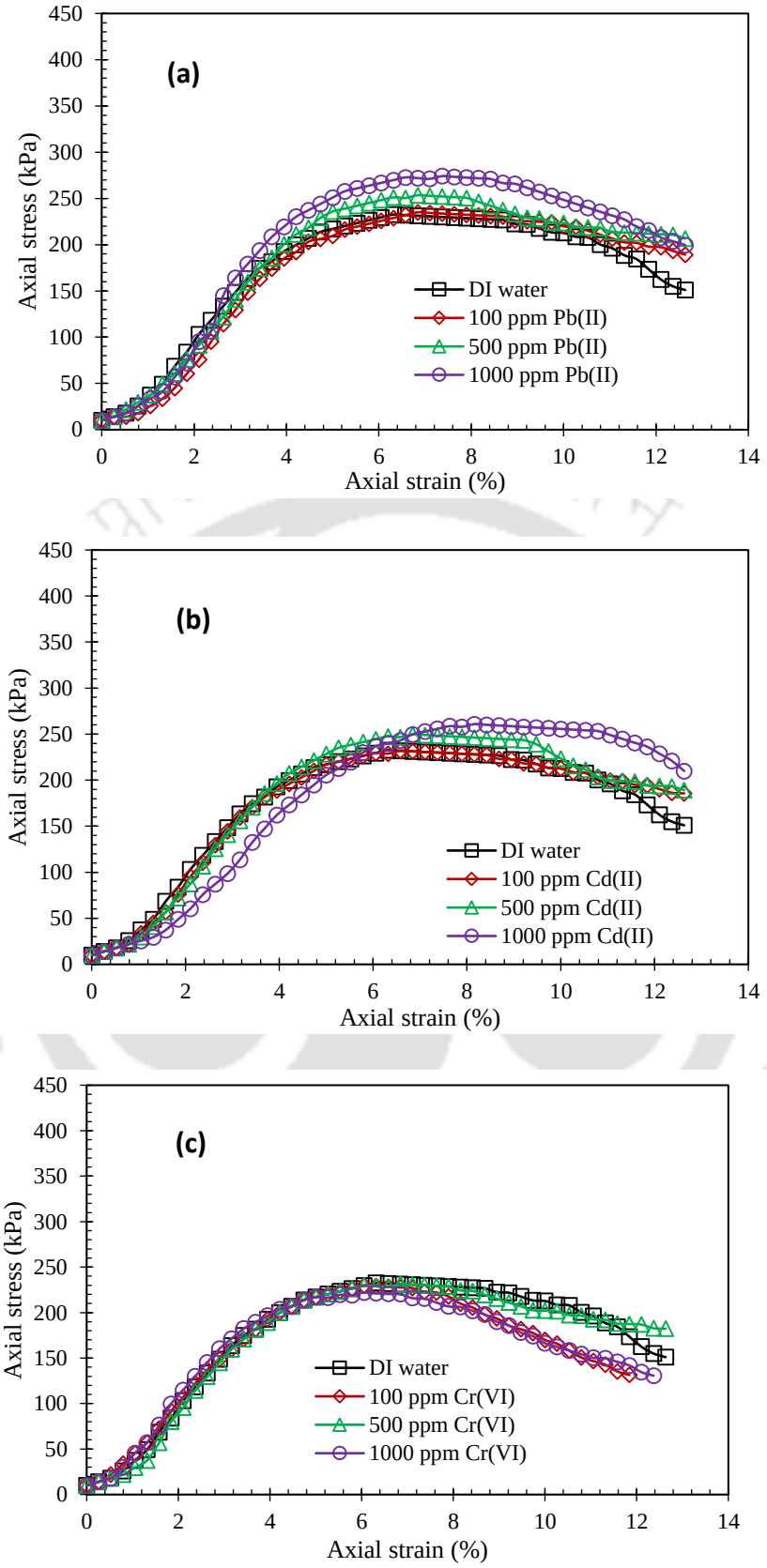

Fig. 6.33. Axial stress vs axial strain curves for 10% fibre-mixed BC soil with various heavy metal permeant concentrations: (a) Lead; (b) Cadmium; (c) Hexavalent chromium.

TH-3665_186104109

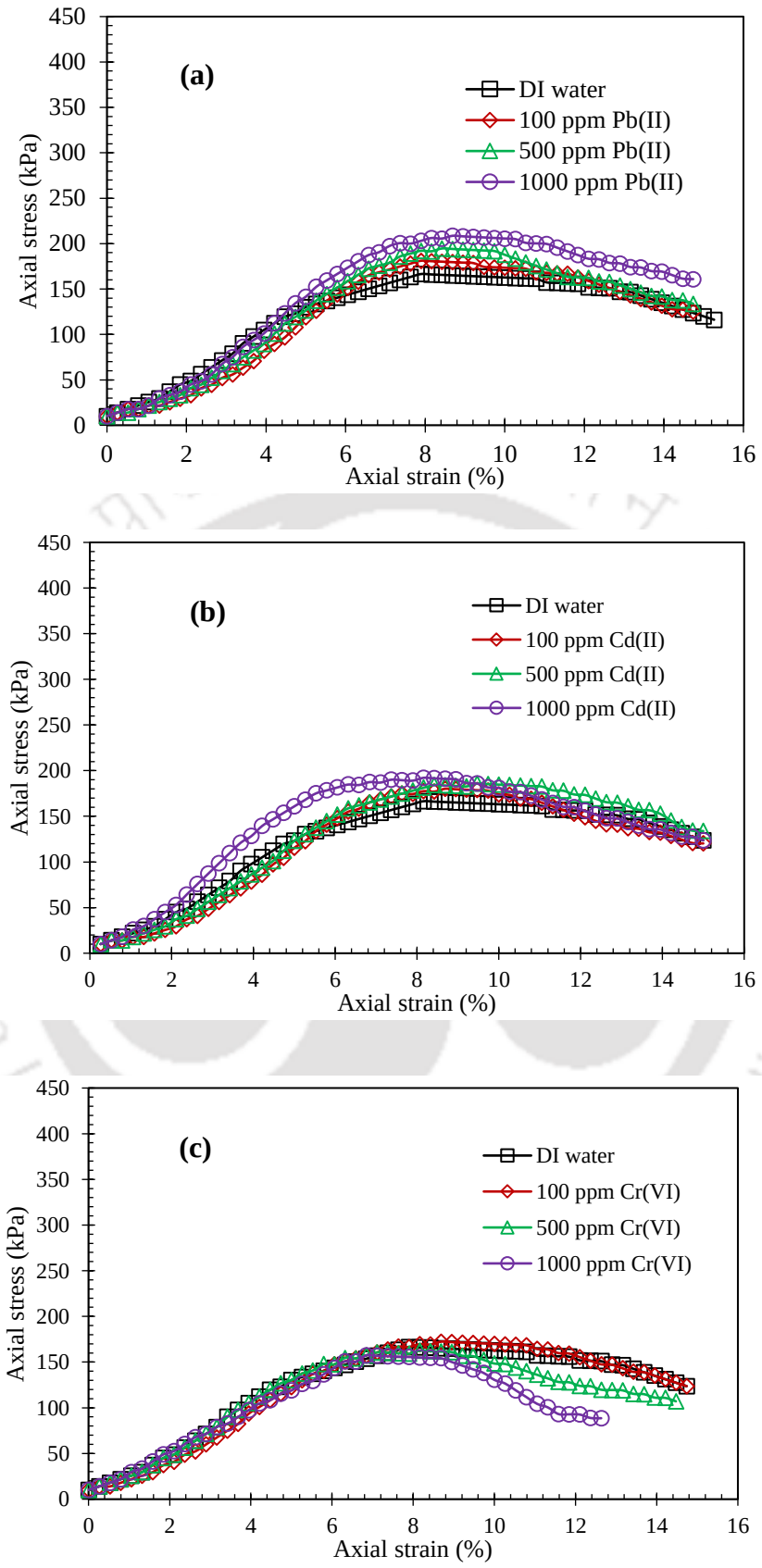

Fig. 6.34. Axial stress vs axial strain curves for 15% fibre-mixed BC soil with various heavy metal permeant concentrations: (a) Lead; (b) Cadmium; (c) Hexavalent chromium.

TH-3665_186104109

Table 6.13. Peak strength values of fibre-mixed BC soil with various heavy metal concentrations

Tire fibre content (%)	Metal concentration (ppm)	Peak strength (kPa)		
		Pb (II)	Cd (II)	Cr(VI)
0	0 (DI water)	594.2	594.2	594.2
	100	600.1	595.9	590.5
	500	637.9	613.1	585.6
	1000	643.3	626.7	570.0
5	0 (DI water)	370.2	370.2	370.2
	100	393.7	383.6	360.1
	500	416.1	402.3	354.6
	1000	432.2	416.1	352.6
10	0 (DI water)	232.6	232.6	232.6
	100	235.0	232.0	229.5
	500	253.5	249.8	231.3
	1000	274.1	260.9	222.1
15	0 (DI water)	166.5	166.5	166.5
	100	181.1	180.1	172.3
	500	194.7	185.7	162.4
	1000	208.6	192.1	157.3

TH-3665_186104109

Table 6.14. Peak strain values of fibre-mixed BC soil with various heavy metal concentrations

Tire fibre content (%)	Metal concentration (ppm)	Peak strain (%)		
		Pb (II)	Cd (II)	Cr(VI)
0	0 (DI water)	5.0	5.0	5.0
	100	5.3	4.7	5.3
	500	5.8	5.0	5.8
	1000	5.0	5.8	5.3
5	0 (DI water)	6.3	6.3	6.3
	100	6.0	5.8	6.0
	500	6.0	5.8	5.5
	1000	5.8	6.0	6.0
10	0 (DI water)	6.3	6.3	6.3
	100	6.8	6.6	6.0
	500	6.8	6.8	6.8
	1000	7.4	8.1	6.0
15	0 (DI water)	7.9	7.9	7.9
	100	7.9	8.4	8.7
	500	8.4	9.2	8.1
	1000	8.7	7.9	6.8

TH-3665_186104109

For 10% fibre-mixed soils, the hike in UCS values was around 17.8 and 12.2% with 1000 ppm lead and cadmium concentrations, respectively, compared with DI water. Similarly, for 15% fibre-mixed BC soil, this hike in UCS values was around 21.3 and 15.4% with 1000 ppm lead and cadmium concentrations, respectively. However, with chromium permeants, a slight reduction in UCS values was observed for all fibre-mixed soils. At 1000 ppm hexavalent chromium concentration, the percentage reduction in UCS values was about 4.8, 4.5, and 5.5% with 5, 10, and 15% fibre-mixed BC soil samples, respectively, compared to DI water. However, not much variation in peak strain values was observed for all fibre-mixed BC soil samples. Therefore, based on experimental UCS results, no significant difference was observed with metal permeants. However, for fibre-mixed samples slight increment in strength was observed with 1000 ppm lead concentrations. Apart from 15% fibre-mixed BC soil samples, all exhibited limiting strength (200 kPa) under permeation of various heavy metal concentrations.

6.3. Summary

This research adopted BC soil as a clay liner material and evaluated its hydromechanical properties under the hazardous heavy metal (lead, cadmium, and hexavalent chromium) permeants at three concentrations ranging from 100 to 1000 ppm. Several laboratory experiments were performed on BC soil to examine its consistency limits, FSI, time-swell relationship, SPr and SPo, hydraulic conductivity, and UCS behaviour under heavy metals environment. However, the swell-shrink phenomenon of BC soil leads to desiccation cracking, which results in a significant rise in hydraulic conductivity, threatening the liner's stability. Therefore, waste tire fibres (5, 10, and 15%) are used as reinforcement materials to control the shrinkage phenomenon. Therefore, the addition of tire fibre to BC soil may alter the hydromechanical properties of liner material. For this reason, all fibre-mixed soil compositions were tested under heavy metal permeants. From these tests, the following significant outcomes were observed;

- Atterberg limits and free swell index of BC soil were reduced slightly for 100 ppm lead, cadmium, and hexavalent chromium permeants. However, this reduction was significant for a rise in the concentrations of metals from 100 to 1000 ppm.
- Time-swelling correlations confirmed that the maximum swelling tendency took place during the primary swelling stage. Moreover, this tendency to swell diminished throughout the primary swelling stage as metal concentrations increased.

TH-3665_186104109

- SPr's and SPo's of BCC were dropped considerably at high metal concentrations. However, this drop in SPr's and SPo's was marginally more for cadmium permeants than lead permeants. For 1000 ppm lead, cadmium, and hexavalent chromium permeants, the fall in SPr values was approximately 19.2, 24.0, and 29.8%, respectively. This fall was about 27.4, 32.0, and 43.2% for SPo values for similar metal levels in the same sequence. In addition, the RH model was established to gain a better understanding of observed swelling in the laboratory, and the results demonstrated a strong correlation between anticipated and measured swelling tendencies.
- An upsurge in coefficient of consolidation (c_v) values of BC soil was observed with the hike in concentration of heavy metal permeants. At 1000 ppm concentration, high c_v values were observed with hexavalent chromium permeant followed by cadmium and lead permeants. Therefore, low t_{90} values were recorded with hexavalent chromium followed by cadmium and lead permeants.
- A slight reduction in void ratios of BC soil was noticed with the hike in the concentration of heavy metal permeants. Relatively low compression indices were reported with hexavalent chromium followed by cadmium and lead permeants.
- Higher concentrations of heavy metals significantly altered BC soil's hydraulic conductivity (k). At 1000 ppm concentration, the upsurge in k values for lead, cadmium, and hexavalent chromium permeants was nearly 3.7, 7.0, and 9.9 times greater than DI water at a void ratio of 0.75.
- From UCS experiments, the peak strengths of BCC samples were enhanced slightly for a rise in the concentration of both heavy metal permeants. These values were reported to be somewhat lower for cadmium permeants than for lead permeants. However, the enhancement percentage in UCS values was about 8.3 and 5.5% for 1000 ppm lead and cadmium permeants, respectively. However, a slight reduction in UCS values was observed at higher concentrations for hexavalent chromium permeants than DI water.
- The swelling heights of BC soil were reduced significantly with the addition of fibre content. Also, these swelling heights of all fibre-mixed BCS were measured in the presence of lead, cadmium, and hexavalent chromium concentrations. A significant reduction in swelling heights was hexavalent chromium permeant followed by cadmium and lead concentrations for all fibre-mixed samples.

TH-3665_186104109

- The SPr and SPo values of BCS were reduced with an increment in tire-fibre content. However, these SPr and SPo values of fibre-mixed soils were further decreased significantly at a greater concentration (1000 ppm) of metal permeants.
- At 784.5 kPa consolidation pressure, the percentage reduction in the t_{90} values of 5% fibre-mixed BCS was 65.6, 75.8, and 82.8% with 1000 ppm lead, cadmium and hexavalent chromium permeants, respectively, compared to DI water. However, a similar trend was observed for the remaining compositions of fibre-mixed BCS.
- Higher hydraulic conductivity values were reported with hexavalent chromium permeants for all fibre-mixed samples compared with cadmium and lead permeants. For 15% fibre-mixed BC soil, hydraulic conductivity exceeded the limiting value for all overburden consolidation pressures except with 392.3 and 784.5 kPa consolidation pressures. The remaining (5 and 10%) are within the limiting criterion, including all permeations impact.
- Not much change in UCS values of fibre-mixed BC soil samples was observed under various heavy metal permeations. However, a slight hike in UCS values was observed with lead permeant, followed by cadmium at 1000 ppm concentrations. A negligible reduction in UCS values was observed with hexavalent chromium solutions with all fibre-mixed samples.

TH-3665_186104109

CHAPTER 7

INFLUENCE OF SYNTHETIC LEACHATES ON THE BEHAVIOUR OF FIBRE-MIXED BC SOIL

7.1. Introduction

Leachates consist of combination of various inorganic salts, heavy metals, organic salts, and other polymers, which would be directly intact with barrier material in a landfill system. The constituents in leachates would vary depending upon the sources of waste dumping in landfills. The numerous categories of waste include municipal solid waste (MSW) leachate, agricultural leachate, sewage sludge leachate, paper mill sludge leachate, and industrial leachate, including fly ash leachate and mining leachate. These leachates would threaten the barrier material purpose due to the various chemical constituents contained in leachates. Therefore, it is essential to study the engineering behaviour of barrier material under various leachates to understand its integrity.

Few studies of the past (Ruhl and Daniel, 1997; Shan et al., 2002; Pivato and Raga, 2006; Bouazza et al., 2013; Xue and Zhang, 2014; Chen et al., 2018; Ray et al., 2021) which studied the behaviour of leachates on liner material's adsorption and hydraulic properties, has already been discussed in Chapter 2. In this study, two synthetic leachates such as synthetic MSW leachate (SML) and synthetic fly as leachate (SFL) were selected as testing leachates due to their prominence and impact in landfills (Li et al., 2015; Ray et al., 2021(a)&2022(b)). Most of the past studies focused to study the influence of these leachates on the beahviour of bentonites, since bentonite has excellent adsorption and swelling capacities. So far no study has been conducted to investigate BC soil engineering behaviour under the permeation of synthetic leachates. Therefore, the primary objective of this chapter is to investigate the impact of two synthetic leachates (SML and SFL) on index properties such as free swell index and Atterberg's limits and engineering properties such as swelling tendency, consolidation characteristics, compressibility, hydraulic conductivity, and shear strength of BC soil.

To overcome the shrinkage problem, this study proposed waste-fibre mixed BC soil as a modified barrier material instead of bentonite-fibre composites and sand-bentonites. Also,

TH-3665_186104109

based on previous chapters and their results, it was evident that the consideration of salts and heavy metals influence is unavoidable with all fibre-mixed BC soil proportions, irrespective of fibre content. Hence, it is important to examine the fibre-mixed BC soil behaviour under synthetic leachates permeation. Therefore, the secondary objective of this chapter is to examine the fibre-mixed BC soils' engineering behaviour under the influence of both SML and SFL permeations.

7.2. Test Result and Discussion

7.2.1. Leachates' influence on Atterberg limits

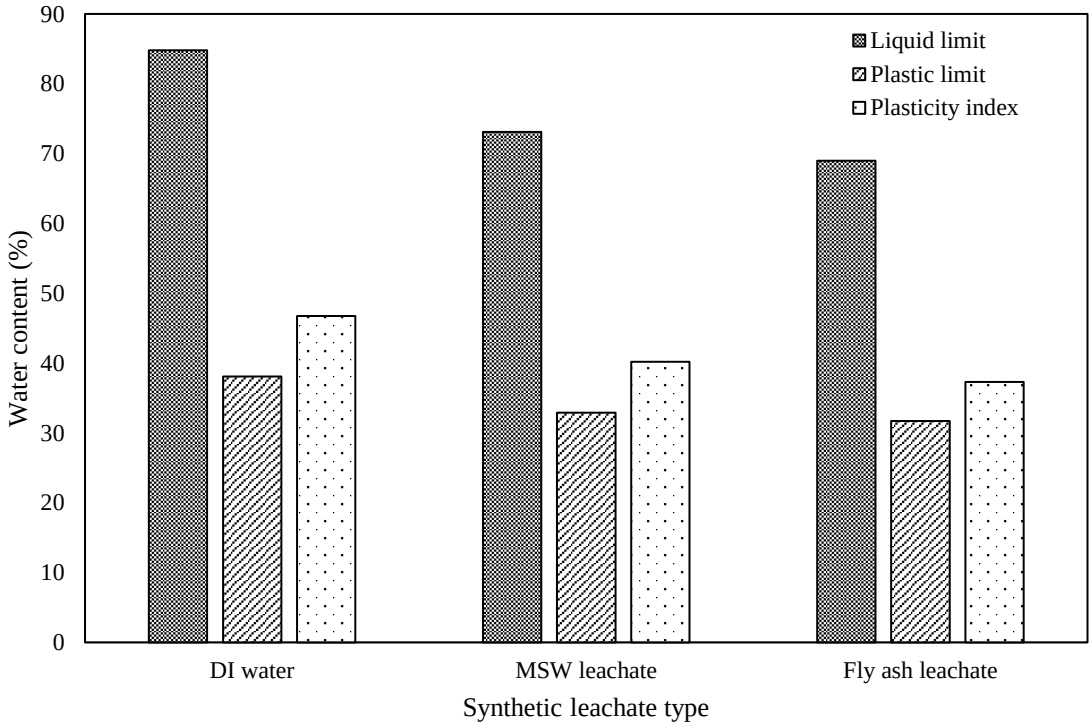

Fig. 7.1. Atterberg limits of BC soil with synthetic leachates.

The Atterberg limits of BC soil were tested in the presence of two synthetic leachates (MSW leachate and fly ash leachate) and the results are shown in Fig. 7.1. The liquid limit of BC soil was dropped from 84.8% (DI water) to 73.1 and 69.0% with synthetic MSW leachate (SML) and synthetic fly ash leachate (SFL), respectively. The percentage reduction in liquid limit was about 13.80 and 18.63% with both SML and SFL, respectively. The higher concentrations of heavy metals and salts in synthetic leachates cause the suppression of DDL thickness, causing a drop in liquid limit values. It was evident from the plot that SFL causes more reduction in liquid limit values than SML due to the presence of higher amount of heavy metals in SFL. The plot also shows that the plastic limit of BC soil also reduced with

TH-3665_186104109

both SML and SFL. The plastic limit value was dropped from 38.07% to 32.9 (13.58% reduction) and 31.7% (16.73% reduction) with both SML and SFL, respectively. Since the plasticity index is the difference between liquid limit and plastic limit, plasticity index values also followed a similar decline trend with leachates as shown in Fig. 7.1.

7.2.2. Influence of leachate on free swell index

The free swell index (FSI) results of BC soil with both SML and SFL are shown in Fig. 7.2. The FSI value of BC soil was reported as 196% with DI water, which reduced to 139 and 130% with both SML and SFL, respectively, as shown in Fig. 7.2. This reduction was about 29.08 and 33.67% with SML and SFL, respectively, compared to DI water. Amadi (2013) also observed similar declining trend in FSI values of lateritic-bentonite soil mix (90:10) with harsh leachate solution. The main reason attributed to this FSI reduction is the mobilization of DDL thickness due to metal ions present in leachate. The high ionic strength of SFL is attributed to more DDL suppression than SML, leading to a high reduction in FSI values.

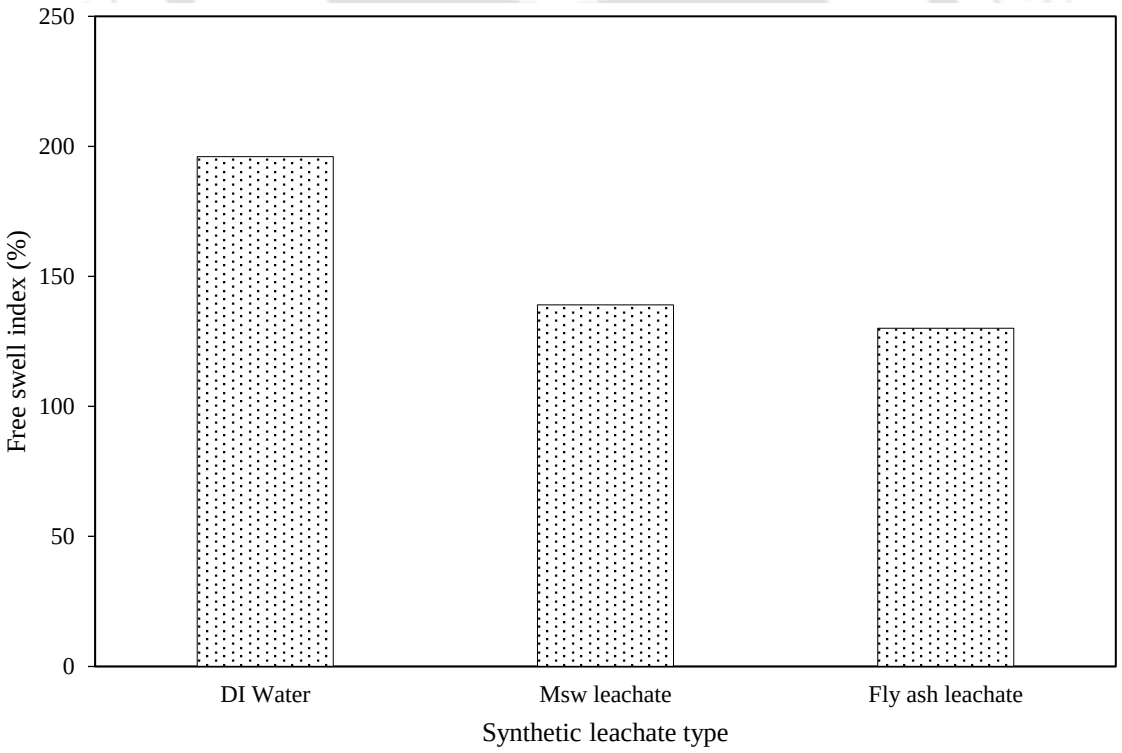

Figure 7.2. Free swell index of BC soil with synthetic leachates.

7.2.3. Influence of leachates on time-swelling relationship

The odometer swelling heights of BC soil under permeation of leachates with respect to time are shown in Fig. 7.3. Irrespective of leachate type all the swelling curves followed a typical

TH-3665_186104109

S shape pattern, which was observed with inorganic salts and heavy metals as well. The oedometer swelling was increased gradually at first, but it then increased rapidly and ultimately reached an asymptomatic level for all samples as displayed in Fig 7.3. Since swelling behaviour is one of the essential properties of barrier material, it is necessary to understand its tendency under leachate conditions. The swelling height of BC soil was reduced from 3.126 mm (DI water) to 1.894 and 1.530 mm with SML and SFL, respectively. A significant reduction in swelling heights was observed with both leachates. This reduction was about 39.4 and 51.5% with SML and SFL leachate permeations, respectively, compared to DI water. However, all soil samples were compacted at OMC and MDD conditions of DI water. Whenever water is used as a permeant, the soil particles in a compacted state start to expand due to the DDL phenomenon, leading to more swelling. On the other hand, leachate permeations cause the replacement of cations leading to shrinkage of the DDL layer causing less swelling height (Mersi and Olson; 1971; Dutta and Mishra, 2018). As explained in the previous chapters, this swelling phenomenon occurs in three stages such as initial, primary, and secondary swelling (Rao et al., 2006; Mishra et al., 2015). The time and amount of swelling that occurred in each stage were measured using tangent lines and reported in Table 7.1. For BC soil, it was clearly noticed that the time taken to complete primary swelling was decreased from 465 minutes (DI water) to 295 and 235 minutes with SML and SFL, respectively. Similarly, the amount of swelling that occurred in the primary swelling stage decreased from 15.45% to 9.80 and 7.22% with SML and SF, respectively, as shown in Table 7.1. The macro swelling phenomenon is attributed to initial swelling and the micro swelling phenomenon is attributed to primary and secondary swelling tendencies. However, irrespective of leachate type, the maximum amount of swelling occurred in the second stage (i.e. primary swelling stage) compared to the other two stages. Also, the time required to reach the asymptotic swelling value of BC soil is dependent on the type of leachate used. SFL exhibited a lower time to reach asymptotic value compared to SML. The other motive of this work is to understand the influence of these leachates on fibre-mixed BC soils. The time-swelling curves of 5, 10, and 15% fibre-mixed soil were depicted in Figs. 7.4 to 7.6. Similar to pure BC soil, these fibre-mixed soil samples also exhibited an S-type curve swelling tendency irrespective of fibre content and leachate type. Also, leachate permeates samples displayed lower swelling tendency compared to DI water, which is significant as shown in Figs. 7.4 to 7.6. For example, the swelling height of 5% fibre-mixed BC soil was decreased from 2.198 (DI water) to 1.176 and 1.030 mm with SML and SFL, respectively.

TH-3665_186104109

This reduction in swelling heights was about 46.50 and 53.14%, respectively. Similarly, this reduction in swelling heights was about 38.24 and 47.03%, respectively with 10% fibre-mixed BC soil for the same order of leachate permeants, respectively, compared to DI water. For 15% fibre-mixed BC soil, this reduction was about 32.04 and 43.65% with SML and SFL, respectively compared to DI water. However, SFL influence is more prominent compared to SML regarding swelling heights of all fibre-mixed samples. Also, the time and percentage of swelling that occurred in three swelling stages were reported in Table 7.1 for all fibre-mixed BC soils. The prominent swelling portion occurred in the primary swelling stage for all fibre-mixed BC soils irrespective of leachate type. All measured swelling values of fibre-mixed BC soils were predicted using the rectangular hyperbola (RH) model (Ye et al. 2015; Solatani et al., 2017) and displayed in Figs. 7.7 to 7.10. It was observed from these linear representations (Figs. 7.7 to 7.10) that the raise in slope with leachate permeants compared to DI water for all samples, indicating that reduction in residual swelling values with leachate permeants.

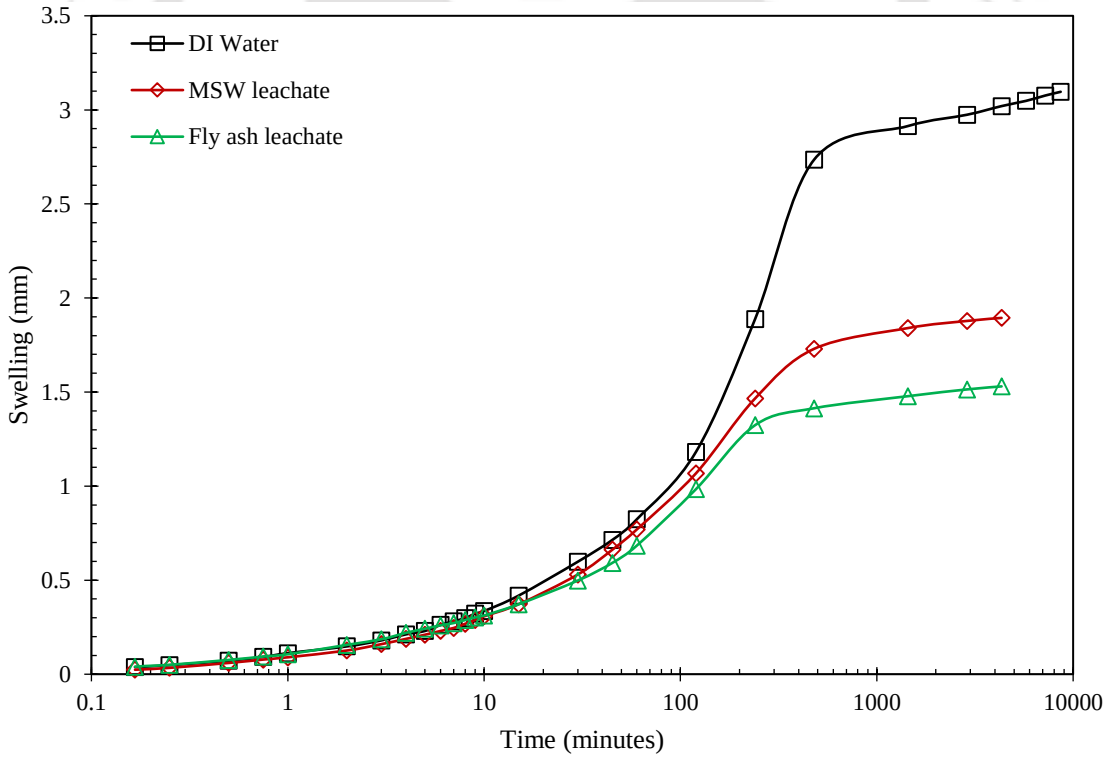

Fig. 7.3. Time-swell plot of pure BC soil under synthetic leachates' permeations.

TH-3665_186104109

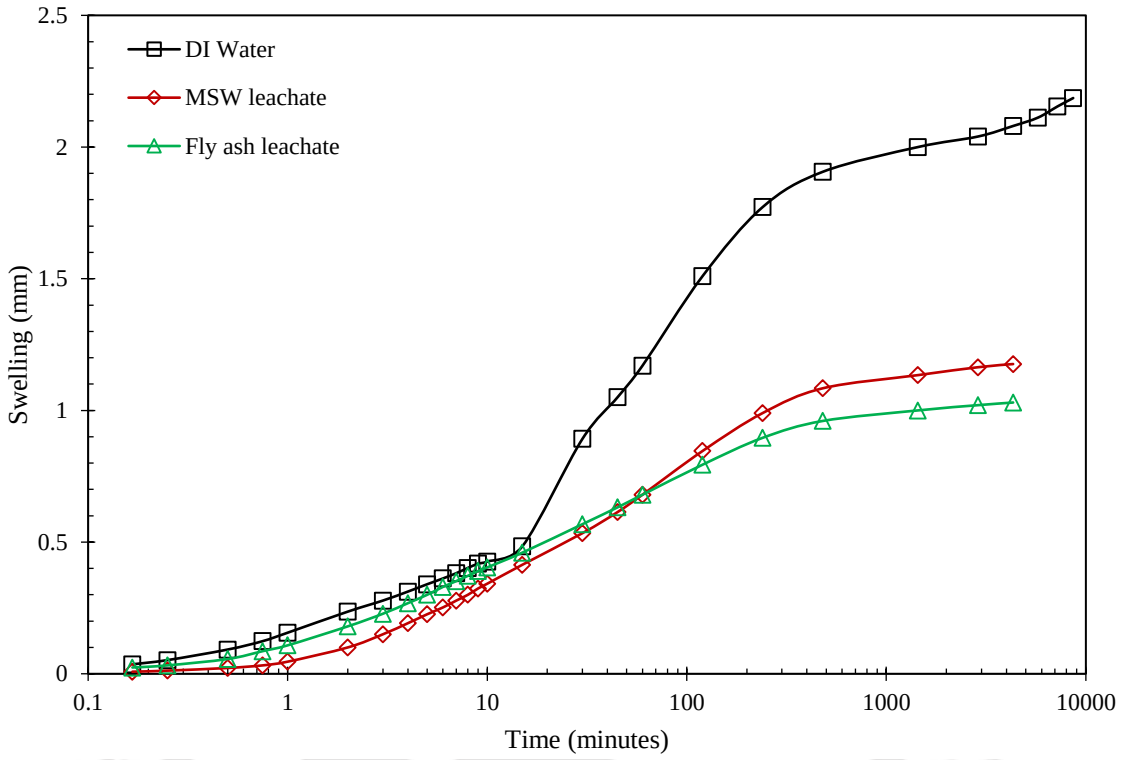

Fig. 7.4. Time-swell plot of 5% fibre-mixed BC soil under synthetic leachates' permeations.

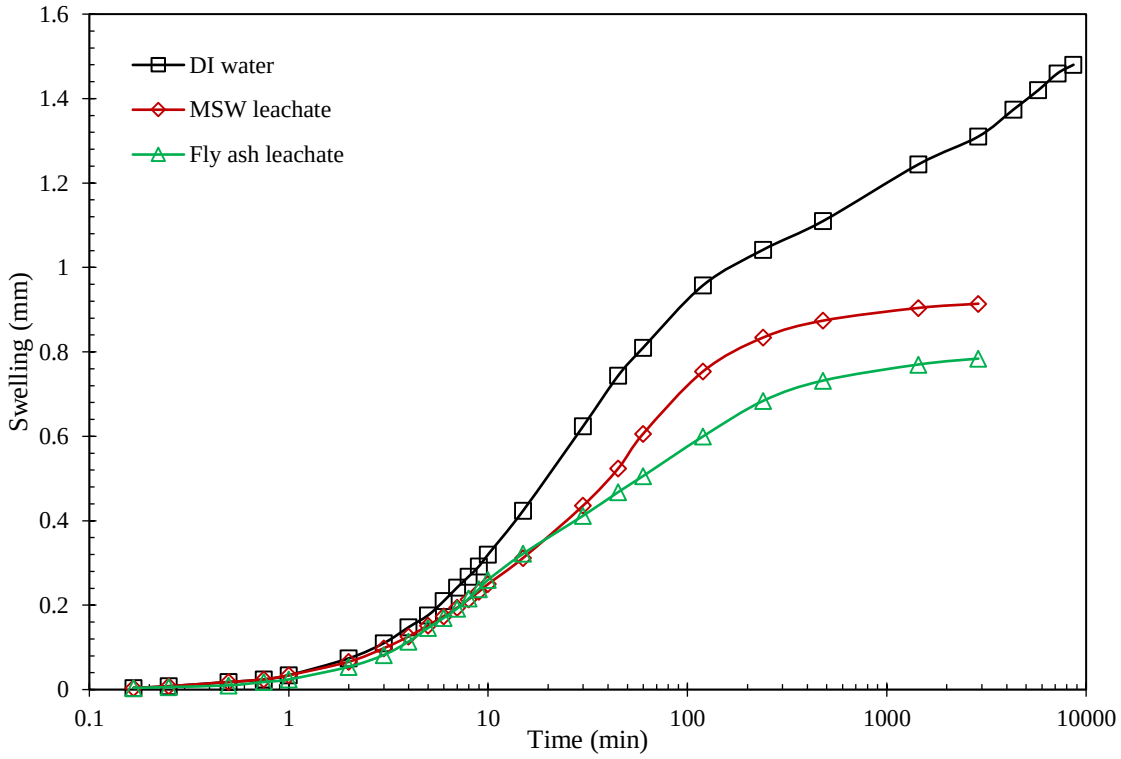

Fig. 7.5. Time-swell plot of 10% fibre-mixed BC soil under synthetic leachates' permeations.

TH-3665_186104109

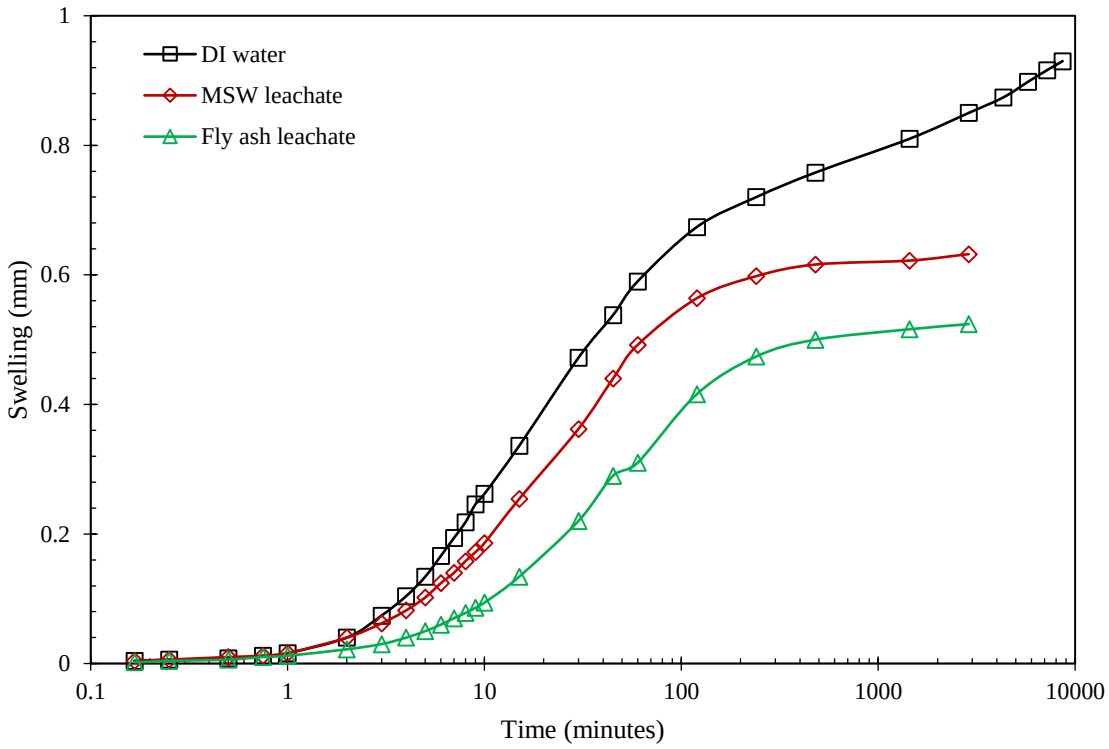

Fig. 7.6. Time-swell plot of 15% fibre-mixed BC soil under synthetic leachates' permeations.

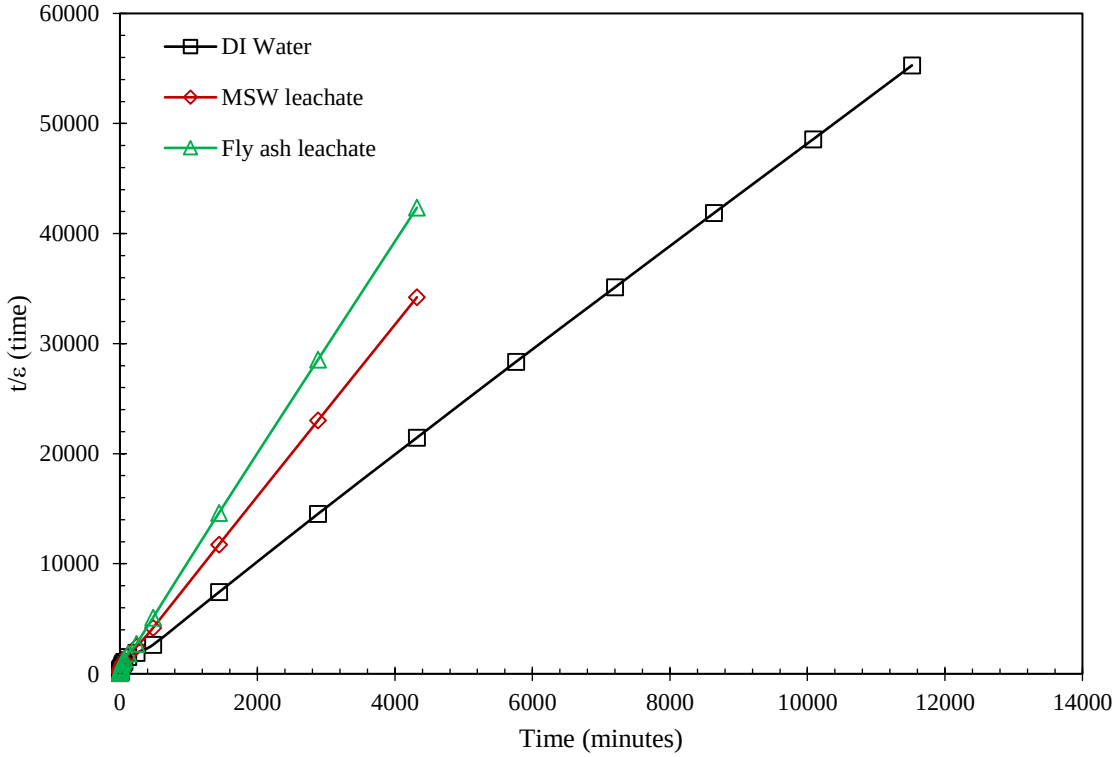

Fig. 7.7. Linearized representation of swelling data for BC soil with RH model permeated with leachates.

TH-3665_186104109

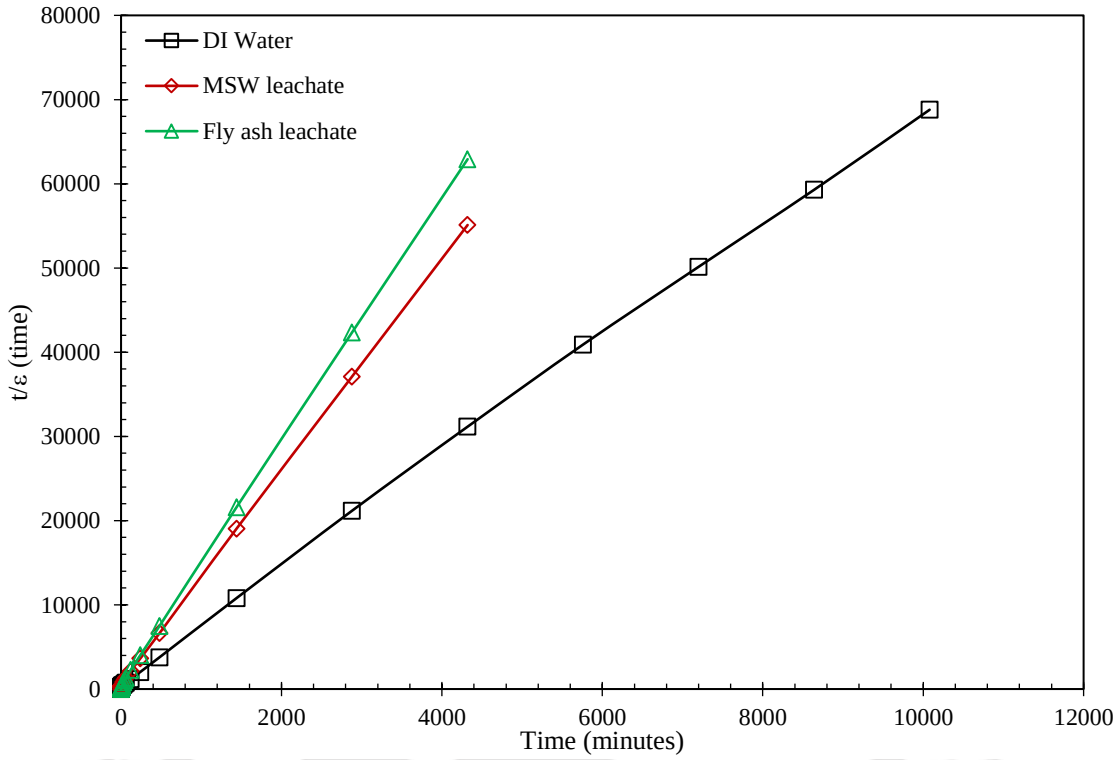

Fig. 7.8. Linearized representation of swelling data for 5% fibre-mixed BC soil with RH model permeated with leachates.

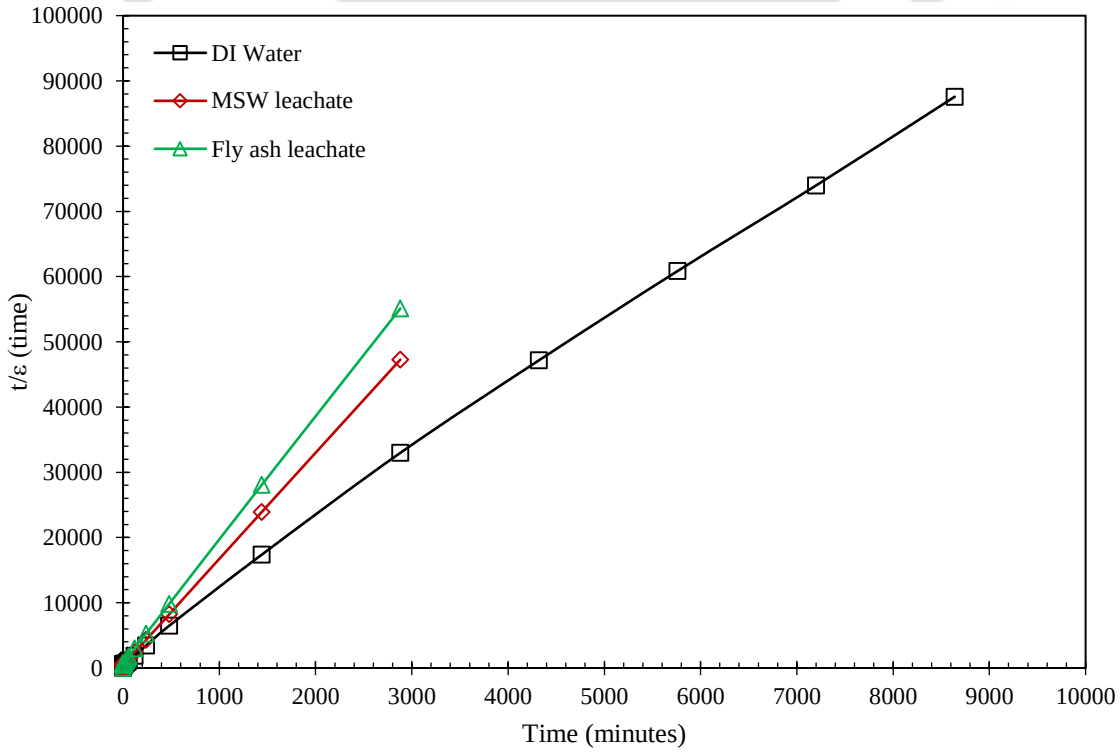

Fig. 7.9. Linearized representation of swelling data for 10% fibre-mixed BC soil with RH model permeated with leachates.

TH-3665_186104109

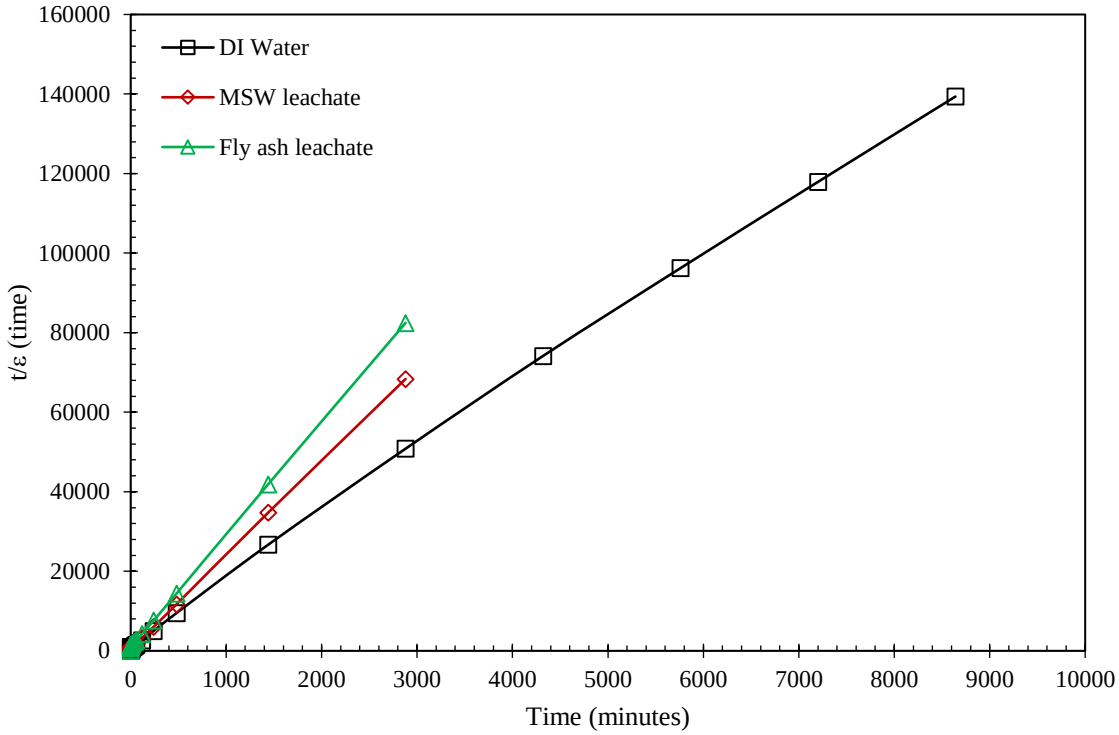

Fig. 7.10. Linearized representation of swelling data for 15% fibre-mixed BC soil with RH model permeated with leachates.

Fig. 7.11. Correlation between measured swell vs observed swell of all fibre-mixed BC soils under permeation of leachates.

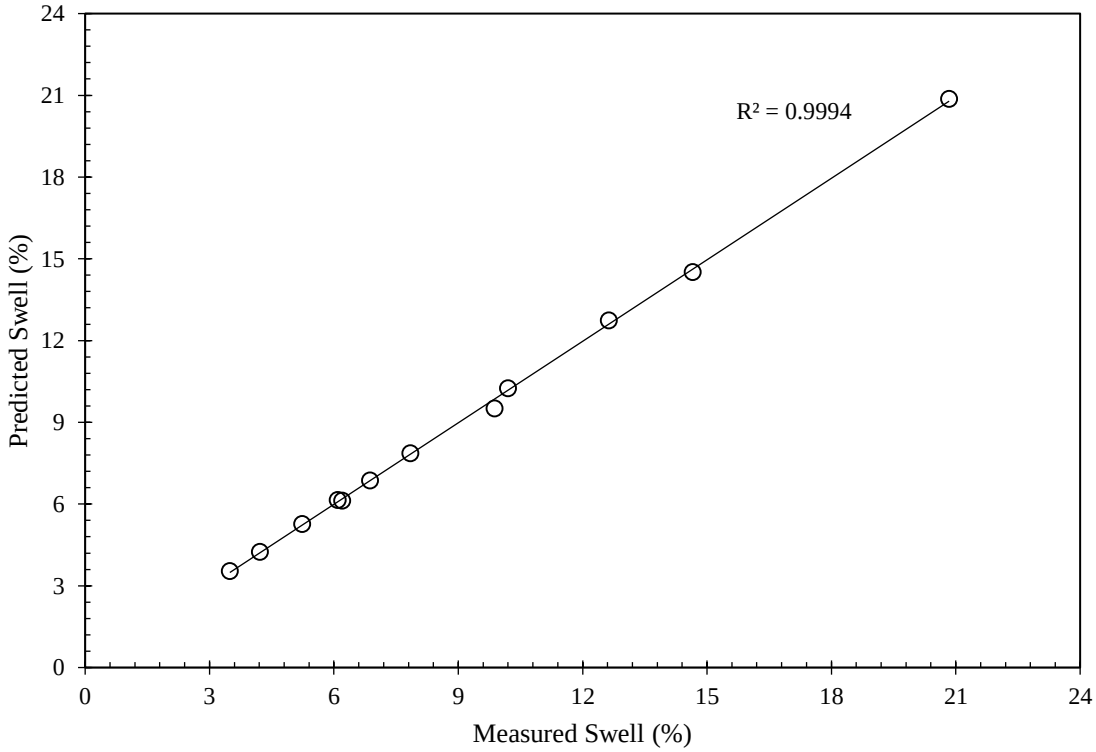

TH-3665_186104109

Table 7.1. Time vs swelling percentage relationship of fibre-mixed BC soil with synthetic leachates

Tire fibre content (%)	Permeant type	Time for completion of swelling in different stages							
		Initial swelling		Primary swelling		Secondary swelling		Total swelling	
		Time in minutes	Swell in percentage	Time in minutes	Swell in percentage	Time in minutes	Swell in percentage	Time in minutes	Swell in percentage
0	DI water	15	2.79	465	15.45	11040	2.6	11520	20.84
	SML	5	1.4	295	9.8	3700	1.43	4000	12.63
	SFL	5	1.61	235	7.22	2640	1.37	2880	10.2
5	DI water	9	2.79	471	9.92	9600	1.94	10080	14.65
	SML	1	0.31	239	6.29	2640	1.24	2880	7.84
	SFL	0.5	0.37	239.5	5.6	2640	0.9	2880	6.87
10	DI water	5	1.17	395	6.13	8240	2.57	8640	9.87
	SML	2	0.44	118	4.59	1880	1.06	2000	6.09

TH-3665_186104109

Tire fibre content (%)	Permeant type	Time for completion of swelling in different stages							
		Initial swelling		Primary swelling		Secondary swelling		Total swelling	
		Time in minutes	Swell in percentage	Time in minutes	Swell in percentage	Time in minutes	Swell in percentage	Time in minutes	Swell in percentage
10	SFL	2	0.44	198	3.98	1800	0.81	2000	5.23
	DI water	4	0.69	296	4.21	6900	1.21	7200	6.20
15	SML	1	0.11	119	3.65	1880	0.45	2000	4.21
	SFL	1	0.08	119	3.02	1780	0.39	1900	3.49

TH-3665_186104109

7.2.4. Influence of leachates on Swelling pressures and swelling potentials

The swelling pressures (SPr's) and swelling potentials (SPo's) of all fibre-mixed BC soil samples were listed in Table 7.3. Swelling pressure is an important engineering property in the design of geoenvironmental structures such as landfill liners since their swelling tendency is significantly impacted by exposure to leachates. To function effectively as impermeable barriers, liners must exhibit high swelling pressure to maintain structural integrity and prevent the formation of cracks and fissures that could compromise their performance. As evidenced in Table 7.3, the swelling pressures (SPr's) of BC soil are profoundly influenced by the presence of leachate permeants. The SPr of BC soil was decreased from 520 kPa (DI water) to 355 and 290 with SML and SFL, respectively. This reduction was about 31.73 and 44.23% with the same order of leachate permeants, respectively. The SFL exhibited a higher reduction in SPr values in comparison to SML. This is due to the higher concentration of cations in FSL leachate which mitigate into montmorillonite layer of BC soil, causing the reduction in DDL thickness. This was evident from the recorded EC values of these leachates. Ray et al. (2022(b)) also observed more reduction in SPr value with fly ash leachate compared with sewage sludge and paper mill leachates. Similarly, all fibre-mixed BC soil samples displayed significant reduction in swelling pressure values in the presence of leachate permeants, as shown in Table 7.3. For example, 5% fibre-mixed BC soil exhibited SPr's as 270, 170, and 155 kPa with DI water, SML, and SFL, respectively. The SPr experienced a reduction of approximately 37.04% and 42.59% when exposed to synthetic municipal SML and SFL, respectively, in comparison to DI water. Similarly, this reduction was about 47.22 and 61.11% with SML and SFL, respectively, with 10% fibre-mixed BC soil. It was 50.00 and 51.43% with 15% fibre-mixed BC soil for the same order of permeant leachates, respectively. This significant decrease in SPr values of all fibre-mixed BC soil samples highlights the impact of leachate type on the swelling behaviour of the soil as well. The SFL significantly influenced all samples, irrespective of fibre content than SML.

Similarly, the swelling potentials of all fibre-mixed BC soil samples under leachate permeants are shown in Table 7.3. The SPos exhibited a similar trend to the SPr response when subjected to leachate permeants, indicating consistent behaviour under varying leachate conditions. The SPo value of BC soil decreased from 20.84% (DI water) to 12.63 and 10.20% with SML and SFL, respectively. Similarly, this trend was observed with all fibre-mixed BC soil samples under leachate permeants, irrespective of fibre content. Also, all SPo values were compared with predicted SPo's using the RH model shown in Table 7.2.

TH-3665_186104109

Hyperbolic parameters of all soil samples were also listed in Table 7.2. Figure 7.11 showed a good correlation between measured swelling potentials and predicted swelling potentials.

Table 7.2 Predicted swelling potentials (RH model) vs measured swelling potential values of fibre-mixed BC soil samples under permeation of leachates

Tire fibre content (%)	**Permeant type**	**Hyperbolic parameters**		**Measured swell (%)**	**Predicted swell (%)**
		a	b		
0	DI water	4.7941	411.71	20.84	20.87
	SML	7.8539	359.76	12.63	12.73
	SFL	9.7652	328.31	10.20	10.24
5	DI water	6.89	329.7	14.65	14.51
	SML	12.725	361.7	7.84	7.86
	SFL	14.571	243.4	6.87	6.86
10	DI water	10.517	712.35	9.87	9.51
	SML	16.263	443.12	6.09	6.15
	SFL	19	523.78	5.23	5.26
15	DI water	16.344	904.35	6.20	6.12
	SML	23.554	573.32	4.21	4.24
	SFL	28.231	1108.7	3.49	3.54

TH-3665_186104109

Table 7.3. Swelling pressures and swelling potentials of fibre-mixed BC soil with synthetic leachates

Tire fibre content (%)	Permeant type	Swelling Pressure (kPa)	Swelling Potential (%)
0	0 (DI Water)	520	20.84
	SML	355	12.63
	SFL	290	10.20
5	0 (DI Water)	270	16.65
	SML	170	7.84
	SFL	155	6.87
10	0 (DI Water)	180	9.87
	SML	95	6.09
	SFL	70	5.23
15	0 (DI Water)	140	6.20
	SML	70	4.21
	SFL	68	3.49

7.2.5. Influence of leachates on coefficient of consolidation (c_v)

The coefficient of consolidation (c_v) parameter helps in understanding the rate of consolidation of soils under various overburden pressures. This would be helpful in calculating time-dependent settlement in saturated soils. The c_v of pure BC soil under permeation of leachate permeants is shown in Fig. 7.12. Irrespective of leachate type, all c_v values decreased with the rise in overburden consolidation pressure. At high consolidation pressures, soil particles are brought closer together, resulting in a reduction in the repulsive forces between them. This leads to densification of the soil, which in turn slows down the rate of consolidation. Also, the impact of leachates on this consolidation rate of BC soil is

TH-3665_186104109

significant as shown in Fig. 7.12. The c_v of BC soil was increased from 1.28×10^{-3} cm^2/s to 2.28×10^{-3} and 6.68×10^{-3} cm^2/s with SML and SFL, respectively, under a consolidation pressure of 49.0 kPa. This hike was around 1.78 and 4.91 times with SML and SFL, respectively, compared to DI water. However, at high consolidation pressure (784.5 kPa), this c_v of BC soil was hiked from 2.36×10^{-5} cm^2/s (DI water) to 2.80×10^{-4} (11.91 times) and 4.43×10^{-4} cm^2/s (18.77 times) with SML and SFL, respectively. Thus, it can be concluded that the c_v values of BC soil were highly influenced by SFL than SML under constant consolidation pressure. The main reason for this hike in consolidation rate is due to elevated concentrations of heavy metals present in SFL compared to SML, which would cause the significant suppression of DDL thickness of BC soil. Similarly, the rate of consolidation behaviour under leachate permeants was observed with all fibre-mixed BC soil samples, displayed in Figs. 7.13 to 7.15. All fibre-mixed BC soil samples exhibited high c_v values with both leachates. For a simple comparison, all c_v values of fibre-mixed BC soil at one consolidation pressure (784.5 kPa) were shown in Fig. 7.16. For example, the c_v value of 5% fibre-mixed was increased from 4.10×10^{-5} cm^2/s to 6.40×10^{-4} (15.61 times) and 9.85×10^{-4} cm^2/s (24.02 times) with SML and SFL permeants, respectively, under the consolidation pressure of 784.5 kPa. For the same order of leachate permanents, this hike was around 17.21 and 33.32 with 10% fibre-mixed BC soil, respectively, under the same consolidation pressure. This hike in cv values of 15% fibre-mixed BC soil was about 34.91 and 64.55 times, respectively. It is evident that SFL had a more significant impact on all fibre-mixed samples compared to SML irrespective of fibre content. Therefore, it is important to consider the leachate impact before suggesting fibre-mixed soils for barrier application.

TH-3665_186104109

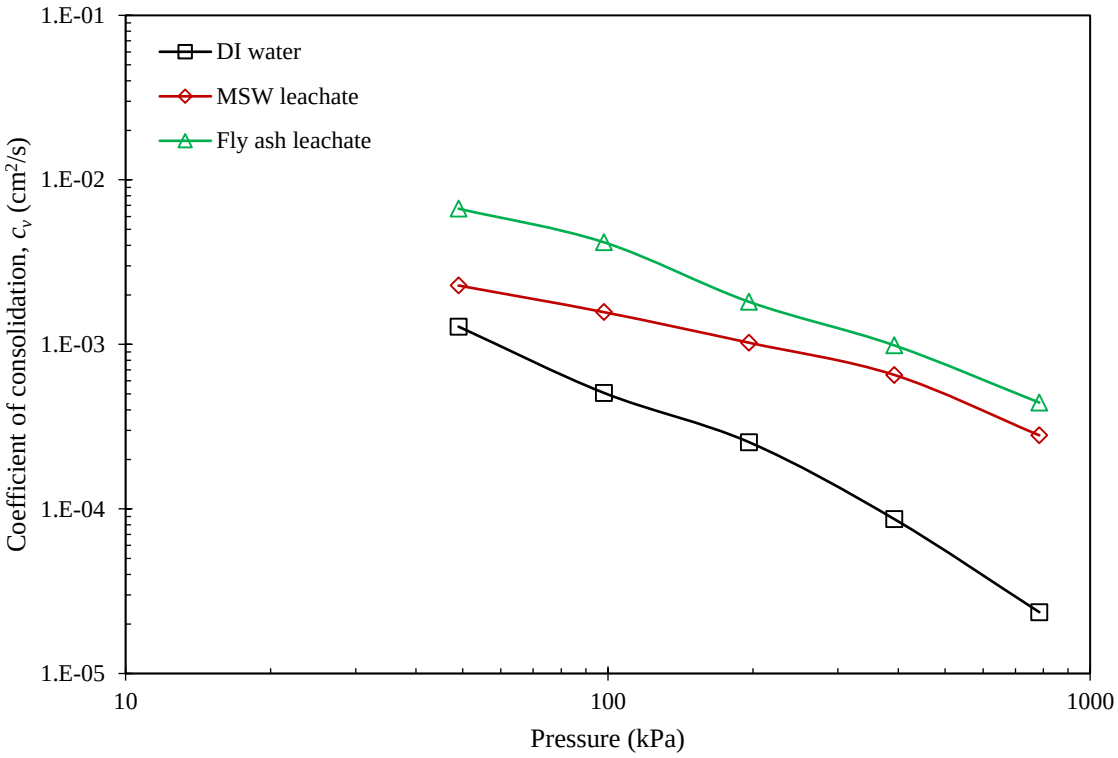

Fig. 7.12. Consolidation pressure vs coefficient of consolidation (c_v) plots for pure BC soil under permeation of synthetic leachates.

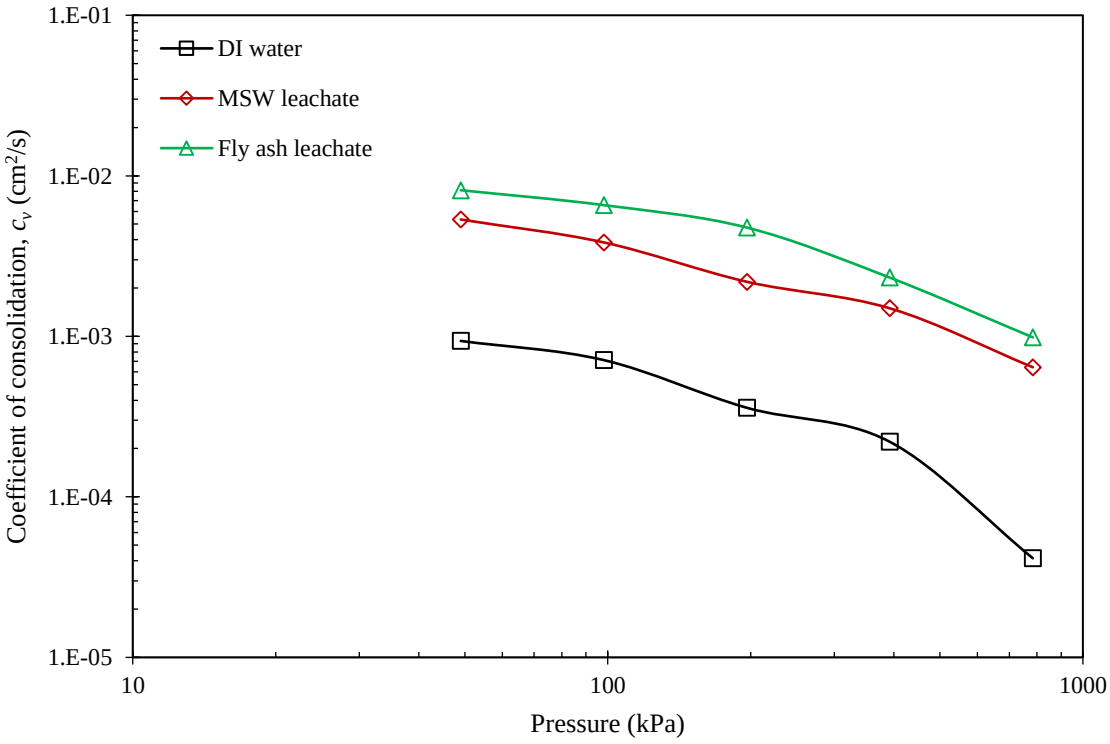

Fig. 7.14. Consolidation pressure vs coefficient of consolidation (c_v) plots for 5% fibre-mixed BC soil under permeation of synthetic leachates.

TH-3665_186104109

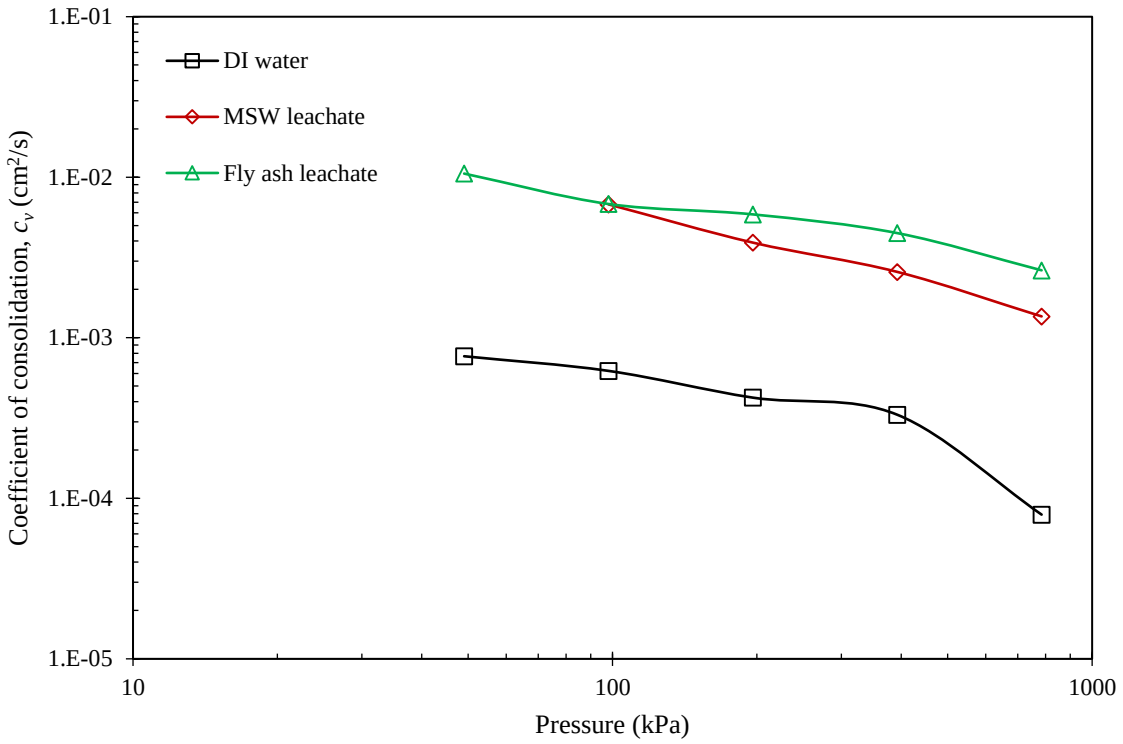

Fig. 7.14. Consolidation pressure vs coefficient of consolidation (c_v) plots for 10% fibre-mixed BC soil under permeation of synthetic leachates.

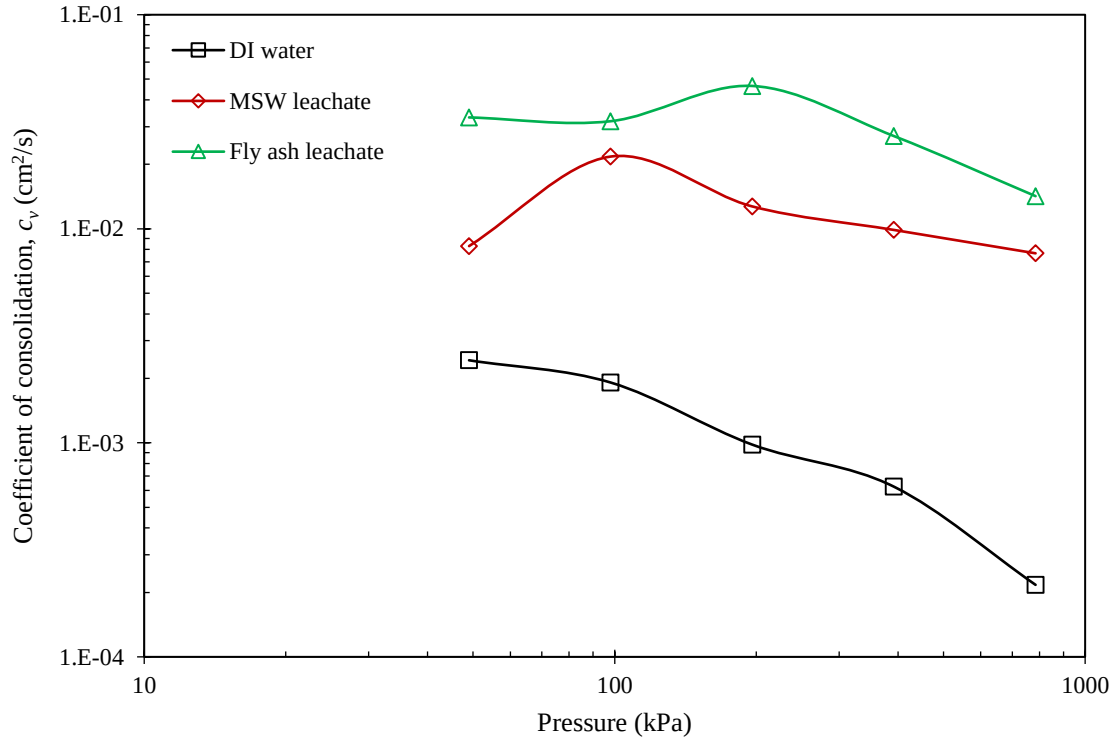

Fig. 7.15. Consolidation pressure vs coefficient of consolidation (c_v) plots for 15% fibre-mixed BC soil under permeation of synthetic leachates.

TH-3665_186104109

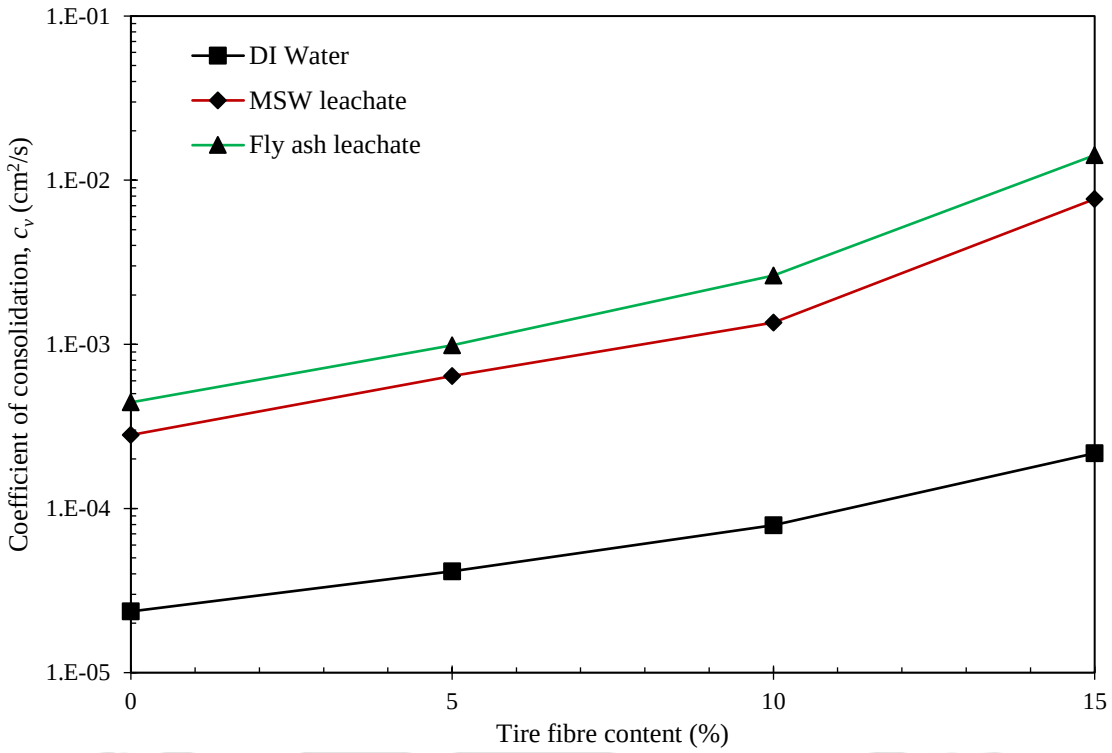

Fig. 7.16. Fibre content vs coefficient of consolidation plot with synthetic leachate permeants at the consolidation pressure of 784.5 kPa.

7.2.6. Influence of leachates on time for 90% consolidation (t_{90})

The time for 90% consolidation (t_{90}) values of all fibre-mixed BC soil samples with respect to various consolidation pressures under permeation of synthetic leachates were depicted in Figs. 7.17 to 7.20. The t_{90} value of pure BC soil was reduced from 9.00 minutes (DI water) to 4.41 (51.00% reduction) and 1.44 (84.00% reduction) minutes with SML and SFL permeants, respectively, under a consolidation pressure of 4.0 kPa. However, this t_{90} value of BC soil decreased from 334.89 to 25.50 (92.38% reduction) and 15.21 (95.46% reduction) minutes with the same order of leachate permeants, respectively, at the consolidation pressure of 784.5 kPa. Therefore, it is clearly seen from the results that at any consolidation pressure, the influence of these synthetic leachates on BC soil is significant. The main reason for this significant reduction in t_{90} values under leachate permeants is due to heavy metal cations present in leachates, which accelerate faster rate of consolidation. Ray et al., (2021b) observed this significant decline trend in t_{90} value of bentonite with MSW leachate. However, SFL influence is relatively more than SML on BC soil consolidation rate. Hence, the focus has been shifted towards the fibre-mixed BCsoil samples' behaviour under these synthetic leachate permeants.

TH-3665_186104109

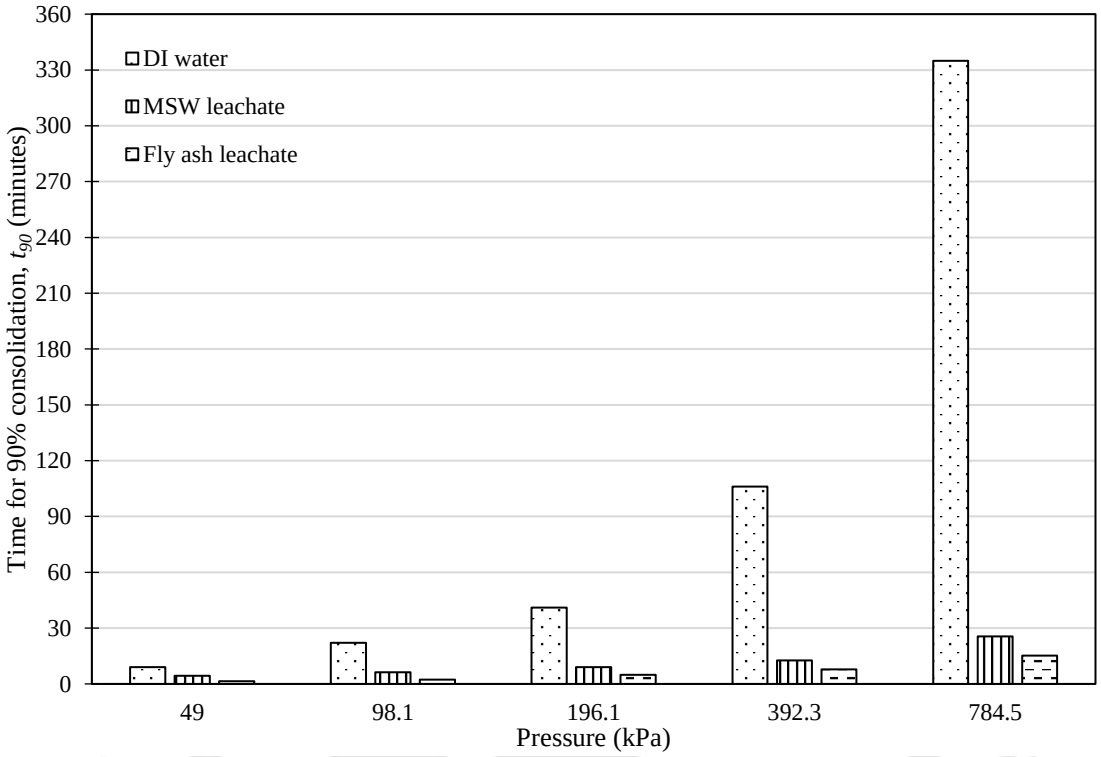

Fig. 7.17. Consolidation pressure vs time for 90% consolidation (t_{90}) plots for pure BC soil under permeation of synthetic leachates.

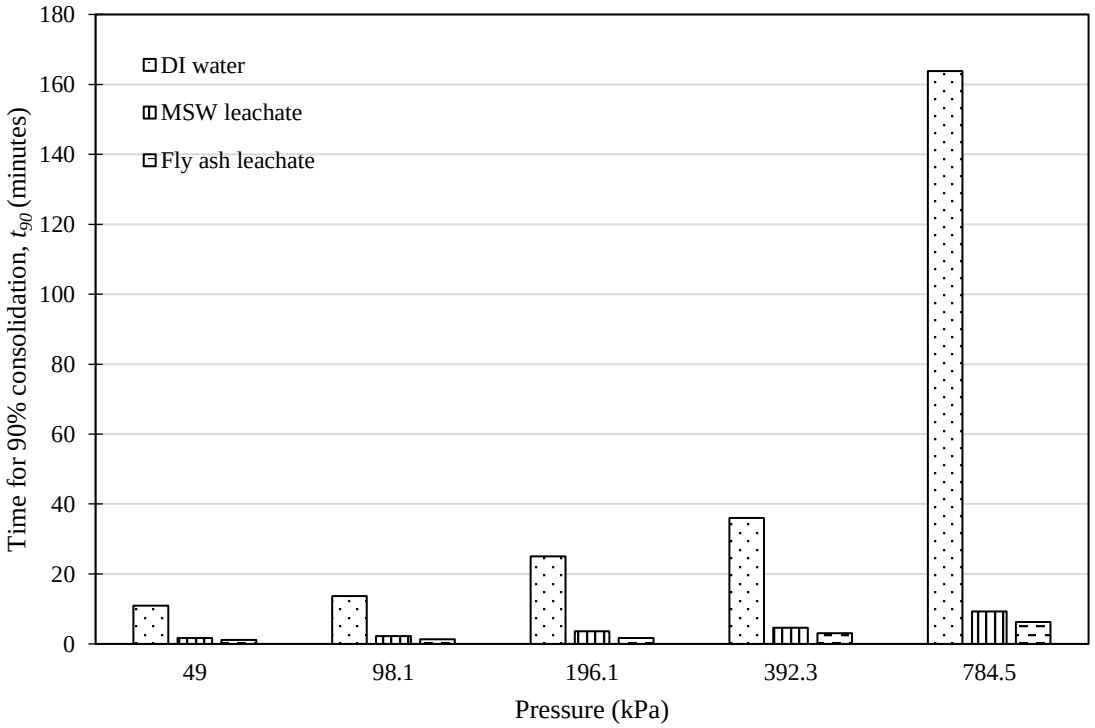

Fig. 7.18. Consolidation pressure vs time for 90% consolidation (t_{90}) plots for 5% fibre-mixed BC soil under permeation of synthetic leachates.

TH-3665_186104109

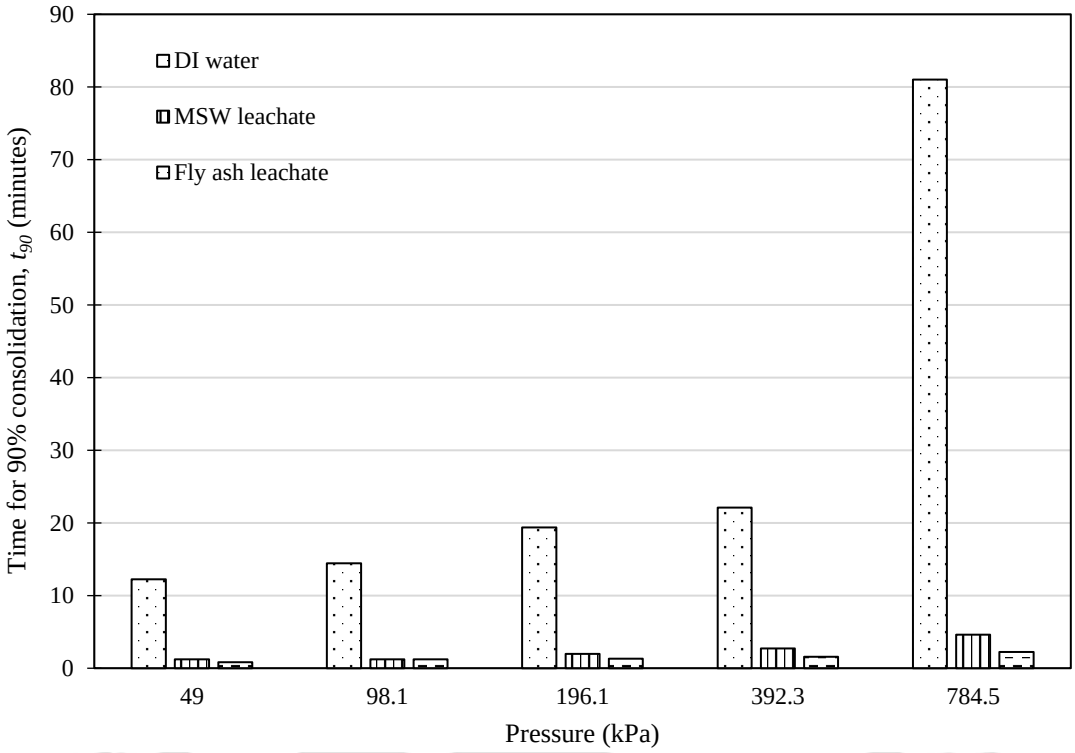

Fig. 7.19. Consolidation pressure vs time for 90% consolidation (t_{90}) plots for 10% fibre-mixed BC soil under permeation of synthetic leachates.

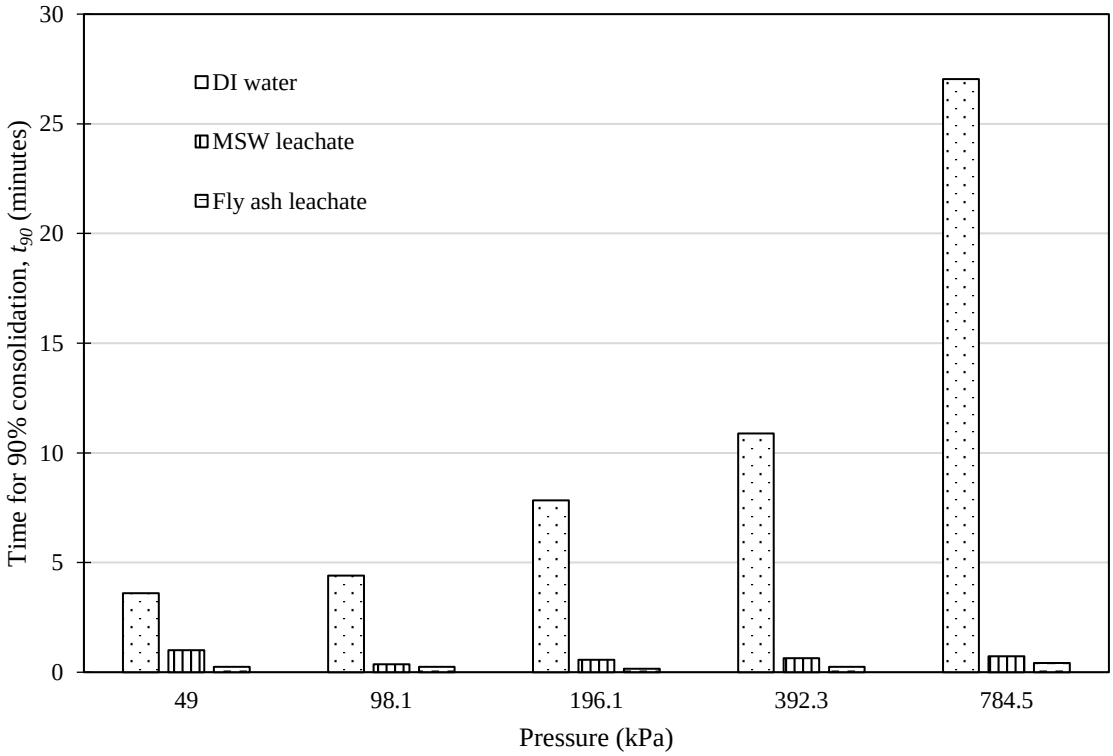

Fig. 7.20. Consolidation pressure vs time for 90% consolidation (t_{90}) plots for 15% fibre-mixed BC soil under permeation of synthetic leachates.

TH-3665_186104109

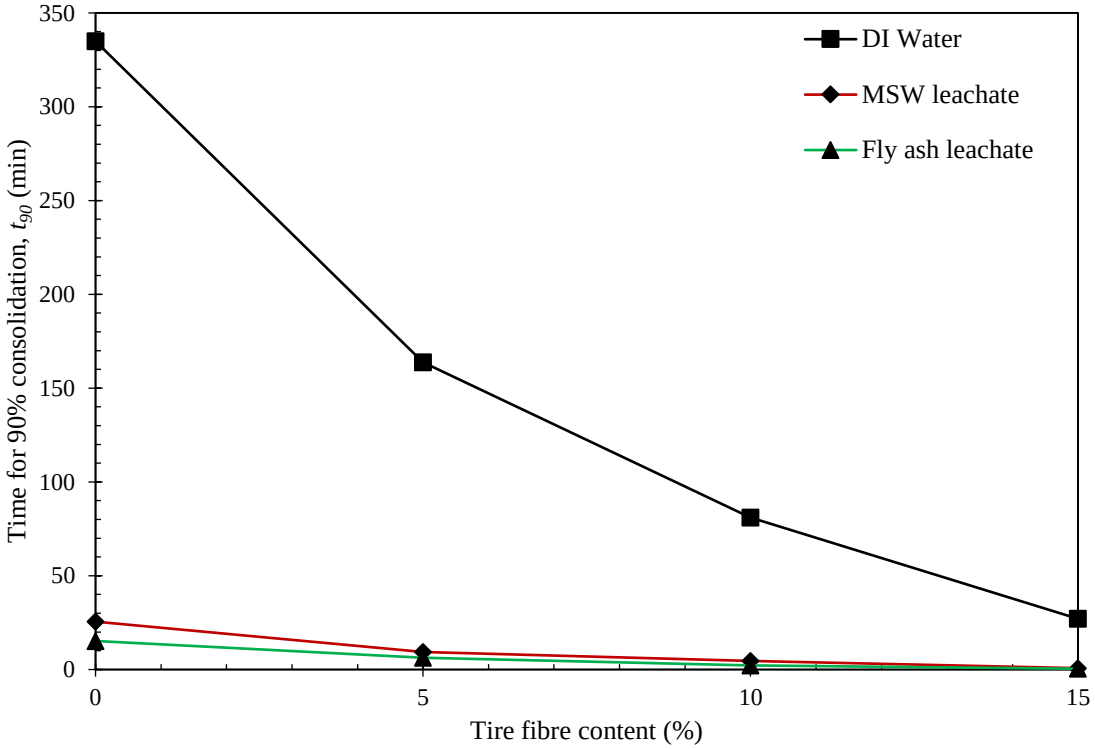

Fig. 7.21. Fibre content vs time for 90% consolidation plot with synthetic leachate permeants at the consolidation pressure of 784.5 kPa.

The time for 90% consolidation (t_{90}) versus consolidation pressures of fibre-mixed (5 to 15%) BC samples were displayed in Figs. 7.18 to 7.20. Irrespective of fibre content, all the plots show considerable diminution in t_{90} values in the presence of synthetic leachate permeants. For a straightforward comparison, the t_{90} values of fibre-mixed BC soil under a consolidation pressure of 784.5 kPa are presented in Fig. 7.21. For example, the t_{90} value of 5% fibre-mixed BC soil was 163.84 minutes with DI water which was diminished to 9.30 (94.32% reduction) and 6.25 (96.185 reduction) minutes with SML and SFL permeants, respectively, at the consolidation pressure of 784.5 kPa. This is both significant and apparent in the way fibre-mixed soil responds to aggressive leachate conditions. For 10% fibre-mixed soil, t_{90} value declined from 81.00 minutes (DI water) to 4.62 and 2.25 minutes with the SML and SFL leachate permeants, respectively, at the consolidation pressure of 784.5 kPa. A similar trend was observed with 15% fibre-mixed soil samples as well., compared to DI water. Therefore, it is evident that leachates have a substantial and notable impact on fibre-mixed soil samples, irrespective of fibre content.

TH-3665_186104109

7.2.7. Influence of leachates on void ratio – pressure (*e*-log*P*) relationship

The relationship between void ratio and consolidation pressure of pure BC soil in the presence of synthetic leachate permeants is depicted in Fig. 7.22. Irrespective of leachate type, the void ratio of BC soil was decreased from 1.13 to 0.67 with the increment in consolidation pressure from 4.90 kPa to 784.5 kPa as displayed in Fig. 7.22. The influence of leachates on the void ratio of soil is also noticeable in Fig. 7.22. The void ratio of BC soil was decreased from 1.12 (DI water) to 1.00 and 0.8 with SML and SFL permeants under 4.90 kPa. At 49.0 kPa consolidation pressure, this void ratio of BC soil dropped from 1.11 to 0.99 and 0.97 with SML and SFL permeants, respectively. Similarly, at 196.1 kPa, this void ratio changed from 0.96 to 0.88 and 0.85 with the same order of leachate permeants. However, at maximum consolidation pressure (784.5 kPa), this void ratio of BC soil declined from 0.67 to 0.62 and 0.58 with SML and SFL, respectively. Therefore, it can be concluded that, at any constant consolidation pressure, a reduction in the void ratio of BC soil was observed with both synthetic leachate permeants. The reason for this reduction in the void ratio is due to the reduction in repulsive forces between clay particles at synthetic leachate permeants, causing the thinning of the DDL layer, subsequently lessening the void ratio. However, elevated metal concentrations in SFL are attributed to more decline in void ratio than SML.

Similarly, the void ratio-consolidation pressure behaviour was observed with all fibre-mixed BC soil samples under the permeation of two synthetic leachates, shown in Figs. 7.23 to 7.25. For example, at a consolidation pressure of 49.0 kPa, the void ratio of 5% fibre-mixed BC soil declined from 1.03 (DI water) to 0.92 and 0.90 with SML and SFL permeants, respectively. For 10% fibre-mixed soil, the void ratio was reduced from 0.92 to 0.83 and 0.82 with the same order of leachate permeants, respectively, at the same consolidation pressure. For a similar order of comparison, this void ratio was dropped from 0.83 (DI water) to 0.79 and 0.76 with SML and SFL permeants, respectively. However, at higher consolidation pressure this difference in void ratio due to synthetic leachate permeants is insignificant and negligible for all fibre-mixed soil samples. However, it can be seen that the void ratios of all fibre-mixed samples showed a declining trend in void ratios with the permeation of leachate permeants, which is relatively more with SFL than SML.

TH-3665_186104109

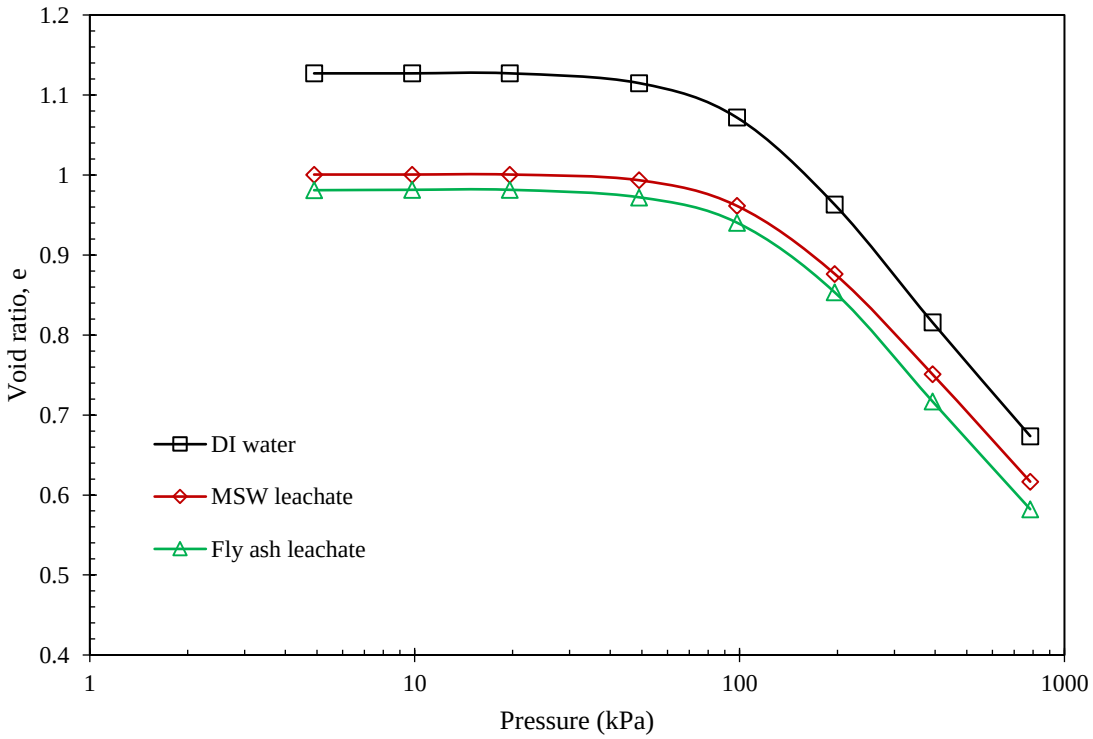

Fig. 7.22. Void ratio (*e*) vs consolidation pressure plots for pure BC soil under permeation of synthetic leachates.

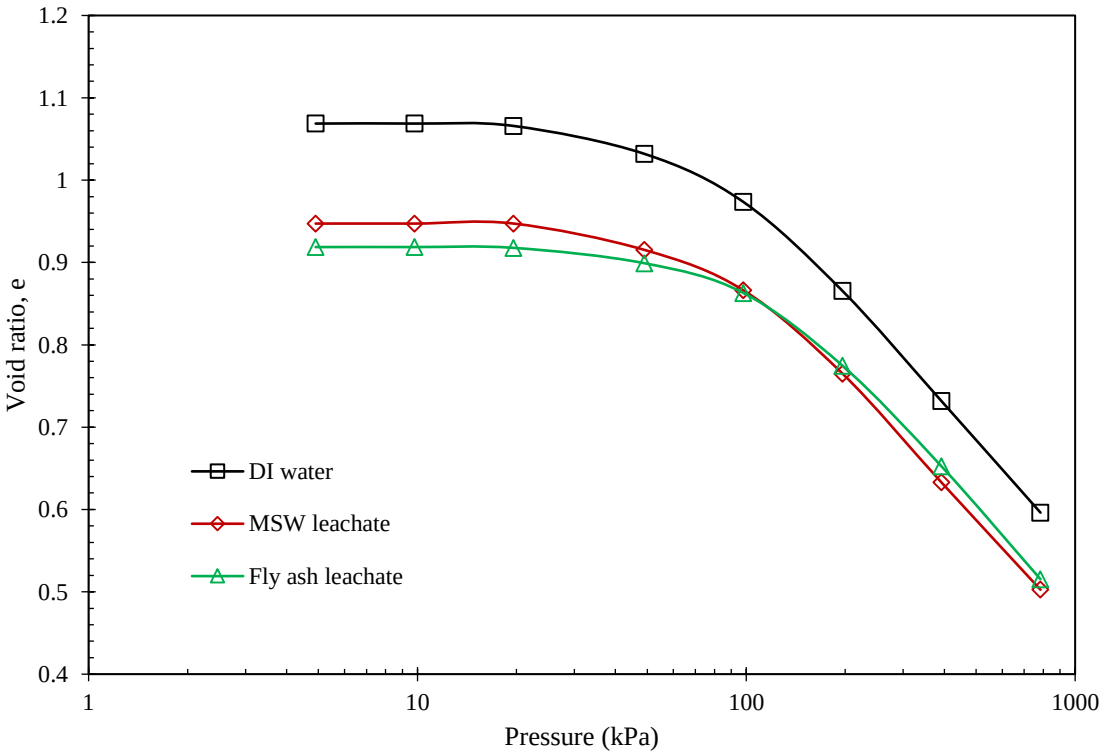

Fig. 7.23. Void ratio (*e*) vs consolidation pressure plots for 5% fibre-mixed BC soil under permeation of synthetic leachates.

TH-3665_186104109

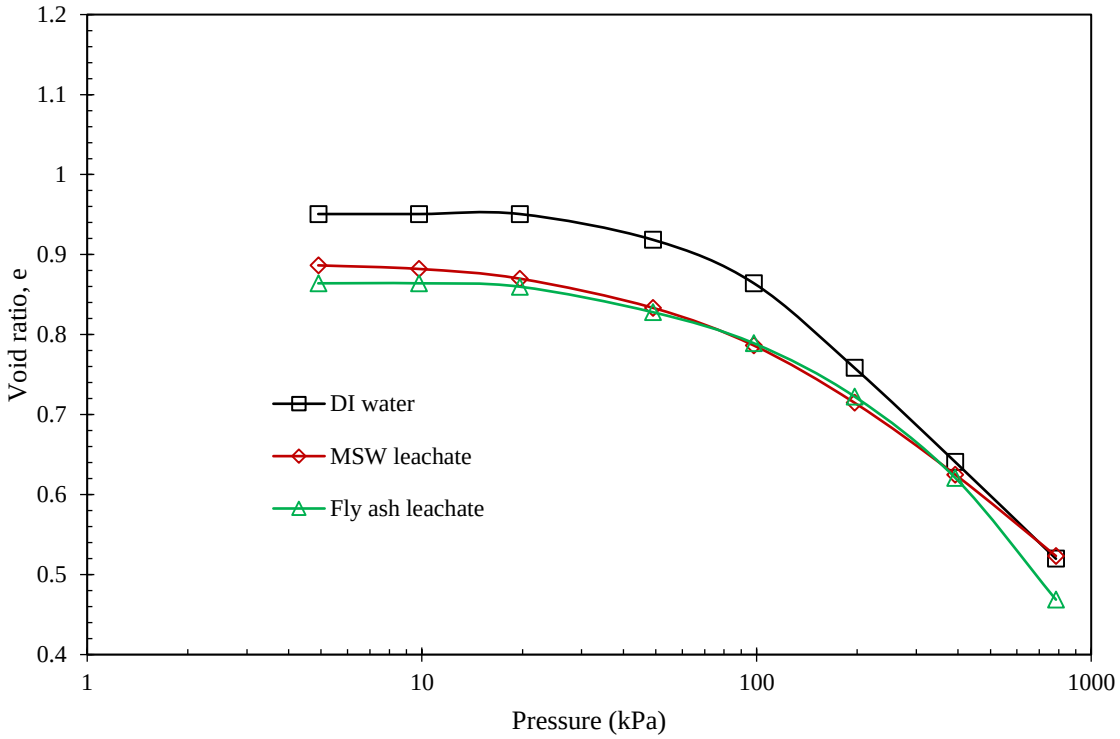

Fig. 7.24. Void ratio (*e*) vs consolidation pressure plots for 10% fibre-mixed BC soil under permeation of synthetic leachates.

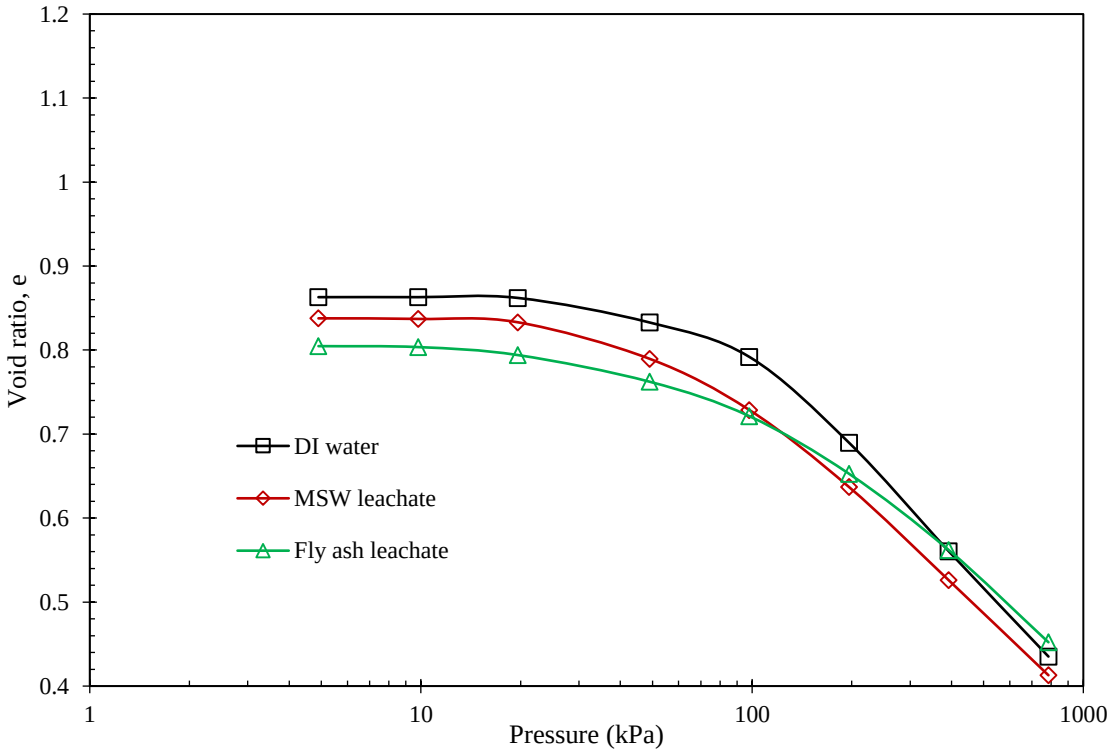

Fig. 7.25. Void ratio (*e*) vs consolidation pressure plots for 15% fibre-mixed BC soil under permeation of synthetic leachates.

TH-3665_186104109

7.2.8. Influence of leachates on compression index (C_c)

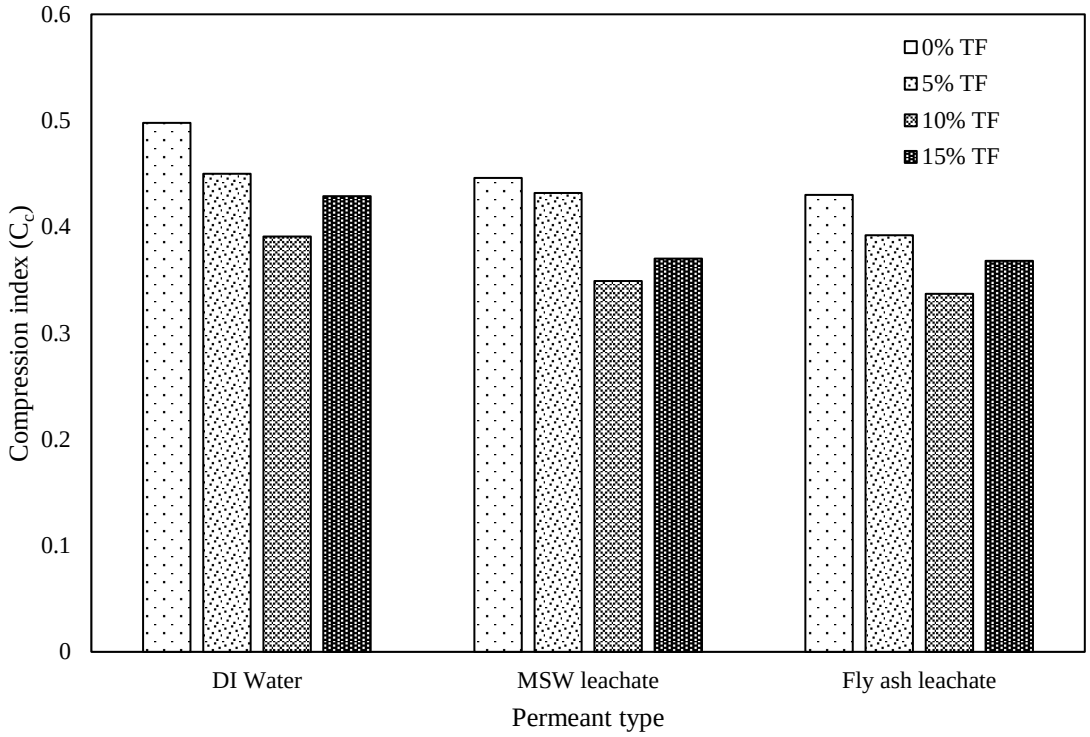

Fig. 7.26. Compression index (C_c) of fibre-mixed BC soil under permeation of synthetic leachates.

The compression indices of all fibre-mixed BC soil samples subjected to permeation with synthetic leachates were determined by examining the linear portion of the void ratio-consolidation pressure curves, as shown in Fig. 7.26. The compressibility behaviour of BC clayey soil is usually influenced by mechanical properties and chemical properties (Bolt, 1956; Dutta and Mishra, 2018, Mukherjee and Mishra, 2021). The compression index (C_c) of BC soil with DI water is reported as 0.498, which was reduced to 0.446 and 0.430 with SML and SFL permeants, respectively. The percentage of reduction in this void ratio was about 10.44 and 13.65% with both SML and SFL, respectively, compared to DI water. The elevated cation concentrations in leachates facilitate the migration of cations into the montmorillonite interlayer, resulting in a substantial reduction in the Diffuse Double Layer (DDL) and a decrease in the compressibility tendency of the soil under these leachate permeants (Sridharan et al., 1986). This compressibility behaviour of all fibre-mixed BC soil samples was also observed under the same SML and SFL leachate permeants and their C_c values were displayed in Fig. 7.26. All fibre-mixed BC soil samples also experienced this declining trend in the C_c values irrespective of fibre content. For example, with the 5% fibre-mixed BCsoil composition, this C_c value was reduced from 0.450 (DI water) to 0.432 (4.00%

TH-3665_186104109

reduction) and 0.392 (12.89% reduction) with SML and SFL permeants, respectively. For the same order of comparison, this reduction in C_c value was about 10.74 and 13.81%, respectively, with 10% fibre-mixed BC soil than DI water. This reduction became 13.75 and 14.22% with 15% fibre-mixed BC soil in the same order.

7.2.9. Influence of leachates on hydraulic conductivity (*k*)

Hydraulic conductivity is an important engineering property, which would help us to understand the mitigation of leachate into clay liners and decide the integrity of the liner based on limiting criteria (USEPA, 1988). The hydraulic conductivity (*k*) of fibre-mixed BC soils with respect to overburden pressures under the permeation of synthetic leachates is shown in Table 7.4. The conductivity value of BC soil with DI water was reported as 2.44×10^{-8} cm/s under the consolidation pressure of 49.0 kPa. At the same consolidation pressure, this *k* value of BC soil was increased to 2.65×10^{-8} (1.09 times) and 1.03×10^{-7} cm/s (4.22 times) with SML and SFL permeants, respectively. Similar observations were made with other consolidation overburden pressures as well, as shown in Table 7.4. For example, at maximum consolidation pressure (784.5 kPa), this *k* value of BC soil was hiked from 4.75×10^{-10} cm/s (DI water) to 5.27×10^{-9} (11.09 times) and 8.53×10^{-9} cm/s (17.96 times) with SML and SFL permenats, respectively. It is clearly observed a prominent hike in *k* values of BC soil at high consolidation pressures under both synthetic leachate permeants. Also, these synthetic leachates cause a significant hike in *k* values compared to DI water. These findings are in accordance with the trends that have been identified in prior research on bentonites (Dutta and Mishra, 2018; Ray et al., 2021(a)). The higher concentrations of cations in synthetic leachates led to this hike in *k* values. DDL undergoes contraction as a consequence of the enhanced binding of ions to the clay surface, which leads to higher hydraulic conductivity and a propensity for a more flocculated soil structure. Similarly, the hydraulic conductivity of BC soil mixed with waste tire fibres ranges from 5 to 15% with respect to consolidation overburden pressures, were shown in Table 7.4. The hydraulic conductivity of BC soil raised significantly with the hike in fibre content, discussed in Chapter 4. The main objective of this chapter is to understand the influence of leachates on the hydraulic characteristics of fibre-mixed soil samples. All fibre-mixed BC soils showed a similar trend of BC soil behaviour in the presence of leachate permeants, irrespective of fibre content. For example, at 784.5 kPa, the *k* value of 5% fibre-mixed BC soil was increased from 7.95×10^{-10} cm/s (DI water) to 1.30×10^{-8} (16.35 times) and 2.00×10^{-8} cm/s (25.16 times) with SML and SFL permeants, respectively. Similarly, this hike was around 14.68 and 42.38 times with

TH-3665_186104109

10% fibre-mixed BC soil, respectively, for the same consolidation pressure and similar order of leachate permeants. Whereas, this hike in *k* value was around 32.71 times and 57.24 times with 15% fibre-mixed BC soil, respectively, for the same order of permeants at 784.5 kPa. This hike in *k* values of all fibre-mixed samples is due to the generation of multiple flow channels because of the high concentration of cations present in leachates. The elevated cation concentrations caused the soil fabric to adopt a flocculated structure by suppressing the thickness of the DDL, resulting in the formation of wider flow channels within the clay medium. Also, the relationship between void ratio and hydraulic conductivity of all fibre-mixed BC soil samples with synthetic leachate permeants was displayed in Figs. 7.27 to 7.30. The results clearly showed a significant hike in conductivity values with both leachates. However, it was understandable that the SFL influenced more on hydraulic behaviour compared to SML for all samples shown in Figs. 7.27 to 7.30 To facilitate a better understanding, the hydraulic conductivity of all fibre-mixed samples was compared at a specific void ratio of 0.75, as illustrated in Fig. 7.31. For example, the *k* value of BC soil was hiked around 23.33 and 51.93 times with SML and SFL permeants, respectively, at the void ratio of 0.75, in comparison to DI water. A similar kind of trend was observed with fibre-mixed BC soil samples as well, depicted in Fig 7.31. For example, 15%fibre-mixed BC soil showed a hike in *k* values about 23.55 and 43.33 times with the same order of comparison and void ratio, respectively. Also, after the completion of testing, microstructural behaviour leachate-permeated samples were tested using FESEM analysis. The FESEM images are shown in Figs. 7.32 and 7.33. The aggregation of clay particles was observed with both leachate-permeated samples. This aggregation was more prominent in the sample permeated with SFL compared to that with SML. These microstructural results supported the hydraulic conductivity investigations on BC soil under the permeation of both synthetic leachates. Therefore, it is evident that the consideration of leachates for all samples, irrespective of fibre content is noticeable for barrier applications. However, 15% fibre mixed samples exceeded the limiting criterion ($>10^{-7}$ cm/s) under both leachate permeants irrespective of the consolidation pressure.

TH-3665_186104109

Table 7.4. Hydraulic conductivity vs consolidation pressure values for fibre-mixed BC soil with synthetic leachate permeants

Tire fibre content (%)	Permeant type	Hydraulic conductivity (cm/s)		
		49.0 kPa	**196.1 kPa**	**784.5 kPa**
0	0 (DI Water)	2.44×10^{-8}	1.37×10^{-8}	4.75×10^{-10}
	SML	2.65×10^{-8}	4.36×10^{-8}	5.27×10^{-9}
	SFL	1.03×10^{-7}	8.01×10^{-8}	8.53×10^{-9}
5	0 (DI Water)	5.03×10^{-8}	1.93×10^{-8}	7.95×10^{-10}
	SML	2.87×10^{-7}	1.20×10^{-7}	1.30×10^{-8}
	SFL	2.59×10^{-7}	2.21×10^{-7}	2.00×10^{-8}
10	0 (DI Water)	4.14×10^{-8}	2.36×10^{-8}	1.43×10^{-9}
	SML	4.52×10^{-7}	1.50×10^{-7}	2.10×10^{-8}
	SFL	5.91×10^{-7}	2.14×10^{-7}	6.06×10^{-8}
15	0 (DI Water)	1.25×10^{-7}	5.49×10^{-8}	4.28×10^{-9}
	SML	6.44×10^{-7}	6.62×10^{-7}	1.40×10^{-7}
	SFL	1.92×10^{-6}	1.81×10^{-6}	2.45×10^{-7}

TH-3665_186104109

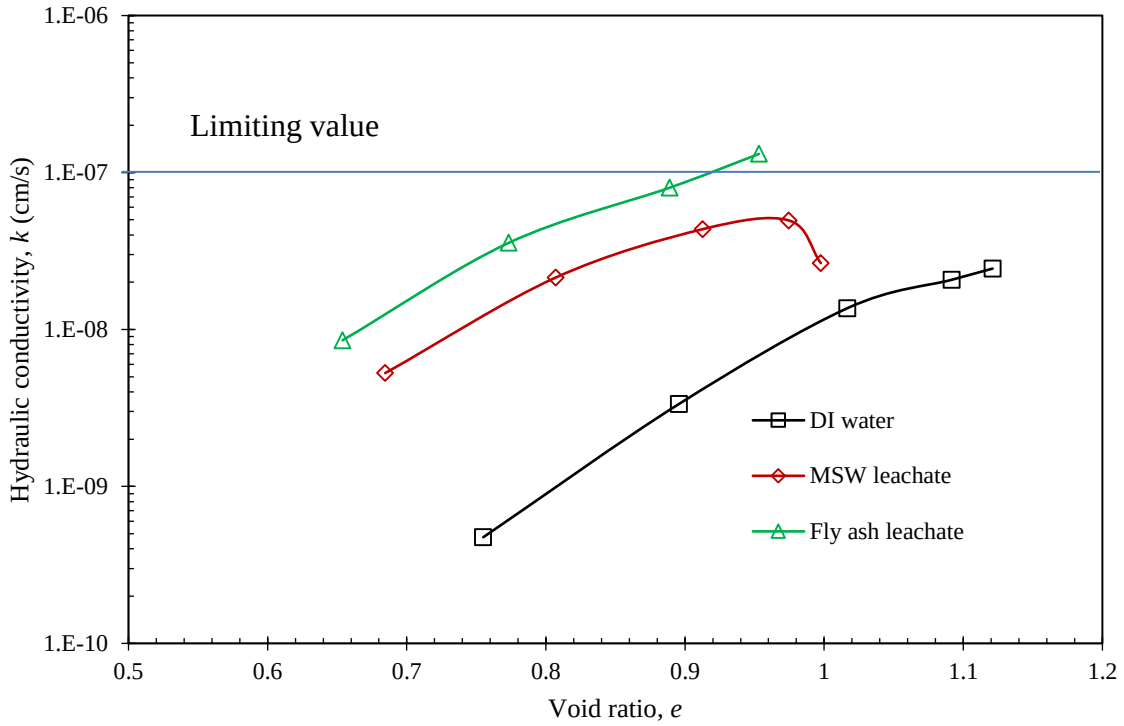

Fig. 7.27. Hydraulic conductivity vs void ratio plots for pure BC soil under permeation of synthetic leachates.

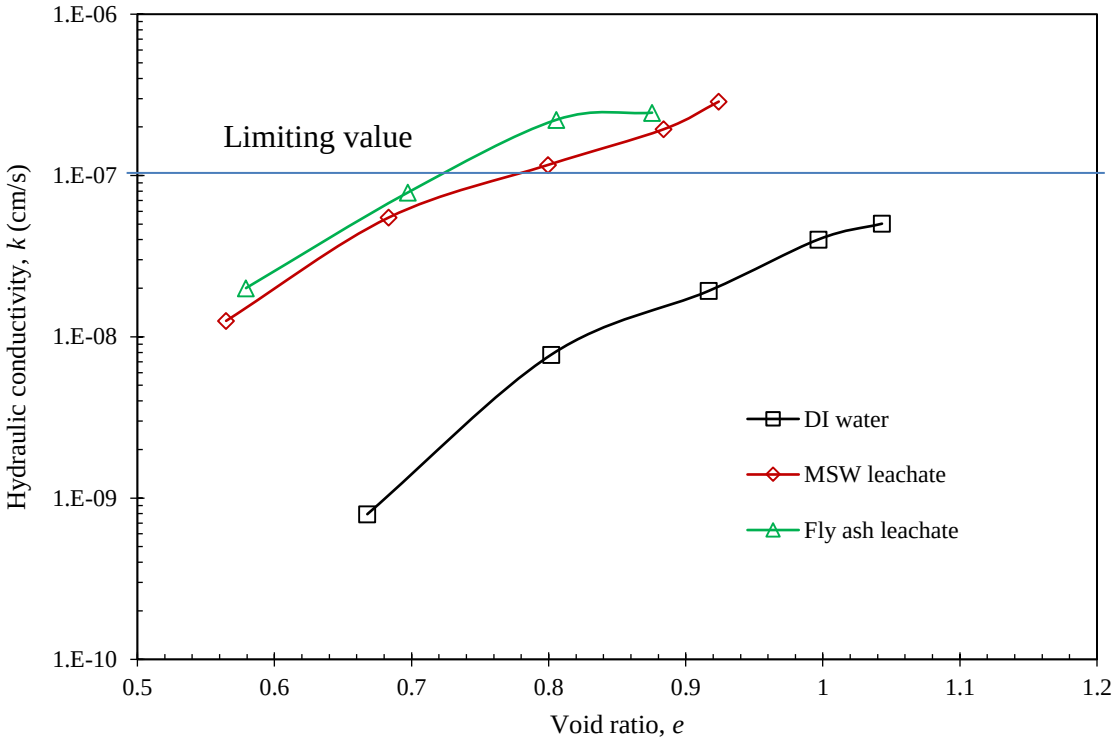

Fig. 7.28. Hydraulic conductivity vs void ratio plots for 5% fibre-mixed BC soil under permeation of synthetic leachates.

TH-3665_186104109

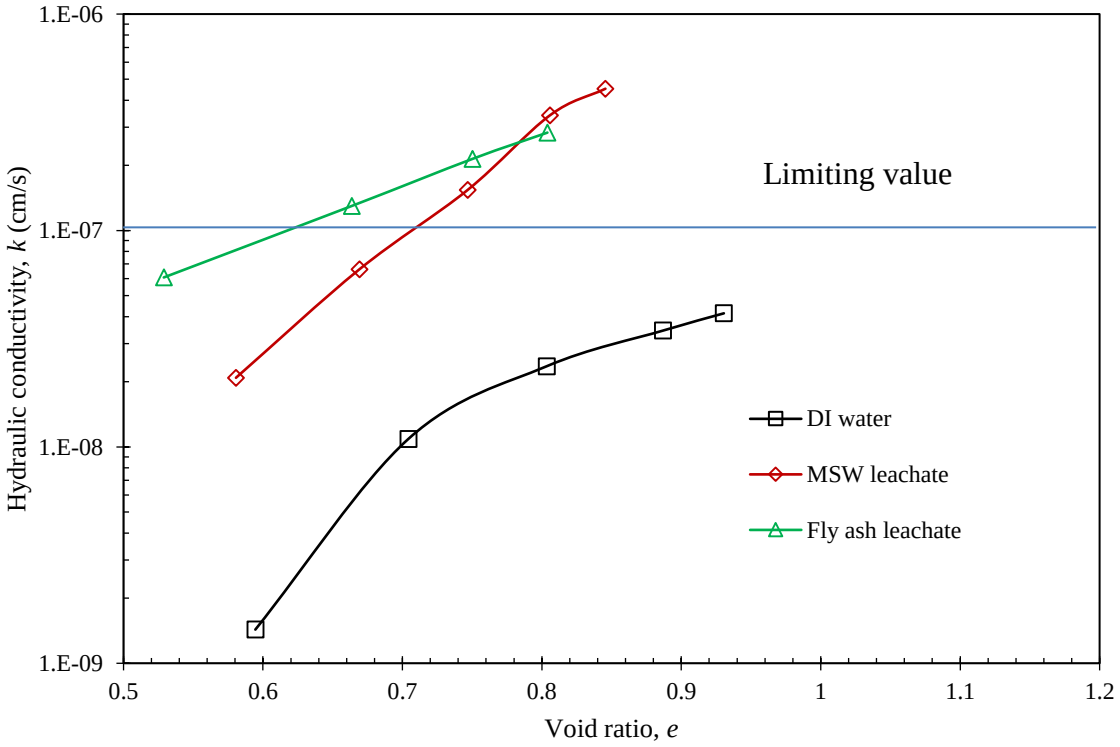

Fig. 7.29. Hydraulic conductivity vs void ratio plots for 10% fibre-mixed BC soil under permeation of synthetic leachates.

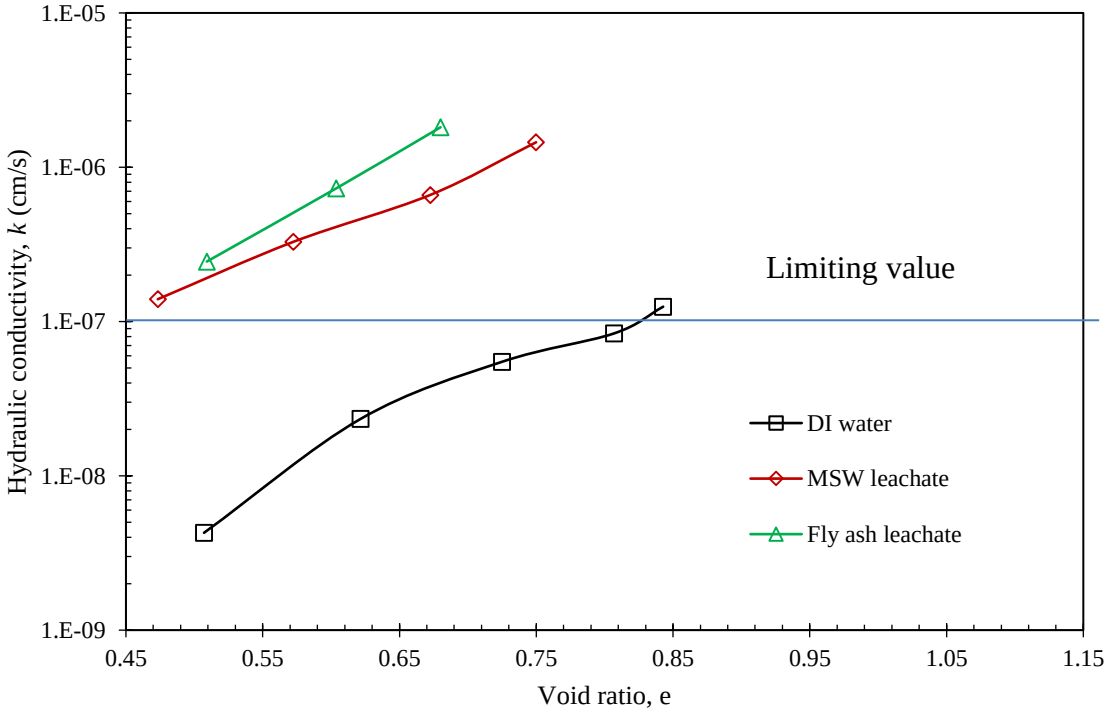

7.30. Hydraulic conductivity vs void ratio plots for 15% fibre-mixed BC soil under permeation of synthetic leachates.

TH-3665_186104109

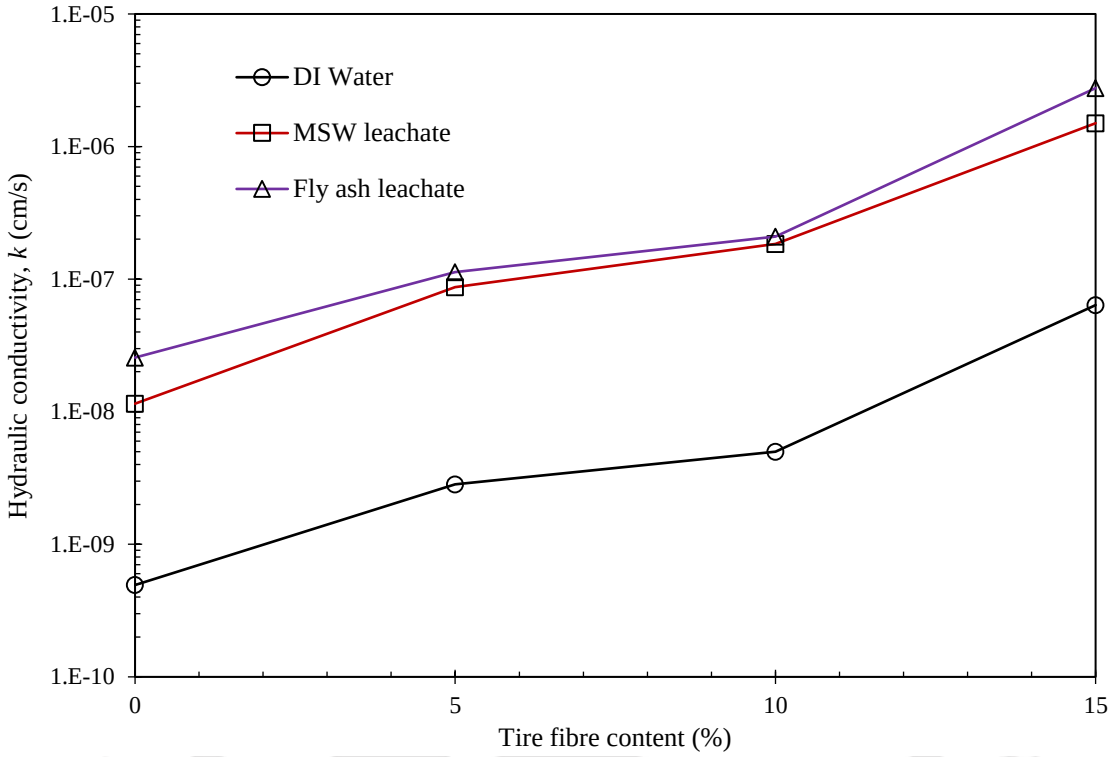

Fig. 7.31. Fibre content vs hydraulic conductivity plots for fibre-mixed BC soil with synthetic leachate permeants cat the void ratio of 0.75.

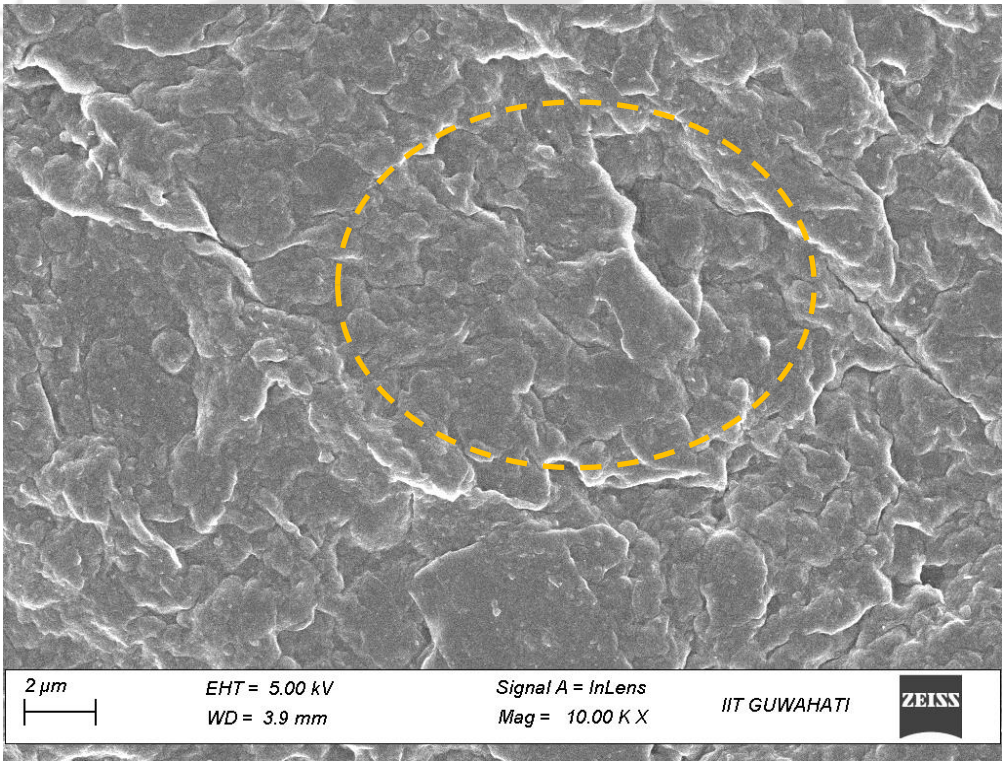

Fig. 7.32. FESEM image of BC soil after permeation of synthetic MSW leachate.

TH-3665_186104109

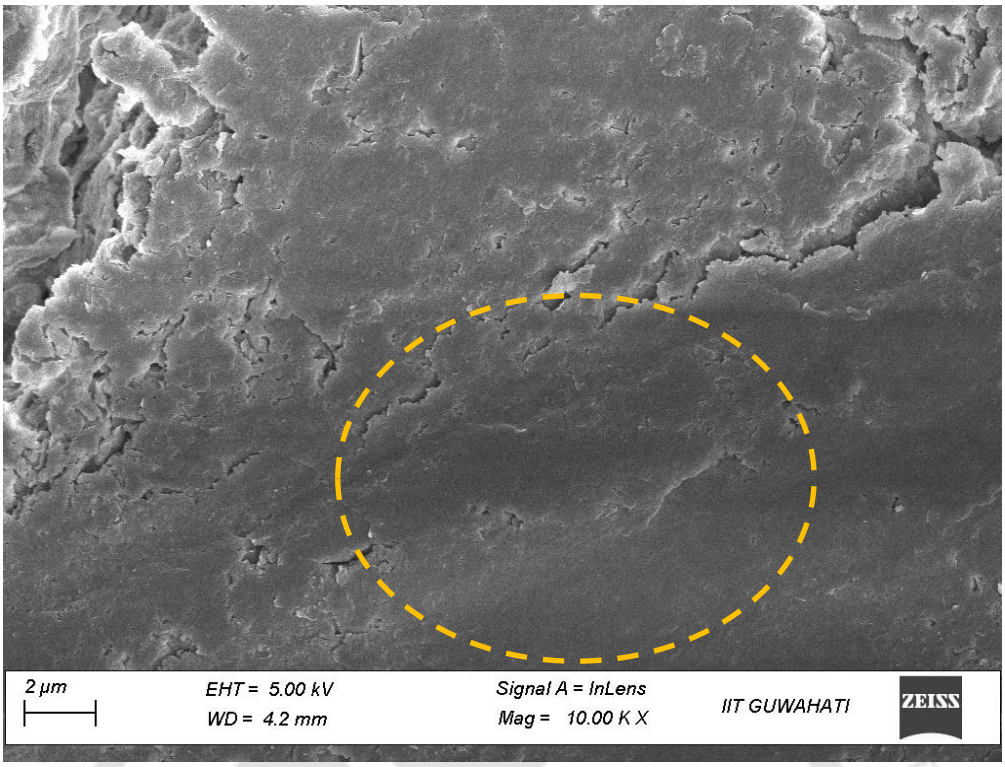

Fig. 7.33. FESEM image of BC soil after permeation of synthetic fly ash leachate.

7.2.9. Influence of leachates on UCS behaviour

The axial stress versus axial strain curves of all fibre-mixed BC soil under two synthetic leachate permeants are depicted in Figs. 7.34-7.37. The results clearly demonstrated that pure BC soil samples reached peak strength values at low strain rates compared to fibre-mixed BC samples, irrespective of leachate type. The peak strength of BC soil with DI water was reported as 594.2 kPa, which was decreased to 522.16 and 511.70 kPa with SML and SFL, respectively, as depicted in Fig. 7.38. It is evident that a slight reduction in peak strength values with both SML and SFL. This reduction in peak strength values was about 12.12 and 13.88% with SML and SFL, respectively, compared to DI water. This reduction in UCS values may attributed to variations in compaction conditions. In this study, all samples including all fibre-mixed soils were compacted at their respective OMC and MDD conditions of DI water. Therefore, the actual compaction conditions of soil samples would vary with respect to leachates (Harun et al., 2013). As leachate increases the MDD (Ray et al., 2022(b)), but the samples were compacted at the MDD corresponding to DI water, the leachate-permeated specimens remained in a looser state, resulting in lower strength. The corresponding peak strains of BC soil were recorded as 5.00, 3.68, and 4.21 with DI water, SML, and SFL, respectively.

TH-3665_186104109

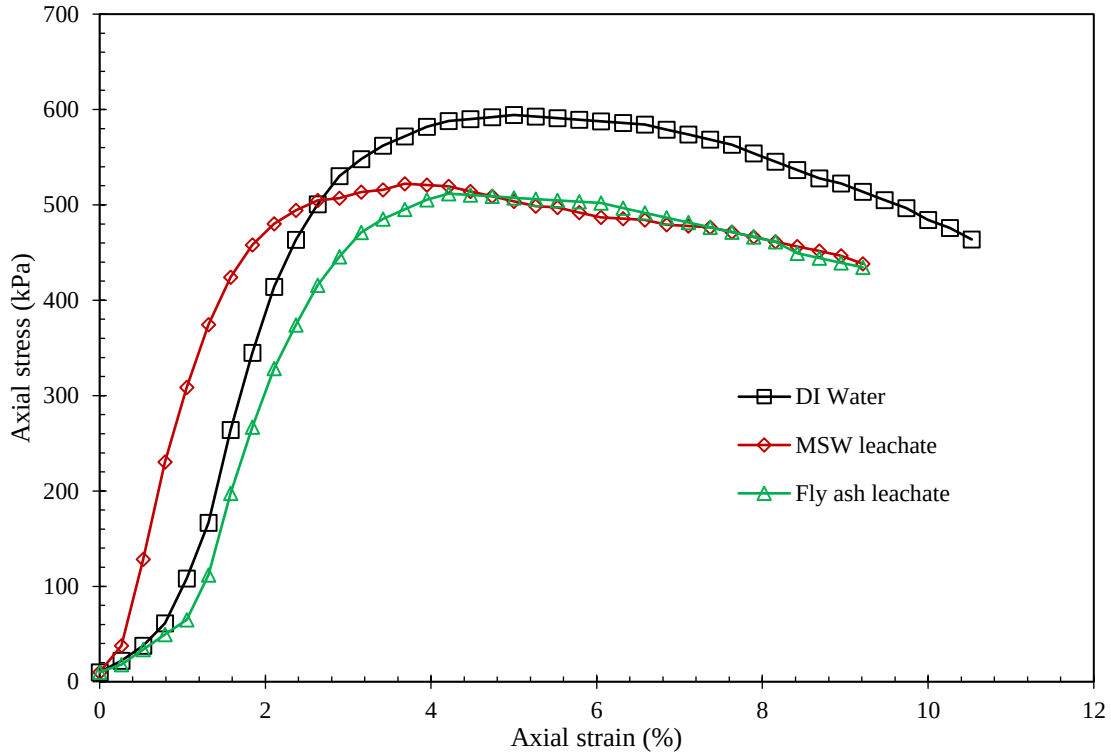

Fig. 7.34. Axial stress vs axial strain behaviour of BC soil with synthetic leachates.

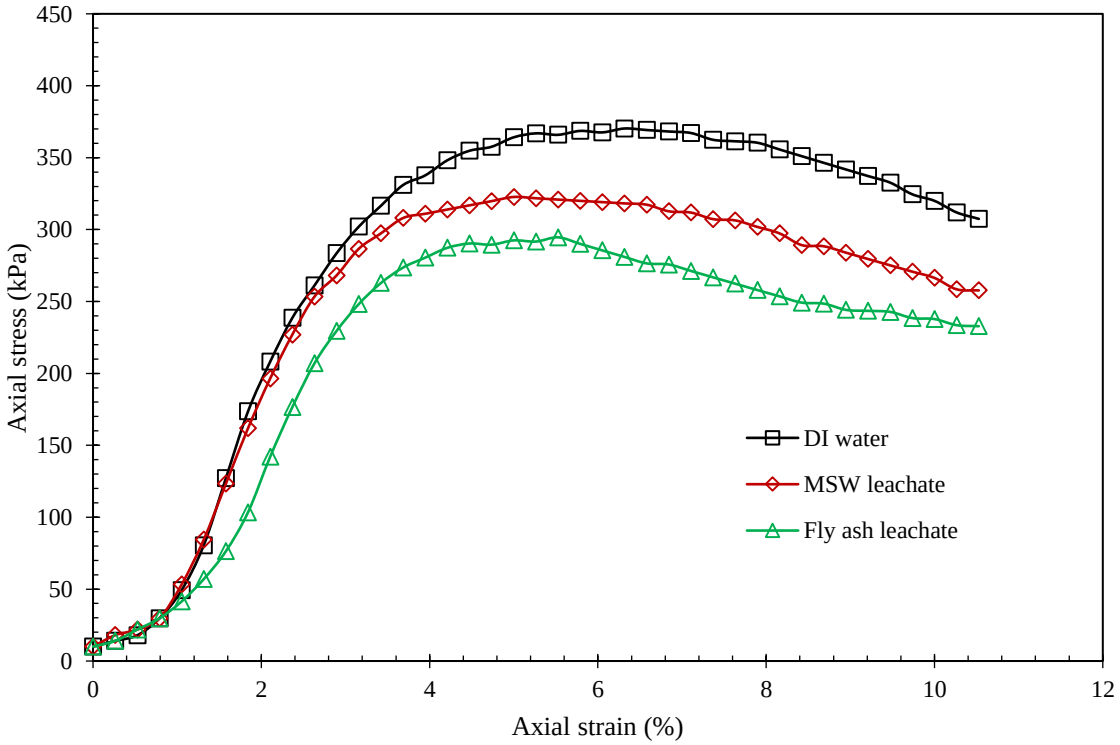

Fig. 7.35. Axial stress vs axial strain behaviour of 5% fibre-mixed BC soil with synthetic leachates.

TH-3665_186104109

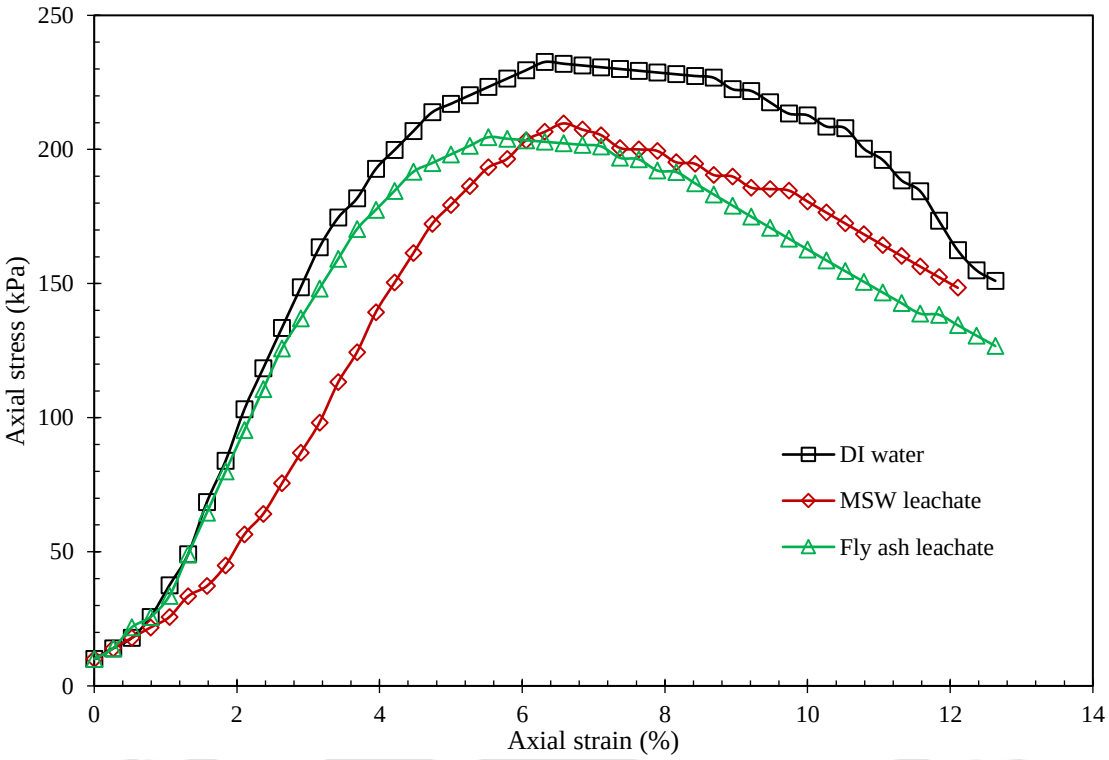

Fig. 7.36. Axial stress vs axial strain behaviour of 10% fibre-mixed BC soil with synthetic leachates.

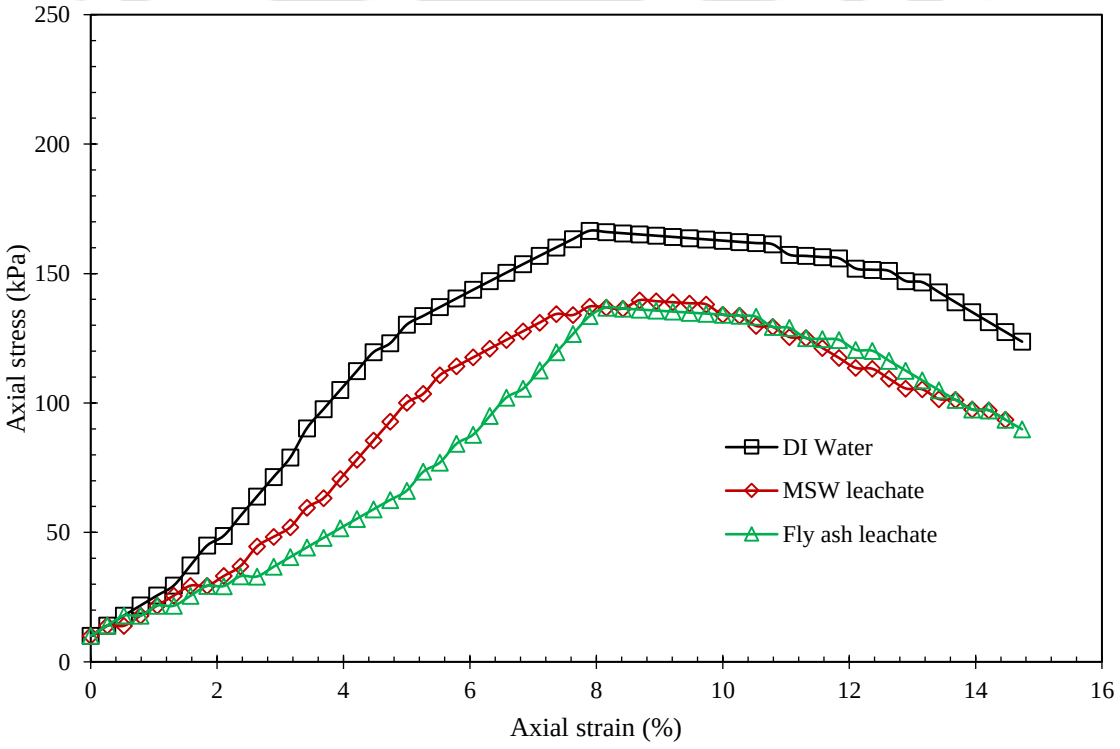

Fig. 7.37. Axial stress vs axial strain behaviour of 15% fibre-mixed BC soil with synthetic leachates.

TH-3665_186104109

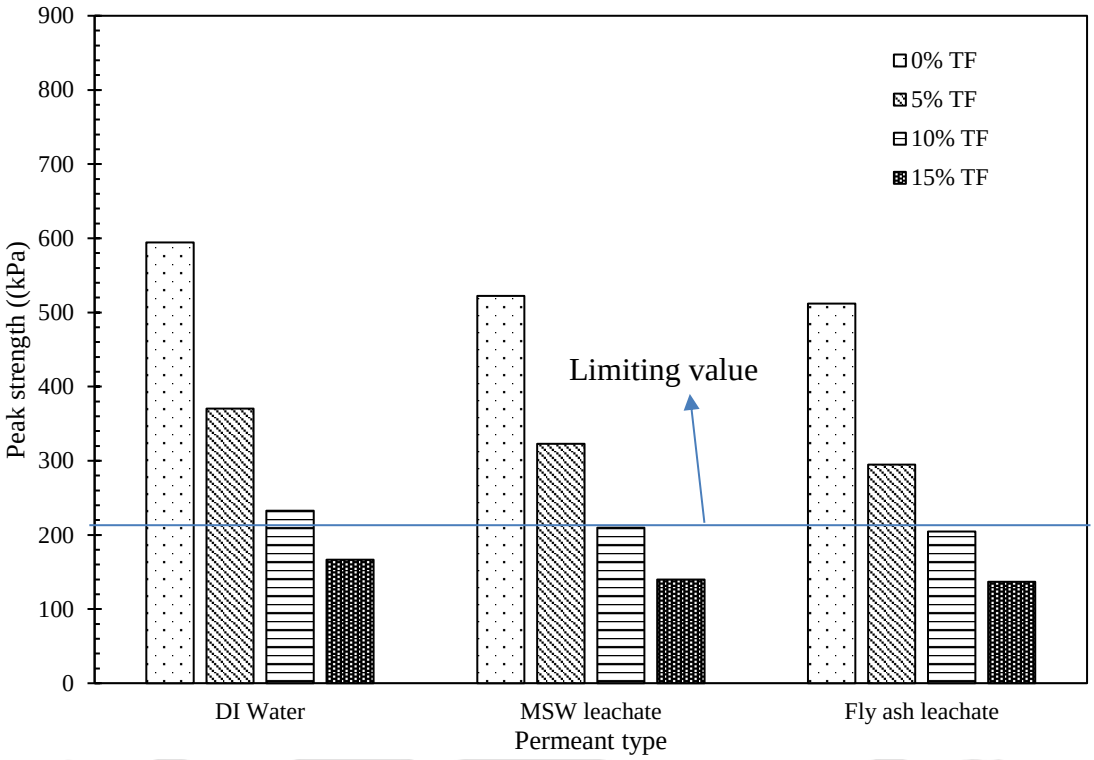

Fig. 7.38. Peak strength values of fibre-mixed BC soil with synthetic leachates.

Similarly, the stress-strain response of 5, 10, and 15% fibre-mixed BC soil samples (Fig. 7.38) displayed similar responses of pure BC soil in strength variations with respect to both synthetic leachates. The peak strength value of 5% fibre-mixed BC soil was determined as 370.2 kPa, which declined to 322.64 and 294.60 kPa with SML and SFL, respectively. The percentage reduction in strength values was about 12.85 and 20.42% with SML and SFL, respectively. However, the peak strains of BC soil were increased with the rise in fibre content, showing the ductile tendency of fibre-soil composite. The peak strains of 5% fibre-mixed BC soil with water, SML, and SFL were reported as 5.26, 5.00, and 5.53%, respectively. Similarly, for 10% fibre-mixed soil, the peak strength values were reduced by about 9.84 and 12.05% with SML and SFL, respectively, compared to DI water. Whereas, for 15% fibre-mixed BC soil, this reduction was about 16.08 and 17.80%, respectively, for the same order of comparison. However, all samples exhibited a limiting strength value (>200 kPa) of barrier material criterion in landfill systems apart from 15% fibre-mixed BC soil samples.

TH-3665_186104109

7.3. Summary

Testing liner material hydromechanical behaviour in the presence of leachate conditions is very crucial. This chapter focused on the index and engineering properties of BC soil under leachate conditions. Also, focused on the influence of leachate permeants on the engineering behaviour of all fibre-mixed (5-15%) BC soils. To achieve this, two synthetic leachates such as synthetic municipal solid waste leachate (SML) and synthetic fly ash leachate (SFL) were prepared in the laboratory. This investigation selected leachates with high concentrations of metals and salts, as identified in previous studies, to evaluate the worst-case scenario. Hence, to achieve these objectives, several laboratory experiments were performed to understand the swelling, consolidation, compressibility, and hydraulic characteristics of barrier material. The experimental results are summarized below:

- Atterberg limits (liquid limit, plastic limit, and plasticity index) and free swell index (FSI) of BC soil were lowered with both synthetic leachates.
- Swelling heights of BC soil were reduced considerably with the permeation of both synthetic leachates. A similar trend was observed with all fibre-mixed BC soil samples, irrespective of fibre content.
- For all samples, the majority of swelling occurred in the primary swelling stage, irrespective of fibre content and leachate type.
- The time required to reach asymptotic swelling was considerably decreased with SFL followed by SML for all fibre-mixed samples.
- The swelling pressures and swelling potentials of BC soil were reduced with both synthetic leachates. More reduction in FSI of BC soil was observed with SFL than with SML.
- A good correlation was observed between measured swelling values and predicted (using the rectangular hyperbola model) swelling values for all samples.
- Coefficient of consolidation and hydraulic conductivity values significantly increased with both synthetic leachates. However, this hike is more with SFL than SML for all fibre-mixed samples.
- Hydraulic conductivity of 15% fibre-mixed BC soil exceeded the limiting criterion under any applied consolidation pressure with both synthetic leachates.
- Unconfined compressive strength values were decreased slightly with the synthetic leachates. This reduction was relatively more with SFL than SML.

TH-3665_186104109

CHAPTER 8

CONCLUSION AND SCOPE FOR FUTURE WORK

8.1. Conclusion

This research work focused on the study of different concentrations of inorganic salts (NaCl and $CaCl_2$), heavy metals (lead, cadmium, and hexavalent chromium), and two types of synthetic leachates (MSW leachate and fly ash leachate) on the geotechnical performance of black cotton (BC) soil mixed with various proportions (0, 5, 10, and 15% by dry weight) of tire fire content. The impact of these chemical concentrations on index properties such as Atterberg limits and free swell index of BC soil and engineering properties such as swelling, consolidation, compressibility, hydraulic conductivity, and shear strength of fibre-mixed BC soil was thoroughly examined by conducting several laboratory experiments. The important conclusions are drawn below:

- Tire-fibres had shown a significant impact on compaction, swelling, consolidation, hydraulic conductivity, compressibility, and unconfined compressive strength (UCS) of black cotton soil. The hydraulic conductivity values of BC soil with all fibre-mixes were observed within the limiting criterion under DI water permeation. However, BC soil exceeded the limiting value from the strength criterion by incorporating 15% tire-fibre content.
- The Atterberg limits and free swell indices were reduced significantly in the presence of inorganic salts, heavy metals, and synthetic leachates. The concentration and the valency of cations play an important role in the behaviour of BC soil.
- All fibre-mixed samples (0, 5, 10, and 15%) were tested under extreme concentrations of inorganic monovalent and divalent salts. However, divalent salt concentrations showed a higher impact on the geotechnical properties of all samples than monovalent salt. This hydraulic conductivity increment was significant for 0.1N and 1.0N concentrations of both salts. However, the $CaCl_2$ permeant showed a great hike compared to NaCl at the same concentration.

TH-3665_186104109

- At any consolidation pressure, the 15% fibre-mixed BC soil exceeded the limiting value for barrier material when subjected to 1.0N monovalent and divalent permeants.
- All fibre-mixed samples were tested under two cationic [Pb(II) and Cd(II)] and one anionic [Cr(VI)] heavy metal concentrations ranging from 100 to 1000 ppm. Consolidation and hydraulic properties of soil samples show only a slight change at lower doses; however, this effect becomes considerable at concentrations of 1000 ppm. Cr(VI) had shown a relatively higher impact on the geotechnical properties of fibre-mixed soil samples, followed by Cd(II). The contribution of K^+ ions from the $K_2Cr_2O_7$ solution and the valency of heavy metal caused this variation in soil properties.
- Leachates had shown a more significant influence on the hydraulic conductivity of fibre-mixed BC soil than individual heavy metal concentrations and low concentrations (0.1N) of inorganic salt solutions. The 15% fibre-mixed BC soil mix exceeded the limiting value for both leachates. However, this hike in hydraulic conductivity value was higher with fly ash leachate than with MSW leachate for all samples, irrespective of fibre content.
- Swelling properties (swelling pressures and swelling potentials) and consolidation parameters (c_v and t_{90}) of fibre-mixed BC soil were significantly influenced by inorganic salts, heavy metals, and synthetic leachates. The synthetic fly ash leachate influence was more significant compared to inorganic salts, MSW leachate, and heavy metal permeants.
- Compression indices of all fibre-mixed BC soil samples were reduced marginally with the increase in concentrations of salts and heavy metals. However, this reduction is more with synthetic leachates followed by inorganic salts and heavy metal permeants.
- Formation of flow channels and aggregation of clay particles observed significantly with high concentrations of inorganic salt, heavy metals, and leachates from FESEM study.
- The UCS values of all fibre-mixed BC soil samples declined marginally with the increase in concentration from 0.1 to 1.0N, irrespective of fibre content.
- There is a slight increment in UCS values of all samples with Pb(II) and Cd(II) concentrations. However, this increment is negligible with 1000 ppm concentrations. On the other hand, slight decrement in UCS values of all samples irrespective of fibre content with Cr(VI) concentrations.
- The reduction in UCS values of fibre-mixed BC soil samples was relatively more with synthetic fly ash leachate compared to synthetic MSW leachate and inorganic salt solutions.

TH-3665_186104109

8.2. Scientific contributions and practical significance

- This study serves as a valuable resource for researchers, design engineers, and site engineers in understanding the index and engineering properties of black cotton soil under the influence of inorganic salts, heavy metals, and leachates. Therefore, it provides an alternative to the use of conventional materials such as bentonites and sand-bentonite mixtures for clay barrier applications.
- Fibre-mixed soils have a wide range of applications in geotechnical, transportation, and geoenvironmental fields. This research has been carried out with a particular focus on landfill barrier application. These results would offer a comprehensive understanding of the influence of various permeants on the hydro-mechanical behaviour of fibre-mixed BC soil.
- The liner material should contain low hydraulic conductivity ($<10^{-7}$ cm/s) and minimum strength (200 kPa) for landfill application. The UCS and hydraulic conductivity results suggested that the naturally available BC soil can be utilized as a barrier material. However, based on the hydraulic conductivity and strength results of fibre-mixed BC soil under different permeants, the acceptable range of tire fibre content was recommended to be up to 10%.
- Finally, many nations would have a solution if these waste tire fibres were utilized for geotechnical and geoenvironmental applications, thereby reducing the significant impact on human health and the environment posed by burning these waste tires and resolving the disposal problem.

8.3. Future scope of the study

The study of BC soil and fibre-mixed BC soil remains an open field with many aspects yet to be fully explored. Future research would focus on the following areas:

- Further investigation is necessary to thoroughly examine tire content's impact on BC soil's desiccation cracking behaviour under varying permeant conditions.
- Further environmental investigations like adsorption studies need to be conducted on BC soil to understand its efficacy in waste containment applications.
- In actual landfill sites, there are numerous organic salts and other dominant heavy metals like zinc, copper, nickel, etc. Further studies need to be done to explore the impact of these contaminants on BC soil and fibre-mixed samples.

TH-3665_186104109

- This study focused on two synthetic leachates. It is also important to study the barrier material under the influence of real MSW and other industrial leachates, such as steel, coke, and waste sewage sludge leachates, which constitute various combinations of heavy metal concentrations.
- The effect of temperature on the geotechnical behaviour of BC soil and fibre-mixed soil samples needs to be considered for further investigations.

भारतीय प्रौद्योगिकी संस्थान गुवाहाटी • Indian Institute of Technology Guwahati •

TH-3665_186104109

REFERENCES

Abbaspour, M., Aflaki, E. and Nejad, F.M., 2019. Reuse of waste tire textile fibers as soil reinforcement. *Journal of cleaner production*, *207*, pp.1059-1071.

Abollino, O., Aceto, M., Malandrino, M., Sarzanini, C. and Mentasti, E., 2003. Adsorption of heavy metals on Na-montmorillonite. Effect of pH and organic substances. *Water research*, *37*(7), pp.1619-1627.

Agamuthu, P., 2013. Landfilling in developing countries. *Waste Management & Research*, *31*(1), pp.1-2.

Akbarimehr, D., Eslami, A., Aflaki, E. and Hajitaheriha, M.M., 2021. Investigating the effect of waste rubber in granular form on strength behavior of Tehran clay. *Arabian Journal of Geosciences*, *14*(18), pp.1-12.

Akbulut, S., Arasan, S. and Kalkan, E., 2007. Modification of clayey soils using scrap tire rubber and synthetic fibers. *Applied Clay Science*, *38*(1-2), pp.23-32.

Al-Tabbaa, A. and Aravinthan, T., 1998. Natural clay-shredded tire mixtures as landfill barrier materials. *Waste Management*, *18*(1), pp.9-16.

Al-Tabbaa, A., Blackwell, O. and Porter, S.A., 1997. An investigation into the geotechnical properties of soil-tyre mixtures. *Environmental technology*, *18*(8), pp.855-860.

Alther, G., Evans, J.C., Fang, H.Y. and Witmer, K., 1985. *Influence of inorganic permeants upon the permeability of bentonite* (pp. 64-73). ASTM International.

Amadi, A.A., 2014. Enhancing durability of quarry fines modified black cotton soil subgrade with cement kiln dust stabilization. *Transportation Geotechnics*, *1*(1), pp.55-61.

Arasan, S. and Yetımoğlu, T., 2008. Effect of Inorganic Salt Solutions on the Consistency Limits of Two Clays. *Turkish Journal of Engineering & Environmental Sciences*, *32*(2).

Arasan, S., Akbulut, R.K., Yetimoglu, T. and Yilmaz, G., 2010. Swelling pressure of compacted clay liners contaminated with inorganic salt solutions. *Environmental & Engineering Geoscience*, *16*(4), pp.401-409.

Arulrajah, A., Mohammadinia, A., Maghool, F. and Horpibulsuk, S., 2019. Tire derived aggregates as a supplementary material with recycled demolition concrete for pavement applications. *Journal of Cleaner Production*, *230*, pp.129-136.

Asadzadeh, M. and Ersizad, A., 2013. Effect of tire-chips on geotechnical properties of clayey soil. In *International Symposium on Advances in Science and Technology* (Vol. 3, No. 2, pp. 117-120).

ASTM D2166, 2013. Standard Test Method for Unconfined Compressive Strength of Cohesive Soil. ASTM International, *West Conshohocken, PA*.

TH-3665_186104109

ASTM D2435, 2010. Standard Test Methods for One-Dimensional Consolidation Properties of Soils Using Incremental Loading, ASTM International, *West Conshohocken*, PA.

ASTM D422, 2007. Standard Test Method for Particle-Size Analysis of Soils, ASTM International, *West Conshohocken*, PA.

ASTM D4318, 2010. Liquid Limit, Plastic Limit, and Plasticity Index of Soils, ASTM International, *West Conshohocken*, PA.

ASTM D6270, 2008. Standard practice of for use scrap tires in civil engineering applications. ASTM International, *West Conshohocken*, PA, USA.

ASTM D698, 2012. Standard Test Methods for Laboratory Compaction Characteristics of Soil Using Standard Effort (12 , 400 ft-lbf / ft 3 (600 kN-m / m 3)), ASTM International, *West Conshohocken*, PA.

ASTM D854, 2014. Standard Test Methods for Specific Gravity of Soil Solids by Water Pycnometer, ASTM International, *West Conshohocken*, PA.

Atahu, M.K., Saathoff, F. and Gebissa, A., 2019. Strength and compressibility behaviors of expansive soil treated with coffee husk ash. *Journal of Rock Mechanics and Geotechnical Engineering*, *11*(2), pp.337-348.

Banchhor, A., Pandey, M., Chakraborty, M. and Pandey, P.K., 2020. Hazardous waste disposal in stromatolitic-limestone terrain and hexavalent chromium contamination in Chhattisgarh state, India. *Journal of Health and Pollution*, *10*(27), p.200907.

Bandipally, S., Cherian, C. and Arnepalli, D.N., 2018. Characterization of lime-treated bentonite using thermogravimetric analysis for assessing its short-term strength behaviour. *Indian Geotechnical Journal*, *48*, pp.393-404.

Bekhiti, M., Trouzine, H. and Rabehi, M., 2019. Influence of waste tire rubber fibers on swelling behavior, unconfined compressive strength and ductility of cement stabilized bentonite clay soil. *Construction and Building Materials*, *208*, pp.304-313.

Benson, C.H. and Othman, M.A., 1993. Hydraulic and mechanical characteristics of a compacted municipal solid waste compost. *Waste Management & Research*, *11*(2), pp.127-142.

Benson, C.H., Daniel, D.E. and Boutwell, G.P., 1999. Field performance of compacted clay liners. *Journal of Geotechnical and Geoenvironmental Engineering*, *125*(5), pp.390-403.

BIS, I., 1977. 2720 Methods of Test for Soils: Part 40 Determination of Free Swell Index of Soils. *Bureau of Indian Standards, New Delhi, India*, pp.1-5.

Bolt, G.H., 1956. Physico-chemical analysis of the compressibility of pure clays. *Geotechnique*, *6*(2), pp.86-93.

Booker, J.R., Quigley, R.M. and Rowe, R.K., 1997. *Clayey barrier systems for waste disposal facilities*. CRC Press.

TH-3665_186104109

Bouazza, A., Liu, Y. and Gates, W., 2013. Effect of strong acidic leachates on hydraulic conductivity of a needle punched GCL. In *Heapleach Conference, Vancouver, Canada*.

Bowders Jr, J.J. and Daniel, D.E., 1987. Hydraulic conductivity of compacted clay to dilute organic chemicals. *Journal of Geotechnical Engineering*, *113*(12), pp.1432-1448.

Bucher F, Müller-Vonmoos M. Bentonite as a containment barrier for the disposal of highly radioactive wastes. Applied Clay Science. 1989 Jun 1;4(2):157-77.

Bušić, R., Miličević, I., Šipoš, T.K. and Strukar, K., 2018. Recycled rubber as an aggregate replacement in self-compacting concrete—Literature overview. *Materials*, *11*(9), p.1729.

Cabalar, A.F., Karabash, Z. and Mustafa, W.S., 2014. Stabilising a clay using tyre buffings and lime. *Road materials and pavement design*, *15*(4), pp.872-891.

Casarett, L.J., 2008. *Casarett and Doull's toxicology: the basic science of poisons* (Vol. 71470514). New York: McGraw-Hill.

Cetin, H., Fener, M. and Gunaydin, O., 2006. Geotechnical properties of tire-cohesive clayey soil mixtures as a fill material. *Engineering geology*, *88*(1-2), pp.110-120.

Chaduvula, U., Viswanadham, B.V.S. and Kodikara, J., 2017. A study on desiccation cracking behavior of polyester fiber-reinforced expansive clay. *Applied Clay Science*, *142*, pp.163-172.

Chai, J.C. and Fu, H.T., 2021. Effect of chemical additives on the consolidation behavior of slurries. *Marine Georesources & Geotechnology*, *39*(7), pp.790-797.

Chai, J.C. and Miura, N., 2002. Comparing the performance of landfill liner systems. *Journal of material cycles and waste management*, *4*, pp.135-142.

Chalermyanont, T., Arrykul, S. and Charoenthaisong, N., 2009. Potential use of lateritic and marine clay soils as landfill liners to retain heavy metals. *Waste Management*, *29*(1), pp.117-127.

Chapman, D.L., 1913. LI. A contribution to the theory of electrocapillarity. *The London, Edinburgh, and Dublin philosophical magazine and journal of science*, *25*(148), pp.475-481.

Chegenizadeh, A., Keramatikerman, M., Dalla Santa, G. and Nikraz, H., 2018. Influence of recycled tyre amendment on the mechanical behaviour of soil-bentonite cut-off walls. *Journal of cleaner production*, *177*, pp.507-515.

Chen, F.H., 2012. *Foundations on expansive soils* (Vol. 12). Elsevier.

Chen, J.N., Benson, C.H. and Edil, T.B., 2018. Hydraulic conductivity of geosynthetic clay liners with sodium bentonite to coal combustion product leachates. *Journal of Geotechnical and Geoenvironmental Engineering*, *144*(3), p.04018008.

Chen, Y.G., Jia, L.Y., Li, Q., Ye, W.M., Cui, Y.J. and Chen, B., 2017. Swelling deformation of compacted GMZ bentonite experiencing chemical cycles of sodium-calcium exchange and salinization-desalinization effect. *Applied Clay Science*, *141*, pp.55-63.

TH-3665_186104109

Christensen, T.H. and Kjeldsen, P., 1989. Basic biochemical processes in landfills. *IN: Sanitary Landfilling: Process, Technology, and Environmental Impact. Academic Press, New York. 1989. p* 29-49.

Cokca, E. and Yilmaz, Z., 2004. Use of rubber and bentonite added fly ash as a liner material. *Waste management*, *24*(2), pp.153-164.

Cokca, E. and Yilmaz, Z., 2004. Use of rubber and bentonite added fly ash as a liner material. *Waste management*, *24*(2), pp.153-164.

Dakshanamurthy, V., 1978. A new method to predict swelling using a hyperbolic equation. *Geotechnical Engineering*, *9*(1).

Daniel, D.E. and Wu, Y.K., 1993. Compacted clay liners and covers for arid sites. *Journal of Geotechnical Engineering*, *119*(2), pp.223-237.

Demdoum, A., Gueddouda, M.K., Goual, I., Souli, H. and Ghembaza, M.S., 2020. Effect of landfill leachate on the hydromechanical behavior of bentonite-geomaterials mixture. *Construction and Building Materials*, *234*, p.117356.

Di Maio, C., Santoli, L. and Schiavone, P., 2004. Volume change behaviour of clays: the influence of mineral composition, pore fluid composition and stress state. *Mechanics of materials*, *36*(5-6), pp.435-451.

Divya, P.V., Viswanadham, B.V.S. and Gourc, J.P., 2014. Evaluation of tensile strength-strain characteristics of fiber-reinforced soil through laboratory tests. *Journal of Materials in civil Engineering*, *26*(1), pp.14-23.

Du, Y.J., Fan, R.D., Reddy, K.R., Liu, S.Y. and Yang, Y.L., 2015. Impacts of presence of lead contamination in clayey soil–calcium bentonite cutoff wall backfills. *Applied Clay Science*, *108*, pp.111-122.

Dunham-Friel, J. and Carraro, J.A.H., 2014. Effects of compaction effort, inclusion stiffness, and rubber size on the shear strength and stiffness of expansive Soil-Rubber (ESR) Mixtures. In *Geo-Congress 2014: Geo-characterization and Modeling for Sustainability* (pp. 3635-3644).

Dutta, J. and Mishra, A.K., 2015. A study on the influence of inorganic salts on the behaviour of compacted bentonites. *Applied Clay Science*, *116*, pp.85-92.

Dutta, J. and Mishra, A.K., 2016(a). Consolidation behaviour of bentonites in the presence of salt solutions. *Applied Clay Science*, *120*, pp.61-69.

Dutta, J. and Mishra, A.K., 2016(b). Influence of the presence of heavy metals on the behaviour of bentonites. *Environmental Earth Sciences*, *75*(11), pp.1-10.

Dutta, J., Mishra, A.K. and Das, P., 2018. Combined effect of inorganic salts and heavy metals on the engineering behaviour of compacted bentonites. *International Journal of Geosynthetics and Ground Engineering*, *4*, pp.1-11.

TH-3665_186104109

Egloffstein, T., 2020. Properties and test methods to assess bentonite used in geosynthetic clay liners. In *Geosynthetic clay liners* (pp. 51-72). CRC Press.

Erenson, C., 2023. Dispersion characteristics of clayey soils containing waste rubber particles. *Journal of Rock Mechanics and Geotechnical Engineering*, *15*(11), pp.3050-3058.

Etim, R.K., Eberemu, A.O. and Osinubi, K.J., 2017. Stabilization of black cotton soil with lime and iron ore tailings admixture. *Transportation Geotechnics*, *10*, pp.85-95.

Fan, R.D., Reddy, K.R., Yang, Y.L. and Du, Y.J., 2020. Index properties, hydraulic conductivity and contaminant-compatibility of CMC-treated sodium activated calcium bentonite. *International Journal of Environmental Research and Public Health*, *17*(6), p.1863.

Gleason, M.H., Daniel, D.E. and Eykholt, G.R., 1997. Calcium and sodium bentonite for hydraulic containment applications. *Journal of geotechnical and geoenvironmental engineering*, *123*(5), pp.438-445.

Gleason, M.H., Daniel, D.E. and Eykholt, G.R., 1997. Calcium and sodium bentonite for hydraulic containment applications. *Journal of geotechnical and geoenvironmental engineering*, *123*(5), pp.438-445.

Gobinath, R., Ganapathy, G.P., Akinwumi, I.I., Kovendiran, S., Hema, S. and Thangaraj, M., 2016. Plasticity, strength, permeability and compressibility characteristics of black cotton soil stabilized with precipitated silica. *Journal of central south university*, *23*, pp.2688-2694.

Gouy, M.J.J.P.T.A., 1910. Sur la constitution de la charge électrique à la surface d'un électrolyte. *J. Phys. Theor. Appl.*, *9*(1), pp.457-468.

Gujre, N., Rangan, L. and Mitra, S., 2021. Occurrence, geochemical fraction, ecological and health risk assessment of cadmium, copper and nickel in soils contaminated with municipal solid wastes. *Chemosphere*, *271*, p.129573.

Gupt, C.B., Bordoloi, S., Sahoo, R.K. and Sekharan, S., 2021. Mechanical performance and micro-structure of bentonite-fly ash and bentonite-sand mixes for landfill liner application. *Journal of Cleaner Production*, *292*, p.126033.

Gupt, C.B., Bordoloi, S., Sahoo, R.K. and Sekharan, S., 2021. Mechanical performance and micro-structure of bentonite-fly ash and bentonite-sand mixes for landfill liner application. *Journal of Cleaner Production*, *292*, p.126033.

Gupt, C.B., Bordoloi, S., Sekharan, S. and Sarmah, A.K., 2020. A feasibility study of Indian fly ash-bentonite as an alternative adsorbent composite to sand-bentonite mixes in landfill liner. *Environmental Pollution*, *265*, p.114811.

Haigh, S.K., Vardanega, P.J. and Bolton, M.D., 2013. The plastic limit of clays. *Géotechnique*, *63*(6), pp.435-440.

TH-3665_186104109

Haq, M., Khan, M.A., Ali, S., Ali, K., Yusuf, M., Kamyab, H. and Irshad, K., 2024. Enhancing clayey soil performance with lime and waste rubber tyre powder: Mechanical, microstructural, and statistical analysis. *Environmental Research*, *256*, p.119217.

Harianto, T., Hayashi, S., Du, Y.J. and Suetsugu, D., 2008. Effects of fiber additives on the desiccation crack behavior of the compacted Akaboku soil as a material for landfill cover barrier. *Water, air, and soil pollution*, *194*(1), pp.141-149.

Harun, N.S., Ali, Z.R., Rahim, A.S., Lihan, T. and Idris, R.M.W., 2013, November. Effects of leachate on geotechnical characteristics of sandy clay soil. In *AIP Conference Proceedings* (Vol. 1571, No. 1, pp. 530-536). American Institute of Physics.

Hasan, H.A., Mohammed, L.H.A. and Masood, L.G.G., 2020, June. Effect of rubber tire on behaviour of subgrade expansive Iraqi soils. In *IOP Conference Series: Materials Science and Engineering* (Vol. 870, No. 1, p. 012066).

Hauser, V.L., Weand, B.L. and Gill, M.D., 2001. Natural covers for landfills and buried waste. *Journal of Environmental Engineering*, *127*(9), pp.768-775.

He, Y., Wang, M.M., Wu, D.Y., Zhang, K.N., Chen, Y.G. and Ye, W.M., 2021. Effects of chemical solutions on the hydromechanical behavior of a laterite/bentonite mixture used as an engineered barrier. *Bulletin of Engineering Geology and the Environment*, *80*(2), pp.1169-1180.

He, Y., Wang, M.M., Wu, D.Y., Zhang, K.N., Chen, Y.G. and Ye, W.M., 2021. Effects of chemical solutions on the hydromechanical behavior of a laterite/bentonite mixture used as an engineered barrier. *Bulletin of Engineering Geology and the Environment*, *80*(2), pp.1169-1180.

He, Y., Ye, W.M., Chen, Y.G., Zhang, K.N. and Wu, D.Y., 2020. Effects of NaCl solution on the swelling and shrinkage behavior of compacted bentonite under one-dimensional conditions. *Bulletin of Engineering Geology and the Environment*, *79*(1), pp.399-410.

He, Z.L., Yang, X.E. and Stoffella, P.J., 2005. Trace elements in agroecosystems and impacts on the environment. *Journal of Trace elements in Medicine and Biology*, *19*(2-3), pp.125-140.

Ho, M.H. and Chan, C.M., 2010. The potential of using rubberchips as a soft clay stabilizer enhancing agent. *Modern Applied Science*, *4*(10), p.122.

Ho, M.H., Chan, C.M. and Bakar, I., 2010. One dimensional compressibility characteristics of clay stabilised with cement-rubber chips. *International Journal of Sustainable Construction Engineering and Technology*, *1*(2), pp.91-104.

Hoornweg, D. and Bhada-Tata, P., 2012. What a waste: a global review of solid waste management.

Hughes, K.L., Christy, A.D., Heimlich, J.E., (2007). Landfill Types and Liner Systems (Extension Fact Sheet CDFS-138). Cincinnati, Ohio: Ohio State University

Ikeagwuani, C.C. and Nwonu, D.C., 2019. Emerging trends in expansive soil stabilisation: A review. *Journal of rock mechanics and geotechnical engineering*, *11*(2), pp.423-440.

Irani, N. and Ghasemi, M., 2019. Effect of scrap tyre on strength properties of untreated and lime-treated clayey sand. *European Journal of Environmental and Civil Engineering*, pp.1-18.

Jadda, K. and Bag, R., 2020. Variation of swelling pressure, consolidation characteristics and hydraulic conductivity of two Indian bentonites due to electrolyte concentration. *Engineering Geology*, *272*, p.105637.

Jafari, M. and Esna-ashari, M., 2012. Effect of waste tire cord reinforcement on unconfined compressive strength of lime stabilized clayey soil under freeze–thaw condition. *Cold Regions Science and Technology*, *82*, pp.21-29.

Jellander, R., Marčelja, S. and Quirk, J.P., 1988. Attractive double-layer interactions between calcium clay particles. *Journal of Colloid and Interface Science*, *126*(1), pp.194-211.

Jo, H.Y., Katsumi, T., Benson, C.H. and Edil, T.B., 2001. Hydraulic conductivity and swelling of nonprehydrated GCLs permeated with single-species salt solutions. *Journal of geotechnical and geoenvironmental engineering*, *127*(7), pp.557-567.

Jones Jr, D.E. and Holtz, W.G., 1973. Expansive soils-the hidden disaster. *Civil Engineering*, *43*(8).

Kalkan, E., 2013. Preparation of scrap tire rubber fiber–silica fume mixtures for modification of clayey soils. *Applied Clay Science*, *80*, pp.117-125.

Kayabali, K., 1997. Engineering aspects of a novel landfill liner material: bentonite-amended natural zeolite. *Engineering Geology*, *46*(2), pp.105-114.

Kim, Y.T. and Kang, H.S., 2013. Effects of rubber and bottom ash inclusion on geotechnical characteristics of composite geomaterial. *Marine Georesources & Geotechnology*, *31*(1), pp.71-85.

Kittrick, J.A., 1969. Interlayer forces in montmorillonite and vermiculite. *Soil Science Society of America Journal*, *33*(2), pp.217-222.

Kjeldsen, P., Barlaz, M.A., Rooker, A.P., Baun, A., Ledin, A. and Christensen, T.H., 2002. Present and long-term composition of MSW landfill leachate: a review. *Critical reviews in environmental science and technology*, *32*(4), pp.297-336.

Koerner, R.M. and Daniel, D.E., (1997). Final covers for solid waste landfills and abandoned dumps. Thomas Telford.

Kraehenbuehl, F., Stoeckli, H.F., Brunner, F., Kahr, G. and Müller-Vonmoos, M., 1987. Study of the water-bentonite system by vapour adsorption, immersion calorimetry and X-ray techniques: I. Micropore volumes and internal surface areas, following Dubinin's theory. *Clay Minerals*, 22(1), pp.1-9.

Kumar, P.R., Kumar, P.S.P. and Maheswari, G., 2017. Laboratory study of black cotton soil blended with copper slag and fly ash. *Int J Innov Res Sci Eng Technol*, *6*(2), p.19601967.

TH-3665_186104109

Laird, D.A., 1996. Model for crystalline swelling of 2: 1 phyllosilicates. *Clays and Clay Minerals*, *44*, pp.553-559.

Laird, D.A., 2006. Influence of layer charge on swelling of smectites. *Applied clay science*, *34*(1-4), pp.74-87.

Lee, J.M. and Shackelford, C.D., 2005. Impact of bentonite quality on hydraulic conductivity of geosynthetic clay liners. *Journal of geotechnical and geoenvironmental engineering*, *131*(1), pp.64-77.

Li, J.S., Xue, Q., Wang, P. and Li, Z.Z., 2015. Effect of lead (II) on the mechanical behavior and microstructure development of a Chinese clay. *Applied Clay Science*, *105*, pp.192-199.

Li, L., Lin, C. and Zhang, Z., 2017. Utilization of shale-clay mixtures as a landfill liner material to retain heavy metals. *Materials & Design*, *114*, pp.73-82.

Li, L.Y. and Li, F., 2001. Heavy metal sorption and hydraulic conductivity studies using three types of bentonite admixes. *Journal of Environmental Engineering*, *127*(5), pp.420-429.

Li, L.Y., Ohtsubo, M., Higashi, T., Yamaoka, S. and Morishita, T., 2007. Leachability of municipal solid waste ashes in simulated landfill conditions. *Waste Management*, *27*(7), pp.932-945.

Liu, L., Cai, G. and Liu, S., 2018. Compression properties and micro-mechanisms of rubber-sand particle mixtures considering grain breakage. *Construction and Building Materials*, *187*, pp.1061-1072.

Liu, L., Cai, G., Zhang, J., Liu, X. and Liu, K., 2020. Evaluation of engineering properties and environmental effect of recycled waste tire-sand/soil in geotechnical engineering: A compressive review. *Renewable and Sustainable Energy Reviews*, *126*, p.109831.

Liu, L., Cai, G., Zhang, J., Liu, X. and Liu, K., 2020. Evaluation of engineering properties and environmental effect of recycled waste tire-sand/soil in geotechnical engineering: A compressive review. *Renewable and Sustainable Energy Reviews*, *126*, p.109831.

Lo, I.M., Luk, A.F. and Yang, X., 2004. Migration of heavy metals in saturated sand and bentonite/soil admixture. *Journal of Environmental Engineering*, *130*(8), pp.906-909.

Long, Y.Y., Shen, D.S., Wang, H.T., Lu, W.J. and Zhao, Y., 2011. Heavy metal source analysis in municipal solid waste (MSW): case study on Cu and Zn. *Journal of hazardous materials*, *186*(2-3), pp.1082-1087.

Lutz, J.F. and Kemper, W.D., 1959. Intrinsic permeability of clay as affected by clay-water interaction. *Soil science*, *88*(2), pp.83-90.

Madsen, F.T. and Müller-Vonmoos, M., 1989. The swelling behaviour of clays. *Applied Clay Science*, *4*(2), pp.143-156.

Maher, M.H. and Ho, Y.C., 1994. Mechanical properties of kaolinite/fiber soil composite. *Journal of Geotechnical Engineering*, *120*(8), pp.1381-1393.

TH-3665_186104109

Malav, L.C., Yadav, K.K., Gupta, N., Kumar, S., Sharma, G.K., Krishnan, S., Rezania, S., Kamyab, H., Pham, Q.B., Yadav, S. and Bhattacharyya, S., 2020. A review on municipal solid waste as a renewable source for waste-to-energy project in India: Current practices, challenges, and future opportunities. *Journal of Cleaner Production*, *277*, p.123227.

Malik, V. and Priyadarshee, A., 2018. Compaction and swelling behavior of black cotton soil mixed with different non-cementitious materials. *International Journal of Geotechnical Engineering*, *12*(4), pp.413-419.

Malik, V. and Priyadarshee, A., 2018. Compaction and swelling behavior of black cotton soil mixed with different non-cementitious materials. *International Journal of Geotechnical Engineering*, *12*(4), pp.413-419.

Marefat, V. & Soltani-Jigheh, H. 2011. Laboratory behavior of clay-tire mixtures, *World Apply Science Journal*, (*13*)5, pp012. 1035-1041.

Mc Bride M (1994) Environmental chemistry of soils., Oxford University Press, New York.

Mesri, G. and Olson, R.E., 1971. Consolidation characteristics of montmorillonite. *Geotechnique*, *21*(4), pp.341-352.

Miller, C.J. and Rifai, S., 2004. Fiber reinforcement for waste containment soil liners. *Journal of Environmental Engineering*, *130*(8), pp.891-895.

Mir, B.A. and Sridharan, A., 2014. Volume change behavior of clayey soil–fly ash mixtures. *International Journal of Geotechnical Engineering*, *8*(1), pp.72-83.

Mir, B.A. and Sridharan, A., 2014. Volume change behavior of clayey soil–fly ash mixtures. *International Journal of Geotechnical Engineering*, *8*(1), pp.72-83.

Mishra, A., Ohtsubo, M., Li, L. and Higashi, T., 2010. Prediction of compressibility and hydraulic conductivity of soil-bentonite mixture. International Journal of Geotechnical Engineering, 4(3), pp.417-424.

Mishra, A.K., Dhawan, S. and Rao, S.M., 2008. Analysis of swelling and shrinkage behavior of compacted clays. *Geotechnical and Geological Engineering*, *26*(3), pp.289-298.

Mishra, A.K., Dhawan, S. and Rao, S.M., 2008. Analysis of swelling and shrinkage behavior of compacted clays. *Geotechnical and Geological Engineering*, *26*(3), pp.289-298.

Mishra, A.K., Dutta, J. and Chingtham, R., 2015. A study on the behavior of the compacted bentonite in the presence of salt solutions. *International Journal of Geotechnical Engineering*, *9*(4), pp.354-362.

Mishra, A.K., Ohtsubo, M., Li, L. and Higashi, T., 2005. Effect of salt concentrations on the permeability and compressibility of soil-bentonite mixtures.

Mishra, A.K., Ohtsubo, M., Li, L.Y., Higashi, T. and Park, J., 2009. Effect of salt of various concentrations on liquid limit, and hydraulic conductivity of different soil-bentonite mixtures. *Environmental geology*, *57*, pp.1145-1153.

TH-3665_186104109

Mistry, M.K., Shukla, S.J., Solanki, C.H. and Shukla, S.K., 2020. Consolidation and Hydraulic Conductivity of High-Plastic Clay Reinforced with Waste Tire Fibers. *Journal of Testing and Evaluation*, *49*(6).

Mitchell, J. K. & Soga, K. (2005). Fundamentals of Soil Behavior, 3rd edition. John Wiley & Sons, Hoboken, NJ, USA.

Mitchell, J.K. and Jaber, M., 1990. Factors controlling the long-term properties of clay liners. *Geotechnical special publication*, (26), pp.84-105.

Moghal, A.A.B., Ashfaq, M., Al-Shamrani, M.A. and Al-Mahbashi, A., 2020. Effect of heavy metal contamination on the compressibility and strength characteristics of chemically modified semiarid soils. *Journal of Hazardous, Toxic, and Radioactive Waste*, *24*(4), p.04020029.

Mohammed, S.A.S., Sanaulla, P.F. and Moghal, A.A.B., 2016. Sustainable use of locally available red earth and black cotton soils in retaining Cd 2^+ and Ni 2^+ from aqueous solutions. *International Journal of Civil Engineering*, *14*, pp.491-505.

Mukherjee, K. and Mishra, A.K., 2017. The impact of scrapped tyre chips on the mechanical properties of liner materials. *Environmental Processes*, *4*(1), pp.219-233.

Mukherjee, K. and Mishra, A.K., 2019(b). Hydraulic and mechanical characteristics of compacted sand–bentonite: Tyre chips mix for its landfill application. *Environment, Development and Sustainability*, *21*(3), pp.1411-1428.

Mukherjee, K. and Mishra, A.K., 2019b. Evaluation of hydraulic and strength characteristics of sand-bentonite mixtures with added tire fiber for landfill application. *Journal of Environmental Engineering*, *145*(6), p.04019026.

Mukherjee, K. and Mishra, A.K., 2021. Recycled waste tire fiber as a sustainable reinforcement in compacted sand–bentonite mixture for landfill application. *Journal of Cleaner Production*, *329*, p.129691.

Murmu, A.L., Dhole, N. and Patel, A., 2020. Stabilisation of black cotton soil for subgrade application using fly ash geopolymer. *Road Materials and Pavement Design*, *21*(3), pp.867-885.

Muththalib, A. and Baudet, B.A., 2019. Effect of heavy metal contamination on the plasticity of kaolin-bentonite clay mixtures and an illite-smectite rich natural clay. In *E3S web of conferences* (Vol. 92, p. 10005). EDP Sciences.

Nagaraj, H., Munnas, M. and Sridharan, A., 2010. Swelling behavior of expansive soils. *International Journal of Geotechnical Engineering*, *4*(1), pp.99-110.

Najim, K.B. and Hall, M.R., 2010. A review of the fresh/hardened properties and applications for plain-(PRC) and self-compacting rubberised concrete (SCRC). *Construction and building materials*, *24*(11), pp.2043-2051.

Namadi, A.H., Motlagh, A.H., Hassanlourad, M. and Hosseinzadeh, M., 2023. Impact of Heavy Metal and Carbonate on Geotechnical Properties of Sand-Bentonite Mixtures. *Indian Geotechnical Journal*, *53*(6), pp.1494-1504.

TH-3665_186104109

Narani, S.S., Abbaspour, M., Hosseini, S.M.M., Aflaki, E. and Nejad, F.M., 2020. Sustainable reuse of Waste Tire Textile Fibers (WTTFs) as reinforcement materials for expansive soils: With a special focus on landfill liners/covers. *Journal of cleaner production*, *247*, p.119151.

Nikkhah Nasab, S. and Abdeh Keykha, H., 2020. Physicochemical changes of lead (II) contaminated sand–clay mixture. *SN Applied Sciences*, *2*(9), pp.1-15.

Norouzi, A., Uygar, E. and Nalbantoglu, Z., 2022. A review on the effects of landfill leachate on the physical and mechanical properties of compacted clay liners for municipality landfills. *Arabian Journal of Geosciences*, *15*(12), p.1174.

Norrish, K. and Quirk, J.P., 1954. Crystalline swelling of montmorillonite: Use of electrolytes to control swelling. *Nature*, 173, pp.255-257.

Norrish, K., 1954. The swelling of montmorillonite. Discussions of the Faraday society, 18, pp.120-134.

Nwaiwu, C., Mshelia, S. and Durkwa, J., 2012. Compactive effort influence on properties of quarry dust-black cotton soil mixtures. *International Journal of Geotechnical Engineering*, *6*(1), pp.91-101.

Olson RE, Mesri G (1970) Mechanisms controlling compressibility of clays. Journal of Soil Mechanics & Foundations Div 96.

Onikata, M., Kondo, M., Hayashi, N. and Yamanaka, S., 1999. Complex formation of cation-exchanged montmorillonites with propylene carbonate: Osmotic swelling in aqueous electrolyte solutions. *Clays and clay minerals*, *47*(5), pp.672-677.

Osinubi, K.J., Yohanna, P. and Eberemu, A.O., 2015. Cement modification of tropical black clay using iron ore tailings as admixture. *Transportation Geotechnics*, *5*, pp.35-49.

Özkul, Z.H. and Baykal, G., 2006. Shear strength of clay with rubber fiber inclusions. *Geosynthetics International*, *13*(5), pp.173-180.

Patil, U., Valdes, J.R. and Evans, T.M., 2011. Swell mitigation with granulated tire rubber. *Journal of materials in civil engineering*, *23*(5), pp.721-727.

Petrov, R.J. and Rowe, R.K., 1997. Geosynthetic clay liner (GCL)-chemical compatibility by hydraulic conductivity testing and factors impacting its performance. *Canadian Geotechnical Journal*, *34*(6), pp.863-885.

Pivato, A. and Raga, R., 2006. Tests for the evaluation of ammonium attenuation in MSW landfill leachate by adsorption into bentonite in a landfill liner. *Waste management*, *26*(2), pp.123-132.

Plum, L.M., Rink, L. and Haase, H., 2010. The essential toxin: impact of zinc on human health. *International journal of environmental research and public health*, *7*(4), pp.1342-1365.

TH-3665_186104109

Posner, A.M. and Quirk, J.P., 1964. Changes in basal spacing of montmorillonite in electrolyte solutions. *Journal of Colloid Science*, *19*(9), pp.798-812.

Priyadarshee, A., Gupta, D., Kumar, V. and Sharma, V., 2015. Comparative study on performance of tire crumbles with fly ash and kaolin clay. *International Journal of Geosynthetics and Ground Engineering*, *1*, pp.1-7.

Prost, R., Koutit, T., Benchara, A. and Huard, E., 1998. State and location of water adsorbed on clay minerals: Consequences of the hydration and swelling-shrinkage phenomena. *Clays and clay minerals*, *46*(2), pp.117-131.

Prudent, P., Domeizel, M. and Massiani, C., 1996. Chemical sequential extraction as decision-making tool: application to municipal solid waste and its individual constituents. *Science of the total environment*, *178*(1-3), pp.55-61.

Qian, X., R. Koerner, and D. Gray., 2002. Geotechnical aspects of landfill design and construction. 1st ed. Englewood Cliffs, NJ: Prentice Hall.

Rahman, Z. and Singh, V.P., 2019. The relative impact of toxic heavy metals (THMs) (arsenic (As), cadmium (Cd), chromium (Cr)(VI), mercury (Hg), and lead (Pb)) on the total environment: an overview. *Environmental monitoring and assessment*, *191*(7), pp.1-21.

Rao, S.M., Thyagaraj, T. and Raghuveer Rao, P., 2013. Crystalline and osmotic swelling of an expansive clay inundated with sodium chloride solutions. *Geotechnical and Geological Engineering*, *31*, pp.1399-1404.

Rao, S.M., Thyagaraj, T. and Thomas, H.R., 2006. Swelling of compacted clay under osmotic gradients. *Geotechnique*, *56*(10), pp.707-713.

Ray, S., Mishra, A.K. and Kalamdhad, A., 2022(c). Influence of various concentration of lead on consolidation parameters of bentonite. *International Journal of Geotechnical Engineering*.

Ray, S., Mishra, A.K. and Kalamdhad, A.S., 2021(b). Influence of real and synthetic municipal solid waste leachates on consolidation and shear strength behaviour of bentonites. *Environmental Science and Pollution Research*, *28*, pp.30975-30985.

Ray, S., Mishra, A.K. and Kalamdhad, A.S., 2022(a). Effect of Lead, Copper, and Zinc on Mechanical Properties of Compacted Bentonites. *Journal of Hazardous, Toxic, and Radioactive Waste*, *26*(2), p.04021067.

Ray, S., Mishra, A.K. and Kalamdhad, A.S., 2022(b). Hydraulic performance, consolidation characteristics and shear strength analysis of bentonites in the presence of fly-ash, sewage sludge and paper-mill leachates for landfill application. *Journal of Environmental Management*, *302*, p.113977.

Ray, S., Mishra, A.K., Kalamdhad, A.S. and Reddy, C.V., 2021(a). Impact of real and simulated municipal solid waste leachates on the hydraulic and swelling behaviour of bentonites for landfill application. *Environmental Monitoring and Assessment*, *193*(11), pp.1-14.

TH-3665_186104109

Rayhani, M.H.T., Yanful, E.K. and Fakher, A., 2008. Physical modeling of desiccation cracking in plastic soils. *Engineering Geology*, *97*(1-2), pp.25-31.

Rayma, H.N., Umesha, T.S. and Lalithamba, H.S., 2018. Effect of sodium chloride on geotechnical properties of black cotton soil. *Journal of Materials Science and Nanotechnology*, *6*(3), pp.302-311.

Razali, N., Sa'don, N.M. and Karim, A.R.A., 2016. Strength and durability effect on stabilized subgrade soil. *Journal of Civil Engineering, Science and Technology*, *7*(1), pp.9-19.

Reddy, P.S., Mohanty, B. and Rao, B.H., 2020. Influence of clay content and montmorillonite content on swelling behavior of expansive soils. *International Journal of Geosynthetics and Ground Engineering*, *6*, pp.1-12.

Robinson, R.G. and Allam, M.M., 1998. Effect of clay mineralogy on coefficient of consolidation. *Clays and clay minerals*, *46*(5), pp.596-600.

Roustaei, M., Ghazavi, M. and Aliaghaei, E., 2016. Application of tire crumbs on mechanical properties of a clayey soil subjected to freeze-thaw cycles. *Scientia Iranica*, *23*(1), pp.122-132.

Rout, S. and Singh, S.P., 2020. Effect of inorganic salt solutions on physical and mechanical properties of bentonite based liner. *Journal of Hazardous, Toxic, and Radioactive Waste*, *24*(4), p.04020053.

Rowe, R. K., R. M. Quigley, and J. R. Booker. (1997). Clayey barrier systems for waste disposal facilities. 1st ed. Boca Raton, FL: Taylor & Francis

Rubinos, D.A. and Spagnoli, G., 2018. Utilization of waste products as alternative landfill liner and cover materials–A critical review. *Critical reviews in environmental science and technology*, *48*(4), pp.376-438.

Ruhl, J.L. and Daniel, D.E., 1997. Geosynthetic clay liners permeated with chemical solutions and leachates. *Journal of geotechnical and geoenvironmental engineering*, *123*(4), pp.369-381.

Saha, P. and Sanyal, S.K., 2010. Assessment of the removal of cadmium present in wastewater using soil–admixture membrane. *Desalination*, *259*(1-3), pp.131-139.

Scalia IV, J., Benson, C.H., Albright, W.H., Smith, B.S. and Wang, X., 2017. Properties of barrier components in a composite cover after 14 years of service and differential settlement. *Journal of Geotechnical and Geoenvironmental Engineering*, *143*(9), p.04017055.

Seda, J.H., Lee, J.C. and Carraro, J.A.H., 2007. Beneficial use of waste tire rubber for swelling potential mitigation in expansive soils. In *Soil improvement* (pp. 1-9).

Shackelford, C.D., Benson, C.H., Katsumi, T., Edil, T.B. and Lin, L., 2000. Evaluating the hydraulic conductivity of GCLs permeated with non-standard liquids. *Geotextiles and Geomembranes*, *18*(2-4), pp.133-161.

TH-3665_186104109

Shan, H.Y. and Lai, Y.J., 2002. Effect of hydrating liquid on the hydraulic properties of geosynthetic clay liners. *Geotextiles and Geomembranes*, *20*(1), pp.19-38.

Shariatmadari, N., Askari Lasaki, B., Eshghinezhad, H. and Alidoust, P., 2018. Effects of landfill leachate on mechanical behaviour of adjacent soil: a case study of Saravan landfill, Rasht, Iran. *International Journal of Civil Engineering*, *16*, pp.1503-1513.

Shariatmadari, N., Salami, M. and Karimpour, F.M., 2011. Effect of inorganic salt solutions on some geotechnical properties of soil-bentonite mixtures as barriers. *International Journal of Civil Engineering*, *9*, pp. 103-110.

Sharma, H.D. and Reddy, K.R., 2004. *Geoenvironmental engineering: site remediation, waste containment, and emerging waste management technologies*. John Wiley & Sons.

Shirazi, S.M., Wiwat, S., Kazama, H., Kuwano, J. and Shaaban, M.G., 2011. Salinity effect on swelling characteristics of compacted bentonite. *Environment Protection Engineering*, *37*(2), pp.65-74.

Shukla, R.P. and Parihar, N.S., 2016. Stabilization of black cotton soil using micro-fine slag. *Journal of the Institution of Engineers (India): Series A*, *97*(3), pp.299-306.

Siddique, R. and Naik, T.R., 2004. Properties of concrete containing scrap-tire rubber–an overview. *Waste management*, *24*(6), pp.563-569.

Siddique, R. and Naik, T.R., 2004. Properties of concrete containing scrap-tire rubber–an overview. *Waste management*, *24*(6), pp.563-569.

Singh, S. and Prasad, A., 2007. Effects of chemicals on compacted clay liner. *Electronic Journal of Geotechnical Engineering*, *12*(D), pp.1-15.

Sivakumar Babu, G.L., Vasudevan, A.K. and Sayida, M.K., 2008. Use of coir fibers for improving the engineering properties of expansive soils. *Journal of Natural Fibers*, *5*(1), pp.61-75.

Sivapullaiah, P.V. and Baig, M.A.A., 2011. Gypsum treated fly ash as a liner for waste disposal facilities. *Waste Management*, *31*(2), pp.359-369.

Sivapullaiah, P.V. and Lakshmikantha, H., 2005. Chemical compatibility of lime stabilized Indian red earth as liner material. *Soil & Sediment Contamination*, *14*(6), pp.515-526.

Sivapullaiah, P.V. and Manju, 2005. Kaolinite–alkali interaction and effects on basic properties. *Geotechnical & Geological Engineering*, *23*, pp.601-614.

Sivapullaiah, P.V., Prashanth, J.P. and Sridharan, A., 1996. Effect of fly ash on the index properties of black cotton soil. *Soils and foundations*, *36*(1), pp.97-103.

Soltani, A., Deng, A., Taheri, A. and Sridharan, A., 2019. Swell–shrink–consolidation behavior of rubber–reinforced expansive soils. *Geotechnical Testing Journal*, *42*(3), pp.761-788.

TH-3665_186104109

Soltani, A., Deng, A., Taheri, A. and Sridharan, A., 2019. Swell–shrink–consolidation behavior of rubber–reinforced expansive soils. *Geotechnical Testing Journal*, *42*(3), pp.761-788.

Soltani, A., Taheri, A., Khatibi, M. and Estabragh, A.R., 2017. Swelling potential of a stabilized expansive soil: a comparative experimental study. *Geotechnical and Geological Engineering*, *35*, pp.1717-1744.

Soltani-Jigheh, H., Asadzadeh, M. and Marefat, V., 2014. Effects of tire chips on shrinkage and cracking characteristics of cohesive soils. *Turk J Eng Environ Sci*, *37*(3), pp.259-271.

Song, Z., Zhang, Z. and Du, X., 2024. Shear strength of compacted bentonite saturated with saline solutions under different specimen saturation methods. *International Journal of Geomechanics*, *24*(3), p.04024004.

Sridharan, A. and Gurtug, Y., 2004. Swelling behaviour of compacted fine-grained soils. *Engineering geology*, *72*(1-2), pp.9-18.

Sridharan, A. and Jayadeva, M.S., 1982. Double layer theory and compressibility of clays. *Geotechnique*, *32*(2), pp.133-144.

Sridharan, A. and Nagaraj, H.B., 2004. Coefficient of consolidation and its correlation with index properties of remolded soils. *Geotechnical testing journal*, *27*(5), pp.469-474.

Sridharan, A. and Prakash, K., 1998. Characteristic water contents of a fine-grained soil—water system. *Geotechnique*, *48*(3), pp.337-346.

Sridharan, A. and Prakash, K., 2000. Classification procedures for expansive soils. *Proceedings of the Institution of Civil Engineers-Geotechnical Engineering*, *143*(4), pp.235-240.

Sridharan, A. and Rao, G.V., 1973. Mechanisms controlling volume change of saturated clays and the role of the effective stress concept. *Geotechnique*, *23*(3), pp.359-382.

Sridharan, A., Rao, S.M. and Murthy, N.S., 1986. A rapid method to identify clay type in soils by the free-swell technique. *Geotechnical Testing Journal*, *9*(4), pp.198-203.

Srivastava, A., Pandey, S., & Rana, J. 2014. Use of shredded tyre waste in improving the geotechnical properties of expansive black cotton soil. *Geomechanics and Geoengineering*, *9*(4), 303-311

Taheri, S., Ebadi, T., Maknoon, R. and Amiri, M., 2018. Predicting variations in the permeability and strength parameters of a sand-bentonite mixture (SBM) contaminated simultaneously with lead (II) and diesel. *Applied Clay Science*, *157*, pp.102-110.

Taheri, S., Ebadi, T., Maknoon, R. and Amiri, M., 2018. Predicting variations in the permeability and strength parameters of a sand-bentonite mixture (SBM) contaminated simultaneously with lead (II) and diesel. *Applied Clay Science*, *157*, pp.102-110.

TH-3665_186104109

Tajdini, M., Nabizadeh, A., Taherkhani, H. and Zartaj, H., 2017. Effect of added waste rubber on the properties and failure mode of kaolinite clay. *International Journal of Civil Engineering*, *15*, pp.949-958.

Tang, C.S., Li, S.J., Wang, D.W., Chen, Z.G., Shi, B. and Inyang, H., 2019. Experimental simulation of boundary condition effects on bentonite swelling in HLW repositories. *Environmental Earth Sciences*, *78*(5), pp.1-15.

Tang, C.S., Shi, B., Cui, Y.J., Liu, C. and Gu, K., 2012. Desiccation cracking behavior of polypropylene fiber–reinforced clayey soil. *Canadian Geotechnical Journal*, *49*(9), pp.1088-1101.

Tatsi, A.A. and Zouboulis, A.I., 2002. A field investigation of the quantity and quality of leachate from a municipal solid waste landfill in a Mediterranean climate (Thessaloniki, Greece). *Advances in Environmental Research*, *6*(3), pp.207-219.

Taylor, D.W., 1948. Fundamentals of soil mechanics (Vol. 66, No. 2, p. 161). LWW.

Terzaghi, K., 1943. Theoretical soil mechanics. johnwiley & sons. *New York*, pp.11-15.

Thanh Duong, N. and Van Hao, D., 2020. Consolidation Characteristics of Artificially Structured Kaolin-Bentonite Mixtures with Different Pore Fluids. *Advances in Civil Engineering*, *2020*(1), p.8856404.

Tripathy, S., Sridharan, A. and Schanz, T., 2004. Swelling pressures of compacted bentonites from diffuse double layer theory. *Canadian Geotechnical Journal*, *41*(3), pp.437-450.

Trouzine, H., Bekhiti, M. and Asroun, A., 2012. Effects of scrap tyre rubber fibre on swelling behaviour of two clayey soils in Algeria. *Geosynthetics International*, *19*(2), pp.124-132.

UNEP (2010) Framework of global partnership on waste management, Note by Secretariat.

United States Environmental Protection Agency (USEPA), 1988. Design, construction and evaluation on of clay liners for waste management facilities.

Van Olphen, H., 1965. Thermodynamics of interlayer adsorption of water in clays. I.—Sodium vermiculite. *Journal of Colloid Science*, *20*(8), pp.822-837.

Wang, Y., Cheng, K., Wu, W., Tian, H., Yi, P., Zhi, G., Fan, J. and Liu, S., 2017. Atmospheric emissions of typical toxic heavy metals from open burning of municipal solid waste in China. *Atmospheric Environment*, *152*, pp.6-15.

Warkentin, B.P., 1961. Interpretation of the upper plastic limit of clays. *Nature*, *190*(4772), pp.287-288. Sridharan, A. and Prakash, K., 1998. Characteristic water contents of a fine-grained soil—water system. *Geotechnique*, *48*(3), pp.337-346.

Wilson, D.N., 1988. Cadmium-market trends and influences. In *Cadmium 87. Proceedings of the 6th International Cadmium Conference, London, Cadmium Association* (Vol. 9, p. 16).

Xiang, G., Ye, W., Xu, Y. and Jalal, F.E., 2020. Swelling deformation of Na-bentonite in solutions containing different cations. *Engineering Geology*, *277*, p.105757.

TH-3665_186104109

Xin, L., He, J., Liu, H. and Shen, Y., 2015. Potential of using cemented soil-tire chips mixture as construction fill: a laboratory study. *Journal of Coastal Research*, (73), pp.564-571.

Xu, Y., Xue, X., Dong, L., Nai, C., Liu, Y. and Huang, Q., 2018. Long-term dynamics of leachate production, leakage from hazardous waste landfill sites and the impact on groundwater quality and human health. *Waste Management*, *82*, pp.156-166.

Xue, Q. and Zhang, Q., 2014. Effects of leachate concentration on the integrity of solidified clay liners. *Waste management & research*, *32*(3), pp.198-206.

Yadav, J.S. and Tiwari, S.K., 2017. Effect of waste rubber fibres on the geotechnical properties of clay stabilized with cement. *Applied Clay Science*, *149*, pp.97-110.

Yang, Y., Reddy, K.R., Zhan, H., Fan, R., Liu, S., Xue, Q. and Du, Y., 2021. Hydraulic conductivity of soil-bentonite backfill comprised of SHMP-amended Ca-bentonite to Cr (VI)-impacted groundwater. *Journal of Contaminant Hydrology*, *242*, p.103856.

Ye, W.M., Zhang, F., Chen, B., Chen, Y.G., Wang, Q. and Cui, Y.J., 2014. Effects of salt solutions on the hydro-mechanical behavior of compacted GMZ01 Bentonite. *Environmental earth sciences*, *72*, pp.2621-2630.

Ye, W.M., Zhu, C.M., Chen, Y.G., Chen, B., Cui, Y.J. and Wang, J., 2015. Influence of salt solutions on the swelling behavior of the compacted GMZ01 bentonite. *Environmental Earth Sciences*, *74*(1), pp.793-802.

Ying, Z., Cui, Y.J., Duc, M., Benahmed, N., Bessaies-Bey, H. and Chen, B., 2021. Salinity effect on the liquid limit of soils. *Acta Geotechnica*, *16*(4), pp.1101-1111.

Yohanna, P., Johnson, P., Victor, B.P., Badamasi, A., Mije, F.G., Ako, T. and Bassey, A.B., 2022. Evaluation of geotechnical properties of black cotton soil reinforced with sisal fibre for waste containment application. *Engineering Science & Technology*, pp.151-168.

Yong, R.N. and Di Perno, N., 1991. Sources and characteristics of waste-with specific reference to Canada.

Yoon, Y.W., Heo, S.B. and Kim, K.S., 2008. Geotechnical performance of waste tires for soil reinforcement from chamber tests. *Geotextiles and Geomembranes*, *26*(1), pp.100-107.

Zayed, A.M. and Terry, N., 2003. Chromium in the environment: factors affecting biological remediation. *Plant and soil*, *249*, pp.139-156.

Zhang, F., Low, P.F. and Roth, C.B., 1995. Effects of monovalent, exchangeable cations and electrolytes on the relation between swelling pressure and interlayer distance in montmorillonite. *Journal of Colloid and Interface Science*, *173*(1), pp.34-41.

Zhang, L. and Jia, D., 2016. Shear strength of GMZ07 bentonite and its mixture with sand saturated with saline solution. *Applied Clay Science*, *132*, pp.24-32.

Zhu, C.M., Ye, W.M., Chen, Y.G., Chen, B. and Cui, Y.J., 2013. Influence of salt solutions on the swelling pressure and hydraulic conductivity of compacted GMZ01 bentonite. *Engineering Geology*, *166*, pp.74-80.

TH-3665_186104109

Zhu, C.M., Ye, W.M., Chen, Y.G., Chen, B. and Cui, Y.J., 2013. Influence of salt solutions on the swelling pressure and hydraulic conductivity of compacted GMZ01 bentonite. *Engineering Geology*, *166*, pp.74-80.

Zhu, F., He, S. and Liu, T., 2018. Effect of pH, temperature and co-existing anions on the Removal of Cr (VI) in groundwater by green synthesized nZVI/Ni. *Ecotoxicology and environmental safety*, *163*, pp.544-550.

TH-3665_186104109

TH-3665_186104109

PUBLICATIONS

INTERNATIONAL JOURNALS

- **Babu, N.M.** and Mishra, A.K., 2022. Effect of salt permeants on the consolidation and hydraulic behaviour of fibre treated black cotton soil for landfill application. *Journal of Cleaner Production*, 369, p.133339.
  DOI: https://doi.org/10.1016/j.jclepro.2022.133339
- **Babu, N.M.** and Mishra, A.K., 2023. Influence of Salt Permeants on The Swelling and Strength Behavior of Fibre Treated Black Cotton Soil. *KSCE Journal of Civil Engineering*, pp.1-11.
  DOI: https://doi.org/10.1007/s12205-023-1453-6
- **Babu, N.M.** and Mishra, A.K., 2024. Geotechnical performance of black cotton clay in the presence of lead and cadmium solutions for geoenvironmental application. *Environmental Technology*, pp.1-15.
  DOI: https://doi.org/10.1080/09593330.2024.2379990

JOURNALS UNDER PREPARATION

- N. Mahesh Babu and Mishra A.K., A study on swell-consolidation-hydraulic characteristics of compacted waste tire fibre-mixed black cotton soil composite under hazardous heavy metal permeants.
- N. Mahesh Babu and Mishra A.K., Geotechnical investigation on the behavior of fibre-mixed BC soil under the permeation of synthetic leachates.

BOOK CHAPTERS

- **Mahesh Babu, N.** and Mishra, A.K., 2022, December. Influence of Inorganic Salt Solutions on the Engineering Behavior of Black Cotton Soil. In *Indian Geotechnical Conference* (pp. 107-116). Singapore: Springer Nature Singapore.
  DOI: https://doi.org/10.1007/978-981-97-2704-9_11
- **Babu, N.M.** and Mishra, A.K., 2023, November. Impact of Waste Tire Fibre on the Hydro-Mechanical Behaviour of Black Cotton Soil Under Different Pore Fluids. In *International Conference on Construction Resources for Environmentally Sustainable Technologies* (pp. 173-183). Singapore: Springer Nature Singapore.
  DOI: https://doi.org/10.1007/978-981-99-9227-0_17

TH-3665_186104109

- **Babu, N.M.** and Mishra, A.K., 2023, October. Heavy Metals Influence on the Geotechnical Performance of Black Cotton Soil for Liner Application. In *International Conference on Environmental Geotechnology, Recycled Waste Materials and Sustainable Engineering* (pp. 107-117). Singapore: Springer Nature Singapore.
  DOI: https://doi.org/10.1007/978-981-97-3823-6_9
- **Babu, N.M.** and Mishra, A.K., 2024. Influence of Lead and Hexavalent Chromium Concentrations on Geotechnical Properties of Black Cotton Soil. In *Advancement in Solid Waste Management and Treatment* (pp. 75-84). Cham: Springer Nature Switzerland.
  DOI: https://doi.org/10.1007/978-3-031-64873-1_6

CONFERENCE

- N. Mahesh Babu and Mishra A.K. (2024) Assessment of Waste Tire Fibre Mixed Black Cotton Clay Engineering Performance Inundated by Various Heavy Metal Concentrations. *An International Conference on Environmental Challenges, Opportunities and Sustainable Solutions*, IIT Guwahati, India.

TH-3665_186104109